University of Southampton

Faculty of Natural and Environmental Science

School of Chemistry

Targeting C-terminal Binding Proteins (CtBPs) using Genetic Selection

By

Sharandip Kaur Nijjar

Thesis submitted for the Degree of Doctor of Philosophy

September 2011

University of Southampton

Abstract

Faculty of Natural and Environmental Science

School of Chemistry

Doctor of Philosophy

Targeting C-terminal Binding Proteins (CtBPs) using Genetic Selection

By Sharandip Kaur Nijjar

There are many protein-protein interactions that are vital for cellular processes such as signal transduction, structural organisation and apoptosis. In this study we decipher the role of the protein-protein interaction of C-terminal Binding Proteins (CtBPs). CtBPs function as transcriptional co-repressors in the nucleus playing key roles in tumorigenesis and metastasis by regulating cellular processes, critical to cell survival, cell migration and senescence. CtBP proteins also play a role in the cytoplasm in regulating mitotic Golgi membrane fission Studies in which the expression or function of CtBPs has been inhibited have independently identified roles for CtBPs in both suppressing apoptosis and promoting cell cycle progression.

Modulation of these interactions with small molecules is a potential therapeutic strategy with benefits over current methods. Our approach in studying protein-protein interactions and uncovering potential inhibitors involves constructing a bacterial Reverse Two Hybrid System (RTHS) linking the dimerisation of the target protein partners to the expression of reporter genes, whose regulation can be monitored via host survival. Subsequent screening of a cyclic peptide library for potential inhibitors was then carried out. The libraries were produced using Split Intein-mediated Circular Ligation Of Peptides and Proteins (SICLOPPS) technology, developed for intracellular synthesis of cyclic peptides. We have used this methodology to identify inhibitors of CtBP dimerisation and better understand the roles of this protein interaction in cell cycle regulation.

Chapter 1 provides an introduction to the work carried out to study protein-protein interactions and finding potential inhibitors. Since our investigations involved the extensive use of the RTHS and SICLOPPS system, the background and work performed by others has been described in detail. A detailed review of CtBPs has also been carried out.

Chapter 2 details our work investigating the homodimeric and heterodimeric protein-protein interaction of CtBPs using the RTHS. This work allowed us to optimise selection conditions and find cyclic peptide inhibitors of the homodimerisation of CtBP1 and CtBP2 using the SICLOPPS process. The synthesis of these inhibitors is described.

Chapter 3 details our work carried out to develop ELISAs for *in vitro* analysis of the selected cyclic peptides. This involved the purification of His- and GST-tagged CtBP1 and CtBP2 proteins. The ELISA conditions were optimised to carry out CtBP homodimeric and hetrodimeric analysis. This work showed that the peptides lead to a reduction in CtBP homdimerisation and heterodimerisation *in vitro*.

Chapter 4 details the *in vivo* effects of the uncovered CtBP dimerisation inhibitors. Using these cyclic peptide inhibitors we have demonstrated that CtBP dimerisation is essential for the regulation of mitotic fidelity, and that inhibition of CtBP dimerisation by the cyclic peptides leads to aberrant segregation of chromosomes during mitosis. We have also shown that inhibition of CtBP dimerisation leads to a reduction in migration of MCF-7 breast cancer cells. Chapter 5 details the experimental procedures used in this work and presents spectroscopic and analytical data for the compounds prepared.

Declaration

The work described in this thesis was carried out at the School of Chemistry and Faculty of Medicine at The University of Southampton. Unless otherwise acknowledged it was the individual work of the author Sharandip Kaur Nijjar.

Acknowledgements

I would firstly like to thank my supervisors Dr Ali Tavassoli and Dr Jeremy Blaydes who have been excellent supervisors. I thank them for all their help, encouragement, guidance and support that they have given me over the last few years.

I would like to thank past and present group members for their friendship and support during my PhD. I have had a great time working with them all and I thank them for making my time an enjoyable and memorable one.

I would like to thank Dr Charles Birts, Dr Patrick Duriez and Matthew Darley for the help and support while I worked in their labs and Marta Chrzan for carrying out the migration assays. With the oversight of my main supervisor, editorial advice has been sought. Thank you also to my sister-inlaw Dr Rajdeep Benning for the proof-reading of this thesis. This is a time consuming job and I am grateful for your help and advise. No changes of intellectual content were made as a result of this advice

And finally I would like to give a big thank you to my husband and family for their support and encouragement throughout my studies.

Abbreviation

A	adenine
aa	Amino acids
3-AT	3-amino-1, 2, 4-triazole
Amp	Ampicillin
ARF	Alternative reading frame
Arg	Arginine
Asp	Aspartic acid
ATP	adenosine triphosphate
Aq	Aqueous
Bcl-2	B cell lymphoma
BARs	brefeldin A-ADP ribosylation substrate
BKLF	basic Krüppel-like factor
bp	base pair
BRCA1	breast cancer 1
BSA	Bovine serum albumin
C	cytosine
CoREST	REST corepressor
CtBP	C-terminal Binding protein
	hCtBP human CtBP
	mCtBP mouse CtBP
	dCtBP drosophila CtBP
Cys	Cysteine

DAPI	(4,6-diamidino-2-phenylindole)
DBD	DNA binding Domain
DCC	N,N'-dicyclohexylcarbodiimide
DCM	Dichloromethane
DIC	N,N'-diisopropylcarbodiimide
DIPEA	*N,N*-diisopropylethylamine
DMAP	4-dimethylamino pyridine
DMEM	Dulbecco's modified Eagle's medium
DMF	*N,N*-dimethylformamide
DMSO	dimethyl sulphoxide
DNA	deoxyribonucleic acid
dNTP	deoxyribonucleotide triphosphate
EBNA3C	Epstein-Barr virus
EC_{50}	half maximal effective concentration
EDC	1-ethyl-3-(3-dimethylaminopropyl) carbodiimide
EDT	Ethane dithiole
EDTA	Ethylenediaminetetraacetic acid
EMT	epithelial-mesenchymal transition
ELISA	Enzyme-linked immunosorbent assay
Et_2OH	Ethanol
eq	equivalents
FCS	Fetal Calf Serum
FITC	fluorescein isothiocyanate

Fmoc	9-Fluorenylmethyloxycarbonyl chloride
FPLC	Fast protein liquid chromatography
G	guanine
Gly	Glycine
GST	Glutathione S-transferase
HAT	Histone acetyl transferase
HDAC	Histone Deacetylase
Hdm2	Human double minute 2 gene
Hdm2	Human double minute 2 protein
His	Histidine
HM ESI	High mass electrospray ionisation
HMTase	Histone methyltransferase
HOBt	Hydroxybenzotriazole
HPLC	High-performance liquid chromatography
HPSS	Hank's Balanced Salt Solution
hr	hour
HRP	Horseradish peroxidise
IC	C-Intein
Ig	Immunoglobulin
IN	N-Intein
IPTG	isopropyl β-D-1-thiogalactopyranoside
IR	Infrared
Kan	Kanamycin

kB	kilo base pair
kDa	kilo Dalton
LB	Luria-bertani Broth
LCI	Live Cell Imager
LSD1	Lysine-specific demethylase
M	Molar concentration
MCS	multiple cloning site
mAb	monoclonal antibody
MCF-7	Michigan Cancer Foundation – 7 (breast cancer cell line)
Mdm2	murine double minute 2 gene
Mdm2	murine double minute 2 protein
MeCN	Acetonitrile
MeOH	Methanol
Met	Methionine
mFIP	Multiple fluorescence
min	minutes
mmol	millimole
mol	moles
MS	Mass spectrometer
MTS	(3-(4,5-dimethylthiazol-2-yl)-5-(3-carboxymethoxyphenyl)-2-(4-sulfophenyl)-2H-tetrazolium)
MW	molecular weight
m/z	mass to charge ratio

NADH	Nicotinamide adenine dinucleotide
NBD	Nucleotide binding domain
NLS	Nuclear localisation signal
NMP	1-methyl-2-pyrrolidinone
NMR	nuclear magnetic resonance
OD	optical density
o/n	overnight
ONPG	ortho-Nitrophenyl-β-galactoside
p300	E1A binding protein p300
PAK1	p21-activated kinase 1
PBS	Phosphate buffered saline
PCR	polymerase chain reaction
pI	isoelectric point
pRB	Retinoblastoma protein
Pro	Proline
P_{Tac}	Tac promoter
PyBop	benzotriazol-1-yl-oxytripyrrolidinophosphonium hexafluorophosphate
Pyr	Pyridine
PXDLS	Proline-X- Aspartic acid-Leucine- serine (X = any amino acid)
RBS	ribosome binding site
RNA	Ribonucleic acid
RNAi	RNA interference
RRT	Arginine-Arginine-Threonine

rt	room temperature
RTHS	Reverse two-hybrid system
SBD	Substrate Binding domain
SDS-PAGE	Sodium dodecyl sulfate polyacrylamide gel electrophoresis
Sec	seconds
Ser	Serine
Sumo	small ubiquitin-like factor
SICLOPPS	Spilt-intein circular ligation of peptides and proteins
siRNA	Small interfering RNA
SOC	Super Optimal broth with Catabolite repression
Spec	Spectinomycin
SPPS	solid phase peptide synthesis
SRC	steroid receptor coactivator
T	thymine
TAE	Tris-acetate-EDTA
Tat	Trans-activator of transcription
TBS	Tris buffered saline
Temp	temperature
TFA	Trifluoroacetic acid
Thr	Threonine
TIS	Triisopropyl silane
TLC	Thin layer chromatography
TNF-α	Tumour necrosis factor alpha

tRNA	transfer RNA
Trp	Tryptophan
Tyr	Tyrosine
Ubc9	Ubiquitin carrier protein 9
UV	Ultra violet
Val	Valine
VMA	Vacuolar Membrane ATPase
wt	wild type
Y2HS	yeast two-hybrid system
ZEB	Zinc finger E-box-binding homeobox
ZnF217	Zinc finger protein

Table of Contents

Table of Figures

1 Introduction

1.1 Protein-Protein interaction

There are a large number of protein-protein interactions that control and regulate many cellular processes, for example metabolic pathway, signal transduction and programmed cell death. For this reason, there is significant current interest in studying the potential of this class of interaction as a general drug target. Low molecular weight chemical compounds that are bound to a protein may prevent the formation of protein dimers. Although typically large and featureless, protein-protein interfaces display an overall match between polar residues through large hydrogen bond networks, often mediated by water molecules and hydrophobic interactions between aliphatic and aromatic patches. Correctly identifying the role of a protein-protein interaction can help assign the true cellular function of a given proteins, investigate the mechanism of intracellular biochemical pathways, understand the primary courses of diseases and could lead to the development of drugs to treat diseases.[1]

Large scale siRNA screening can be used to investigate the function of genes individually in a high throughput manner with respect to biological function and cellular processes. Treatment with siRNA leads to gene silencing by destroying mRNA that encodes a protein therefore preventing the protein from being synthesised. Methods of introducing siRNA into the cells include introducing an expression vector, which allows the cells to express the siRNA. An advantage of this method is that it allows persistent gene silencing after stable integration of the vector into the host genome. This leads to complete knock out of the protein. This process is complicated, time consuming and more expensive than other methods. Another method involves the synthesis and transfection of long double stranded (ds) siRNA (200 nt). Once introduced into the cell ds siRNA can be cleaved by the DICER complex forming siRNA. This method is easier and more cost effective. Small siRNA can be created *in vitro* and transfected into the cells once present in the cells ds siRNA is denatured and bound by the RISC complex. Small siRNA can be purchased directly, complete knock down is not guaranteed.[2, 3] There are many therapeutic uses of siRNA, for example treatment of cancer, viral and genetic diseases.[4]

Advantages of siRNA screening include:

- Quick method to knock down a specific gene.
- siRNA can be labeled.
- Ease of transfection.
- Chemical modifications to enhance stability are possible.
- Allows the depletion of any protein as long as the sequence is known.
- Perfect drug for the specific blocking of unwanted or disease causing genes

Disadvantages of siRNA screening include:

- May not work in cell lines difficult to transfect.
- Is expensive for larger experiments.
- Short-term, transient knock down only.
- Chemically synthesized siRNA is short lived.
- Results in transient inhibition of gene expression.
- Off-target effects resulting in knock down unintended genes due to mismatches and gaps between small RNA and target RNA sequences.
- Degree of knock down is variable.
- The protein is removed from the system, therefore further analysis is required to identify the underlying mechanism of the cellular process of interest.

Manipulation of protein-protein interactions has proven challenging. Unlike enzyme based drug discovery, there is a no clear starting point for drug design, because in nature, few small molecules bind at protein-protein surfaces. Protein-protein interfacial surface areas are typically large, suggesting that macromolecules may be better suited as inhibitors (as opposed to small molecules).[5] Other difficulties include the fact that interacting surfaces are often shallow and featureless compared to the well-defined binding pockets for enzyme active sites. This may cause problems with selectivity, because on such surfaces there is not enough contact to achieve specificity through shape recognition for a small molecule, as typically observed in deep binding enzyme pockets. Studies focusing on protein interfaces have shown that binding energies are not uniformly distributed, but instead there are certain important residues called hot spots. These residues comprise a small fraction of interfaces but account for the majority of the binding energy.[6] Typically, the larger the interface then the more hot spots there are.

However, in most cases there is only one hot spot present at the interface and on average it has a surface area of 1560 ± 340Å upon binding.[7] It is therefore difficult to know where on the interface these hot spot areas are and often there is no associated crystal structure, which makes rational design very difficult.[8]

A great deal of work has gone into understanding protein-protein interactions and trying to find potential inhibitors. Traditional drug development involves random screening of molecules this process is very lengthy, expensive and gives low yields. Computational methods have been proposed to predict protein-protein interactions, for example computer-aided drug design (CADD). The CADD method refers to the application of a variety of computational methods to drug discovery and design. It is possible to identify appropriate binding sites to be targeted during virtual database screening. CADD exploits state-of-the-art technology to speed up the drug development process. Advantages of CADD process are as follows: It is target specific and structure based, fast, automatic and has a low cost.[9] Disadvantages of the process are as follows: due to combinatorial attachment, a number of diverse chemical components arise that in reality, may be synthetically unfeasible structures; many ligands are produced that are chemically unstable and although a diverse set of chemical building blocks are used, the manner of attachment depends entirely on the developer of the software.

Another methodology used to identify interacting proteins or to study protein interactions is the yeast two-hybrid system (YTH), which is used to identify mutations that affect protein-protein interactions. YTH is also used to find proteins that interact with a single protein of interest and used to confirm suspected interactions and to define interacting domains.[10] It provides direct evidence of physical protein-protein interactions in high-throughput analysis.[11] Detection of protein-protein interactions in the YTH is based on the reconstitution of transcription factors divided into a DNA binding domain (DBD) and a DNA activation domain (AD). One of the proteins is fused to the DBD and the other to the AD. Productive interaction of the proteins of interest will bring the two domains together and will trigger the transcription of an adjacent reporter gene for example lacZ. However, there are some limitations to this process: the location of the interaction is restricted to the nucleus, which is not suitable for the study of membrane proteins and large size proteins. Also transcription factors can auto activate the reporter gene and that leads to false positive results. Proteins that

cannot be targeted to the nucleus may not yield a transcription signal even though it may potentially interact, causing false negatives. [12]

The bacterial two-hybrid (BTH) system is similar to the yeast two-hybrid system. It allows the identification of protein-protein interactions in *Escherichia coli*. This technique enables a fast and simple approach to identifying protein-protein interactions.[12a] Both the YTH and BTH system are limited to positive selection for protein-protein association events and do not allow the detection of dissociation events for examples mutations in one of the interacting proteins or introduction of an inhibitor.

1.2 Reverse Two Hybrid Systems (RTHS)

The original forward two hybrid systems can be altered to couple cell growth to the disruption of protein complexes, and this methodology is referred to as the reverse two-hybrid system (RTHS). An important feature of the RTHS is the incorporation of reporter genes to monitor the protein-protein interaction, whose product is toxic to growing cells. Allowing selective pressure against the formation of the two-hybrid complex, Vidal *et al* developed a RTHS in yeast where *URA3* was used as a reporter gene. The *URA3* gene encodes an enzyme required for the biosynthesis of uracil. Yeast cells that express *URA3* fail to grow on media containing 5-fluoro-orotic acid (5-FOA) because the URA3 enzyme transforms 5-FOA into a toxic compound.[13, 14] When the proteins of interest interact the *URA3* gene is expressed leading to the death of yeast cell on media containing 5-FOA. When the protein-protein interaction is disrupted either by a mutation or the presence of an inhibitor the *URA3* gene is no longer expressed therefore cells are able to survive on media containing 5-FOA. This process allows the screening of libraries of randomly generated mutation and potential drugs.

Another reporter gene used was *LacZ*, which allows quantification of the protein-protein interactions through β-galactosidase assays. Hannick *et al* [15] reported that biochemical assays for *LacZ* expression were relatively insensitive and lead to high frequency of false positives. They therefore developed a system dependent on cell viability, for example the introduction of a selective marker *HIS3*. The *HIS3* genes encode a yeast auxotroph of imidazole glycerol phosphate dehydratase, needed for the

synthesis of histidine and is able to complement the growth defect of cells bearing a deletion in the homologous.[16]

The RTHS[17] can be used for both studying protein-protein interactions and for rapid screening of inhibitors of protein-protein interactions. The RTHS used in this study is based on the bacteriophage regulatory system, linking the disruption of the interaction between the two target proteins, expressed as hybrid fusion of a chimeric repressor complex, to the expression of three reporter genes. The λ phage active repressor is a homodimer formed by 2 cI molecules. The λ cI is a transcriptional repressor that controls the lytic/lysogeny cycle of bacteriophage λ, the N-terminal domain is responsible for DNA operator, recognition and binding. The C-terminal domain mediates dimerisation. The N-terminal domain alone can not form an active repressor, but if bound to a protein able to dimerise a functional chimeric repressor can be restored.[18] The bacteriophage 434 is a close relative of bacteriophage λ and encodes a regulatory protein that both activates and represses transcription.[19] Repressor dimers bind cooperatively to a region of the phage chromosome called (O_R) that contains three repressor binding sites (O_R1, O_R2, O_R3). P_R and P_{RM} are promoter regions present with in O_R. The *Salmonella* phage P22 and the coli-phage 434 and λ repressor all share sequence similarities within the C-terminal domain.[19, 20, 21] These proteins can only form homodimers. The dimerisation interface of the 434 repressor is located within 15 amino acids of the C-terminal end of the protein. In order to study protein heterodimerisation G. Di Lallo *et al* [22] generated a chimeric operator in which the DNA sequence coding for the amino acids in this region were replaced with the homologous region of p22 repressor. The operator can be recognised and bound only by a hybrid repressor formed by two chimeric monomers. Only proteins, which allow dimerisation of the two chimeric reporters allow the formation of a functional repressor able to bind the P22-434 hybrid operator and prevent synthesis of down-stream reporter genes.

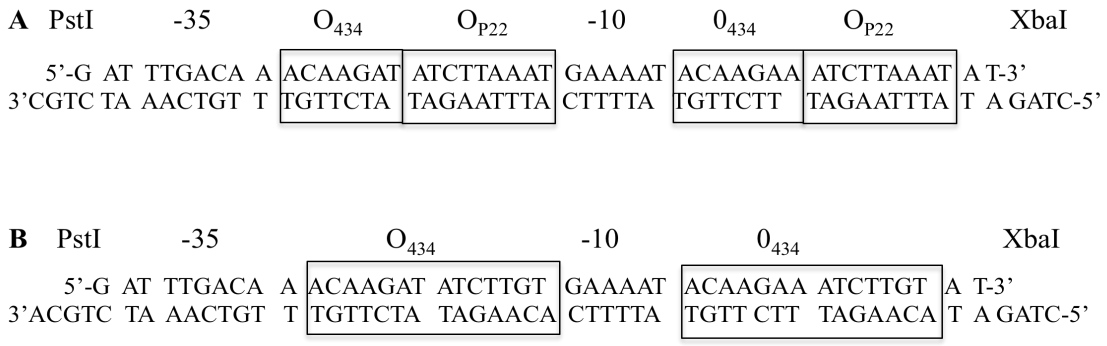

Figure 1.1 (A) Chimeric 434 and P22 promoter, (B) Wild-type 434 promoter.[17b]

Our homodimeric RTHS uses the 434 binding protein and the heterodimeric RTHS uses a mutant 434, p22 and the wild-type 434 binding protein (Figure 1.1). A plasmid, which codes for two fusion proteins, is constructed. Each fusion protein consists of one of the protein partners of the protein-protein interaction under investigation and one half of the repressor. Once the plasmid is introduced into the cell and transcribed, protein partners are able to come together forming the protein complex. This brings the two halves of the repressor into contact, reconstituting the active repressor that will bind its corresponding operator sequence that has been incorporated onto the chromosome. The repressor has control over downstream reporter genes that are essential for the life of the cell on minimal media; the formation of the active repressor prevents their transcription and leads to cell death.[17b] In this system, potential inhibitors of the dimerisation can be introduced and cells containing active inhibitors can easily be identified on selective media, as they are the ones able to survive (Figure 1.2).[17a, 23]

The reporter construct is engineered onto the chromosome of the *E.coli* host cell strain containing a HisB deletion. HisB codes for imidazole glycerol-phosphate (IGP) dehydratase and histidinol-phosphate (HOL-P) phosphatase which catalyse the sixth and eighth step of histidine biosynthesis, respectively[24]. The reporter construct consists of three reporter genes: *HIS3*. The second reporter is Kan^R, which codes for aminoglycosidase 3'-phosphotransferase for kanamycin resistance. These two reporters are chemically tuneable and conditionally selective for reporter genes. The third reporter gene is *Lac Z* (β-galactosidase).[13] Formation of the protein complex inhibits the growth on minimal media by blocking *HIS3* expression. Residual background can be adjusted with 3-amino-1, 2, 4-triazole (3-AT, a competitive inhibitor of imidazole

glycerol phosphate dehydratase and so inhibits histidine biosynthesis and growth) and kanamycin. Figure 1.2 shows an example of how the RTHS system works.[17]

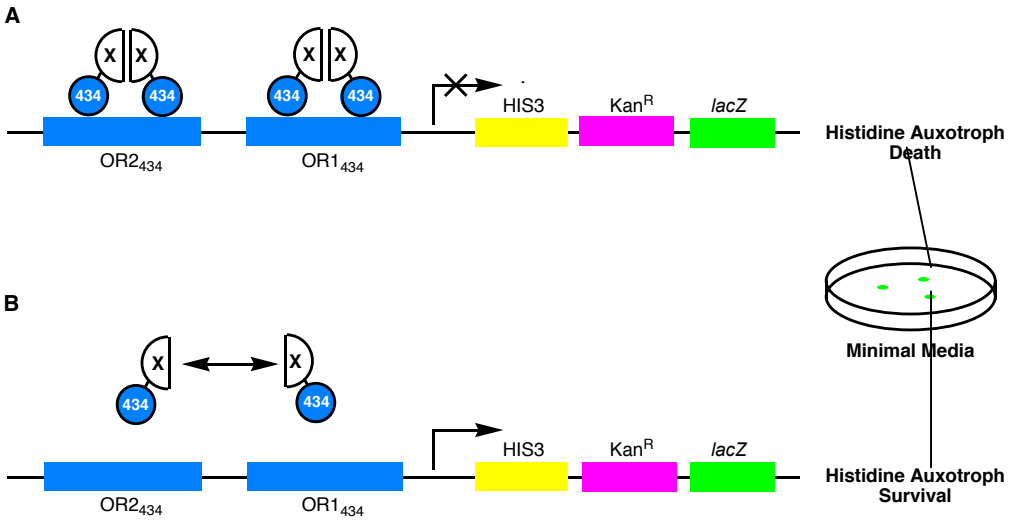

Figure 1.2 RTHS, (A), homodimerisation of two fusion proteins leads to the transcription of an active repressor protein, preventing the transcription of *HIS3* reporter gene, therefore causing non-growth of phenotypes on the plate without histidine. (B), Mutation or introducing a small molecule allows *HIS3* expression and survival of cells as the repressor is not formed.[17a]

The RTHS has been used to decipher interactions used by the influenza virus non-structural protein1 (NS1) protein to silence the host antiviral sensor protein, retinoic acid inducible gene-1 (RIG-1). NS1 is widely regarded as a factor that antagonises the host's immune responses. RIG-1 acts as a sensor for influenza and other negative strand RNA viruses. The gene encoding the Influenza A NS1 was cloned into the N-terminal fusion with 434, while RIG-I or tripartite motif protein 25 (TRIM25) was cloned as an N-terminal fusion with P22. The resulting plasmids were integrated into the chromosome of the RTHS strain (SNS126). The protein-protein interaction was quantified using *o*-nitrophenol-β-galactoside (ONPG) assays. A direct interaction between NS1: RIG-I and NS1: TRIM25 was observed.[25]

In this study we have combined the RTHS with a biosynthetic library of ~10^8 cyclic peptides, produced using split intein-mediated circular ligation of peptides and proteins (SICLOPPS). The advantage offered by this approach is the ability to link both the

cyclic peptide inhibitor and target protein to DNA encoding and compartmentalise the entire assay with cells, which allows for genetic selection to be performed instead of a screen. This has previously been used to indentify small molecule inhibitors of the homdimeric interaction of ATIC[17a] which is involved in the production of purines and the heterodimerisation of p6 and UEV involved in HIV budding[26]. This current study looks into the protein-protein interaction of C-terminal binding proteins (CtBPs) using the RTHS (Figure 1.3). This will then be combined to SICLOPPS to uncover potential cyclic peptide inhibitors.

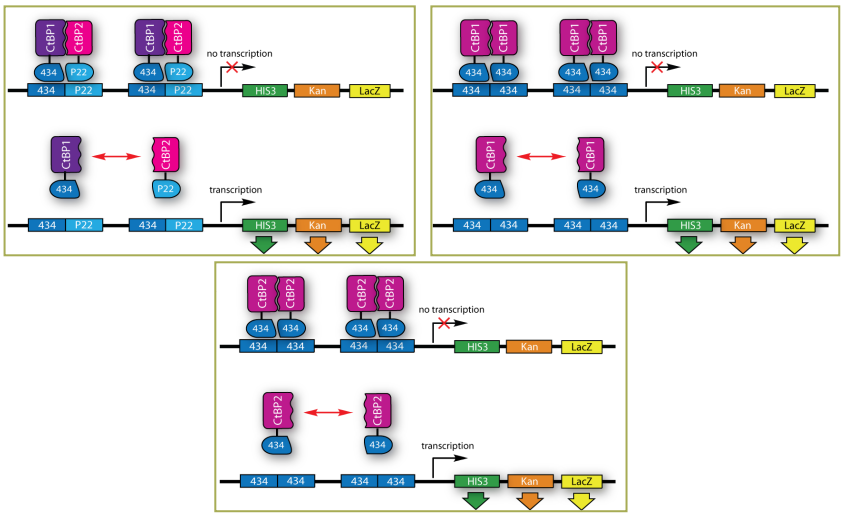

Figure 1.3 RTHS constructs for CtBP heterodimerisation, CtBP1 and CtBP2 homodimerisation.

1.3 Split intein-mediated circular ligation of peptides and proteins (SICLOPPS):

Both synthetic and genetic methods have been extensively employed to generate molecular libraries. Both methods have their advantages and disadvantages. Synthetic methods readily generate libraries of small, drug-like molecules rich in chemical diversity. Moderate library sizes of 10^3-10^5 members are attainable by these approaches. Genetic encoding enables the generation and screening of large libraries (10^6-10^{10}) *in vivo*.[27] Many genetically encoded libraries have been developed for the discovery of potential drug targets. DNA-encoded chemical libraries allow the discovery of small molecules ligands against target proteins of biological or pharmaceutical importance. This involves the covalent attachment of individual compounds to unique DNA

fragments. These libraries can then go through affinity-based selection; this involves the incubation of the library with a target protein of choice immobilised on a solid support. The non-binding molecules can be removed by washing the solid support. The DNA code of the bound molecule can be amplified via PCR. High throughput sequencing allows for the identification of the compound. Which can then be synthesised for biological or biochemical assays. A disadvantage of this process is that it is difficult to discriminate between ligands with different binding affinities, which depends on the coating densities of the target protein on the solid support.[28]

DNA-encoded chemical libraries share features with biological and biochemical display technologies such as phage display technology, which allows the isolation of billions of polypeptides. The gene encoding a specific protein is inserted into the genome of a non-lytic phage. After production of the phages in bacteria the DNA encoded polypeptide is displayed on a defined coat protein of the respective phage. This can also be applied to ribosome display and yeast display. A drawback of these methods is that they are limited to the display and selection of polypeptides and proteins. Display of small molecules showed to be more complex and led to smaller library sizes.[29, 28]

In this study we use cyclic peptide libraries encoded by split inteins (SICLOPPS). Cyclic peptides are an important class of therapeutics with pharmacological function ranging from immunosuppressants to antineoplastic, antibacterial and antiviral agents. Many natural products with a wide range of pharmacological activities are derived from cyclic polypeptides. Production of cyclic peptides is advantageous in that they are more resistant to cellular catabolism such as degradation by proteases than their linear counterparts therefore have a longer drug half-life.[23] Like peptide aptamers and disulfide-linked peptides, the constrained scaffolds of cyclic peptides enhances their binding affinity compared to the linear counter-part and that improves the binding ability for target sites. Giebel *et al* showed that cyclic peptides had 100-fold to 1000-fold higher affinity than the liner counterpart.[30] Peptides are particularly well suited to be modulators of protein-protein interface as they are themselves composed of amino acids.[23, 31]

Post-translational rearrangement was discovered in the *Saccharomyces cerevisaiae* vascular ATPase where a segment of over 400 amino acids was excised out of the VMA host protein (extein) and the two flanking halves were ligated to form the functional VMA subunit.[32] It was shown that this type of rearrangement occurred independently of

other cellular entities via a self catalysed post-translational process in which an intervening sequence (intein) excises itself out of precursor polypeptide resulting in linkage of the flanking sequence (extein) by a native bond. There is little homology in the extein sequence, therefore it can be replaced with a foreign sequence without major effect on the splicing and cleavage process.[23] However, the efficiency of the intein-mediated protein ligation is known to depend on the identity of the extein amino acid residues immediately adjacent to I_C and I_N. The extein residue immediately adjacent to the C-intein (I_C+1) serves as a nucleophile for the transesterification reaction, generating the branched and lariat intermediates in protein splicing and circular ligation, respectively. Only three residues occupy the I_C+1 position in active inteins: cysteine, serine and threonine. Cysteine serves as the transesterification nucleophile for the wild-type Ssp DnaE intein. C.P. Scott *et al*. evaluated the dependence of circular ligation on the identity of the transesterification nucleophile. The cyclic peptide production was evaluated following *in vitro* incubation and elution from the chitin affinity column. All three constructs were well expressed and showed evidence for the post-translational processing by PAGE (Polyacrylamide gel electrophoresis) analysis.[33] Inteins catalyze a highly specific N-(S/O) acyl shift at the N-terminal splice junction followed by transesterification, which joins the N-extein to the C-extein (Figure 1.4). Cyclisation of the intein C-terminal asparagine results in breakage of the C-terminal splice junction yielding free intein and (thio) ester linked extein. A spontaneous (O/S)-N acyl shift restores the natural amide bond. *Trans*-acting split intein follow the same reaction pathway after the N- and C- terminal intein fragment rapidly associate to form active intein.[32]

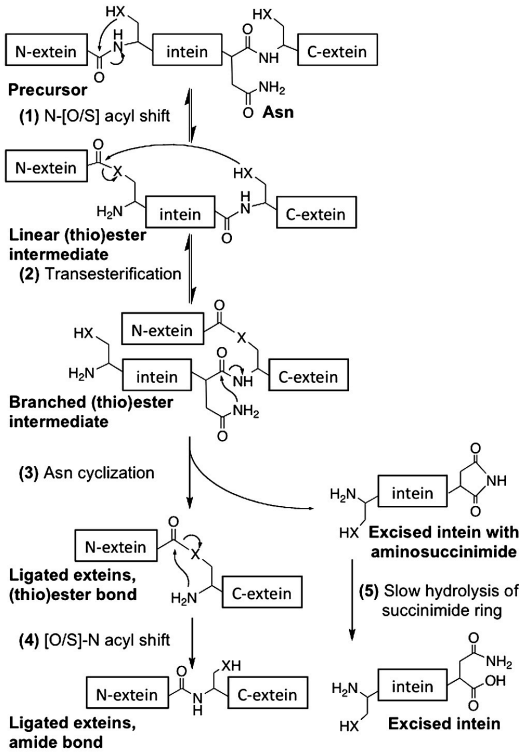

Figure 1.4 Mechanism of intein mediated protein splicing. X represents either oxygen or sulfur in the side chain of either serine, threonine or cysteine.[32]

Application of inteins for the *in vivo* production of cyclic peptides by Scott *et al*.[34] and Evans *et al*. has improved the feasibility of developing peptide-base therapeutics. Cyclic peptides are created by inverting the placement of the N- and C- domains of a naturally occurring split-intein found in the *Synechocystis* sp. PCC6803 *DnaE* gene. Similar cyclic peptides can also be obtained using the TWIN system, which employs two inteins on the N- and C- terminus of the target protein.[32] The Methodology of Split-Intein Circular Ligation of Peptides and Proteins (SICLOPPS) allows for genetic encoding of libraries by introducing random peptide sequences as the extein sequence via oligonucleotide synthesis using error prone PCR, followed by cloning into plasmids that code for the rearranged intein. After translation of intein:peptide:intein:fusion, the intein catalyses the formation of a peptide bond between the first and last amino acid thereby creating a cyclic peptide (Figure 1.5).[35] SICLOPPS libraries were designed by introducing codons for five variable amino acids between the C- and N- intein genes. The variable region was encoded by NNS where N represents any of the four DNA bases (A, C, G or T) and S represents C or G. The NNS sequence generates 32 codons

(4X4X2) and encodes all 20 amino acids while eliminating both ochre (UAA) and opal (UGA) stop codons from the library. Amber stop codons (UAG) are represented in the library at a frequency of 1/32.

SICLOPPS may be used for the cyclisation of peptides of a variety of sizes, even protein.[34] Benkovic *et al*. were able to synthesise the cyclic octapeptide pseudostellarin F in *E.coli* and demonstrated its inhibitory effect on tyrosinase *in vivo*. An advantage of SICLOPPS is that libraries of up to 10^8 members are rapidly generated and screened *in vivo* using standard molecular biology techniques and genetic selection, it has proven large flexibility towards peptide length and composition. Library sizes are several orders of magnitude larger than those possible by conventional synthetic methods.[31 17a]

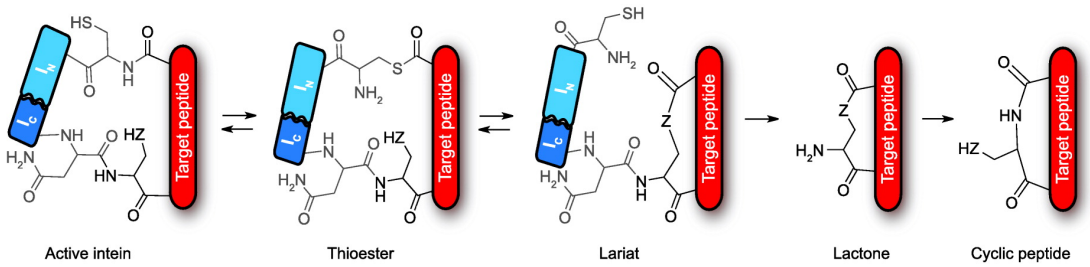

Figure 1.5 An expressed fusion protein folds to form an active intein, which undergoes a series of rearrangements to generate a cyclic peptide with randomly encoded amino acids. Z = S or O (cysteine or serine).[26]

This methodology also has some drawbacks. A particularly difficult challenge is that molecules attainable by SICLOPPS are limited both by the specificity of the intein and the ability of the peptide to form a tight loop structure. Although the Ssp DnaE intein shows a usefully broad specificity, it is far from random in the sequence it will cyclise. Since less than 70% of randomly selected clones generally showed detectable levels of *in vivo* cyclisaton, it is impossible to correlate library size with the cyclic peptide sequence space actually tested. Growth phenotypes may reflect active component expression levels and not necessarily the inhibitor with the best binding affinity or efficacy because *in vivo* requirements for growth are often threshold based. Additionally, genetic selection and screens often produce false positives, so target molecules require further validation to confirm the mode of activity. Similar results are found in all types of genetic selections and aptamer-based small molecule screens. This highlights the importance of secondary

selections and screens to eliminate false positives. Solid phase synthesis of peptides is straightforward and cyclisation of small peptides is facile. The ability to synthesise large quantities of the selected peptides assures the availability of sufficient quantities for *in vitro* and *in vivo* testing.

Despite the above drawbacks, SICLOPPS has successfully identified inhibitors of E. coli Dam methyltransferase,[36] C1pXP[37] as well as inhibitors of HIV Gag protein recognition of the human endocytotic protein TSG101.[26] This technology has also proven useful for the discovery of cyclic peptides that disrupt the dimerisation domains of ribonucleotide reductase and 5-aminoimidazole-4-carboxyamide-ribotide transformylase. SICLOPPS coupled with genetic selection has facilitated the rapid identification of numerous cyclic peptides with micromolar IC_{50} values that serve as valuable leads for further drug development.

SICLOPPS has also been used for the production of libraries of random cyclic peptides in mammalian cells using retroviral technology to enable the intracellular delivery. This led to the identification of cyclic peptide inhibitors that block interleukin-4 mediated IgE class switching in B cells.[38] Deschuyteneer *et al*[35] have also evaluated the possibility to perform split intein-mediated polypeptide cyclisation in the periplasm of *E.coli* and further secrete the peptides in the extracellular medium. They created various libraries of randomised precursors, and a large proportion of the clones were shown to efficiently produce backbone cyclic peptides in periplasm. They also postulated that using an SXXXXXG library, with a G at the splice junction would greatly improve the efficiency of the random libraries. By expressing a phage pore protein in the outer membrane of *E.coli*, they showed that cyclic peptides could diffuse in the extracellular medium. These new possibilities of producing libraries of cyclic peptides either in the periplasm or outside the bacteria opens a wide potential of development of selection-based strategies for identifying compounds that would act on exported or membrane proteins or that would interfere with competing organisms. The target sequence for cyclisation is cloned in frame between genes encoding the two fragments of the Ssp and DnaB split intein ($DnaBI_C$ and $DnaBI_N$) in a permuted order and behind the arabinose controlled pBAD promoter. The pPBla construct in Figure 1.6 illustrates the intein-TEM-1 β-lactamase precursor. Splicing will occur in the linker region containing the N- and C-termini of the enzyme and that's made possible by imposing a serine (+1) and a glycine (-1) at the splicing junction. The pPL6-8 constructs for cyclisation of hexa-, and

octa-peptides libraries in the periplasm of *E.coli*. The randomised codons encoding four, five, or six amino acids are cloned between the fixed codons of the serine and glycine residues. The degeneracy of the codons is NNB (B encodes C, T, or G).[35]

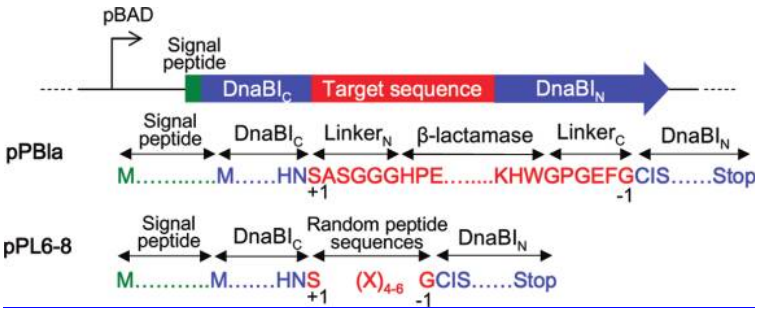

Figure 1.6 Construct for protein and peptide cyclisation in the periplasm of *E.coli*.[35]

This project was conducted jointly with the Faculty of Medicine to uncover cyclic peptide inhibitors of the C-terminal binding proteins homodimerisation.

1.4 C-terminal Binding Proteins:

The adenovirus E1A proteins are expressed during the early phase of the viral life cycle and they induce cell proliferation. The N-terminal region of E1A along with the conserved region 1 (CR1) interacts with histone acetyl transferases (HATS) to modulate chromatin modification and transcription, whereas CR2 interacts with the tumour suppressor protein pRb and related proteins, p130 and p107. Through these interactions, E1A exon 1 drives cell cycle into the S-phase and cooperates with other oncogenes to transform primary cells. C-terminal Binding Proteins (CtBPs) were first identified in 1993 as a 48 kDa protein that bound the C-terminal CR4 domain of the adenovirus E1A oncoprotein containing the conserved PLDLS motif.[39] Interaction of CtBP with E1A C-terminal region was found to negatively modulate oncogenic transformation by E1A.

CtBP family proteins are highly conserved among invertebrates and vertebrates. Invertebrates contain a single CtBP whereas vertebrates contain two highly homologous CtBP proteins (CtBP1 and CtBP2). CtBPs show distinct functions according to their cellular localization. In the nucleus, CtBPs act as transcriptional co-repressors modulating the activity of a large number of transcriptional repressors. They form

functional interactions with multiple cellular proteins, allowing them to act as transcriptional co-repressors that can regulate many cellular processes including development, proliferation, differentiation, transformation and apoptosis. The transcriptional activity of CtBPs is regulated by NAD(H)-binding and metabolic status of the cell. In the cytoplasm they are involved in maintenance of the Golgi playing a key component of the machinery controlling Golgi tubule fission and endocytic membranes. CtBP fission inducing activity was shown to participate in the fragmentation of the Golgi complex during mitosis and in intracellular membrane traffic. They also perform diverse function associated with central nervous system synapses and in regulation of the microtubule cytoskeleton. The control of CtBP nuclear vs. cytosolic localisation involves posttranslational modifications such as phosphorylation and sumoylation.

There are four CtBP isoforms that are generated from the two distinct mammalian genes, CtBP1 and CtBP2. The *CtBP1* gene is located on chromosome 4 of humans and on chromosome 5 of mice. The CtBP1 locus codes for two protein isoforms: CtBP1-L and CtBP1-S (CtBP3/brefeldin A-dependent ADP ribosylation substrate (BARS) protein). Both are identical except for a thirteen amino acid region at the N-terminus. The *CtBP2* gene maps to chromosome 10 of humans and in chromosome 7 of mice. The *CtBP2* gene codes two protein isoforms, CtBP2 and the second isoform, designated as RIBEYE is a 120 kD protein that is predominantly expressed in sensory neurons. CtBP1 and CtBP2 are very similar in sequence; they share 78% in amino acid identity and 83% in similarity.

CtBPs exhibit homology to NAD-dependent 2-hydroxy acid dehydrogenase. This homology includes the conserved NAD binding motif (GXGXXG) and a catalytic His residue at the active site.[40] The CtBP central domain (~ 195 residues) plays an important role as the dimerisation site (Figure 1.7), allowing the formation of homo- and hetrodimerisation between CtBP1 and CtBP2 that would act as an aggregation scaffold for multimeric nuclear protein complexes.[41] Each monomer in the CtBPs dimer is divided into large and small domains. The dimerisation interface is extensive, burying ~3368 $Å^2$ of solvent accessible surface area per monomer.[42] Dimerisation is stimulated by occupation of the dinucleotide-binding site within the central domain. The preferred ligand is NADH, which binds to the site with greater than 100-fold higher affinities than NAD^+. CtBP has been postulated to be a redox sensor that links the cellular metabolic status to transcription regulation. The unique NADH-dependence of CtBP1's action not

only highlights the importance of hypoxia and an aerobic glycolysis in promoting tumour formation through the activation of CtBP1, but also reveals a potential therapeutic approach.

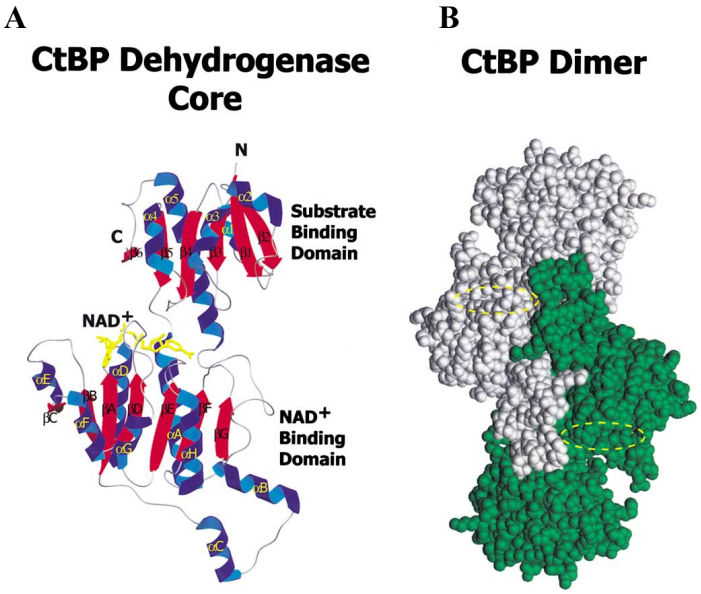

Figure 1.7 CtBP structure: (A) the dehydrogenase domain contains a substrate-binding domain linked via flexible hinge to NAD^+ binding domain. NAD^+ (yellow) binds in the active site cleft. (B) The van der Waals surface of CtBP dimer, one monomer in green the other in grey.[42]

Binding NAD(H) promotes the stabilization of a compact dimeric form of the protein, with the substrate- and nucleotide-binding domains tightly wrapped around the bound NAD(H), which is required for providing a stable core for the formation of multimeric repression complexes (Figure 1.8).[43] Loss of NAD/NADH binding induced a dramatic decrease in the homodimerisation efficiency and transcriptional repression activity in both CtBP1 and CtBP2. Studies by Nardini *et al* showed a mutation of the Gly172 to Glu which resulted in complete disruption of the dimer.[44] Mutation of the NAD(H)-binding motif (G183A/G186A) in CtBP1 leads to a protein that is deficient in dimerisation compared to the wild type.[45] Also, the amino acid substitution at G189, in the conserved NAD(H) binding motif, abrogates the ability of CtBP2 to homodimerise and leads to a dramatic decrease in corepressor activity. The ability of NADH to stimulate CtBP dimerisation contributes indirectly to the enhanced binding of PXDLS

motif containing transcription factors. A double mutant G189R/R272L which also introduces an amino acid substitution at a highly evolutionarily conserved arginine residue implicated in substrate binding for bacterial 2HAD family members, completely inhibited mCtBP transcriptional repression activity.[46]

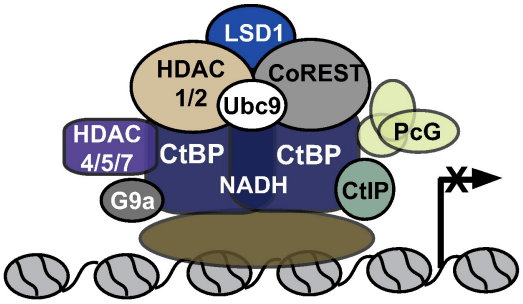

Figure 1.8 CtBP mediated transcriptional repression. CtBP is recruited to the chromatin by its interaction with negative regulators of transcription. NADH is involved in dimerisation and repressor activity of CtBP. Transcription repression is brought about by its interaction with CtIP, polycomb complex and involves HDACs and HMTases (G9a). CtBP and its interaction with HDAC1/2, CoREST/LSD1 and Ubc9 also form a multiprotein complex involved in SUMOylation of transcriptional regulators.[43]

Both CtBP1 and CtBP2 contain a conserved substrate binding domain (consisting of ~155 residues that are mainly N-terminal) involved in the binding of transcription factors possessing consensus Pro-X-Asp-Leu-Ser (PXDLS) peptide motif (where X is any amino acid).[41] This motif was identified within the C-termini of E1A and EBNA3C. Deletion of these regions from either of these two proteins markedly alters their ability to transform cells into cooperation with mutant RAS, providing evidence for the key role of CtBP in cellular transformation. Subsequent work has confirmed that the vast majority of DNA-binding factors that recruit CtBP family proteins that contain related motifs (Figure 1.9). Peptides as small as 15 residues encompassing this motif can bind CtBP *in vitro*. Quantitative binding assays have confirmed the importance of the Pro, Asp/Asn, Leu and Ser/Thr residues, through the mutations in any one of these residues does not usually eliminate binding. There is evidence that the binding of CtBP proteins to NADH significantly increases their affinity for PXDLS motif containing nuclear transcription factors, and so it is possible that this serves to drive CtBPs to the nucleus.

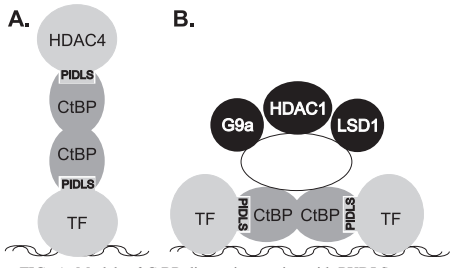

Figure 1.9 Models of CtBP dimers with PXDLS partners. (A) Model of CtBP as a bridging molecule linking a transcription factor (TF) and an effector. An elongated dimer of CtBP as a link between a promoter-bound transcription factor containing a PIDLS and the effector molecule HDAC4, which also contains a PIDLS motif. (B) Model where a CtBP dimer is localised to a promoter by binding two PIDLS motif-containing transcription factor and then recruits effectors through a different surface.[47]

The C-terminus of CtBP1 contains a PDZ-binding motif, which is implicated in nuclear export of CtBP1 in association with PDZ domain containing partners. CtBP is thought to act as a molecular bridge between DNA binding proteins and enzymes associated with transcriptional repression such as histone deactylases. Various DNA-binding repressors recruit CtBP through this region. A second protein interaction groove has been identified which interacts with a RRT motif. Even though the RRT binding site has no direct contact with the nucleotide-binding site, the close proximity of the two sites in the same domain may influence interaction of RRT-containing proteins with CtBP in the presence of NAD(H). While DNA-binding proteins such as ZEB1/2 interact with CtBP primarily through PLDLS-like motifs, factors such as ZnF217 interact through both PLDLS-like and RRT motifs.[48]

Attempts to crystallise full length CtBP have been unsuccessful. A possible explanation for this could be the high mobility, or disorder, of the C-terminal region in the full-length protein that, contrary to the substrate- and nucleotide-binding domains, may maintain an unstructured conformation, which prevents the formation of productive crystal contacts. Analysis of CtBP C-terminal sequence illustrates the presence of bulky hydrophobic residues, and a high proportion of 'disorder promoting' residues, in particular Gly and Pro. The lack of order-promoting residues and of aromatic amino

acids undermines one of the basic contributions to the thermodynamic stabilisation of the protein hydrophobic core. ^{1}H-NMR analysis carried out by Nardini *et al* [41] indicates that large portions of the C-terminal protein backbone experiences dynamic fluctuation, lacking a well-defined 3D structure.

There is strong evidence that CtBP1 and CtBP2 are found in transcriptional complexes in the nucleus, indicating that CtBP proteins must be imported into the nucleus from the cytoplasm. Control of subcellular localisation is emerging as an important mechanism whereby CtBP1 functions are regulated. It is possible that this translocation of the vertebrate CtBP may be a regulatory event by which the transcriptional regulatory activity of CtBP in the nucleus may be disrupted. Alternatively, it may also play a role in providing CtBP for the cytoplasmic functions such as those observed in Golgi.[49] Phosphorylation of CtBP1 at Ser158 by p21-activated kinase 1 (PAK1) results in cytoplasmic localisation and inhibition of its corepressor activity under certain growth conditions. Pak1 regulation of CtBP represents a new transcriptional regulatory pathway whereby a signalling kinase can inactivate a corepressor and stimulate dissociation of a corepressor regulatory complex from an endogenous gene promoter. In the presence of NADH, Pak1 super-phosphorylated CtBP and inhibited CtBP dehydrogenase activity, suggesting that preferential phosphorylation of active CtBP may alter secondary structures and influence protein-protein interaction, enzymatic and corepressor function.[50]

Certain PxDLS-containing transcriptional repressors are able to recruit CtBP1 to the nucleus, for example Ets family member NET, tumour suppressor protein HIC1 and transcription factor BKLF (basic Krüppel-like factor). CtBP is also modified by covalent addition of the small ubiquitin-like modifier (Sumo). HPC2 has been shown to enhance SUMOylation of CtBP at a single K428 of CtBP1 by functioning as SUMO E3 ligase activity of the polycomb protein PC2. This in conjunction with protein-protein interactions involving C-terminal PDZ-binding domain, regulates the nuclear localisation and is critical for the repression activity of CtBP1.[41, 51] It has been reported that neuronal nitric oxide synthase binds and causes translocation of CtBP1 from the nucleus into the cytoplasm.[49] CtBP2 lacks both this sumoylation site and the PDZ binding domain. However, CtBP2 contains a unique nuclear localisation signal (NLS, amino acids 8-13) located in the N-terminus that plays a key role in controlling the nuclear-cytoplasmic distribution of the protein.[52] When expression constructs encoding

amino acids 1-119 of CtBP2 fused to EGFP are transfected into MCF-7 cells, the fusion protein localises primarily to the nucleus. This localisation is dependent upon the NLS, as a protein lacking amino acids 4-14 is localised primarily in the cytoplasm.[52] Zhao *et al* demonstrated that this region does not, in fact, function as classical NLS, but rather that it is necessary for the lysine 10 within it, to be acetylated for it to direct localisation into the nucleus. They specifically showed that the lysine in this sequence is acetylated *in vivo* and this is likely to be through the action of the p300 acetyltransferase, a known CtBP binding protein. CtBP1 lacks the NLS region but CtBP2 can heterodimerise with CtBP1and direct both proteins into the nucleus. Transcriptional reporter assays have shown that CtBP2 repressed E1A transcriptional activity whereas CtBP1 did not. CtBP2 mediated repression not only requires PLDLS-dependent interaction with E1A C-terminal domain and also the NLS of CtBP2.

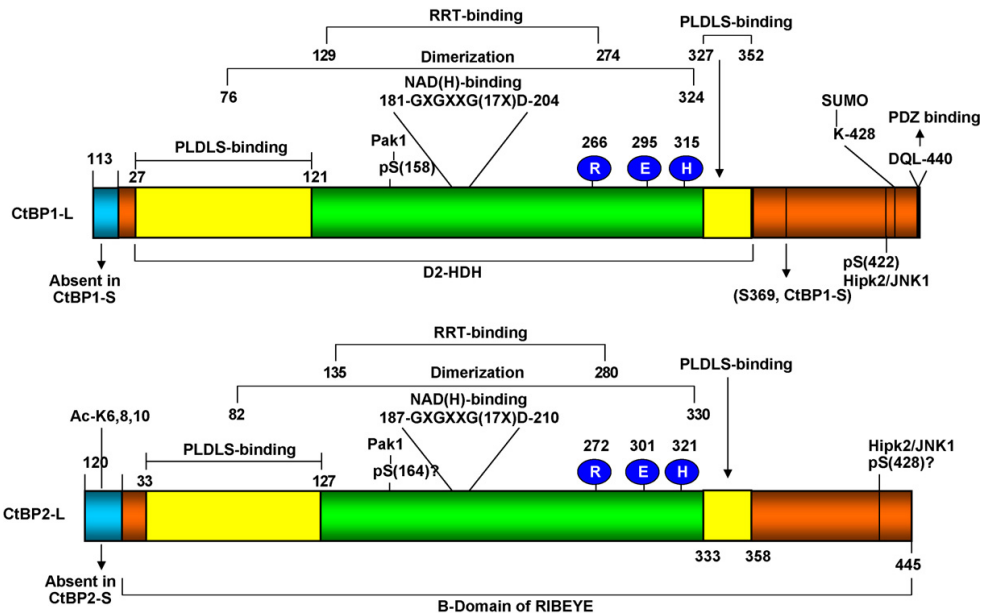

Figure 1.10 Domain structure of mammalian CtBP family protein. Shows the two proteins CtBP1 (top) and CtBP2 (bottom).[53]

1.5 Nuclear Function

1.5.1 Transcriptional Repression

The vertebrate CtBPs, and the Drosophila homolog, dCtBP function as a transcriptional corepressor in the nucleus. A large number of DNA-binding transcription repressors

mediate their activity by recruiting CtBP through the PLDLS motif (0). The Mouse basic Krüppel-like factor (BKLF) interacts with mCtBP through the PXDLS motif. When mCtBP2 was targeted to the promoter through the BKLF Zn-finger domain, the chimeric protein repressed transcription efficiency, demonstrating that CtBP has direct transcriptional repressor activity.[49] As a corepressor, CtBPs primarily function as a scaffold to recruit chromatin modifying enzymes including histone deacetylases, histone methyltransferases, and polycomb-group proteins to DNA-binding transcription factors. The precise mechanism by which CtBP mediates transcriptional repression remains to be elucidated. Repression of transcription plays a critical role in the regulation of cellular processes, with various repressor proteins exerting their effect through protein-protein interactions with corepressor that in turn bind chromatin-modifying enzymes.

Transcription Factor	Family	Adapter	CtBP
mBKLF, hKLF8	Krüppel-type Zn finger	Direct	mCtBP2
mIkaros,	Krüppel-type Zn finger	Direct	hCtBP1
hZEB, mδEF1	Homeodomain Zn finger	Direct	hCtBP1, mCtBP1, 2
hTGIF	TALE family homeodomain	Direct	hCtBP1
mFOG1, mFOG2, hFOG2	Zn finger	Direct	mCtBP2
xFOG	Zn finger	Direct?	Not none
hEvi-1, mEvi-1	Zn finger	Direct	hCtBP1, mCtBP2
mNet	Ets	Direct	mCtBP1
xTcf-3	HMG-box	Direct	xCtBP
hPc2, xPc	Polycomb	Direct	hCtBP1, 2, xCtBP
mSOX6	HMG-box	Direct	mCtBP2
hHuntingtin	Polyglutamine	Direct	hCtBP1
hBRCA-1	Ring finger	hCtIP	hCtBP1
hE2F4, 5	E2F/DP	pRb/p130-hCtIP	hCtIP
mMEF2	MADS family	mMIRT, hHDAC4, 5, mHDAC7	mCtBP1, 2
NHR	Nuclear receptor	mRIP140	hCtBP1

Table 1.1. Vertebrate CtBP-Interacting Transcriptional Factors.[49]

One of the best-characterised mechanisms of gene repression is the recruitment of histone deacetylase enzymes (HDACs). These are thought to remove acetyl groups from the N-terminal tail of histones, thereby increasing their positive charge and affinity for

DNA, and facilitating the compaction of chromatin, thus preventing gene expression in the targeted region. CtBPs link DNA-binding repressors and histone-modifying enzymes to mediate transcriptional repression. HDAC contains a PXDLS motif that allows them to bind CTBP (Figure 1.11). This observation suggests a simple model by which the dimerisation of CtBP enables it to serve as a link between DNA-binding protein, containing a PXDLS motif, and a histone deacetylase protein with a similar motif. It has been documented that CtBP can interact with multiple HDACs both *in vivo* and *in vitro*. The addition of trichostatin A, a specific inhibitor of HDACs blocked CtBP-dependent repression. It has also been shown that CtBP-dependent repression can still occur in the presence of trichostatin A and there is no detectable HDAC activity associated with CtBP. This suggests that CtBP may utilize multiple mechanisms to regulate transcription.[54]

Other proteins shown to interact with CtBP include co-REST, histone methyltransferase (G9a and HMTase), and a polyamine oxidase. The association of CtBP with polycomb protein PC2 led to its sumoylation. Polycomb (Pc) is part of a Pc group (PcG) protein that are involved in the stable and heritable repression of gene activity during *Drosophila* and vertebrate development. PcG proteins do not typically bind DNA directly but are components of chromatin and are thought to repress gene expression by co-ordinating the formation of densely packed heterochromatin.[55] PcG protein HPC2 recruits CtBP1 and Ubc9 to the PcG bodies resulting in sumoylation of CtBP1 at a single Lys (K428) residue. Ubc9 recruited by CtBP1 and HPC2 may also target other transcription factors and histone H4.

Repression by CtBP1 has been suggested to play a key role in cell survival. Decreased CtBP1 expression allows cancer cells to become hypersensitive to apoptosis. A decrease in the level of CtBP1 proteins is sufficient to trigger apoptosis in p53-null cells. Upon apoptotic stimuli, CtBP1 undergoes proteasome-dependent degradation, which results in derepression of pro-apoptotic genes and allows apoptosis to proceed. The p160/steroid receptor coactivator (SRC) family is a well-studied family of transcriptional coregulatory proteins that function through histone tail modification, altering chromatin structure, and facilitating transcription initiation. SCR1 and SCR3 have been shown to have histone acetyltransferase (HAT) activity, which is necessary for the formation of an open chromatin structure. SCR coactivators also interact with general coactivators such as the CREB binding protein (CBP) and p300 and thus may help nuclear receptors

to recruit more HAT enzymes to the vicinity of target sites upon ligand binding.[50] Additionally, the CtBP complex contains the corepressor CoREST. The CoREST protein complex also contains HDAC1/2 and LSD1 (lysine specific demethylase-1).

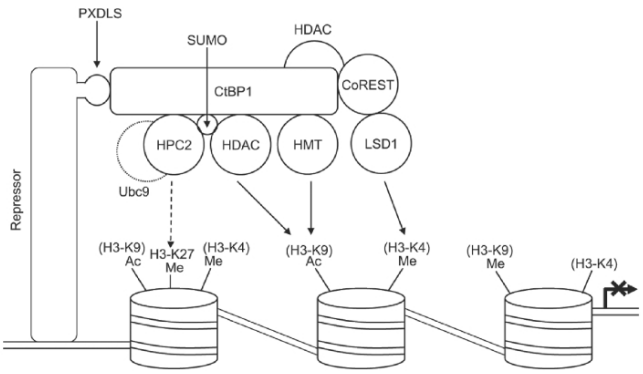

Figure 1.11 Transcriptional repression by CtBP1.

1.5.2 Transcriptional Activation

Although CtBPs function predominantly as transcriptional corepressors linking various chromatin-modifying components to DNA-binding repressor, under certain conditions they may function as transcriptional activators. CtBP-null mouse embryos which exhibit axial truncation phenotypes have revealed that expression of one of the target genes of Wnt3A, Brachyury (T), is lower in E10.5 embryos[54] compared to normal looking E9.5 embryos. That suggests that CtBP2 may function as a transcriptional activator of Brachyury. The Brachyury promoter contains a consensus-binding site for the Wnt transcription TCF as well as for the E box transcription regulator. The potential effect of CtBP2 on Brachyury expression is due to *trans*-activation function encoded by CtBP2 or due to interaction between CtBP2 and factors simultaneously recruited by both TCF and E-box transcription factor. CtBP2 undergoes post-translation modification such as acetylation by p300 and a lower level of SUMO modification, which contribute to the context-dependent transcriptional activation function.[48]

Studies by Fang *et al* have demonstrated that dCtBP can directly activate transcription of certain Wnt target genes after stimulation with Wnt, while repressing others in the absence of Wnt. Upon Wnt stimulation, stabilised β-catenin binds to TCFs, converting them into transcriptional activators. The Wnt/β-catenin pathway is used throughout

animal development to control a variety of cell fate decisions and promotes oncogenesis by maintaining a proliferative, stem cell fate.[48, 56]

1.6 Role in Oncogenesis and Apoptosis

The mammalian CtBPs modulate oncogenesis by regulating the activities of tumor suppressor genes and cellular and viral oncogenes, consistent with a role in tumor suppression as well as tumor promotion. CtBPs promote tumorigenesis by inhibiting genes involved in the epithelial to mesenchymal transition. CtBP transcriptional repressors are attractive cancer targets since they encode a potentially "druggable" dehydrogenase domain and their silencing by RNAi results in anti-cancer effects, including apoptosis and abrogation of cancer cell migration or invasion.[57] CtBP dimers and CtBP repression complexes are also detectable in cancer cells in the absence of hypoxic or nutrients, and siRNA-mediated knockdown of CtBPs in cancer cell lines leaves them hypersentive to p53-independent apoptosis.[58,59,60] The multiple pro-oncogenic activities of CtBPs are well established, with CtBP being the target of multiple tumour suppressors. CtBP-dependent transcriptional regulation also plays an important role in the control of tumor cell migration. The pro-survival role of CtBPs has recently been shown to arise from their role in maintaining mitotic fidelity. CtBP siRNA results in reduced association of aurora B with mitotic chromatin and an increase in the frequency of aberrant mitosis.[58] This results in cell death, particularly in cells containing mutant p53, which fails to undergo a protective post-mitotic cell cycle arrest.

1.6.1 E1A Model

A biological role for CtBP was first demonstrated by genetic dissection of the oncogenic activity of E1A. Mutation in the conserved PLDLS motif causes enhanced transformation phenotype in ras cooperation assays. Tumors expressing the E1A mutants are also highly metastatic, while tumors expressing wt E1A are not. These results are consistent with the concept that the interaction of CtBP with E1A negatively regulates oncogenesis. [49, 61] It has been postulated that the interaction of CtBP with E1A would restrain the cell proliferation activity of the N-terminal region of E1A. E1A disrupts the interaction of CtBP with repressors. One possible way of E1A doing that is

for E1A to up-regulate cellular genes. Cells from CtBP knockout mice were hypersensitive to a wide variety of apoptotic stimuli, mimicking the effect of E1A.[62]

1.6.2 CtBP1/Bcl-3

Bcl-3 is a proto-oncogene that belongs to the IκB family. Elevated levels of Bcl-3 have been detected in a number of cancers, including breast cancer and anti-apoptotic effects of Bcl-3 in cancer have been reported. Bcl-3 is also responsible for the down regulation of p53 activity by enhancing the transcription of Hdm2 in normal and cancer cells, leading to inhibition of DNA damage induced apoptosis. Bcl-3 can also negatively regulate lipopolysaccaride (LPS)-induced tumour necrosis factor alpha (TNF-α) synthesis in macrophages when bound to histone deacetylase 1 (HDAC1) and HDAC3. Bcl-3 prevents the degradative polyubiquitination of p50 inhibitory homodimers.

CtBP was identified as a binding partner of Bcl-3 via nano-flow liquid chromatography/tandem mass spectrometry (LC-MS/MS) analysis; direct binding was confirmed via GST pull-down assay. A PXDLS/R sequence located in the N-terminal region of Bcl-3 was recognised. This motif found within CtBP1-binding proteins allows them to associate with CtBP1. CtBP is crucial in the biology of Bcl-3: this corepressor is required for the stabilisation of Bcl-3 and for Bcl-3 to repress gene transcription. Both Bcl-3 and CtBP1 are known to exert anti-apoptotic effects. Binding of Bcl-3 to CtBP1 blocked ubiquitination of CtBP1 leading to its stabilisation. Therefore, over expression of Bcl-3 made cells resistant to apoptotic stimuli due to sustained maintenance of CtBP1-mediated repression of pro-apoptotic genes. This role of Bcl-3 is independent of p53 since the repression was maintained in H1299 cell, where functional p53 is absent.

1.6.3 CtBP/BRAC1

Breast cancer is one of the leading causes of death in women worldwide. BRAC1 (breast cancer 1) is a human tumour suppressor gene, which produces a protein called breast cancer type 1 susceptibility protein, responsible for DNA repair, cell regulation and transcriptional regulation. Deficiency in BRAC1 leads to accelerated proliferation, aberrant mitosis, tumorigenesis and reduced genome stability. It also leads to impaired cell cycle checkpoints, reduced efficiency in homologous recombination and defective

DNA repair following genotoxic insults. Individual harbouring germline mutations in the BRAC1 carry an 80% lifetime risk of developing breast cancer. Li-Jun Di *et al* have demonstrated that CTBP assembles at BRAC1 promoter as part of a dynamic, multicomponent co-repressor complex containing p130, BRAC1 and HDAC1 that represses local histone acetylation at the BRAC1 promoter and BRAC1 transcription. Disruption of this complex by estrogen stimulation and/or changes in NAD+/NADH ratio leads to CtBP dismissal, HDAC1 eviction, increased histone acetylase and subsequently increased BRAC1 transcription from the BRAC1 promoter.[63]

Patients with germline mutations in Fanc/Brca genes have high incident of head and neck squamous cell carcinomas (HNSCCs) at a young age. The BRAC1 promoter is controlled by a complex and dynamic array of DNA binding proteins, transcriptional co-activators and co-repressors. Knocking down CtBP1 expression via siRNA led to a three-fold increase in BRAC1 mRNA, suggesting that CtBP1 on its own regulates BRAC1 expression in HNSCC cells. Y Deng *et al* investigated whether CtBP1-mediated repression of BRAC1 gene is sensitive to NADH levels. They showed that hypoxia increases free cellular NADH levels, which affects CtBP1 activity without affecting its levels. Cells exposed to hypoxia showed a 2.5-fold increase in CtBP1 recruitment to the proximal region of BRAC1 promoter resulting in a decrease in BRAC1 mRNA levels.[64]

1.6.4 CtBP in Epithelial-Mesenchymal Transition (EMT)

Carcinomas, representing the majority of human cancers, develop from epithelial cells. Epithelial cells possess prominent cell-cell and cell-matrix adhesion that partly regulate critical functions such as selective permeable barrier assembly, cell polarity, developmental pattern formation, and epithelial gene expression. High turnover cells are programmed to undergo apoptosis on their release from the extracellular matrix, preventing the colonization of mislocalised cells. As carcinoma cells progress to malignancy, the cells lose expression and self-differentiation of certain epithelial-specific genes in a process known as epithelial-mesenchymal transition (EMT).[65] A hallmark event in the EMT is the downregulation or loss of the E-cadherin, a homotypic cell-to-cell interaction molecule ubiquitously expressed on epithelial cells.[66]

E-cadherin-mediated cell-cell adhesion is essential for maintaining the homeostasis and structure of epithelial tissues; its function is lost in a majority of epithelial cancers. E-Cadherin (encoded by *CDHI* gene), serves as a widely acting suppressor of invasion and metastasis by epithelial cancers.[67] The E-cadherin promoter contains two E-box elements, which are thought to be involved in silencing it in E-cadherin non-expressing cells. The rapid growth and poor vascularisation of solid tumours exposes cancer cells to hypoxia leading to increased levels of NADH in the cells enhancing CtBP-mediated repression of the E-cadherin promoter as a result of increased interaction with cellular repressors such as ZEB. Consistent with the results on E-cadherin repression, hypoxia was reported to increase tumor cell migration (Figure 1.12).[68] CtBP dependent recruitment of E-box repressors such as ZEB1/2 and methylation (HMTases, G9a-GLP) has been linked to repression of E-Cadherin promoter, suggesting that CtBP is important in promoting epithelial-to-mesenchymal transition (EMT). This is a step that contributes to the malignant property of tumour cells due to loss of intracellular adhesion in tumours, acquisition of motile and invasive phenotypes and increased resistance to apoptosis.[69] Cell mobility was reduced by siRNA-mediated depletion of CtBP, suggesting that the effect was independent of HIF-1α or other E-cadherin repressors. CtBP1 and hypoxia-inducible factor transcription factor are thought to be involved in the activation of cell migration. Like hypoxia-inducible factor CtBP corepressors directly sense and respond to the intracellular metabolic changes that accompany hypoxia. CtBP-mediated stimulation of hypoxia-induced cancer cell migration may be due, in part, to repression of epithelial adhesion genes such as *E-cadherin*.

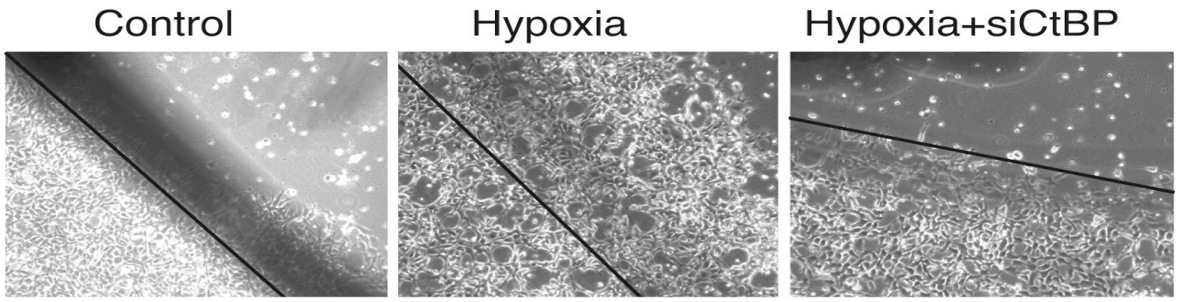

Figure 1.12 CtBP mediates the hypoxia-induced migration of H1299 lung cancer cells. H1299 cells grown for 20 h in 20% O_2 (Control) or 1% O_2 (hypoxia) were assayed for their migration onto the matrix deposited by cells scraped away at the beginning of the assay.[68]

ZEB1 and ZEB2 are transcriptional repressors that contain zinc-finger motifs in their DNA binding domains, and both recognise the same E-boxes in their target genes. ZEB1 and ZEB2 are transcription factors that control key regulatory genes during embryonic development and cell differentiation. ZEB1 is expressed in many tissues including immune system and plays an important role in regulating both muscle and lymphoid differentiation. ZEB1 has also been shown to block the function of a range of transcription factors involved in the regulation of immune genes and has been shown to have two means of repression: direct competition for binding of activators to certain E-box sites and trans-repression involving both an N-terminal region and the (PXDLS) motif region of the protein.[70] ZEB1 represses E-cadherin transcription by binding to two E box sequences in its promoter region. Expression of ZEB1 in epithelial cells induces an EMT and promotes tumour invasiveness *in vitro* and *in vivo* models.[71]

ZEB1 contains an N-terminal region that binds the coactivator p300 and P/CAF, acteyltransferases that loosen chromatin structure. Moreover binding of P/CAF to ZEB1 acetylates several lysine residues close to the CtBP interaction domain of ZEB1, displacing CtBP and switching ZEB1 from a repressor to an activator. ZEB2 does not interact with p300 or P/CAF and thus only serves as a transcriptional repressor. Experimental results obtained by Pena et al illustrated that *CtBP* and *p300* levels are important factors in the control of the expression of genes crucial for EMT, and therefore, for tumor progression, at least in human colon cancer.[72] Wang *et al* demonstrated that ZEB1 could function with CtBP2 and HDAC1 to repress IL-2

promoter activity. IL-2 is a key cytokine for T cell proliferation and homeostasis. The cooperation of ZEB1 with HDAC1 requires the co-expression of CtBP2 leading to the speculation that CtBP2 may behave as a scaffold protein in repressor complexes.[70]

Other E-cadherin repressors include δEF1; knockout of δEF1 in mice causes severe skeletal defects. Another human member of this family, slug causes epithelial to mesenchymal transition when overexpressed.[73] Expression of *Drosophila* ZEB homologue zfh-1 is controlled by members of the SNAIL family of transcription factors. SNAIL has been proposed as an alternative E-cadherin repressor. Vitamin D induces the expression of *CDHI* in cells expressing vitamin D receptor (VDRs). SNAIL also represses VDR expression in tumor cell lines and its induction in human colorectal carcinomas is associated with *CDHI* and VDR down regulation.[72]

Epithelial cells are sensitive to 'anoikis' (a form of apoptosis mediated by the loss of contact from the extracellular matrix), wherein apoptosis is triggered by the loss of appropriate integrin-mediated cell-matrix contacts, causing cell survival to be anchorage-dependent. E1a-CtBP interaction was required for the induction of epithelial gene expression. In the case of E-cadherin promoter, this resulted from E1a' disruption of a complex involving CtBP and δEF1/ZEB, a zinc finger-homodomain repressor protein that controls muscle and lymphoid differentiation. Anoikis-sensitivity resulted from the interaction of E1a-CtBP.[73]

1.6.5 CtBP as an Apoptosis Antagonist

It is thought that apoptosis might be regulated through changes in cellular CtBP. Work on E1A has also revealed a potential apoptosis antagonist activity of CtBP. Tumor cell lines expressing E1A mutants defective in interaction with CtBP were less sensitive to anoikis. Genetic knockdown of the transcriptional co-repressor CtBP in mouse embryonic fibroblast results in up regulation of several genes involved in apoptosis such as *PERP* (p53-effector related to pmp-22), *P21*, Bax and *NOXA*.[69, 74]

Additionally, HIPK2 mediates the phosphorylation of p53 in the response to UV irradiation, thereby activating p53 function and promoting apoptosis. Studies by Wang *et al* showed that HIPK2 also promotes apoptosis through its effect on CtBP. UV irradiation also appears to activate the CtBP degradation pathway and similarly

promotes apoptosis in cells. The mitogen-activated protein kinase (MAPK) family member-Jun NH2 terminal kinase 1 (JNK1) plays an important role in triggering apoptosis in response to cellular stresses such as UV irradiation and cytokines. JNK1 phosphorylate Ser 422 of CtBP and triggers CtBP degradation. Both UV and cisplatin induced sustained JNK activation and decreased CtBP levels. This pathway promotes p53-independent apoptosis in tumor cells, suggesting a possible novel cancer therapy by targeting JNK1 mediated CtBP degradation.[74] Pro-apoptotic effects have been demonstrated to occur indepentantly of p53, however recently Birts *et al* have demonstrated that loss of CtBP1 and CtBP2 does lead to p53 activation, and this can protect against CtBP siRNA-induced chemosensitisation in breast cancer cells.[75]

1.6.6 ARF/CtBP

ARF ($p19^{ARF}$ in mouse [mARF] and $p14^{ARF}$ in human [hARF]) is a potent tumour suppressor that antagonises the oncoprotein Hdm2. ARF is also a negative regulator of p53, inhibiting the interaction of p53 with transcriptional co-activators, driving its export from the cytoplasm and degradation by proteosome. Under hypoxic conditions that would favour an increase intracellular NADH concentration, a decrease in interaction between Hdm2 and CtBP2 resulted in the relief of p53 mediated repression. ARF exerts tumour suppression function utilizing both p53 dependent and independent pathways. CtBP is a putative target for p53 independent ARF function, where ARF-dependent CtBP degradation correlated with ability of ARF to physically interact with CtBP. ARF expression in human colon cancer cells lacking p53 induced efficient apoptosis.[76]

ARF can also downregulate CtBP by targeting it for proteasomal degradation, inducing Bik-dependent apoptosis. However apoptosis was also observed after CtBP knockdown alone, suggesting that CtBP lies directly downstream of ARF in its pathway of apoptosis induction. Loss of ARF has been linked to tumour invasiveness and metastasis in mouse and skin models. Notably, an antiapoptotic survival signal(s) is necessary for tumour cells to escape their normal microenvironment, invade and metastasise.[77]

ARF is also capable of blocking CTBP mediated repression of PTEN and by doing so, ARF can inhibit CtBP-dependent hypoxia-induced, cancer cell migration.[57] Suppression of tumour invasion and metastasis by ARF, especially in a setting of p53 inactivation, might therefore be explained by its ability to induce apoptosis through inhibiting targets of CtBP. CtBP transcription factors have been shown to induce epithelial-to-mesenchymal transition and to stimulate cell migration. Therefore regulation of CtBP's activity is an important tumour suppressor function.[40,78] Depletion of CtBP1 or CtBP2 reduces cell invasion. Ectopic CtBP2 expression enhances tumour cell migration and invasion. The Evi-1 oncoprotein responsible for acute myelogenous leukaemia requires interaction with CtBPs to mediate transformation. Therefore, agents designed to disrupt this interaction may be useful therapeutically.[79] Various studies carried out suggest that CtBP maintains a certain antiapoptotic "tone" in cells through repression of proapoptotic gene transcription. Such repression might be abrogated via ARF-induced CtBP degradation, resulting in derepression of such genes.

The CtBP dehydrogenase substrate 4-methylthio-2-oxobutyric acid (MTOB) can act as CtBP inhibitor at high concentration, and is cytotoxic to cancer cells . Treatment with MTOB induced p53-independent apoptosis in a variety of human cancer cell lines. MTOB displaced CtBP from the promoter of the pro-apoptotic gene Bik, increasing Bik expression in a dose dependant manner. MTOB induces apoptosis in human colorectal cancer cell lines. *In vivo* test by Straza *et al* showed that MTOB in colon cancer peritonaeal xenograft demonstrated it to be a safe, well-tolerated therapy, with an ability to limit tumor growth and ascites production and possibly prolong survival.[57]

1.6.7 CtBP/Bcl-2

Mitochondria are essential organelles that are responsible for cellular energy production and cell death by regulating the balance between pro-apoptotic and anti-apoptotic proteins such as Apoptosis Inducing Factor (AIF), Smac/Diablo and cytochrome C. These factors are released from the mitochondria following the formation of a pore in the mitochondrial membrane called permeability Transition pore, or PT pore. These pores are thought to form through the action of the pro-apoptotic members of the bcl-2 family of proteins which are often found in the cytosol where they act as sensors for cellular damage or stress. Following apoptotic stress, free radical damage or growth

factor deprivation they relocate to the surface of the mitochondria where the anti-apoptotic proteins are located[80]. Bcl-2 family members play a critical role in regulation of the mitochondrial pathway that leads to apoptotic cell death by directly targeting mitochondria and are frequently over-expressed in many tumors. J H Kim *et al* found that mitochondria-dependent apoptosis occurred in response to glucose deprivation and this apoptosis was mediated by the activation of Bcl-2 associated X protein (BAX) gene expression. They also found that CtBP associated with and repressed BAX promoter and was dissociated from the promoter in response to glucose deprivation. In addition, mitochondrial morphological changes and decreased mitochondrial activities were observed in ctbp-knockout cells, and the knockdown of Bax in CtBP-knockout cells recovered the mitochondrial morphology and function.[60]

1.6.8 CtBP/ACP, Wnt signalling

CtBP plays an important role in modulating the Wnt signalling pathway during development and oncogenesis in mammals. The activation of Wnt signalling results in an increase in the levels of β-catenin. In the absence of this signalling, the level of β-catenin is downregulated by the tumour suppressor protein, adenomatous polyposis coli (ACP). ACP gene is a key tumour suppressor gene, which promotes degradation of β-catenin.[49] During human colon carcinogenesis,[57] inactivation of the ACP/β-catenin pathway services to block the progress of enterocytes in the colonic crypt into a differentiated, post mitotic state.[67] Genetic studies using mutant mouse models have demonstrated that mutations in the *Acp* gene are responsible for intestinal tumorigenesis. Homozygous *Acp* mutation in mice leads to embryonic lethality, and conditional deletion of the gene in the adult mouse disrupts homeostasis not only in the intestine but also in other tissues. ACP inhibits β-catenin/TCF transcription through interaction of β-catenin or CtBP.[79] The APC protein has also been demonstrated to control CtBP protein turnover and may be involved in the auto-regulation of CtBP abundance. APC is known to regulate the abundance of CtBP1 but did not have this effect on CtBP2 suggesting a CtBP2-selective regulatory mechanism, or it could be that CtBP1 may be more abundant in cells than CtBP2, so that knockdown of CtBP2 results in undetectable relative increase in CtBP1 abundance to restore total CtBP protein levels.[75]

1.7 Role in Membrane Fission and Transport

The Golgi complex in mammalian cells is composed of stacks of flattened membrane disks that in mammals are connected laterally to form a single ribbon. The Golgi ribbon is localised to perinuclear area, and it has an essential role in secretory trafficking, lipid biosynthesis, protein modification and the sorting and transport of protein.[81] Many factors contribute to the formation and maintenance of the structure of the Golgi complex, including Golgi 'matrix' proteins and GTPase, specialised cytoskeleton-base motors, determine the Golgi perinuclear location and a constant membrane input from the endoplasmic reticulum (ER). When cells divide they must segregate not only their genetic material but also their cytoplasmic or organelles equally between two daughter cells. During cell division, the Golgi undergoes extensive fragmentation that begins prophase and initially involves the severing of tubules connecting adjacent stacks. The isolated Golgi stacks are shortened and transformed into tubular networks that fragment into clusters of vesicles and tubules. A number of molecular proteins have been characterised through *in vitro* assays of Golgi mitotic fragmentation reassembly. These include numerous kinases, such as Cdc2, RAF/MEK1/ERKc1, PlK1 and plK3 (Figure 1.13).[82]

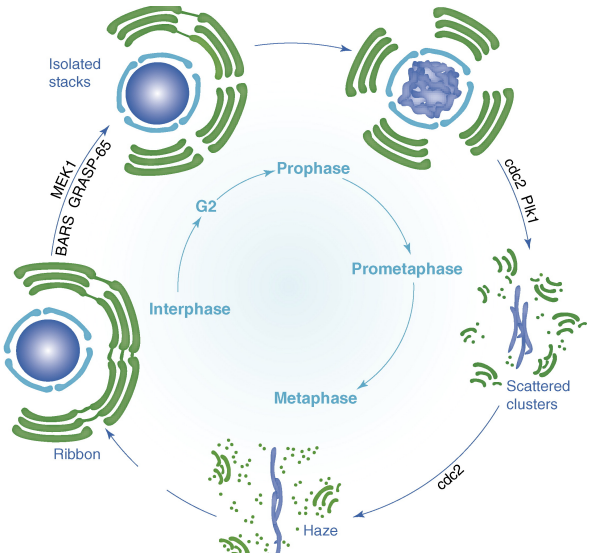

Figure 1.13 The Golgi ribbon undergoes sequential fragmentation steps during mitosis in mammalian cells. Schematic representation of the Golgi complex partitioning during mitosis.[82]

A third CtBP homologue (CtBP3) was identified initially as a 50 kD protein that is ribosylated when rat cells are treated with the fungal toxin Brefeldin-A. Hidalgo Carcedo *et al* report that the protein CtBP3/BARS [C-terminus binding protein 3/brefeldin A (BFA) adenosine diphosphate-ribosylated substrate], has homology to CtBP1 and 2 but lacks the first 11 amino acids relative to CtBP1. CtBP3 remodels lipid bilayers, which is an essential regulator of Golgi membrane fission, fission of vesicles involves in basolateral transport from the Golgi to plasma membrane, in dynamin-independent endocytosis and in transcriptional regulation. The fragmentation of the Golgi complex by CtBP is required for cells to enter mitosis and both CtBP3 and CtBP1 possess this activity. Spyer *et al* showed that a sub-population of CtBP migrates to and associates with centrosomes during the transition from G_2 to mitosis or in very early prophase. CtBP then remains localised with the centrosomes throughout mitosis. It reassociates with chromatin when daughter nuclei are forming during late telophase.[51,81]This suggests that drugs acting on BARS should have the potential to control G_2-propase transition stage of this cycle and prevent the proliferation of cancer cells. Anti-sense and siRNA directed against CtBP causes a reduction of mitotic index and accumulation of cells in G_2 of the cell cycle.

Golgi fission is required for proper entry of cells to start dividing suggesting the existence of a novel 'Golgi mitotic checkpoint' dedicated to linking the state of assembly of the Golgi complex with the process of entry into mitosis. The main evidence for this checkpoint is that the inhibition of Golgi fragmentation via a functional block of the proteins involved in this process. Immunodepletion of BARS inhibited Golgi fragmentation by more than 80%, and the addition of recombinant BARS to depleted extracts completely restored their fragmentation activity.[82] Moreover, in cells that already have Golgi membranes that are organised as isolated stack, microinjection of the BARS blocker does not affect G2/M transition, indicating that the absence of a ribbon organisation of the Golgi, BARS becomes necessary for mitotic entry.[81] BARS are active also in the fission of transport carriers during interphase traffic, but this activity may be enhanced by mitotic phosphorylation. CtBP/BARS-dependent fission requires long-chain acyl-CoAs as essential cofactors. These acyl-CoAs were originally proposed to be acyl donors for a lipid specific acyl-transferase activity of CtBP/BARS, which leads to the conversion of lysophosphatidic acid (LPA)

into phosphatic acid (PA). This activity facilitates, but is not essential for several fission-requires activities of BARS. CtBP1 exhibits fissioning activity when it binds acyl-CoA and assumes an open structural configuration as a monomer and participates in transcriptional regulation when in the dimeric form bound to NAD(H).

BARS is involved in membrane fission at several transport steps, including that from the Golgi complex to the basolateral membrane in epithelial cells, fluid-phase endocytosis and retrograde transport of the KDEL receptor to the ER by COPI-coated vesicles. The later requires an interaction between BARS and the COPI-vesicle component ARFGAPI, which is in turn regulated in an opposite fashion by palmitoyl-CoA and NAD^+, the cofactor of BARS.[82] The core complex of Coat Protein I (COPI), coatomer, is sufficient to induce coated vesicular-like structures from liposomal membrane. Coat proteins play a key role in intracellular transport by coupling the deformation compartmental membrane from vesicle formation with cargo sorting that involves coats binding to specific sequences in the cytoplasmic domain of cargo proteins for their proper packaging into nascent vesicles. Upon activation of the small GTpase ADP-Ribosylation Factor 1 (ARF1), coatomer becomes recruited onto Golgi membrane. J-S Yang *et al* showed that BARS plays a critical role in the fission step of COPI vesicle formation by multiple approaches.[83]

1.8 Mitotic Fidelity

The pro-survival role of CtBPs has recently been shown to arise from their role in maintaining mitotic fidelity. During mitosis aurora B first localises to centromeres in prophase and remains concentrated at centromeres until it relocalises to the central spindle at the start of anaphase where it subsequently concentrates at the midbody. CtBPs are required for the optimal association of aurora B with the chromatin during mitosis. CtBP siRNA results in reduced association of aurora B with mitotic chromatin and an increase in the frequency of aberrant mitoses. This results in cell death, particularly in cells containing mutant p53, which fail to undergo a protective post-mitotic cell cycle arrest. Bergman *et al* found three mitotic phenotypes in CtBP siRNA treated cells: 1) lagging chromosome during mitosis and, interphase cells, micronuclei that contain primarily centromere-containing chromatin; together indicative of entry into anaphase prior to completion of amphitelic attachment of paired sister chromatids

to microtubules; 2) an extended average time spent in mitosis, mitosis being delayed predominantly at the prometaphase stage and 3) failure of cytokinesis in a proportion of cells, resulting in the generation of binucleate cell progeny. Bergman *et al* analysed the phenotype of CtBP depleted cells by morphological analysis of DAPI-stained cell nuclei and identifying multiple morphological defects consistent with aberrant transit through mitosis. There was a significant increase in occurrence of binucleate cells, suggesting that a portion of cells undergo cell division without segregating their DNA and is consistent with the modest increase in cells with 4N DNA content which was also seen in flow cytometry. CtBP siRNA also caused a three- to four-fold increase in micronuclei. Micronuclei can arise from whole chromosomes that lag at mitosis due to, for example, a damaged kinetochore or faulty spindle apparatus or from acentric chromosome fragments created by DNA breaks. There was no gross effect of CtBP siRNA on Golgi morphology, suggesting that the aberrant mitotic phenotype might not be a consequence of abnormal Golgi maintenance.[84] CtBP siRNA causes both an extended period of transit through mitosis, and a post-mitotic G_1 arrest.[85] Birts *et al* microinjected GST-CtBP^{DN}, into the cytoplasm of MCF-7 cells, which also caused a significant increase in aberrant mitosis (showed in the montage in Figure 1.14). CtBP function in the nucleus is critical for the regulation of mitotic fidelity, as are its interaction with cellular factors that associate with the PxDLS-binding cleft.

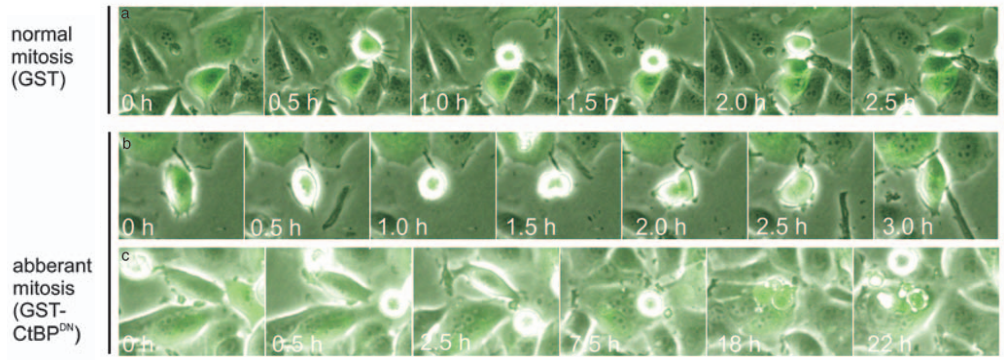

Figure 1.14 Microinjection of GST-CtBP2(1–110) (CtBP^{DN}) induces aberrant mitosis. At 20 h post-release, cells were microinjected into the cytoplasm with the indicated proteins plus FITC-Dextran. Cells were then monitored by fluorescent time-lapse imaging for the subsequent 65 h. Representative time-lapse montages of cells.[86]

The cell cycle transition from interphase into mitosis requires several dramatic cellular events, which include chromosome condensation. Reversible chromosome condensation limits transcriptional machinery access to chromosomal DNA and inactivates chromatin-remodelling complexes.[87] D. Cimini *et al* supports this idea that chromatin-remodelling process is strongly altered when histones are hyperacetylated during mitotic condensation, producing mitotic chromosomes with altered three-dimensional structure. Inhibition of histone deacetylation shortly before mitosis produces defects in chromosome condensation in living cells. A complex of chromosomal passenger proteins, notably aurora B kinase and its regulators surviving, borealin and INCENP regulates many aspects of mitosis. Inhibiting the expression and/or activity of chromosomal passenger proteins results in severe mitotic defect. Cell death may occur as a consequence of such defects, and thus proteins such as survivin and aurora B kinase are currently under investigation as targets for potential anti-cancer therapeutics. Aurora B-depleted *Drosophila* cultured cells showed altered chromosome condensation and defective association of the condensing Barren protein together with reduced H3 phosphorylation.[88]

The mitotic check points maintain the fidelity of this process by sensing proper microtubule attachment with the kinetochores and the tension between the kinetochores of sister chromatids.[87] The spindle assembly checkpoint is the cell cycle control mechanism that acts during mitosis to ensure the fidelity of chromosome segregation by preventing premature entry into anaphase. Thus preventing the chromosome instability and polyploidy associated with cancer.[89] This checkpoint is activated for longer in CtBP compromised cells compared to controls.

Histone modification also plays a key role in regulating mitotic checkpoint activation,[87] with inhibition of HDAC activity prolonging mitotic arrest leading to chromosomal stability and segregation defects.[88, 90] As cell cycle checkpoints are often defective in cancer, HDAC inhibitors are often selectively cytotoxic to tumour cells, causing rapid and extensive apoptosis. HDACs are therefore increasingly viewed as holding much potential for development of novel therapeutics for a variety of diseases (including cancer) with the majority of current approaches focused on inhibiting individual HDACs with small molecules. The use of HDAC inhibitors has shown the ability of CtBPs to repress transcription in a partially HDAC dependent way. Along with their effect on gene transcription, HDAC inhibitors also induce effects on mitotic fidelity that

are highly comparable to those observed upon inhibition of CtBP expression or targeting of the CtBP chromatin modifying complex. These effects include activation of the spindle assembly checkpoint, aberrant chromosomal segregation, failure of cytokinesis and reduced association of chromosomal passenger proteins with mitotic chromatin. Mitotic fidelity is thus dependent upon both HDACs, and an intact CtBP chromatin modifying complex; further dissection of the mechanism of regulation of mitosis by these proteins will be required to establish whether recruitment of HDACs by CtBPs is required for a normal mitotic phenotype.

1.9 CtBPs in central nervous system synapses

Chemical Synapses are highly specialised cell-cell contacts that mediate efficient communication between nerve cells. The release and reception of neurotransmitters occurs at the pre- and postsynaptic region. A unique type of chemical synapse, structurally specialised for the tonic release of neurotransmitter in the dark, is the photoreceptor ribbon synapse. The presynaptic ribbon constitutes an electron-dense band of large surface area that extends from the site of transmitter release into the presynaptic cytoplasm and is covered by hundreds of synaptic vesicles. The ribbon is defined and organised by a scaffold of proteins. One of these proteins is the kinesin motor protein KIF3A and is enriched at ribbons. Two other integral components of photoreceptor ribbon synapses are Bassoon and Piccolo.[91] Another protein is RIBEYE, which is a protein that is enriched in dense bodies at ribbon synapses and is likely to function in synaptic vesicle exocytosis through the interaction with active zone proteins. CtBP is also present at the synaptic terminals (Figure 1.15).

The N-terminal A domain can form aggregates in cultured cells and bears no recognisable similarity to other proteins or protein domains. The C-terminal B domain is identical to a transcriptional corepressor, C-terminal binding protein 2, but without the first 20 residues encoded by the first coding exon.[91-92] The A domain mediates assembly of RIBEYE into large structures whereas B domain binds NAD^+ with high affinity, similar to 2-hydroxyacid dehydrogenases.[93] RIBEYE lacks the N-terminal 20 amino acid domain of CtBP2 and is localised to the cytoplasm. Ultra structural studies have revealed that both RIBEYE and CtBP1 may meet the need of tonic rate release of neurotransmitter. CtBP1/BARS is present at photoreceptor ribbon synapses and at

conventional synapses of retina and brain and has been identified as a constituent of the conventional chemical synapses that do not express RIBEYE. CtBPs play a role in the molecular assembly and function of central nervous system synapses.[94] Depletion of RIBEYE in zebra fish has shown to result in shorter synaptic ribbons.[95]

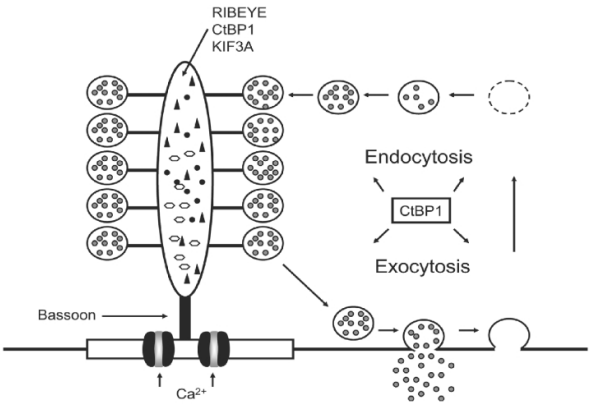

Figure 1.15 CtBPs in ribbon synapse. The RIBEYE protein is postulated to be the predominant constituent of the ribbon. Other constituents of the ribbon include CtBP1 and the kinesin motor molecule KIF3A. The ribbon is anchored to the presynaptic membrane by the protein Bassoon, which is associated with voltage-gated Ca^{2+} channels. CtBP1 is suggested to play a role in membrane turnover during exocytosis and endocytosis of the synaptic vesicles.

1.10 Role of CtBP in developmental processes

Tightly regulated gene expression is critical for the correct embryonic development and adult growth. CtBP plays a crucial role during early embryo development and during later development processes in *Drosophila*, they have been found in complex with several known DNA-binding transcription factors that participate in a wide variety of developmental and adult biological pathways and processes. These include Wnt and BMP/TGFβ signalling, the action of GATA factors, cell-cell adhesion and apoptosis, myogenesis and vascularisation and segmentation in flies.[54] In *Drosophila*, the single *CtBP* gene encodes two major isoform generated through alternative RNA splicing. These isoforms, termed $CtBP_L$ and $CtBP_S$ are highly conserved in insects. The proteins are identical at the N-terminus but differ in the C-terminal region: CtBPL has an

extended C-terminus, which is lacking in CtBPS. These two isoforms have similar repression activity, but distinct development expression profile.[96]

Reduction in the level of maternal dCtBP results in severe segmentation and patterning defects, and homozygous mutations are embryonic lethal.[97] Gene dosage experiments in Drosophila have shown that CtBP is required for the activity of the repressors Krüppel, SNAIL, Knirps and biochemical assays have confirmed these genetic interaction.[49] Knirps is a nuclear receptor protein that controls the segmentation of the abdomen, whereas SNAIL is a zinc finger protein that establishes a boundary between the presumptive mesoderm and neurogenic ectoderm.[98] The Notch signalling pathway is important in cell fate decisions during *Drosophila* development. During Notch signalling, the intracellular domain of Notch associates with DNA binding protein suppressor of Hairless.[49] Hairy is another Drosophila pre-cellular repressor that has shown to bind dCtBP. Hairy is also known to recruit the Groucho co-repressor. Mouse embryos lacking CtBP1 are small but viable, whereas CtBP2 deficient embryos die mid-gestation and display defective development of several tissues. This shows the importance of CtBPs in mammals and drosophila.[40, 99, 100]

In addition to the identified functions in *Drosophila*, CtBP has also been implicated in human development. Mutation in the human TGIF (which maps to the *HPE4* locus) leads to holoprosencephaly, a condition resulting from defects in craniofacial development. One of the *HPE4* alleles encode a protein with a single amino acid substitution I a consensus binding site for CtBP, suggesting that CtBP-dependent branch of TGIF-mediated transcriptional repression is required for proper craniofacial development in humans. The full repressor activity of TGIF is dependent on its ability to bind both CtBP and histone deacetylase (HDAC).[54] In animal models CtBPs are widely expressed during numerous developmental processes, as well as in adult cells. Indeed homozygous knockout Drosophila (dCtBP-/-) exhibits lethal phenotypic abnormalities. Similar effects have been demonstrated in mouse embryo models, CtBP1-/- animals are small and have a significantly shorter life expectancy while CtBP2-/- embryos die in utero. In addition, the phenotypic defects seen in the neurological, cardiovascular and musculoskeletal systems of CtBP2-/- embryos are worsened if they are also CtBP1-/-, indicating that the two proteins, while having distinct roles, may share considerable functional overlap. These differences suggest that the two proteins have different roles *in vivo* or they are expressed in slightly different

places during the course of development. Hildebrand *et al* have shown that there are clear differences in the expression of CtBP1 and CtBP2 during placental morphogenesis. Specifically, CtBP2 is readily detected in the forming placenta while CtBP1 is not. CtBP1 is expressed throughout embryogenesis and into adulthood.[54, 97, 101]

CtBP2 interacts physically with key factors in the stem cell regulatory network. Embryonic stem cell (ESC) assays carried out by Tarleton and Lemischka indicate that a knockdown of *Ctbp2* expression affects the balance between self-renewal and differentiation towards self-renewal even when differentiation is forced. There are only two mechanisms by which a stem cell could increase in prevalence, these being to divide more rapidly or to experience a change in symmetry of fate decisions. It was hypothesised that the later mechanism was responsible for this observation, as cell cycle assays verified that this change was not due to changes in the rate of cell division.

1.11 Control of Plant Microtubule Cytoskeleton

The genome of terrestrial plants also codes for a CtBP family member, ANGUSTIFOLIA (AN). The *AN* gene was first identified in *Arabidopsis thaliana* and this gene controls N polarity-dependent leaf cell expansion, possibly through controlling the arrangement of the microtubule cytoskeleton. The N-terminal region of the AN protein shares sequence similarity with three protein classes, which also show similarities with each other in the region: dehydrogneases, CtBPs and BARS. AN proteins lack amino acid residues important for the D2-HDH catalytic function and also lacks the consensus NAD(H)-binding motif. It has been shown that AN was thought to repress transcription similar to the function of CtBP; however AN lacks some of the structural features that are conserved in animal CtBPs.[102] Mutations in *AN* gene results in leaves that are narrower and thicker than normal.[103]

1.12 The aim of the project

The aim of this project was to combine the RTHS with SICLOPPS in order to study the protein-protein interaction of CtBP and uncover cyclic peptide inhibitors. This will help us further understand the role of these proteins in the cell. CtBPs exist as both monomer and dimers in cells and they dimerise in response to NADH levels. Current tools do not allow us to know whether the effect of CtBP on mitotic fidelity, reduced proliferation

and colony forming potential is due the loss of CtBP or the break up dimerisation. siRNA leads to a loss off protein abundance in the cell where as the peptides do not.

2. **Screening and Selection of Peptides**

Construction Of CtBP1 RTHS

Building construct

Repression using ONPG assay and Minimal media plates

Construction of CtBP2 RTHS

Building construct

Repression using ONPG assay and Minimal media plates

NADH domain mutation

Construction of CtBP heterodimeric RTHS

Building construct

SICLOPPS Library Construction

Selection CtBP1

Selection CtBP2

Peptide synthesis

Synthesis of Peptide 61

Synthesis of Peptide 6

Tat

Synthesis of Peptide 61 Tat-Tagged

Synthesis of Peptide 6 Tat-Tagged

Synthesis of Peptide 32

Synthesis of Peptide 33

2.1. Construction of RTHS

The pTHCP16 plasmid constructed by Horswill *et al*[17b] (Figure 2.1) was used to build a homodimeric Reverse Two Hybrid System (RTHS) construct for CtBPs. This plasmid contains the sequence for wild type 434 repressor, under the control of P_{tac} promoter induced by isopropyl-β-D-thiogalactopyranoside (IPTG). The multiple cloning sites (MCS) have been placed to allow for construction of C-terminal fusion with the 434 repressors. The MCS consists of *Sac*I, *Bam*HI, *Nru*I and *Sac*I restriction sites.

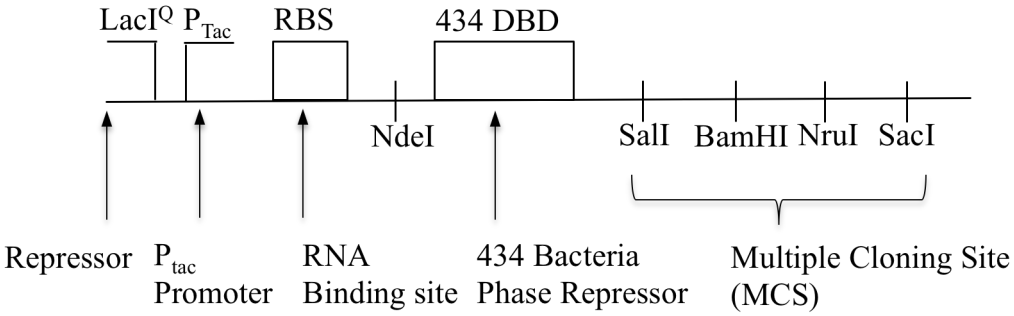

Figure 2.1. pTHCP16 plasmid.

The pTHCP14 plasmid constructed by Horswill *et al*[17b] (Figure 2.2) was used to build our heterodimeric RTHS construct for CtBPs . As shown, this plasmid contains the sequences for the wild-type 434 repressor and a mutant 434 repressor (referred to as P22) with P22 binding specificity, under the control of a P_{TAC} promoter induced by IPTG. Multiple cloning sites (MCS) have been placed to allow for construction of C-terminal fusions with the repressors. The MCS following P22 contains *XhoI, SpeI, SmaI*, and *KpnI*, while 434 is followed by *SalI, BamHI, NruI*, and *SacI*.

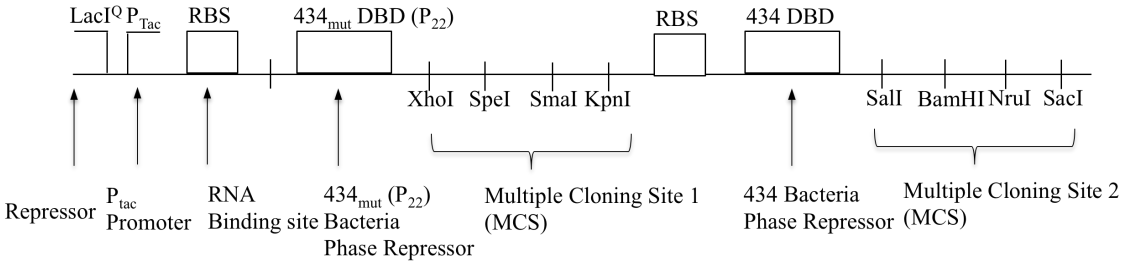

Figure 2.2. pTHCP14 plasmid

Two primers were designed for PCR: a forward primer to extend from the start codon (ATG) towards the stop codon (TAG) of template DNA, and a reverse primer that extends from the stop codon towards the start codon. Appropriate restriction enzymes were chosen that do not cut within the gene of interest. The distance between restriction sites is also considered, and where feasible sites were chosen to be as far apart as possible to improve efficiency of digestion by allowing more efficient binding of the restriction enzyme to the DNA.

For the forward primer, 21bp from the beginning of the desired gene were taken and for the reverse primer the reverse complement from the end of the gene was taken. Ideally a cytosine or guanine was taken as the last 3' nucleotide as this allows for stronger binding interaction and a more efficient PCR reaction. A stop codon (TAG) was introduced for the reverse primer. A GTTGTT sequence was introduced at the start of the primer, to act as a handle to allow the restriction enzyme to bind more efficiently to the DNA. The general sequence for the forward primer was GTTGTT-sequence of restriction enzyme-21bp and for the reverse primer the general sequence was GTTGTT-Complementary reverse of restriction enzyme-CTA-reverse complement of 21bp.

The next step was to amplify the gene that codes for the protein of interest; this was done via the polymerase chain reaction (PCR). PCR was carried out using a high fidelity polymerase with exonuclease activity for example Deep Vent (New England Biolabs) or Pfu (Promega). The annealing temperature was calculated using pDRAW software. It is important to note that when calculating the annealing temperature, only bases that are complementary to template DNA were used, and the restriction site was not incorporated in the calculation.

After the PCR reaction the length of the amplified DNA was determined by gel electrophoresis. The PCR product was then purified and stored ready for the next step. Bacterial strains containing pTHCP16 was grown overnight and the plasmid was then isolated and purified. The Plasmid and PCR product were then digested with the relevant restriction enzymes (which were chosen when designing the primers), using standard condition (section 6.1.2.5). Digestion was followed by purification with QIAGEN QIAquick Spin Columns. The digested PCR product and plasmid were then ligated using NEB T4 ligase; this resulted in the insertion of the target gene into the RTHS plasmid. This plasmid was then transformed into DH5α cells, and grown on agar plates containing the appropriate antibiotic marker for the plasmid (ampicillin). For maximum transformation efficiency, the cells were thawed on ice and resuspended by carefully agitating the tube. It was found that cold and dry plates lower transformation efficiency and therefore the plates were pre-warmed at 37 °C. Colony PCR was run to identify colonies with the correct insert.

Nitrophenyl-β-D-Galactoside (ONPG) assay

The SNS118 cell strain constructed by *Horswill et al*[17b] contains the RTHS reporter construct as a chromosomal insert, composed of the lacZ gene encoding ß-galactosidase, under the control of the binding region of the reconstituted 434. The use of the *lacZ* reporter gene in the RTHS allows the targeted protein-protein interaction to be monitored by ONPG assay. IPTG is used to induce the production of the fusion proteins, increasing the levels of IPTG produces a higher concentration of fusion protein, which potentially reduces levels of β-galactosidase because its transcription is hindered by the increase in dimerised repressor. This links protein dimerisation to the levels of β-galactosidase present and can be quantified by ONPG assays. ONPG is a colorimetric substrate used for the detection of β-galactosidase activity. β-galactosidase hydrolyses ONPG to otho-nitrophenyl (ONP), which is yellow in colour. Enzyme activity can be measured by the rate of appearance of the yellow colour using a spectrometer and measuring the absorbance at OD_{420}. If excess ONPG is added, the amount of ONP formed is proportional to the amount of β-galactosidase and time of reaction. The reaction is stopped by the addition of Na_2CO_3, which shifts the reaction

mixture to pH 11. At this pH, ONP is converted to a coloured anionic form and β-galactosidase is inactivated.

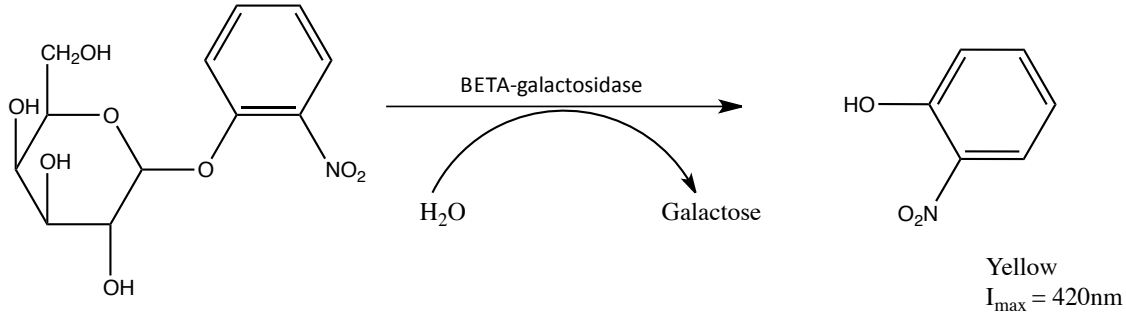

Figure 2.3. Hydrolysis of ONPG by β-galactosidase to ONP and galactose.

2.2. Construction of CtBPs RTHS

The plasmids containing cDNA of CtBP1 and CtBP2 were available in house. The gene encoding full-length human CtBP1 and CtBP2 was cloned into the RTHS as a C-terminal fusion of the bacteriophage 434-repressor DNA binding domain under the control of an IPTG inducible promoter. The whole protein was used in the RTHS in order to include any regulatory domains as well as the dimerisation domain.

2.2.1. CtBP1 RTHS

The CtBP1 coding sequence was amplified via PCR using designed primers, which allows the introduction of restriction sites into the sequence. The gene contained a *SalI* site near the end of the sequence, which was removed by a silent mutation (GUC to GUU) to allow *SalI* to be used to clone the gene into the RTHS. The CtBP1 gene was incorporated between the *Sal*I and *Nru*I restriction sites (Figure 2.4). As the *Nru*I restriction enzyme is unable to cleave DNA methylated with Dam methyltransferase, a Dam negative strain was used to incorporate CtBP1. The pTHCP16 plasmid was therefore transformed into GM2929, a dam negative strain, which is maintained by chloamphenical resistance gene within the dam gene. The isolated plasmid was cut once with *HpaI* to confirm its length (~7103) and a PCR was carried out to confirm the insert was present (Band at 1320bp) (Figure 2.5). The presence and fidelity of the cloned sequence was verified by sequencing.

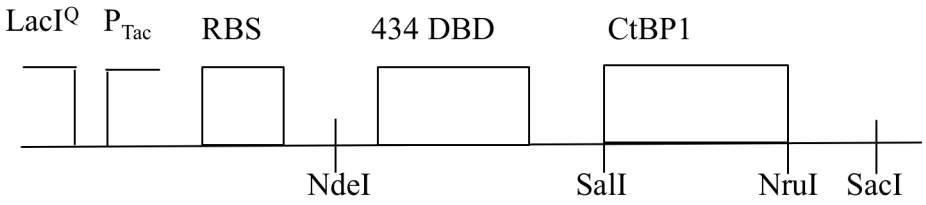

Figure 2.4. RTHS construct of CtBP1.

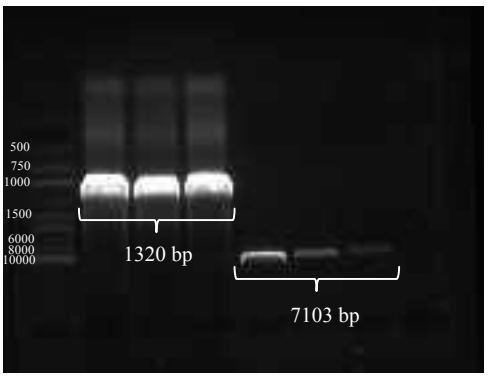

Figure 2.5. Gel confirming the presence of CtBP1 in pTCHP16. First three lane: PCR product using CtBP1 primers (1320 bp). Last three lane: pTCHP16-CtBP1 plasmids digested HpaI (7103 bp).

To confirm the interaction between the fusion proteins, the CtBP1-pTCHP16 plasmid was transformed into the reporter strain SNS118 and an ONPG assay was conducted (section 6.1.3.9).[26] The standard activity (SA) for the above reaction is calculated using the following equation:

$$SA = A_{420}/t \times V\ OD_{600,}$$

Where t is the incubation time in sec; V is the sample volume; OD_{600} is the optical density of the culture at 600 nm, which relates to the density of cell culture and A_{420} is the absorbance at 420 nm, which relates to the ONP produced.

The ONPG assay showed there was interaction between the fusion proteins with a twofold repression of the reporter construct at IPTG levels of 50 μM, indicating the formation of a CtBP1 homodimer in the RTHS (Figure 2.6).

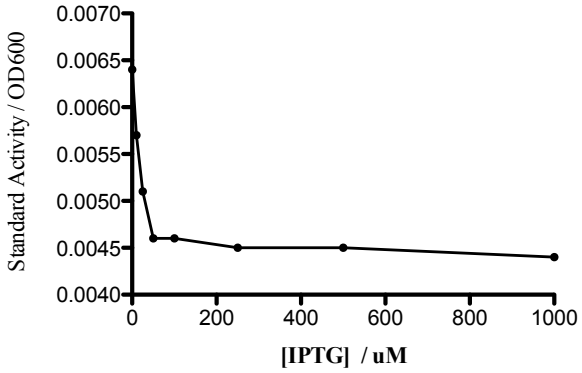

Figure 2.6. ONPG assay of CtBP1-pTCHP16 in SNS118. An increase in IPTG led to a decrease in standard activity. Repression was observed at 50μM concentration of IPTG.

It is important that the optimal IPTG levels are obtained for the screen, as excessively high levels would lead to too much protein in the cytosol, making screening and inhibitor identification difficult. Dimerisation of the target proteins results in the formation of a functional repressor that prevents the transcription of reporter genes downstream, leading to cell death on selective media. The reporter construct consists of three reporter genes: *HIS3*, which encodes a yeast auxotroph of imidazole glycerol phosphate dehydratase, needed for the synthesis of histidine. The second reporter is Kan^R, which codes for aminoglycosidase 3'-phosphotransferase for kanamycin resistance. These two reporters are chemically tuneable and conditionally selective for reporter genes. 3-amino-1,2,4-triazole (3-AT) is a competitive inhibitor of HIS3. Kanamycin and 3-AT are used to fine tune leaky expression of HIS3 and Kan^R reporter genes. The third reporter gene is *Lac Z* (β-galactosidase), which allows quantification of the protein-protein interactions through ONPG assays mentioned above.

Then to identify the optimal levels of IPTG required for high-throughput screening, a series of minimal media selection plates were prepared. The target protein-protein interaction was visualized by drop spotting ten-fold dilutions of different putatives of CtBP1-pTCHP16 in SNS118 (Figure 2.6) (with positive and negative controls) onto selective media containing a range of 3 –AT (2.5-5 μM) and kanamycin (25-50 μg/mL) in the absence and presence of IPTG (0-50 μM). A lower rate of growth cell was

observed on plates containing 3 –AT (5 μM) and kanamycin (50 μg/mL) even in the absence of IPTG, indicating that these conditions were too harsh. The experiment was repeated using 3-AT (2.5 μM) and Kan (25 μg/mL) and a range of IPTG (0, 15, 25, 50 μM). The optimal levels required for expression of fusion proteins and blocking transcription of reporter genes downstream were 3-AT (2.5 μM) and Kan (25 μg/mL) and IPTG (25 μM) (Figure 2.7). The drop spotting data also confirmed the CtBP1 homodimeric interaction in the RTHS. To eliminate the possibility that the growth inhibition is due to the toxicity of the expressed protein, the RTHS strains were drop spotted onto LB agar with 25 μM IPTG (Figure 2.8). All strains grew to the same extent on plates with and without IPTG; the observed growth inhibition on selective media can therefore be attributed to the targeted protein-protein interactions.

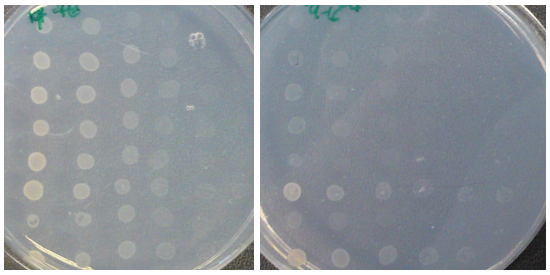

Figure 2.7. Drop spotting of CtBP1 RTHS construct, 0 μM IPTG (left) to 25 μM IPTG (right).

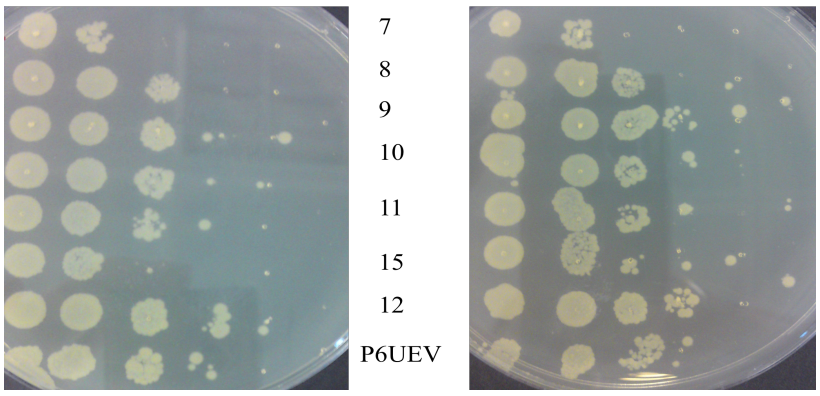

Figure 2.8. Drop spotting of CtBP1 RTHS construct on to rich media, 0 μM IPTG (left) to 25 μM IPTG (right).

The cassette coding for the CtBP1-434 repressor fusion was integrated onto the chromosome of the *E*. coli reporter strain by phage specific recombination using the HK022 phage integrase as previously reported.[17a, 104] Chromosomal integration stabilises expression levels of the CtBP1-434 repressor protein, and eliminate false positives arising (during selection) from plasmid ejection. The method employed to achieve this was the CRIM (conditional-replication, integration, and modular) integration system (Figure 2.9). The CRIM plasmid used (pAH68), contains unique sites within the MCS, which include *Sph*I, *Pst*I, *Sal*I, *Xba*I, *BamH*I, *Sma*I, *Kpn*I, *Sac*I and *Eco*RI. The pAH68 plasmid also contains a phage site (attP), which can be integrated into the chromosome of the host bacterium at bacterial attachment sites (attB). Integration is carried out by phage integrase enzyme (*Int* protein). This enzyme is encoded by the helper plasmid (pAH69), under the control of temperature sensitive cI857 repressor.[104]

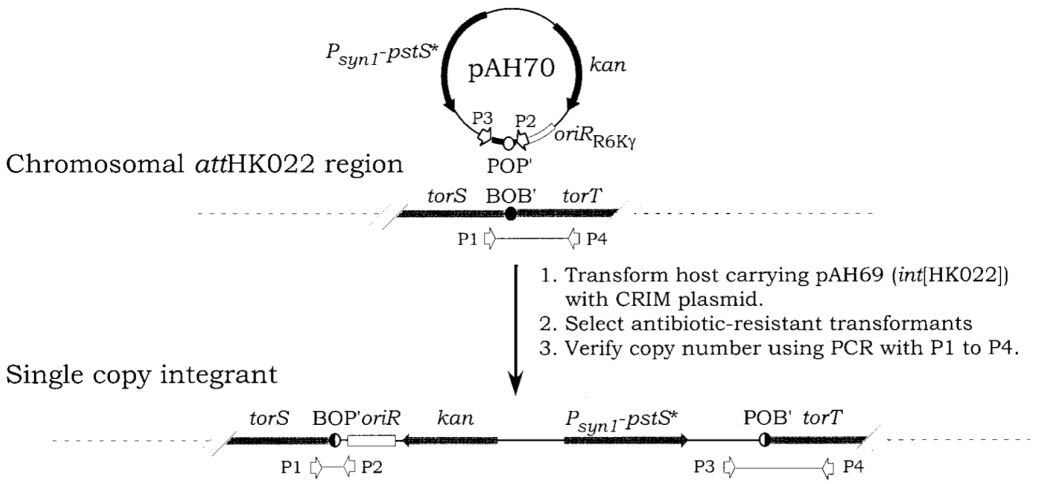

Figure 2.9. Integration of CRIM pAH68 plasmid into phage attachment site attHK022. Positive integration identified by PCR product of primers P1, P2, P3 and P4.[104]

The CtBP1 construct was cut out of pTHCP16 using *Hpa*I and *Nru*I. *Sac*I cuts the CtBP1 gene and therefore that could not be used. The cassette was ligated to pAH68 plasmid, which was cut once with *Sma*I. The problem with this is that insert can ligate to the vector in both directions or the vector can easily re-ligate. The pAH68 plasmid was treated with shrimp alkaline phosphatase, which catalyses the removal of

5' phosphate group from DNA, to prevent backbone re-ligation. The correct orientation of the insert was confirmed by PCR using the reverse primer from pAH68 plasmid (this binds 500bp outside the MCS of pAH68) and the forward primer for CtBP1 (giving a band of 1820 bp). PCR was also run using both the forward and reverse CtBP1 primers (giving a band at 1320 bp). The plasmid was digested once to check the length of the plasmid (4634 bp). Five different putatives of pAH68-CtBP1 were tested. Figure 2.10 a shows that the CtBP coding sequence is present in all five but only the first putative is in the right orientation and of the correct length.

The pAH68-CtBP1 construct was then integrated on to the chromosome of SNS118 using the HK022 integrase expressed from the pAH69 helper plasmid. Production of *int* protein was suppressed by initial recovery in SOC at 30 °C for 1 h, then allowed to begin by shifting the temperature to 42 °C for a further 30 min. Positive integrants were identified using pre-designed primer P1, P2, P3 and P4 (Figure 2.9). Positive integrants give two bands, one at 289 nt and one at 824 nt, corresponding to the PCR products of P1/P2 and P3/P4 PCR product (Figure 2.10 B). Unsuccessful integration results in a band at 740 nt from the PCR product of P2 and P3 from the unaltered pAH68 plasmid. Initially the yield of positive integrant was low. An alternative method for preparing electrocompetent cells was followed as described by Lu Zhou, Ke Zhang and Barry L. Warnner in Methods in molecular biology: Reviews and Protocols.[105] Cells were grown at 30 °C OD_{600} 0.5 with 100 μg/mL amp present (to maintain helper plasmid) then kept for a further 20min at 42 °C. Rapid temperature change was obtained by using a water bath. This did not lead to an improvement in integrant yield. There could possibly have been a fault with the helper plasmid pAH69, which may have prevented it from either producing the cI857 repressor protein or the crucial *Int* protein. Therefore, a fresh source of pAH69 was obtained from The Coli Genetic Stock Centre at Yale University (USA). The new batch led to a dramatic increase in the amount of positive integrant colonies.

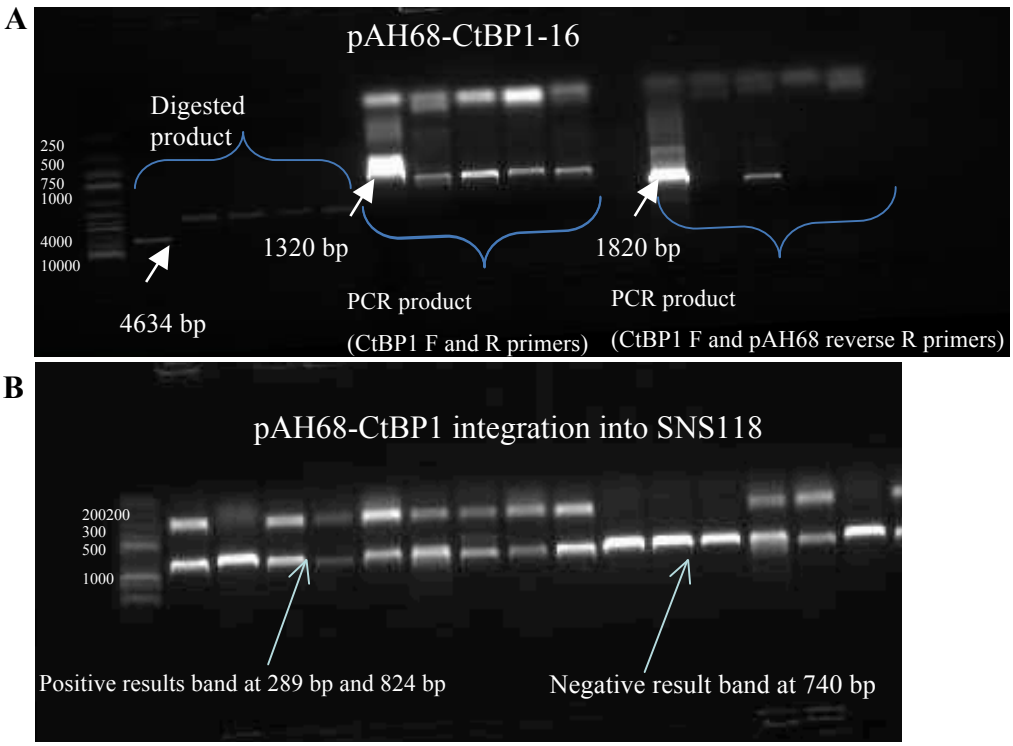

Figure 2.10. Gels of CtBP1 constructs, (A) Check to test positive integration into pAH68, (digestion of product, PCR using CtBP1 F and R primers, and PCR using CtBP1 F and pAH68 reverse primer). (B) Colony PCR checking for positive integrants on the chromosome of SNS118.

Putatives containing the CtBP1 construct on the chromosome of SNS118 were cultured; PCR was run to confirm the presence of the CtBP1 gene. These were then drop spotted on minimal media plates to investigate the formation of a functional repressor when the CtBP-434 fusion protein was expressed from the chromosome (Figure 2.11). The experiments were run using 3-AT (2.5 μM) and Kan (25 μg/mL) and a range of IPTG (5, 10, 12.5, 25, 30 and 50 μM). It was found that 25 μM of IPTG was sufficient to repress the reporter construct; therefore these conditions were used for SICLOPPS selection.

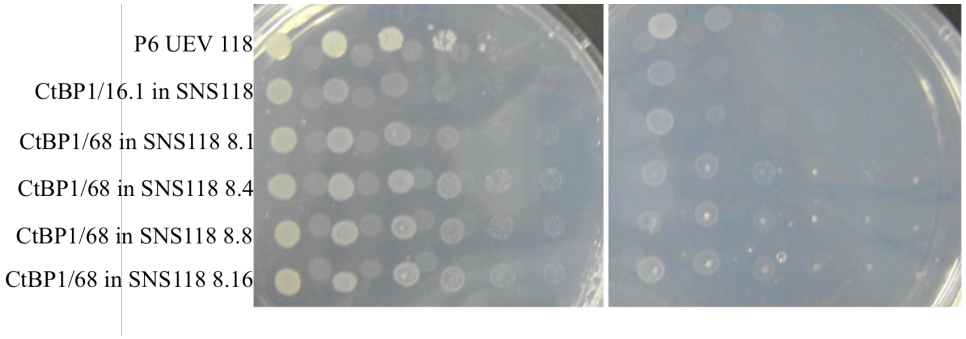

Figure 2.11. Drop spotting of CtBP1/68-SNS118 putatives on minimal media plates with and without IPTG, respectively. P6 UEV SNS118 and CtBP1/16.1 in SNS118 were used as positive controls.

2.2.2. CtBP2 RTHS

The CtBP2 gene was cloned as fusion with the DNA-binding domain of of bacteriophage 434- repressor and placed under the control of an IPTG inducible promoter. The CtBP2 coding sequence was amplified via PCR using designed primers, which allow the introduction of restriction sites into the sequence. The CtBP2 cDNA sequence contains a *Sal*I site and therefore this restriction enzyme could not be used. So, *Xho*I was used instead as its cohesive ends are compatible with *Sal*I. The CtBP2 gene was incorporated in to the pTCHP16 Plasmid (Gm2929 strain) using *Xho*I and *Nru*I restriction sites (Figure 2.12). The isolated plasmid was digested with *Hpa*I to confirm its length (~7121) and a PCR was carried out to check the insert was present (Band at 1338bp) (Figure 2.13).

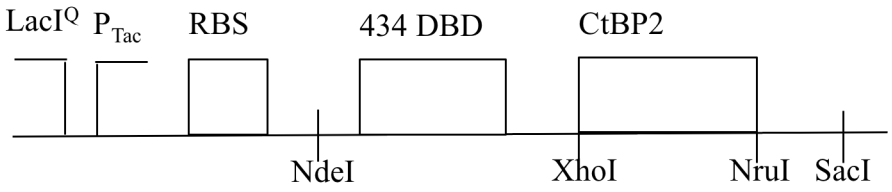

Figure 2.12. RTHS construct of CtBP2.

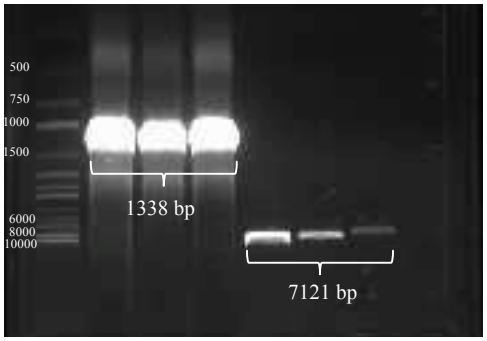

Figure 2.13. Gel confirming the presence of CtBP2 in pTCHP16. First three lane: PCR product using CtBP2 primers (1338 bp). Last three lane: pTCHP16-CtBP2 plasmids digested HpaI (7121 bp).

To confirm the interaction between the fusion proteins, the CtBP2 fusion protein in our RTHS was transformed into SNS118 and an ONPG assay was carried (Figure 2.14). The ONPG assay showed there was some interaction between the fusion proteins with a one-fold repression of the reporter construct at IPTG levels of 50µM.

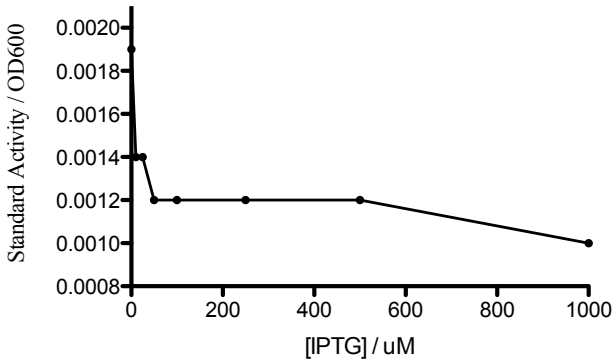

Figure 2.14. ONPG assay of CtBP2-pTHCP16 in SNS118. An increase in IPTG led to a decrease in standard activity. Repression was observed at 50µM concentration.

To find the levels of IPTG required for complete repression of the reporter genes, minimal media plates were prepared for drop spotting (cells were diluted 10 fold). The resulting CtBP2 RTHS showed IPTG-dependent inhibition of cell growth on minimal media, indicating that CtBP homodimerisation leads to the formation of a functional repressor in the RTHS blocking production of the reporter gene (Figure 2.15).

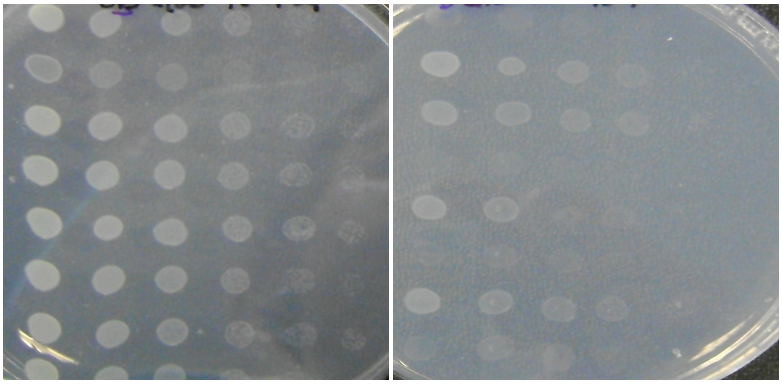

Figure 2.15. Drop spotting of CtBP2 RTHS construct, 0 μM IPTG (left) to 25 μM IPTG (right).

The cassette coding for the CtBP2-434 repressor fusion was integrated onto the chromosome of the *E*. coli reporter strain as previously reported,[17a, 104] to stabilize expression levels of the CtBP2-434 repressor protein, and eliminate any false positives arising (during selection) from plasmid ejection.

The CtBP2-pTHCP16 plasmid was digested using *HpaI* and *NruI*, as there is a *SacI* digestion site within the CtBP2 gene. The cassette was ligated to pAH68 plasmid, which was cut once with *Sma*I. Once the CtBP2-pAH68 plasmid was constructed, the CtBP2 RTHS construct was integrated onto the chromosome of SNS118 (Figure 2.16 A).

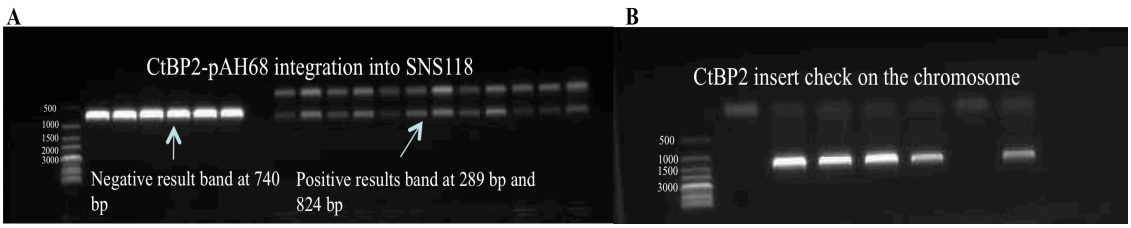

Figure 2.16. Gels confirming integration of the CtBP2 construct onto the chromosome of SNS118; (A) colony PCR run using P1, P2, P3 and P4 primers, (B) PCR run using CtBP2 primer to confirm the presence of the CtBP2 gene.

Putatives containing the CtBP2 construct on the chromosome of SNS118 were cultured; PCR was run to confirm the presence of the CtBP2 gene (Figure 2.16 B). These were then drop spotted on minimal media plates to investigate repression from the

chromosome Figure 2.17. The optimal level of IPTG for selection was determined to be 25 μM.

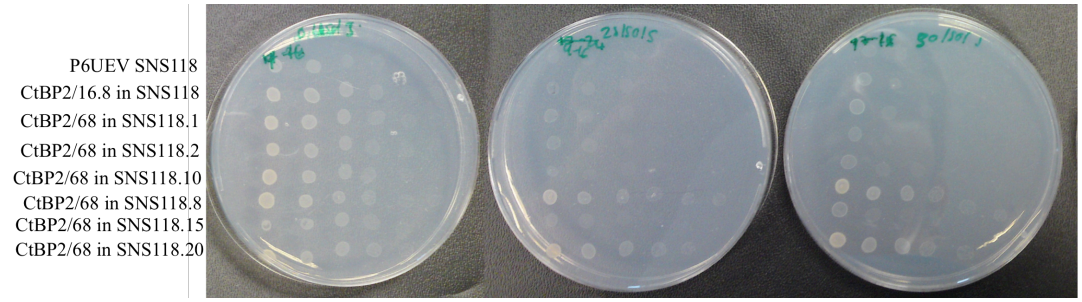

Figure 2.17. Drop spotting of CtBP2-pAH68 putatives in SNS118. P6UEV SNS118 and CtBP2/16.8 in SNS118 were used as positive controls. From left to right increasing amounts of IPTG from 0, 25 to 50 μM.

2.2.3. Construction of CtBP2mut

CtBPs contain a central NAD(H) binding domain, and binding of NAD(H) to CtBPs promotes dimerisation. Point mutation in the NAD(H) binding motif leads to a dramatic decline in homdimerisation efficiency and transcriptional activity of CtBP1 and CtBP2 isoforms. To confirm the observed formation of the functional repressor was due to CtBP dimerisation, we used the monomeric CtBP mutants as a negative controls. This specific point mutation (G189A) in the NAD(H) binding motif of hCtBP2 (GXGXXG) was chosen. The alanine substitution in CtBP2 NAD(H) binding domain makes CtBP2 insensitive to NADH. The mutation was introduced via PCR mutagenesis (Figure 2.18). Two PCR reactions were carried out to amplify the 5'- and the 3'- portions of the DNA to be mutated (Figure 2.19 A). Two PCR products were mixed and used for another PCR using just the CtBP2 primers (Figure 2.19 B). The PCR product was then sub-cloned into the pTCHP16. The construct was then cloned into the pAH68 plasmid (Figure 2.19 C) and integrated onto the chromosome of SNS118 (Figure 2.19 D).

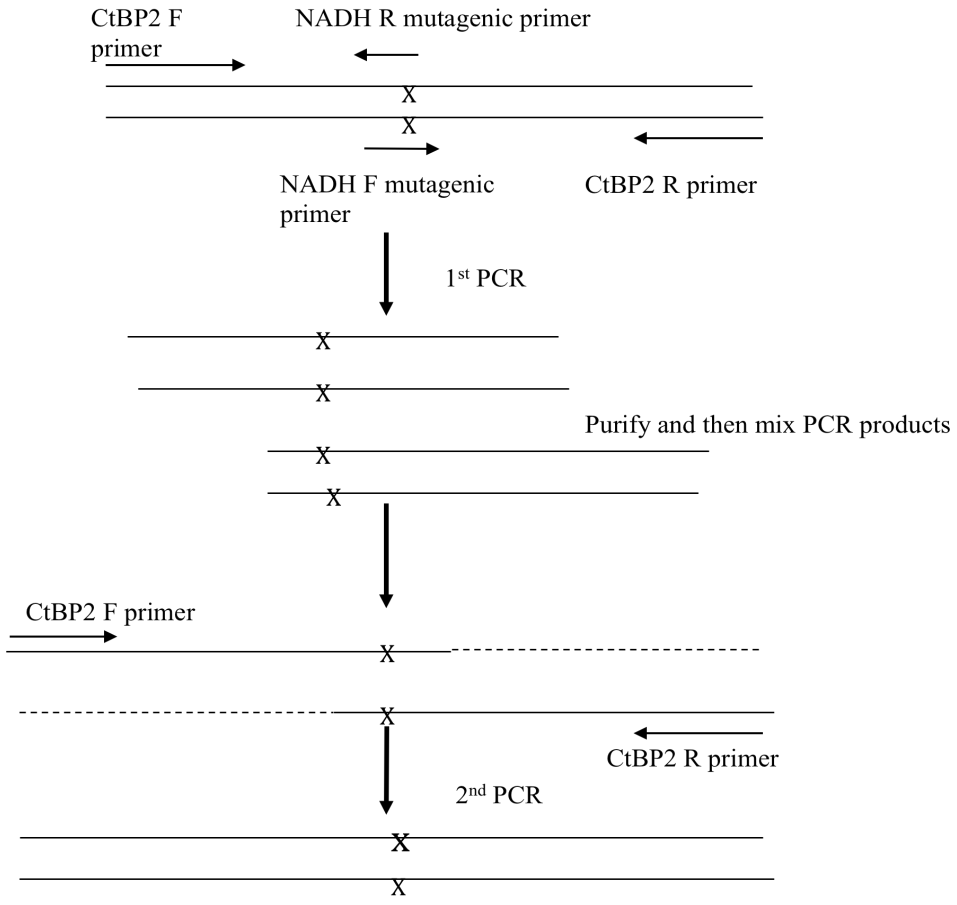

Figure 2.18. Diagram illustrating the PCR mutagenesis methodology.

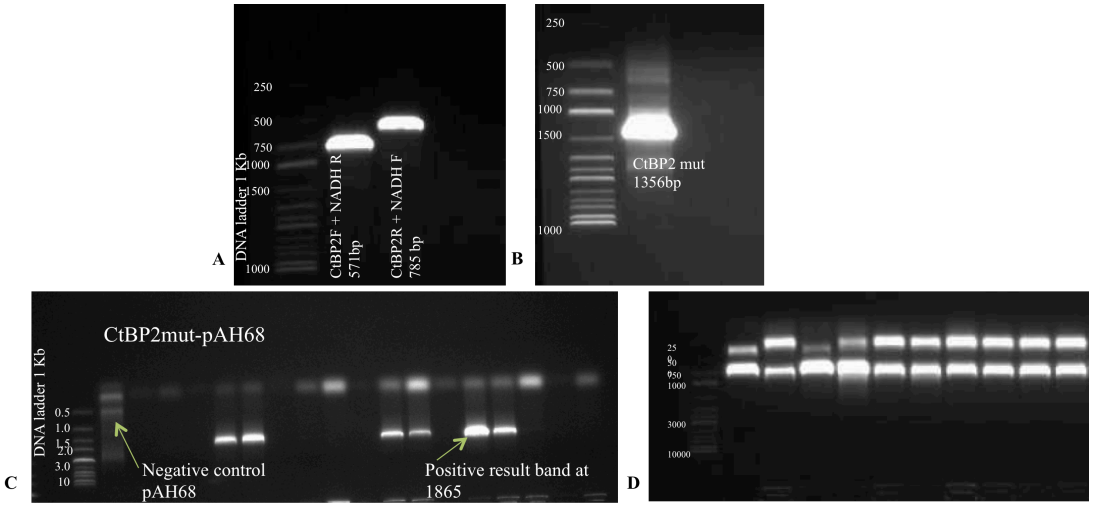

Figure 2.19. (A) Gel of PCR product from the 1st PCR, (B) gel of PCR product from the 2nd PCR both illustrated above (Figure 2.18) (C) gel of colony PCR to check the insertion of CtBP2mut into pAH68. (D) gell of integration of CtBP2mut on to the chromosome.

Figure 2.20 shows a set of minimal media plates with increasing amount of IPTG. P6UEV and CtBP2wt were used as controls and four different putative of CtBP2mut were drop spotted in dilutions of 10 from left to right. The addition of IPTG leads to dimerisation and the production of fusion proteins. That leads to the active repressor being formed which results in inhibition of transcription of the reporter genes downstream, which results in cell death. On the plate with zero IPTG all the cells grew but as the amount of IPTG was increased the cells struggled to grow on the more diluted spots. These results show that there is dimerisation occurring in CtBP2mut albeit less that the wt.

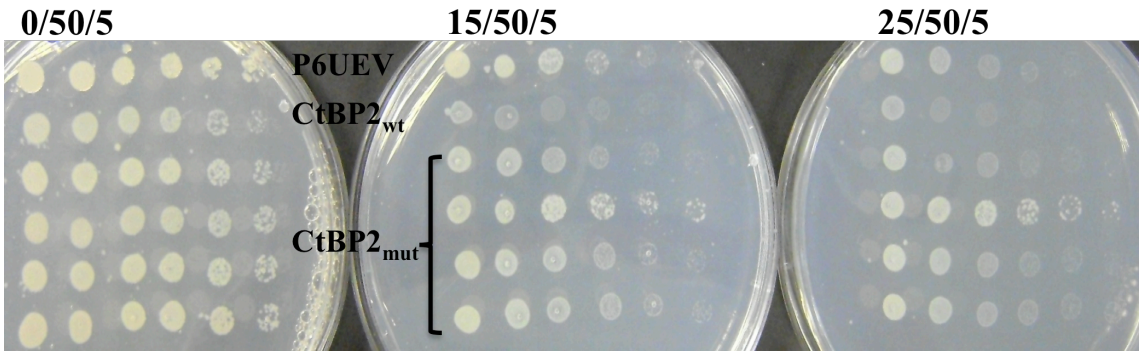

Figure 2.20. Minimal media plates, cultures drop spotted in dilutions of 10 from left to right. P6 UEV and $CtBP2_{wt}$ were used as controls, followed by 4 putatives of $CtBP2_{mut}$. Levels of IPTG added to the plate's increases from left to right.

2.2.4. CtBP Heterodimeric RTHS

Due to most of the restriction sites in the pTCHP14 MCS being present within the CtBP1 and CtBP2 gene, truncations containing the CtBP dimerisation domains (CtBP1dim and CtBP2dim) were used to construct the CtBP1/CtBP2 heterodimeric RTHS. For CtBP2, amino acids 82 to 330 were amplified via PCR. The CtBP2dim gene was incorporated into pTCHP14 Plasmid using *SalI* and *Sac*I restriction sites. For CtBP1, amino acids 76 to 324 were amplified via PCR. The CtBP1dim gene was incorporated into pTCHP14 Plasmid using *SmaI* and *Kpn*I restriction sites (Figure 2.21). The RTHS construct was then integrated into pAH68. Attempts were made to incorporate the construct onto chromosome of SNS118. Again, from the colony PCR there were no positive colonies. Due to time constraints no further work was carried out on the CtBP heterodimeric system.

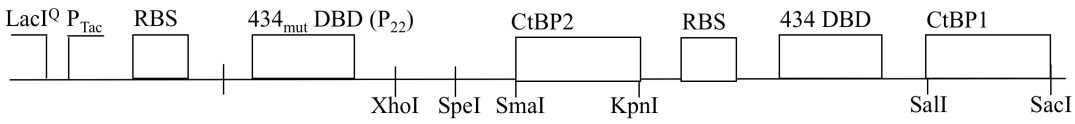

Figure 2.21. CtBP2 heterodimeric construct.

2.3. SICLOPPS

2.3.1. Construction of Library

To identify cyclic peptides that inhibit CtBP1 homodimeric interaction, SICLOPPS[31 34] library was constructed using degenerate oligonucleotides that code for the C- and N-terminus of the Synechocytis sp PCC6803 DnaE split inteins joined by a predetermined number of random amino acids. A PCR-based technique was used in which the random oligonucleotides of the library are incorporated into the forward primer between the region that binds the 3' end of I_C and the 5' end of I_N. The reverse primer anneals to the chitin-CBD, amplifying the I_N-CBD fusion gene (CBDr primer). The variable region was encoded from of NNS, where N represents any of the four DNA bases (A, C, G or T) and S represents C or G. The NNS sequence generates 32 codons (4X4X2) and encodes all 20 amino acids while eliminating both ochre (UAA) and opal (UGA) stop codons from the library. Amber stop codons (UAG) are represented in the library at a frequency of 1/32.[33] The intein chemistry requires the first amino acid to be a nucleophilic cysteine or serine. There is no limit on the number of amino acids in the target peptide.

It had been previously reported that after the first PCR, half of the amplified DNA fragments contain mismatches in the random nucleotide region,[34, 106] and this may be due to the complexity of the library. A second PCR using a "zipper" primer corresponding to the 3' end of I_C was therefore used to ensure the annealing of all DNA sequences to their complimentary strand. Either Deepvent or Gotaq polymerases were used for PCR but the PCR efficiency was greater when using Gotaq and more DNA was obtained. The PCR product and pARCBD plasmid were digested with BglI and HindIII. Digested products were gel purified. The pARCBD was treated with shrimp alkaline phosphotase to prevent re-ligation of the backbone plasmid. A 1:1 plasmid/insert overnight ligation at 4 °C was set up, and a control was also run using pARCBD plasmid and water. It was important to have high transformation efficiency in order to have a high library size. Therefore, after ligation the enzyme was heat killed and then dialysed to remove salt and contaminant, which are known to decrease efficiency. For dialysis, a Millipore membrane was floated shiny side up on deionised water in a falcon tube, and the sample was carefully pipetted on to the centre of the membrane. The tube was covered and left for 2 hr before transformation of the dialysed mixture into

NEB10β electrocompetent cells. The electroporation cuvettes were pre-chilled on ice before transformation, and it was also important to add recovery solution immediately after electroporation as a delay of 1 min was found to cause a 3-fold reduction in efficiency.

Upon intercellular expression of the SICLOPPS intein for the transformed plasmid, the split inteins process to give a library of cyclic peptides. Combining the bacterial RTHS with SICLOPPS enables the rapid screening of a large library of compounds against a chosen protein-protein interaction.[17a, 17b] The selection process links survival of a bacterial cell on minimal media to the distruption of a chosen protein-protein interaction. Inhibition of dimerisation by a cyclic peptide distrupts the repressor, allowing the expression of the reporter genes, resulting in the survival of the host cell on selective media.

Four SICLOPPS libraries were constructed for screening the CtBP RTHS, One encoding SGWXXXX (X = any amino acid) cyclic heptomers, another encoding SGWXXXXX cyclic octamers and the other two encoding SGWXXXXXX cyclic nonamers and C+5 cyclic hexamers as previously described.[31] The SGW sequence allows efficient circular ligation. The SGW cyclic peptide libraries were designed to contain an invariable motif of serine (required nucleophile for intein processing), glycine (avoids racemisation during chemical synthesis and tryptophan (functions and a chromophore for HPLC purification). The C+5 cyclic peptide libraries were designed to contain an invariable motif of cysteine (required nucleophile for intein processing).

2.3.2. Screening of peptides in the CtBP1 RTHS

The SICLOPPs library was transformed into the CtBP1 RTHS strain and plated onto histidine-free minimal media plate supplemented with arabinose (inducer of SICLOPPS), IPTG (Inducer of selection strain), Kan and 3-amino-1,2,3-triazole (3-AT, a competitive inhibitor of HIS3 gene product). The plates were incubated until colonies were readily visible (Figure 2.22A). Individual colonies were picked and restreaked onto rich media plates containing Spectinomycin (resistance from the selection strain) and Chloramphenicol (resistance from the SICLOPPS plasmids) (Figure 2.22 B). To eliminate false positives, several filtering steps were developed that enabled rapid and

convenient assessment of candidates. Aberrant selectants could arise because of the possibility of damage to the expression of SICLOPPS or the CtBP fusion and they were detected by (1) the failure of IPTG to inhibit growth; (2) the inability of arabinose to improve growth; and (3) the inability to confirm the expected phenotype upon retransformation of the plasmid.

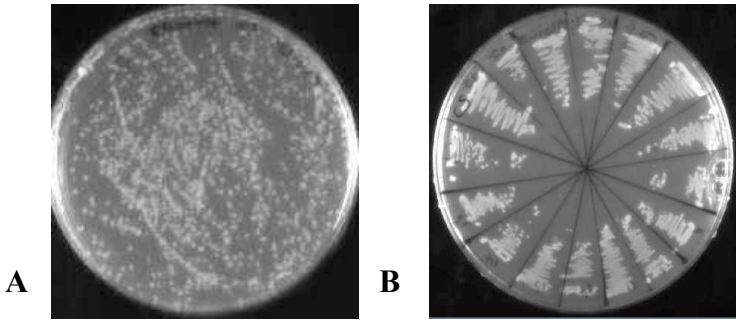

Figure 2.22. (A)Typical selection plate, (with IPTG and Arabinose), (B) restreaking of colonies from selection plate.

Surviving colonies were harvested overnight and then drop spotted onto selection minimal media plates with and without arabinose in order to screen against arabinose-dependent growth advantage to eliminate false positives (Figure 2.23). Plasmids showing growth advantage on plates with arabinose were isolated and retransformed into the CtBP1 selection strain to confirm the expected phenotype. After isolation of the SICLOPPS plasmids containing potential inhibitors and retransforming into the CtBP1-68-8.1 selection strain, 44 potential peptides showing growth advantage on arabinose plates were isolated (Figure 2.24).

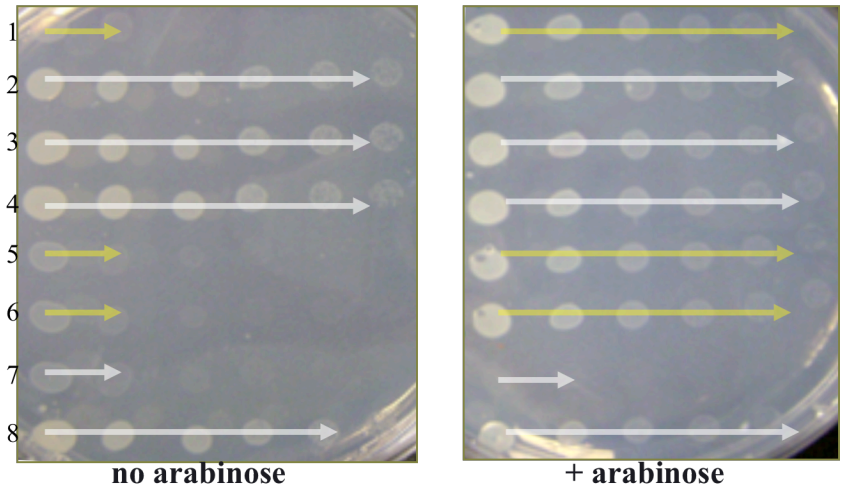

Figure 2.23. +/- arabinose Drop spotting of potential cyclic peptide inhibitor in the reporter strain CtBP1-68-8.1.

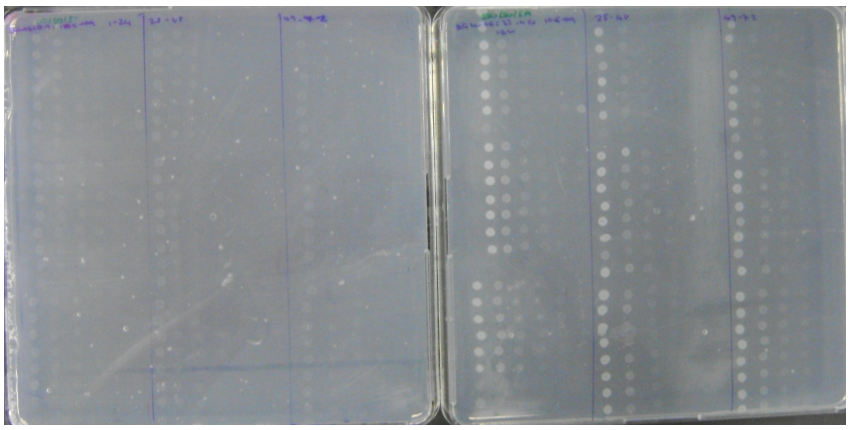

Figure 2.24. Retransformation of CtBP1 SGW+6 SICLOPPS plasmids into CtBP1 selection strain.

To assess the selectivity of the identified peptides, the corresponding SICLOPPS plasmids were retransformed into a RTHS monitoring the interaction of an unrelated protein, ATIC[17a] (a homodimeric enzyme in the de novo purine biosynthesis pathway). This step identifies any false positive results due to binding to regions of the RTHS unrelated to CtBP1 (example shown in Figure 2.25).

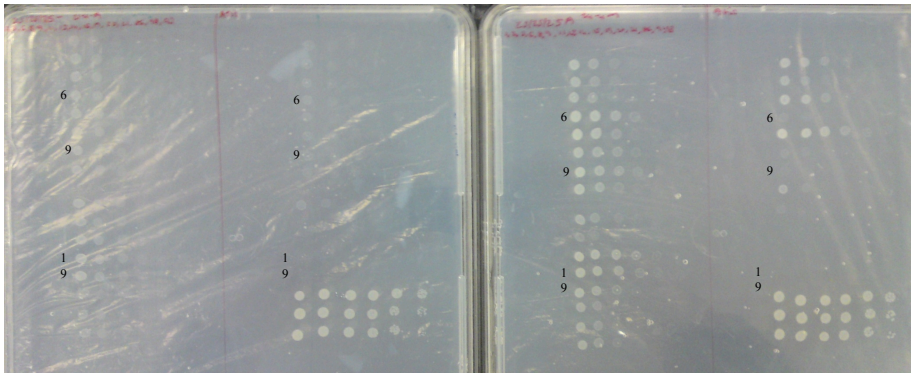

Figure 2.25. Drop spotting of Potential Peptides inhibitors (1-3, 6-9, 11, 13-15, 19-21) for CtBP1 transformed in CtBP1 (left on both plates) and ATIC (right on both plates) on minimal media plates without (left) and with (right) arabinose. Peptides that made it through all the screens are highlighted.

23 plasmids showed specificity for CTBP1. These plasmids were then transformed into the CtBP2-68-118-10 selection strain (Figure 2.26). CtBP1 and CtBP2 are very similar in sequences; they share 78% in amino acid identity and 83% similarity. So, it was interesting to find that some of these peptides were specific inhibitors of CtBP1.

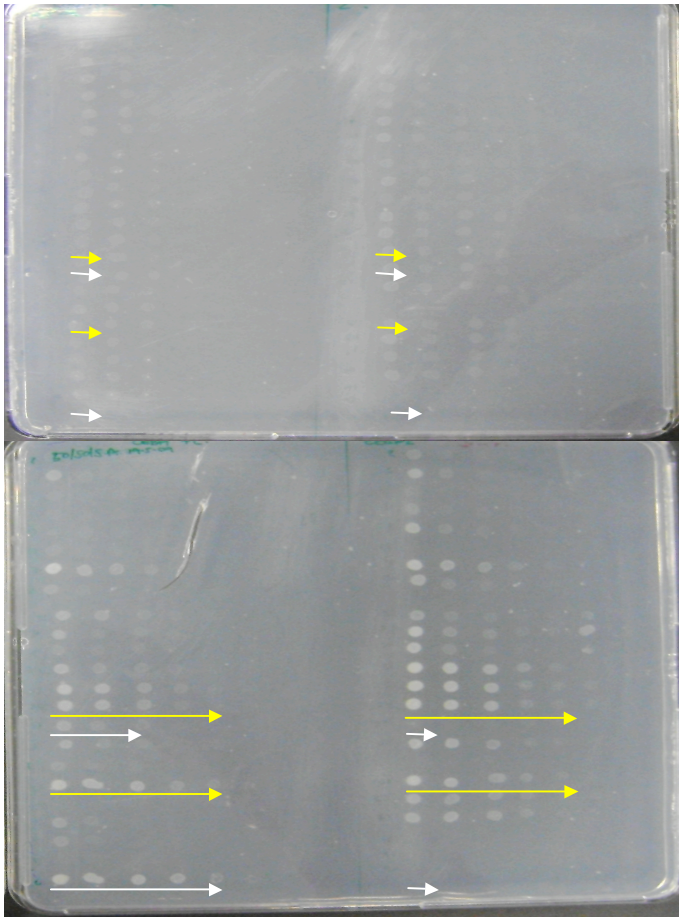

Figure 2.26. Drop spotting of Potential Peptides inhibitors for CtBP1 transformed in CtBP1 (left on both plates) and CtBP2 (right on both plates) on minimal media plates without (above) and with (below) arabinose. Examples of putative showing growth advantage in CtBP1 are highlighted in white, and those showing growth advantages in both CtBP1 and CtBP2 are highlighted in yellow.

One of the benefits of genetically encoded combinatorial libraries is the ease of deciphering their chemical composition, compared to synthetically derived libraries. SICLOPPS plasmids were sent for DNA sequencing to determine the amino sequence of the variable region present on the selected SICLOPPS plasmid (Figure 2.27). Peptide 6, 9, 19 and 31 were selective for both CtBP1, 10 other peptides that the showed activity in both the CtBP1 and CtBP2 screen were sequenced.

A

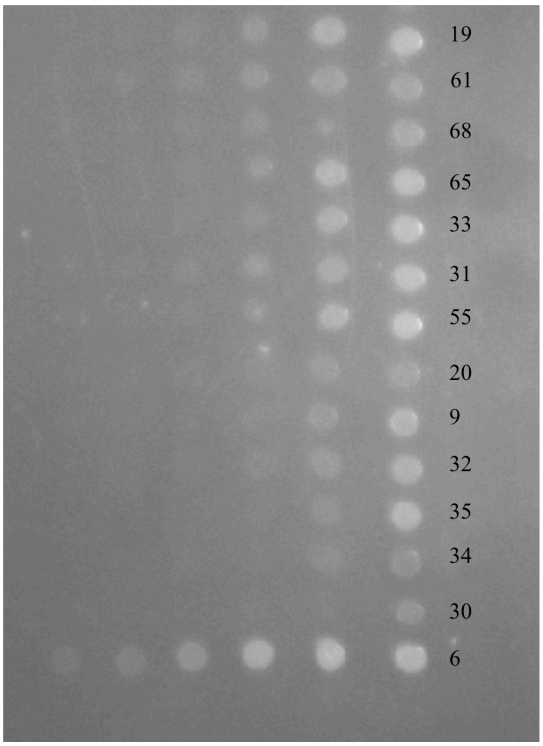

B

Activity	Name	Peptide sequence
1	19	T Y S V S G W
1	61	T V V R M Y S G W
1	68	P L S T W Y S G W
1	65	R L I R L Y S G W
1	33	N R Y Y F C
1	31	L L I V V C
1	55	V I W W L C
2	20	-
2	9	R V Y F L C
2	32	R Y F N V C
2	35	R V Y F L C
2	34	T I Y L Y C
2	30	I I L W Y C
1*	6	N T V R S S G W

Figure 2.27. Sequenced selected SICLOPPS peptides, (A) Drop spotting, (B) Table showing peptide sequence and scoring of activity (1* most active, 1 active 2 least active). Peptides 6, 9, 19 and 31 were selective for both CtBP1, the other peptides showed activity for both CtBP1 and 2. Sequencing for peptide 20 failed.

2.3.3. Screening of peptides in the CtBP2 RTHS

The SGW+6 and C+5 libraries were transformed into the CtBP2-68 in SNS118 strain. The initial drop spotting showed that all the colonies picked from the screening plate had growth advantages on arabinose plates. The corresponding SICLOPPS plasmids were isolated and retransformed into the CtBP2 strain. When retransforming CtBP2 SICLOPPS plasmid into the CtBP2 selection strain, the colonies did not grow as expected with colonies showing a growth advantage on both +/- arabinose plates. Different libraries and different selection conditions were tried but the same results were observed, which indicated a fault in the RTHS construct. Due to time constraints the CtBP2 selection was not carried further, and peptides from the CtBP1 screen were synthesised for testing in mammalian cells.

2.4. Peptide Synthesis

The selected peptides were synthesized and purified to examine their effect on CtBP activity *in vitro*. Due to the low yields obtained when using SICLOPPS to produce cyclic peptide production *in vivo*, all peptides were synthesized via solid phase peptide synthesis (Figure 2.28). Peptides were made using Fmoc solid-phase chemical synthesis, starting with the carboxy-terminal amino acid attached to the Wang resin, and adding one amino acid at a time to the amino terminal end to build the peptide. One of the advantages of the Fmoc method is that it allows for milder deprotection conditions to be used. This method utilizes 20% piperidine as a base in DMF in order to remove the Fmoc group, which exposes the α-amino group for subsequent reaction with an incoming activated amino acid. Unlike the BOC method, which uses acid to deprotect the α-amino group, Fmoc SPPS uses a base for deprotection, and thus the exposed amine is neutral. Therefore, no neutralisation of the peptide is required after deprotection. Along with development of Fmoc SPPS, different resins have been developed in order to remove the peptide from the resin by TFA.

There are many advantages to solid phase peptide synthesis:

- The reactions can be driven to completion by the addition of excess reagents, and any excess reagents can be removed by washing the resin with suitable solvents.
- Reactions, which show low chemoselectivity can be directed by the attachment to an appropriate resin.
- Resins allow for the rapid diffusion of reagents and accommodate increasing peptide length.

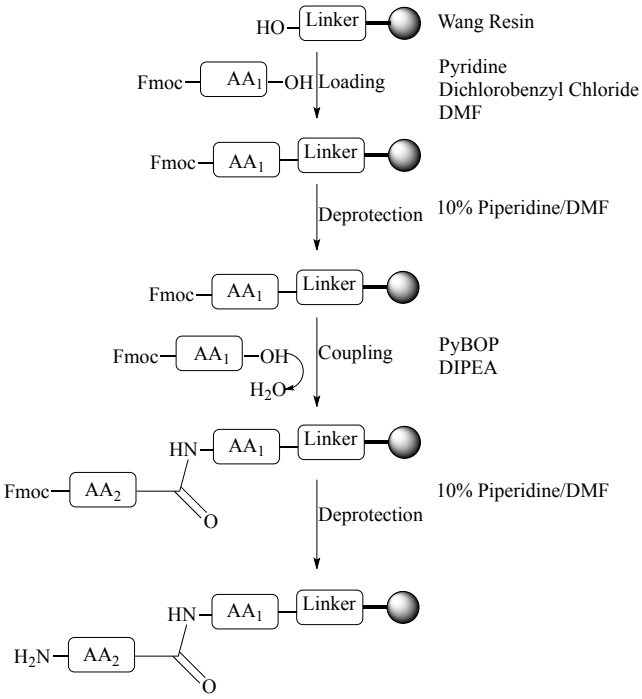

Figure 2.28. Standard reaction scheme for solid phase peptide synthesis.

Monitoring the reactions in the solid phase is not as straight forward as in the solution phase. It is not possible to use TLC, NMR and IR to monitor the reactions in the solid phase because the product is attached to the polymeric support. To utilize these characterization methods, a small sample of the product has to be cleaved from the resin. However, this was not a viable option with our work because the reactions were initially performed on a small scale. Instead, the Kaiser test was used (Figure 2.29). The Kaiser test is a qualitative test for the presence or absence of a free amino group, and it can be a useful indication for the completeness of a coupling step. The test is based on the reaction of ninhydrin with primary amines, which gives a characteristic dark blue colour on removal of the Fmoc group and a straw yellow colour in the presence of an Fmoc protected amino group. The test requires minimal amount of analyte and is completed within a few minutes. The Kaiser test was therefore used after every coupling and deprotection step to determine if the reaction was successful.

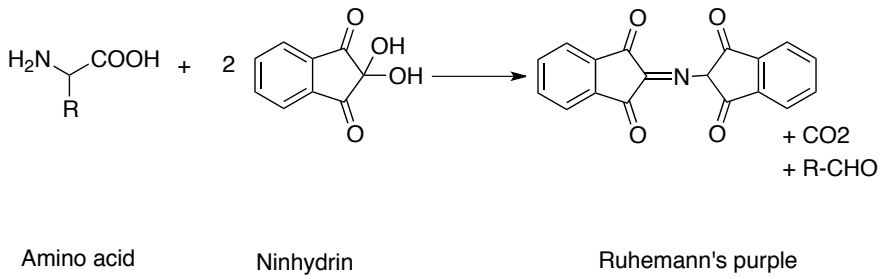

Figure 2.29. Reaction scheme for the Ninhydrin test.

After total synthesis of the peptides, they were cleaved from the resin and deprotected. The cysteine of cysteine containing peptides was subsequently protected with 2,2'-Dithiodipyridine (Aldrithiol). Once peptides were synthesised, they were characterized by mass spectroscopy and analytical HPLC. The peak corresponding to the cyclic peptide was isolated from the HPLC and the mass ion obtained from the mass spectroscopy showed that the desired sequence was observed.

Transport of proteins and peptides across the cell membrane is challenging, due to the impermeable nature of the cell membrane that restrict cellular drug uptake to small (<600 Da) and to hydrophobic molecules. Methods of cellular delivery include microinjection, electroporation, receptor-mediated endocytosis and scrape loading. There are certain drawbacks each of these methods such as cell toxicity, low transfer efficiency and being time consuming. To improve cyclic peptide delivery into targeted mammalian cells, a short peptide sequence derived from the 86-mer trans-activating transcriptional activator (Tat) protein encoded by the Human immunodeficiency virus type 1 (HIV-1) was attached to the cyclic peptides through a disulfide bond between two cysteines. The Tat sequence has previously been shown to aid the translocation of a variety of proteins across the plasma membrane of mammalian cells.[107] The region responsible for the cell penetrating properties has shown to be confined to a stretch of 9 basic amino acids RKKRRQRRR. The cationic charges of the peptide and the anionic charges of the membrane component initiate the membrane adsorption of the peptide. The cationic charge plays a role in the uptake process and a single deletion or substitution of basic charges induced a reduction of the cell association of the peptide.[108] The non-random region of the cyclic peptide was changed from SGW to

CGW and a cysteine was added to the beginning of Tat to enable the joining of the cyclic peptide to Tat via a disulphide bond.

Peptides 6 and 61 were chosen initially for synthesis, as peptide 6 was the most potent inhibitor of CtBP1 and peptide 61 was the most active inhibitor for both CtBP1 and CtBP2.

2.4.1. Peptide 61

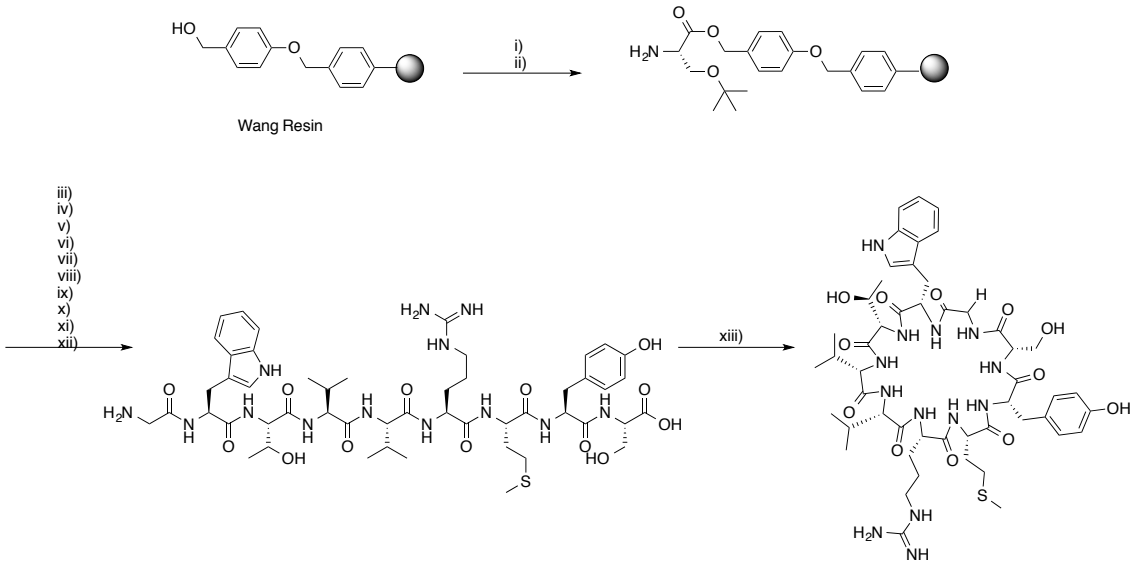

Scheme:1 (i) Fmoc-Ser(tBu)-OH, DMF 15 min, rt ; (ii) Pyridine, 2,6 dichlorobenzyl chloride, 15 hr rt; (iii) Fmoc-Tyr(tBu)-OH, PyBop, DIPEA; 2 hr rt; (iv) Fmoc-Met-OH, PyBop, DIPEA; 2 hr rt; (v) Fmoc-Arg(Pmc)-OH, PyBop, DIPEA; 2 hr rt; (vi) Fmoc-Val-OH, PyBop, DIPEA; 2 hr rt; (vii) Fmoc-Val-OH, PyBop, DIPEA; 2 hr rt; (viii) Fmoc-Thr(tBu)-OH, PyBop, DIPEA; 2 hr rt; (ix) Fmoc-Trp(Boc)-OH, PyBop, DIPEA; 2 hr rt; (x) Fmoc-Gly-OH, PyBop, DIPEA; 2 hr rt; (xi) 94% TFA, 2.5% EDT, 2.5% water, 1% TIS 3 hr, rt; (xii) EDC, HOBt, DCM, 24 hr, rt.

As Scheme:1 shows, the first step in the synthesis of peptide 61 is to load the Wang resin with serine residue. After washing, any remaining hydroxyl groups of the resin were benzoylated with 150 µl 2, 6-dichlorobenzoyl chloride and 150 µl pyridine in 4 ml DMF for 2 h. It has been reported that the use of 2, 6-dichlorobenzoyl chloride procedure did not lead to the formation of dipeptides due to premature cleavage of the

Fmoc-group under basic condition when using DCC/DMAP.[109] The Kaiser test was carried out to test for the coupling of an amino acid and the removal of the Fmoc group.

On completion of the linear peptide the peptide was cleaved from the resin using TFA. During this process highly reactive cationic species are generated from the protecting groups and the linkers on the resin, and these can, unless trapped, react with and hence modify those residues containing nucleophilic functional groups: Trp, Met, Tyr and Cys. To prevent this, various nucleophilic reagents (known as scavengers) are added with TFA to quench these ions. In our case, TIS and water were added. The amino acids Met, Cys, Trp are extremely susceptible to alkylation by cations produced during the cleavage process. When these amino acids are present the most commonly used scavenger is EDT as it is a good scavenger for *t*-butyl cations. It also assists in the removal of the trityl protecting group and is particularly effective in preventing acid catalysed oxidation of Trp residues.

Crude peptide mixtures were subjected to reverse-phase chromatography, on a Waters HPLC system by using water/acetonitrile gradient with 0.1% trifluoroacetic acid. A typical program was 95:5 (water:acetonitrile) for 10 min and then the flow was then changed to 50:50 and held for 15 minutes before reducing the flow was reduced to 95:5 for 5 min. Mass analysis was performed via HM ESI+ mass spectrometry .

After HPLC purification, the solvent was removed on the rotary evaporator and dried in the desiccator overnight to ensure the peptide was dry. It was also important to ensure that the glassware used in the reactions was dry, and that dry DMF was also used as the reaction solvent for cyclisation. This was necessary because the presence of water resulted in a low yield of cyclic peptide and ~50% of the peptide remaining linear (Figure 2.30).

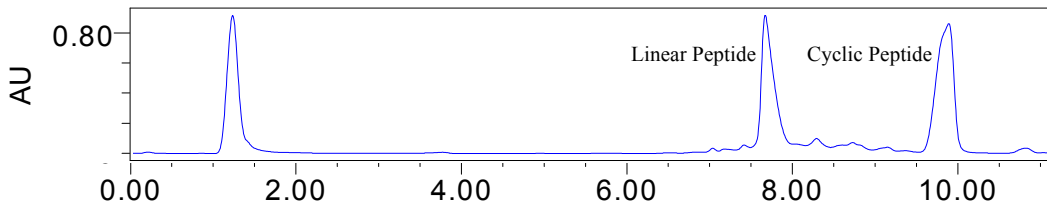

Figure 2.30. HPLC trace of the cylisation reaction.

The cyclisation also needed to be performed under high dilution, in order to prevent oligomerisation. Cyclisation was carried out by mixing the linear peptide with EDC, which is used as a carbonyl activating agent for coupling of primary amines to yield an amide bond. HOBt was also added to the reaction mixture, and this is one of the most widely used reagents in peptide synthesis due to the excellent reactivity and chiral stability of OBt esters of amino acids and peptides. The crude cyclised product was purified via HPLC (prep6040 (50:50 flow changed to 60:40 for 10 min)). Mass analysis was performed via HM ESI+ mass spectrometry

2.4.2. Pep6

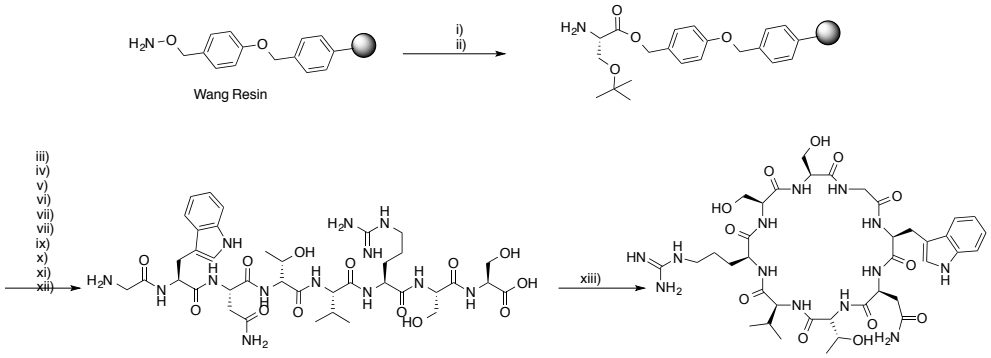

Scheme:2 (i) Fmoc-Ser(tBu)-OH, DMF 15 min, rt ; (ii) Pyridine, 2,6 dichlorobenzyl chloride, 15 hr rt; iii) Fmoc-Ser(tBu)-OH, PyBop, DIPEA; 2 hr rt; (iv) Fmoc-Arg(Pmc)-OH, PyBop, DIPEA; 2 hr rt; (v) Fmoc-Val-OH, PyBop, DIPEA; 2 hr rt; (vi) Fmoc-Thr(tBu)-OH, PyBop, DIPEA; 2 hr rt; (vii) Fmoc-Asn(Trt)-OH, PyBop, DIPEA; 2 hr rt; (viii) Fmoc-Trp(Boc)-OH, PyBop, DIPEA; 2 hr rt; (ix) Fmoc-Gly-OH, PyBop, DIPEA; 2 hr rt; (x) 94% TFA, 2.5% EDT, 2.5% water, 1% TIS 3 hr, rt; (xi) EDC, HOBt, DCM, 24 hr, rt.

Scheme:2 shows the synthesis of peptide 6; the same procedure as for peptide 61 was followed. Peptide 6 is soluble in water due the presence of two hydrophilic serine amino acids, an arginine, a threonine and an asparagine amino acid.

2.4.3. Tat

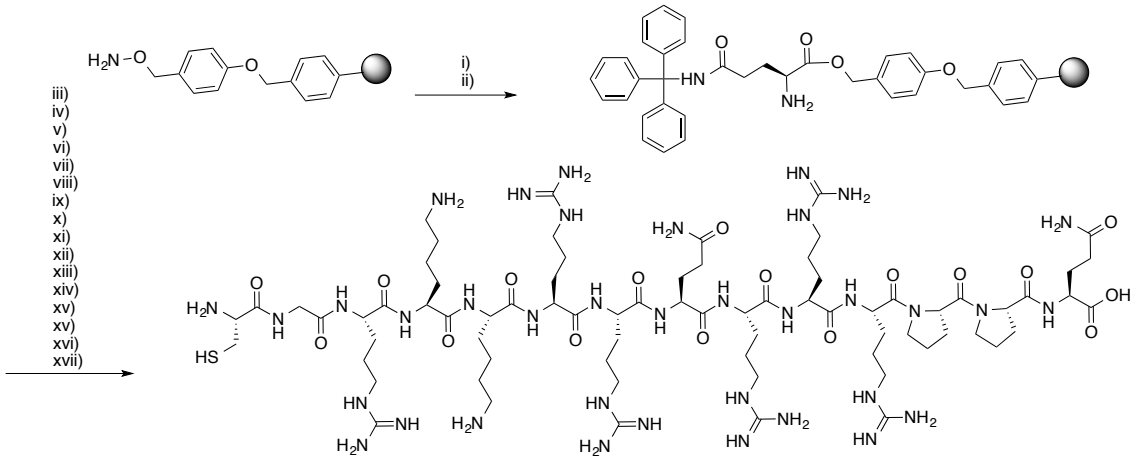

Scheme:3 (i) Fmoc-Gln(Trt)-OH, DMF 15 min, rt ; (ii) Pyridine, 2,6 dichlorobenzyl chloride, 15 hr rt; iii)Fmoc-Pro-OH, PyBop, DIPEA; 2 hr rt; (iv) Fmoc-Pro-OH, PyBop, DIPEA; 2 hr rt; (v) Fmoc-Arg(Pmc)-OH, PyBop, DIPEA; 2 hr rt; (vi) Fmoc-Arg(Pmc)-OH, PyBop, DIPEA; 2 hr rt; (vii) Fmoc-Arg(Pmc)-OH, PyBop, DIPEA; 2 hr rt; (viii) Fmoc-Gln(Trt)-OH, PyBop, DIPEA; 2 hr rt; (x) Fmoc-Arg(Pmc)-OH, PyBop, DIPEA; 2 hr rt; (ix) Fmoc-Arg(Pmc)-OH, PyBop, DIPEA; 2 hr rt; (x) Fmoc-Lys(Boc)-OH, PyBop, DIPEA; 2 hr rt; (xi) Fmoc-Lys(Boc)-OH, PyBop, DIPEA; 2 hr rt; (xii) Fmoc-Arg(Pmc)-OH, PyBop, DIPEA; 2 hr rt; (xiii) Fmoc-Gly-OH, PyBop, DIPEA 2 hr rt; (xiv) Fmoc-Cys(Trt)-OH, PyBop, DIPEA 2 hr rt. (xv) 94% TFA, 2.5% EDT, 2.5% water, 1% TIS 3 hr, rt; (xvi) Aldrithiol, DMF, rt, 15hr; xvii) Tcep, DMF, 1 hr, rt.

Scheme:3 shows the synthesis of Tat. The standard procedure for the synthesis of linear peptides was followed. Tat can be attached to cyclic peptides in order to aid the internalisation of the peptides into mammalian cells. One challenge facing peptide synthesis is the γ-lactam formation of arginine (Figure 2.31). The formation of the γ-lactam occurs when the internal nitrogen of the guanidine attacks the activated ester,

irreversibly forming the lactam ring. This reaction is competitive with peptide-bond formation, and it greatly reduces the coupling efficiency of arginine. For efficient coupling of arginine the coupling reaction was carried out twice.

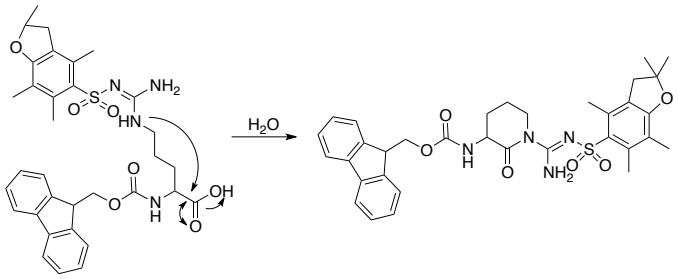

Figure 2.31. γ-Lactam Formation.

After cleavage of the peptide from the resin the sulphur of the cysteine residue was protected using aldrithiol (2,2'-Dithiodipyridine) to prevent any side reactions. The linear peptide was purified prior to cyclisation.

2.4.4. 61 Tat-Tagged

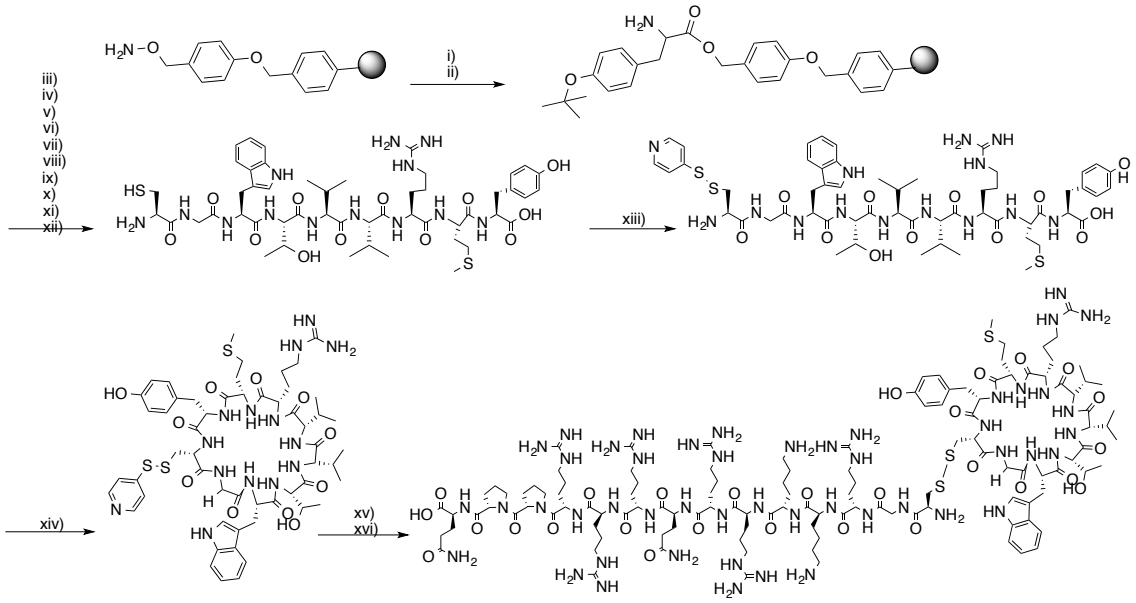

Scheme:4 (i) Fmoc-Tyr(tBu)-OH, DMF 15 min, rt ; (ii) Pyridine, 2,6 dichlorobenzyl chloride, 15 hr rt; iii) Fmoc-Met-OH, PyBop, DIPEA; 2 hr rt; (iv)Fmoc-Arg(Pmc)-OH, PyBop, DIPEA; 2 hr rt; (v) Fmoc-Val-OH, PyBop, DIPEA; 2 hr rt; (vi) Fmoc-Val-OH, PyBop, DIPEA; 2 hr rt; (vii) Fmoc--Thr(tBu)--OH, PyBop, DIPEA; 2 hr rt; (viii) Fmoc-Trp(Boc)-OH, PyBop, DIPEA; 2 hr rt; (ix) Fmoc-Gly-OH, PyBop, DIPEA 2 hr rt;(x) Fmoc-Cys(Trt)-OH, PyBop, DIPEA 2 hr rt; (xi) 94% TFA, 2.5% EDT, 2.5% water, 1% TIS 3 hr, rt; (xii) Aldrithiol, DMF, rt, 15hr (xiii) EDC, HOBt, DCM, 24 hr, rt; (xiv)Tcep, DMF, 1 hr, rt; xv)Tat-s-s-py, DMF, rt.

Scheme:4 shows the synthesis of peptide 61 Tat-tagged. The same reaction scheme as peptide 61 (Scheme:1) was followed; the serine was replaced with a cysteine in order to carry out the Tat-tagged reaction. On cleavage from the resin the cysteine was protected using aldrithiol to avoid any side reactions. The linear protected peptide was purified via HPLC prior to cyclisation. The aldritiol protecting group was removed using *tris*(2-carboxyethyl)phosphine (TCEP). TCEP is often used as a reducing agent to break disulfide bonds (Figure 2.32). TCEP has advantages over other common reducing agents such as being odourless, a more powerful reducing agent, an irreversible reducing agent, more hydrophilic and more resistant to oxidation in air. Initially 1,3-propanedithiol was used to reduce the disulphide bond via thiol exchange. A

disadvantage of this process is that the reaction takes 6 hr compared to 1 hr reaction time with TCEP. The deprotected peptide was then mixed with Tat and DMF for the final step of the Tat-tagging.

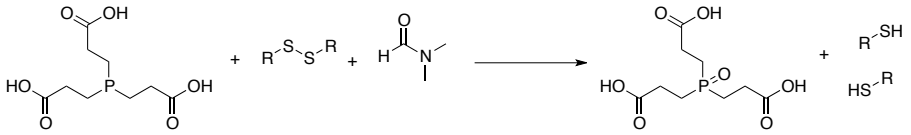

Figure 2.32. Reaction Scheme for TCEP disulphide bond reduction.

2.4.5. Peptide 6 Tat-Tagged

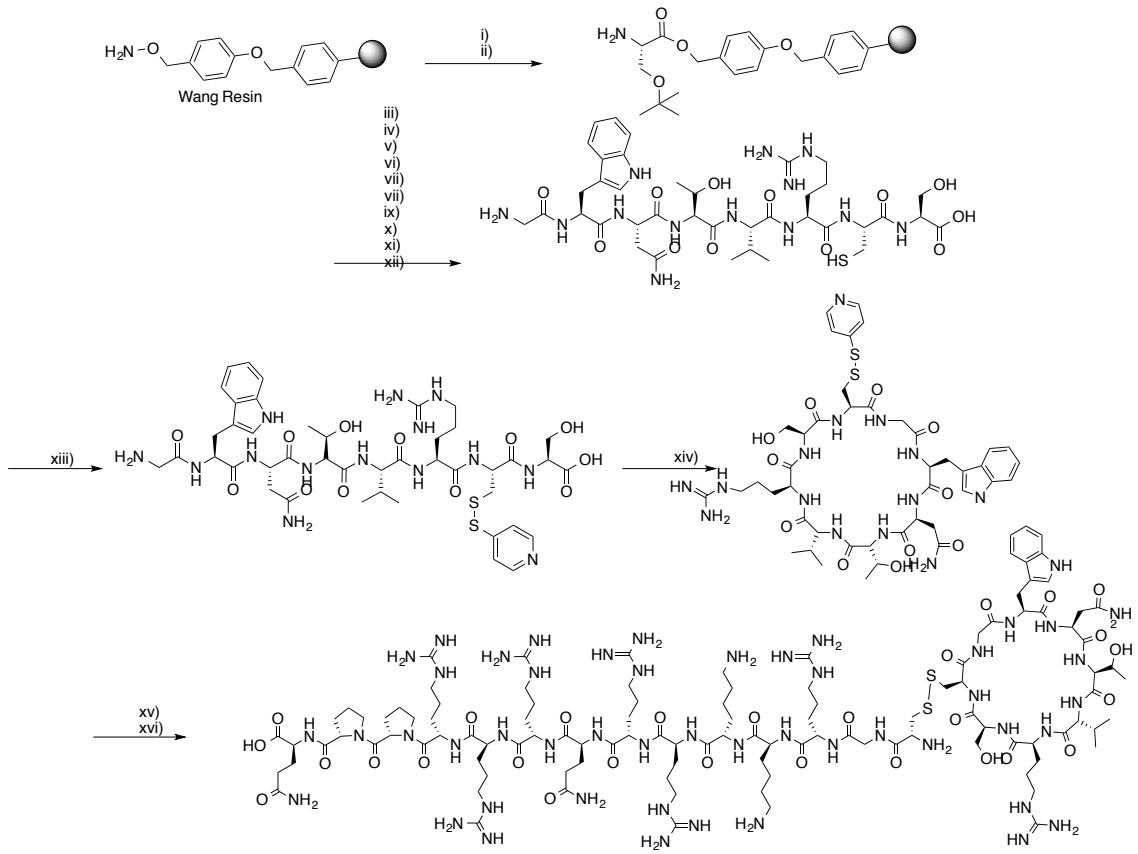

Scheme:5 (i) Fmoc-Ser(tBu)-OH, DMF 15 min, rt ; (ii) Pyridine, 2,6 dichlorobenzyl chloride, 15 hr rt; iii) Fmoc-Arg(Pmc)-OH, PyBop, DIPEA; 30 min rt; (iv) Fmoc-Val-OH, PyBop, DIPEA; 30 min rt; (v) Fmoc-Thr(tBu)-OH, PyBop, DIPEA; 30 min rt; (vi) Fmoc-Asn(Trt)-OH, PyBop, DIPEA; 30 min rt; (vii) Fmoc-Trp(Boc)-OH, PyBop, DIPEA; 30 min rt; (viii) Fmoc-Gly-OH, PyBop, DIPEA 30 min rt; (ix) Fmoc-Cys(Trt)-OH, PyBop, DIPEA 30 min rt; (x) 94% TFA, 2.5% EDT, 2.5% water, 1% TIS 3 hr, rt; (xi) Aldrithiol, DMF, rt, 15hr (xii) EDC, HOBt, DCM, 24 hr, rt; (xiii)Tcep, DMF, 1 hr, rt; xiv)Tat-s-s-py, DMF, rt.

Scheme:5 illustrates the synthesis of peptide 6 Tat-tagged. Again the serine was replaced with cysteine so that the peptide could be attached to Tat via a disulfide bond. The linear peptide was synthesised on the peptide synthesiser (CEM Liberty1 microwave peptide synthesiser). The preloaded resin was added to the reaction vessel. All the amino acid coupling and deprotection reagents were made up in bottles and connected to the machine. The Liberty1 system features microwave peptide synthesis,

which offers several advantages over conventional synthesis conditions including shorter reactions resulting in fast cycle times and higher purity peptides than conventional synthesis. Coupling time was reduced from 2 hr to 30 min. The last amino acid was left protected. On completion, the linear peptide was removed and deprotected as normal. The peptide was then cleaved from the resin. The standard procedure for cleavage from the resin, cysteine protectection, cyclisation and Tat-tagging was followed.

2.4.6. Peptide 32

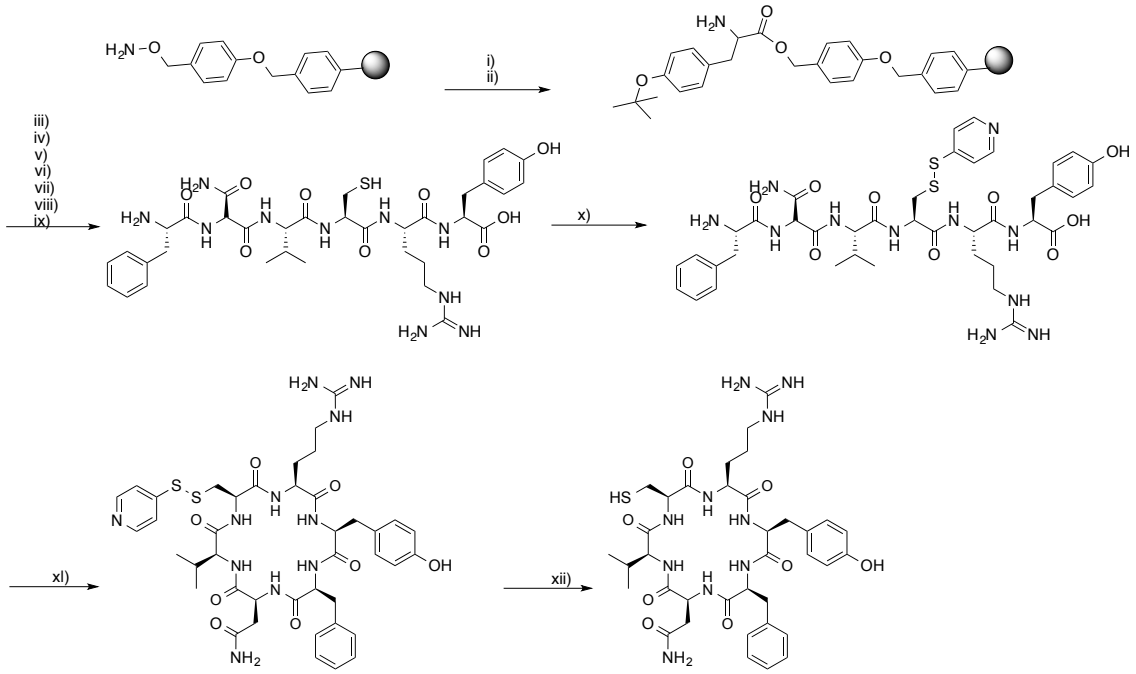

Scheme:6 i) Fmoc-Tyr(tBu)-OH, DMF 15 min, rt ; (ii) Pyridine, 2,6 dichlorobenzyl chloride, 15 hr rt; (iii) Fmoc-Arg(Pmc)-OH, PyBop, DIPEA; 2 hr rt; (iv) Fmoc-Cys(Trt)-OH, PyBop, DIPEA 2 hr rt; (v) Fmoc-Val-OH, PyBop, DIPEA; 2 hr rt; (vi) Fmoc-Asn(Trt)-OH, PyBop, DIPEA; 2 hr rt; (vii) Fmoc-Phe-OH, PyBop, DIPEA 2 hr rt; (viii) 94% TFA, 2.5% EDT, 2.5% water, 1% TIS 3 hr, rt; (ix) Aldrithiol, DMF, rt, 15hr; (x) EDC, HOBt, DCM, 24 hr, rt; (xi) Tcep, DMF, 1 hr, rt.

Scheme:6 was followed for the synthesis of peptide 32. Standard procedures were followed.

2.4.7. Peptide 33

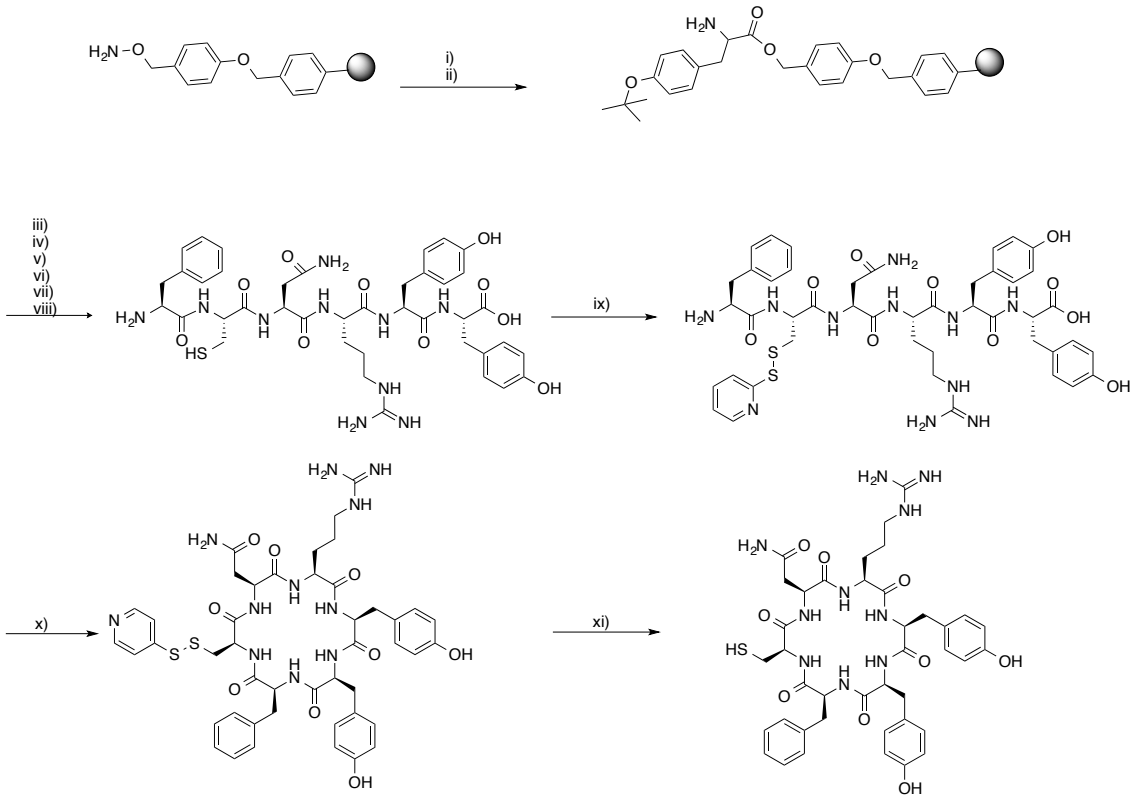

Scheme:7 i) Fmoc-Tyr(tBu)-OH, DMF 15 min, rt ; (ii) Pyridine, 2,6 dichlorobenzyl chloride, 15 hr rt; (iii) Fmoc-Tyr(tBu)-OH, PyBop, DIPEA; 2 hr rt; (iv) Fmoc-Arg(Pmc)-OH, PyBop, DIPEA; 2 hr rt; (v) Fmoc-Asn(Trt)-OH, PyBop, DIPEA; 2 hr rt; (vi) Fmoc-Cys(Trt)-OH, PyBop, DIPEA 2 hr rt; (vii) Fmoc-Phe-OH, PyBop, DIPEA 2 hr rt; (viii) 94% TFA, 2.5% EDT, 2.5% water, 1% TIS 3 hr, rt; (ix) Aldrithiol, DMF, rt, 15hr; (x) EDC, HOBt, DCM, 24 hr, rt; xi)Tcep, DMF, 1 hr, rt.

Scheme:7 was followed for the synthesis of peptide 33. Standard procedures were followed.

The RTHS has confirmed the homodimeric interaction of CtBP1 and CtBP2. The RTHS and SICLOPPS system have been combined to successfully uncover inhibitors of CtBP1 and CtBP2. The most active inhibitors were first synthesised to test *in vitro* (Chapter 3) and *in vivo* (Chapter 4) assays.

The selection of CtBP2 was not completed, it would be useful get inhibitors that just inhibit CtBP2. CtBP1-pTCHP14 and CtBP2-pTCHP14 plasmid have been constructed, these need to be integrated onto the chromosome. It will be interesting to see if these peptides inhibit the heterodimerisation of CtBPs in the RTHS/SICLOPPS screen.

3 *In* Vitro Analysis of Peptides

CtBP Protein Expression and Purification

Cloning CtBP1 into pET28 vector bacterial expression vector

Cloning CtBP2 into pET28 vector bacterial expression vector

Purification

CtBP1 Purification

CtBP2 Purification

Development of ELISA

Chapter two goes into details of the discovery and synthesis of the peptide inhibitors of CtBP1 and CtBP2. The aim of this chapter was to build an *in vitro* assay of NADH-dependant CtBP dimerisation in order to test the peptides on CtBP1/2 homodimer and heterodimers. We decided to set up an ELISA, using proteins tagged with two different tags (His-tag and GST-tag) to allow the capture and detection of the proteins. The GST reagents were already available in JPB lab therefore, we first started by making the His-tagged reagents.

3.1 CtBP Protein Purification

The expression and purification of recombinant proteins facilitates production and detailed characterisation of virtually any protein. Figure 3.1 illustrates an overview of the steps required for the expression and analysis of recombinant proteins. Recombinant DNA techniques permit the construction of fusion proteins in which specific affinity tags are added to the protein sequence of interest. The use of affinity tags simplifies the purification of the recombinant fusion proteins by employing affinity chromatography methods. In order to purify CtBP the full-length gene was cloned into the T7 expression vector pET28. The pET28 vectors carry an N-terminal His-Tag/thrombin/T7-Tag configuration plus an optional C-terminal His-Tag sequence. The His-Tag contains 6 consecutive histidine residues, which allows strong binding of the protein to a chromatography column bearing Ni^{2+} ions.

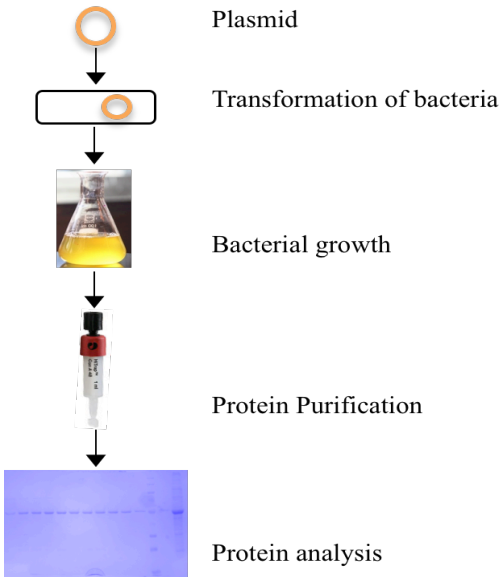

Figure 3.1. Overview of the steps involved in expression and analysis of recombinant proteins.

3.1.1 Cloning CtBP1 into pET28 vector bacterial expression vector

The full-length CtBP1 coding sequence (1320 bp) was amplified by PCR. The PCR and isolated pET28 vector were digested with *XhoI* and *NdeI* (giving a N-terminal His-tag). The digested PCR product and plasmid were then ligated using NEB T4 ligase; this resulted in the insertion of the target gene into the pET28 plasmid (Figure 3.2). This plasmid was then transformed into BL21(DE3)pLysS competent cells (Promega). BL21(DE3)pLysS also contains a plasmid, pLysS, which carries the gene encoding T7 lysozymes. T7 lysozyme is a natural inhibitor of T7 RNA polymerase and reduces the background expression levels of target genes under the control of the T7 promoter. The level of protein produced upon induction by IPTG is not affected.

3.1.2 Cloning CtBP2 into pET28 vector bacterial expression vector

The full-length CtBP2 gene (1338 bp) was amplified by PCR. The PCR and isolated pET28 vector were digested with *XhoI* and *NdeI* (giving a N-terminal His-tag). The digested PCR product and plasmid were then ligated using NEB T4 ligase; this resulted in the insertion of the target gene into the pET28 plasmid (Figure 3.2). This plasmid was then transformed into BL21(DE3)pLysS competent cells (Promega).

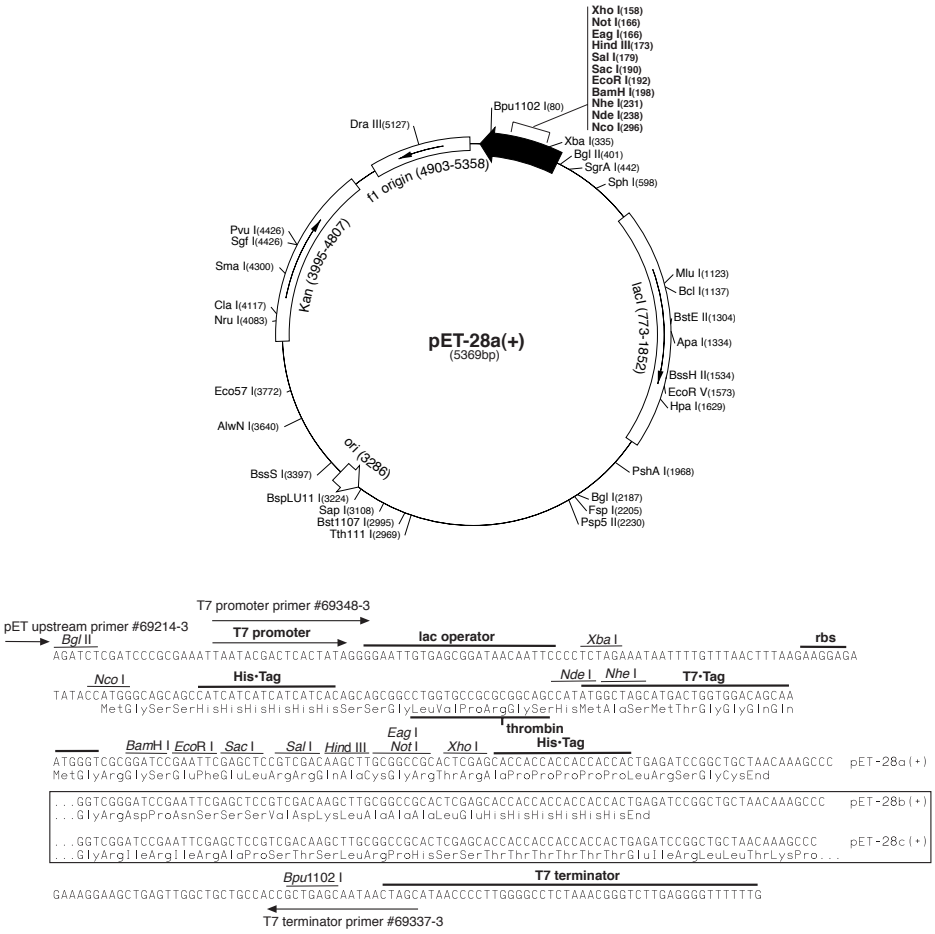

Figure 3.2. pET28 Plasmid map and sequence.

3.2 Purification

CtBP1-pET28 and CtBP2-pET28 was transformed into both BL21(DE3)pLysS and BL21-CodonPlus*(DES)-RIPL competent cells (Stratagene) to compare the purification. BL21-CodonPlus*(DES)-RIPL (RIPL) competent cells contain extra copies of rare *E.coli* argU, ileY, leuW, proL tRNA genes which correct for codon bias and dramatically improve expression of sequence from other organisms. The induction of recombinant protein expression is effected by the addition of the *lac*-inducer IPTG. It is important to identify the optimal conditions when expressing the protein in order to get the maximum amount of soluble protein. Induction in bacteria can be performed using one of two basic methods. One method is fast induction and that does not work for all proteins and can give suboptimal yield. The second method is by slow induction and can enhance the solubility of some proteins. Growing cells at lower temperature is

better, mainly because at slower growth rates proteins that may otherwise not fold well during expression will fold more efficiently, thus increasing the yield and minimising inclusion bodies (which is what happens when the protein is expressed and precipitates out). Incubation time is important and induction should be carried out at OD 0.6-0.7. At this OD most cells would have reached exponential growth, with the vast majority of cells alive and healthy, which makes them ideal for protein expression. At an OD that is too high (over 1 or higher) the culture will start to collect dead cells, which do not express protein. An OD that's too low (<0.4) has a negative impact, as most of the culture is media so there are not enough cells to make protein. Shorter induction times and lower temperatures are considered best for maintaining recombinant solubility.

500 ml cultures of CtBP1-pET28 and CtBP2-pET28 were grown at 37 °C, induction was carried out once an OD of 0.6 was reached using 0.2 mM IPTG. The flask was transferred to an incubator for 1 h 30 min at rt. The culture was centrifuged and the pellet was collected and frozen till used. The cell pellet was re-suspended in 10 ml of lysis buffer per gram of cells, which is made up of reagents used to break up the cells and release the protein. The lysis buffer contains: 0.2% Triton X 100 which helps to solubilise the protein; lysozyme which cuts the wall of the bacteria; DNAse I which cuts the DNA into small pieces and protease inhibitor which stops proteases from breaking up the protein. The cells were frozen, thawed and sonicated to further help break the bacteria. The cells were then centrifuged to separate the soluble material (supernatant) from the insoluble material (pellet). Samples were collected before and after induction, and before and after centrifugation in order to load on to the gel for analysis.

The supernatant was loaded on to the FPLC (fast protein liquid Chromatography), HisTrap crude affinity columns (GE healthcare). HisTrap crude affinity columns were used during the purification of His-tagged CtBP1 and CtBP2. These columns are ready-to-use columns and are pre-packed with pre-charged Ni Sepharose 6 Fast flow. This pre-packed column is intended for purification of histidine-tagged recombinant proteins.

For the ELISA it is important that the CtBP1 and CtBP2 proteins are purified in a predominantly monomeric form. In order to achieve this the Cell lysate was incubated with pyruvate (0.25 mM) made up in binding buffer (TrisHCl (20 mM) and NaCl (350 mM) pH 7.4) for 30 min once loaded onto the column. Pyruvate has been found to be a substrate for CtBP dehydrogenase activity although pyruvate is a relatively poor

substrate, its addition caused a release of the bound NAD(H).[110] NAD(H) binds to the nucleotide binding domain of CtBPs and promotes dimerisation.[41]

The GST-CtBP1FL and GST-CTBP2FL constructs were available in the Blaydes lab.[111] 500 ml cultures of GST-CtBP1$_{FL}$ and GST-CTBP2$_{FL}$ were grown at 37 °C. Induction was carried out once an OD of 0.6 was reached using 0.25 mM IPTG. The flask containing the mix was transferred to an incubator for 2 h at rt. Cell lysis was carried out using the same procedure as the CtBP-His proteins. The supernatant was loaded on to the FLPC, GSTrap affinity columns were used during the purification of GST-tagged CtBP1 and CtBP2. The GSTrap affinity columns are pre-packed, ready-to-use columns containing Glutathione Sepharose 4 Fast Flow. The columns are designed for a one step purification of GST fusion proteins.

3.2.1 His-CtBP1 purification

Initially the protein was lysed with lysis buffer (Table 6.18), the supernatant was filtered and loaded onto the column. Washes at lower concentration of imidazole (made up in binding buffer, Table 6.19) were carried out to try to remove any contaminants (10 mM (4%) and 20 mM (8%)) before a10 ml gradient from 20 mM to 250 mM was applied to remove bound protein. The yield and purity of protein was low (Figure 3.3) (fractions 43-49) compared to Figure 3.5 (fractions 26-40)). Proteins were expressed in both BL21(DE3)pLysS and BL21-CodonPlus*(DES)-RIPL (RIPL) competent cells. After purification it was found that more protein and less contaminants were obtained when expressed in RIPl.

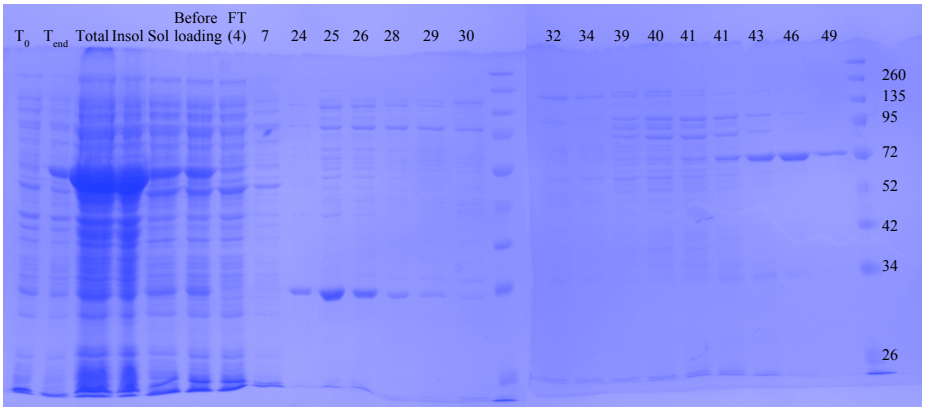

Figure 3.3. Purification of His-CtBP1 on HisTrap T_o = Sample before induction (lane 1), T_{end} = sample after induction (lane 2), Total = total cell lysate (lane 3), Insol = insoluble protein (lane 4), Sol = soluble protein (lane 5), sample before loading (lane 6), FT (4) = fraction collected from the flow through (lane 7), lanes 8-14, 16-25 are the fractions collected.

Therefore, it was decided to express the protein in the RIPL strain. Batch binding was carried out instead of column binding. The protein was captured on Ni^{++} superflow beads before applying to a column on the FPLC. A switch was made from column binding to batch binding in order to try and obtain a higher yield of protein. Batch purification allow for more efficient binding of the protein, it could be seen from Figure 3.3 the flow through fraction (lane 7) contains unbound protein. Also, a more of a shallow imidazole gradient was used to try and remove some of the contaminant observed previously. 2 ml of 50% beads were prepared by taking 1.5 ml of 75% beads and washing with 15 ml PBS. The 50% beads were added to the supernatant and incubated overnight at 4 °C on a rotator. The mixture was centrifuged at 1300 rpm (the supernatant was kept as unbound). The beads were washed twice with 50 ml of binding buffer (20 mM Tris-HCl pH 7.4, 350 mM NaCl, (wash 1 and wash 2)). The beads were then incubated with binding buffer and 0.25 mM Sodium Pyruvate for 30 min, keeping the conditions the same as the purification on the column (wash 3). The beads were incubated at 4 °C on the rotor with binding buffer and 20 mM imidazole for 20 min (wash 4). The beads were transferred onto a column and mounted onto the FPLC. 40 mM imidazole (16%), 50 mM (20%) and 60 mM (24%) was used to see if contaminants seen previously could be removed. An 18 ml gradient from 60 mM to

250 mM was run to remove bound protein. As can be seen in Figure 3.5 the protein obtained was more pure.

Fractions 30 to 33 (4ml) and fractions 28, 29 and 34 to 41 (Figure 3.5) were pooled together and dialysed against 2 L of PBS with 15% glycerol using 12 kDa MWCO (molecular weight cut-off) dialysis tubing overnight at 4 °C. The buffer was replaced with 2 L of fresh PBS and dialysis was continued for a further 2 hr. After dialysis the material was collected and the protein concentration was determined using Bio-Rad. The concentration of His-CtBP1 was 0.3 µg/µl. Gel analysis was also carried to confirm the protein concentration. The protein was aliquoted into 5 µl single use aliquots, then snap frozen and stored at -80 °C.

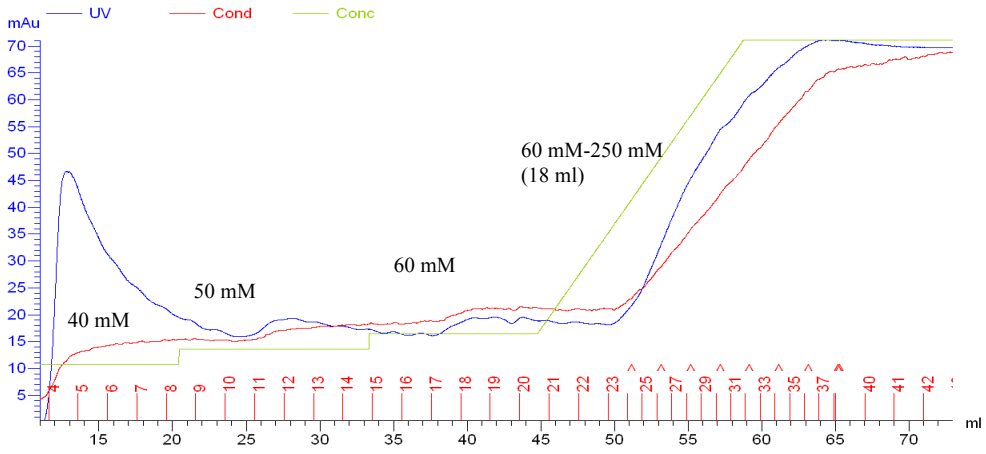

Figure 3.4. Purification of His-CtBP1 on 1 ml Ni-NTA superflow column.

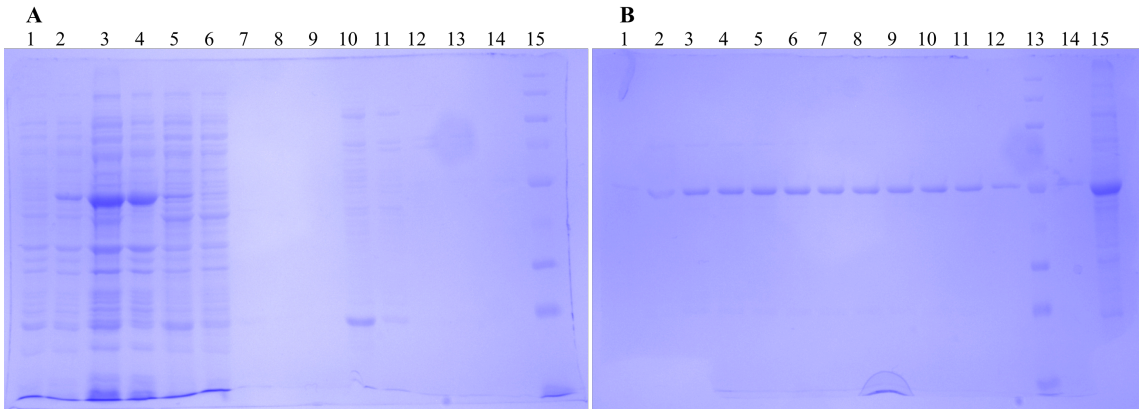

Figure 3.5. His-CtBP1 Purification fractions Gel (**A**) **1**.To (sample before induction), **2**.Tend (sample after induction), **3**.Total, **4**.Insoluble, **5**.Soluble, **6**.Unbound, **7**.Wash1 with binding buffer, **8**.Wash2 with binding buffer, **9**.Wash3 with binding buffer + 0.25 mM sodium pyruvate, **10**.Wash4 with binding buffer + 20 mM imidazole, **11**.Fraction #4, **12**.Fraction #8, **13**.Fraction #12, **14**.Fraction #19, **15**.Marker. His-CtBP1 Purification fraction Gel (**B**) **1**.Fraction #24, **2**.Fraction #26, **3**.Fraction #28, **4**.Fraction #29, **5**.Fraction #30, **6**.Fraction #31, **7**.Fraction #32, **8**.Fraction #33, **9**.Fraction #35, **10**.Fraction #36, **11**.Fraction #37, **12**.Fraction #40, **13**.Marker, **14**.Fraction #45, **15**.Beads after elution.

3.2.2 GST-CtBP1 Purification

Before purification of GST-CtBP1 was carried out a gel was run after induction to determine whether the protein was expressed, Figure 3.6 shows that after induction the protein is expressed (T_2).

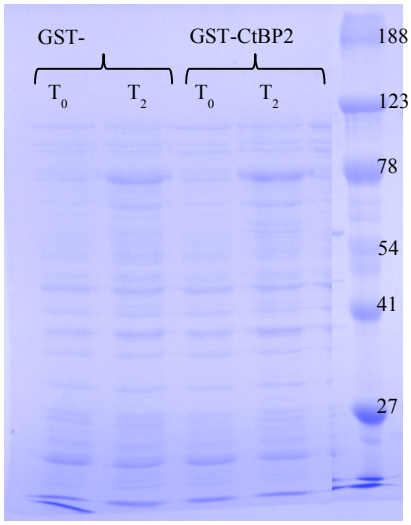

Figure 3.6. Induction of GST-CtBP1 and GST-CtBP2 (T_0 – Before induction, T_2 – After induction).

After the Bacteria were lysed, the solution was prepared for purification on 1 ml GSTrap column. Once the sample was applied to the column, the column was washed with PBS (back to baseline). Then 15 ml of 0.55 mM sodium pyruvate in binding buffer was applied to fill line A and the column, the FPLC was paused for 20 min. Then the same solution was applied for another 10 min before changing back to PBS. The total contact time with sodium pyruvate was 30 min.

There were still impurities in the GST-CtBP1, therefore requiring further purification. Fractions 27 to 30 were pooled together and diluted with 50 ml of buffer A (20 mM tris HCl pH 8 and 10 mM NaCl) to be further purified via ion exchange, using anion exchanger Q HP 1 ml column form GE (Figure 3.7). Ion exchange separates molecules or groups that have different charges. To optimise binding of all charged molecules, the mobile phase is generally a low to medium conductivity solution (i.e. low to medium salt concentration). Adsorption of the molecules to the solid support is driven by the ionic interaction between oppositely charged ionic groups in the sample molecule and functional ligands of the support. By increasing salt concentration (linear salt concentration) molecules with the weakest ionic interaction start to elute first, stronger interactions elute later. These interactions can be controlled by varying conditions such as ionic strength and pH. The pH of the mobile phase buffer must be between pI (isoelectric point) or pKa of the charged molecule and pKa of the charged group on the

solid support.[112] A pI 6.32 was calculated online (expasy.org, it requires you to enter the protein sequence). The pH needs to be greater than 1 unit above the pI ie greater then or equal to 7.5. Therefore a strong anion exchanger (Q) was used to bind the protein of interest and a start buffer with pH 8 was used.

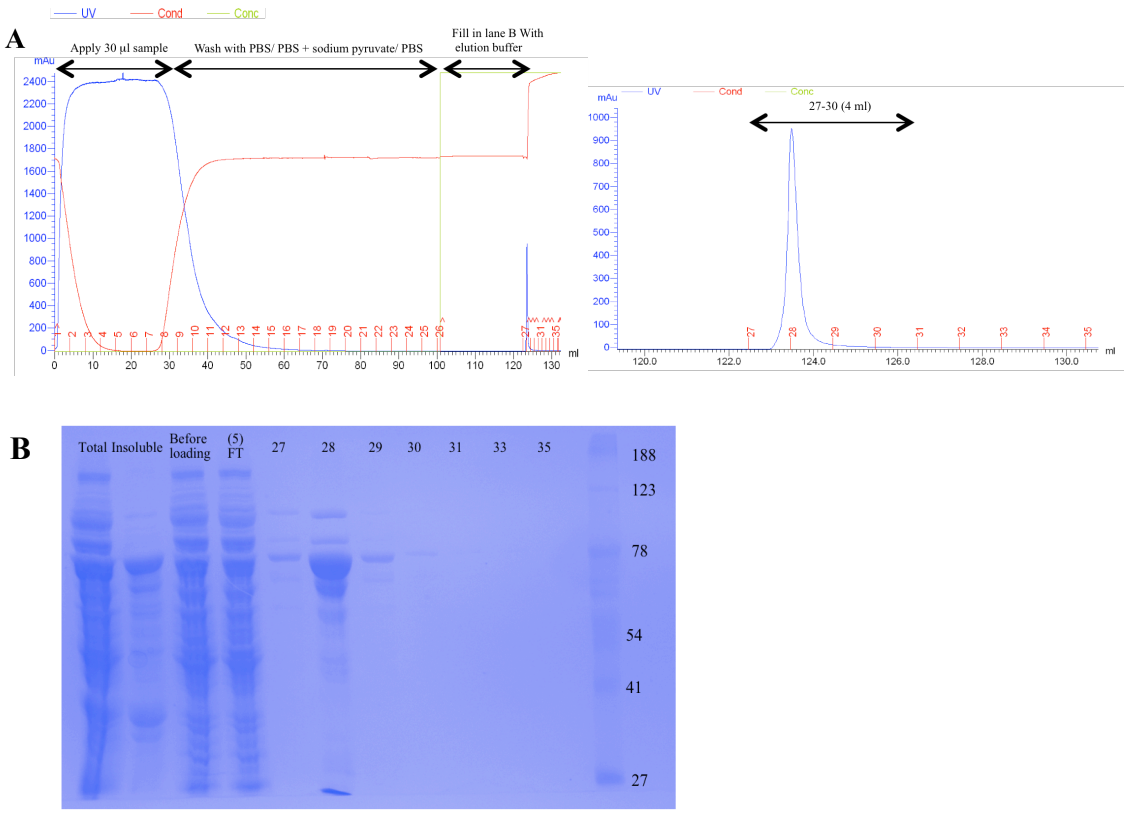

Figure 3.7. Purification of GST-CtBP1 FL on 1 ml GSTrap. (A) FPLC trace, (B) Gel of fractions collected during purification, Total cell lysate (lane 1), insoluble protein (lane 2), cell lysate before loading onto the column (lane 3), Faction from the flow through (lane 4), fraction collected during elution (lane 5-11), marker (lane 12)

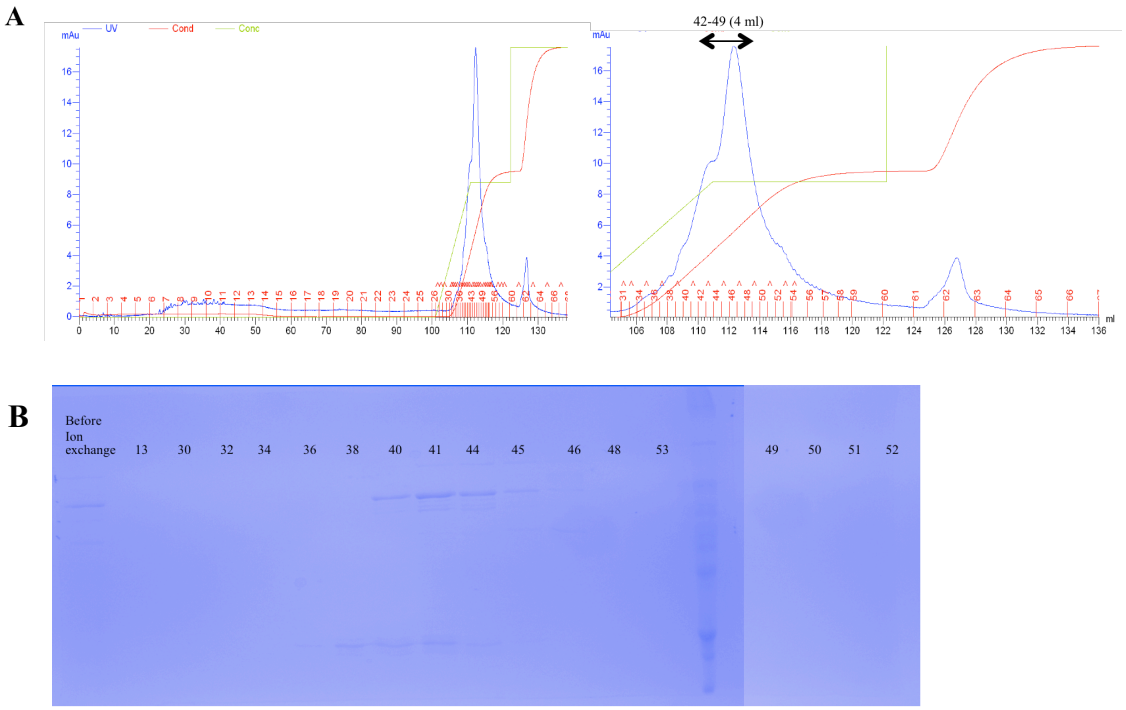

Figure 3.8. Purification of GST-CtBP1 on Q HP column. (A) FPLC trace, (B) Gel of fractions collected during purification.

After purification, fractions 40 to 44 were collected (Figure 3.8) and dialysed in 12-14 kDa MWCO dialysis tubing against 1 litre of PBS and 15% glycerol at 4 °C overnight. After dialysis the material was collected and the protein concentration was determined using Bio-Rad. The concentration of GST-CtBP1 was 0.25 µg/µl. Gel analysis was also carried to confirm the protein concentration (0.2 µg/µl) (Figure 3.13). The protein was aliquoted into 5 µl single use aliquots, then snap frozen and stored at -80 °C.

3.2.3 His-CtBP2 purification

As for His-CtBP1 due to low yield and purity the purification was repeated this time capturing the protein on Ni^{++} superflow beads before applying to a column on the FPLC. Also, a more shallow imidazole gradient was used to try to remove some of the contaminant. The same procedure as His-CtBP1 was followed. As can be seen in Figure

3.10 purer protein was obtained. Fractions 30 to 41 (18 ml) were pooled together and dialysed against 2 L of PBS with 15% glycerol using 12 kDa MWCO dialysis tubing overnight at 4 °C. The buffer was replaced with 2 L of fresh PBS and dialysis was continued for a further 2 hr. After dialysis the material was collected and the protein concentration was determined using Bio-Rad. The concentration of His-CtBP1 was 0.4 µg/µl. Gel analysis was also carried to confirm the protein concentration. The protein was aliquoted into 5 µl single use aliquots, then snap frozen and stored at -80 °C.

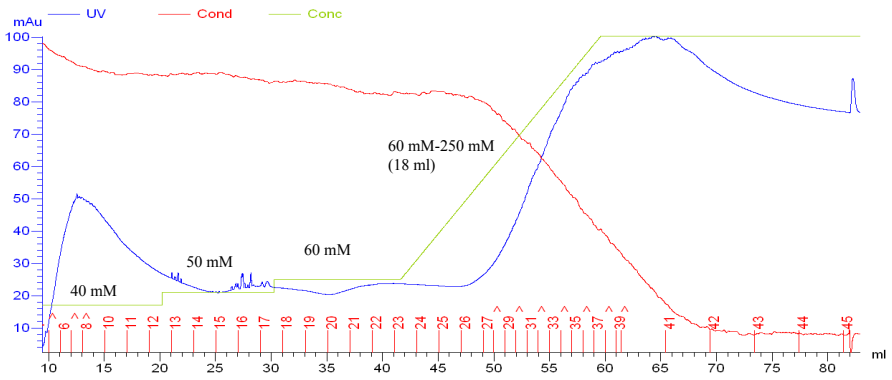

Figure 3.9. Purification of His-CtBP2 on 1 ml Ni-NTA superflow column.

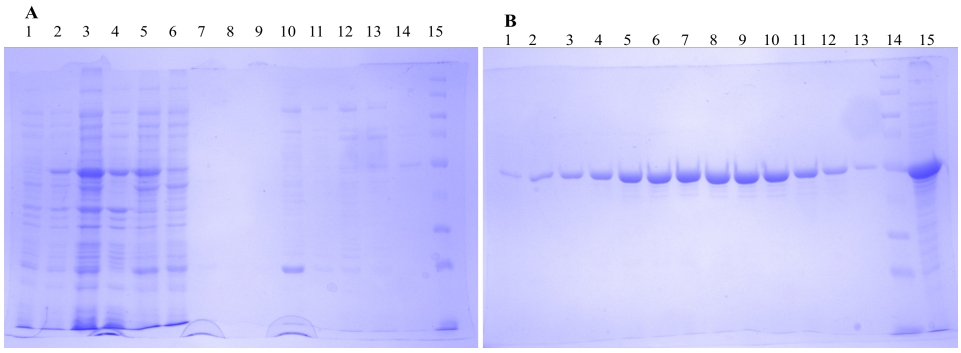

Figure 3.10. His-CtBP2 Purification fractions Gel (**A**) **1**.To, **2**.Tend, **3**.Total, **4**.Insoluble, **5**.Soluble, **6**.Unbound, **7**.Wash1 with binding buffer, **8**.Wash2 with binding buffer, **9**.Wash3 with binding buffer + 0.25 mM sodium pyruvate, **10**.Wash4 with binding buffer + 20 mM imidazole, **11**.Fraction #5, **12**.Fraction #7, **13**.Fraction #10, **14**.Fraction #16, **15**.Marker. His-CtBP2 Purification fractions Gel (**B**) **1**.Fraction #22, **2**.Fraction #28, **3**.Fraction #29, **4**.Fraction #30,**5**.Fraction #32, **6**.Fraction #33, **7**.Fraction #35,**8**.Fraction #36, **9**.Fraction #38, **10**.Fraction #40, **11**.Fraction #41, **12**.Fraction #42, **13**.Fraction #44, **14**.Marker, **15**.beads after elution.

3.2.4 GST-CtBP2 Purification

The same procedure as for GST-CtBP1 was carried out and the GST-CtBP2 was more pure in comparison. Even though GST-CtBP2 was pure enough ion exchange was still carried to ensure both proteins were treated the same. A pI of 6.53 was calculated online and therefore an anion exchanger was used. Fractions 35 to 40 (Figure 3.11) were pooled together and diluted in 50 ml of buffer A (20 mM tris HCl pH8 and 10 mM NaCl) and applied to the column.

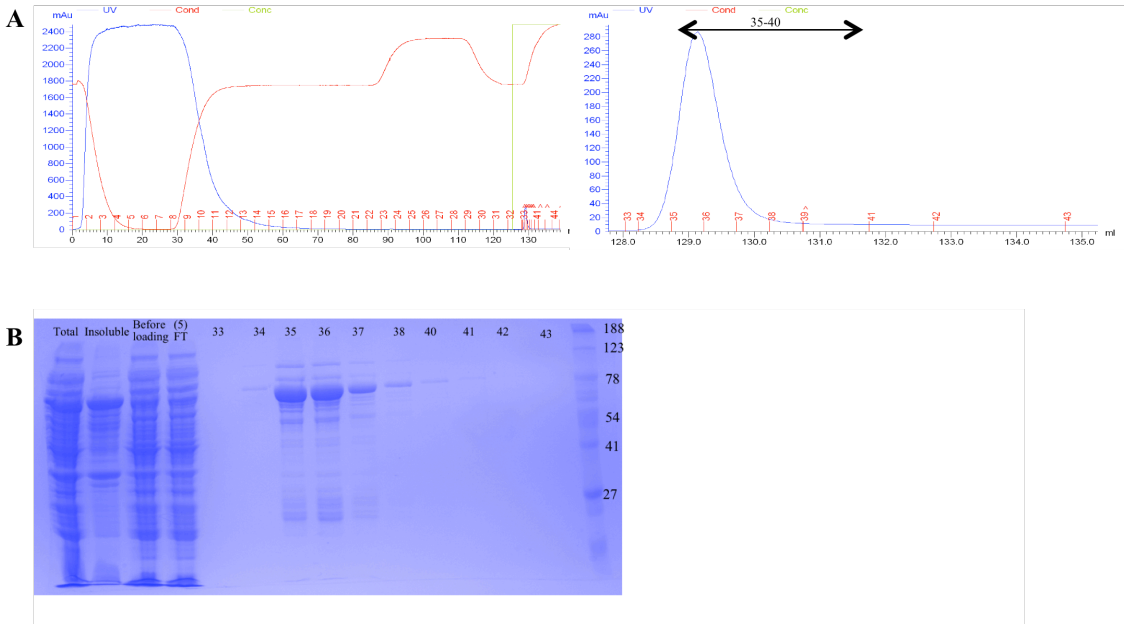

Figure 3.11. Purification of GST-CtBP2FL on 1 ml GSTrap, (A) FPLC trace, (B) gel of fractions collected.

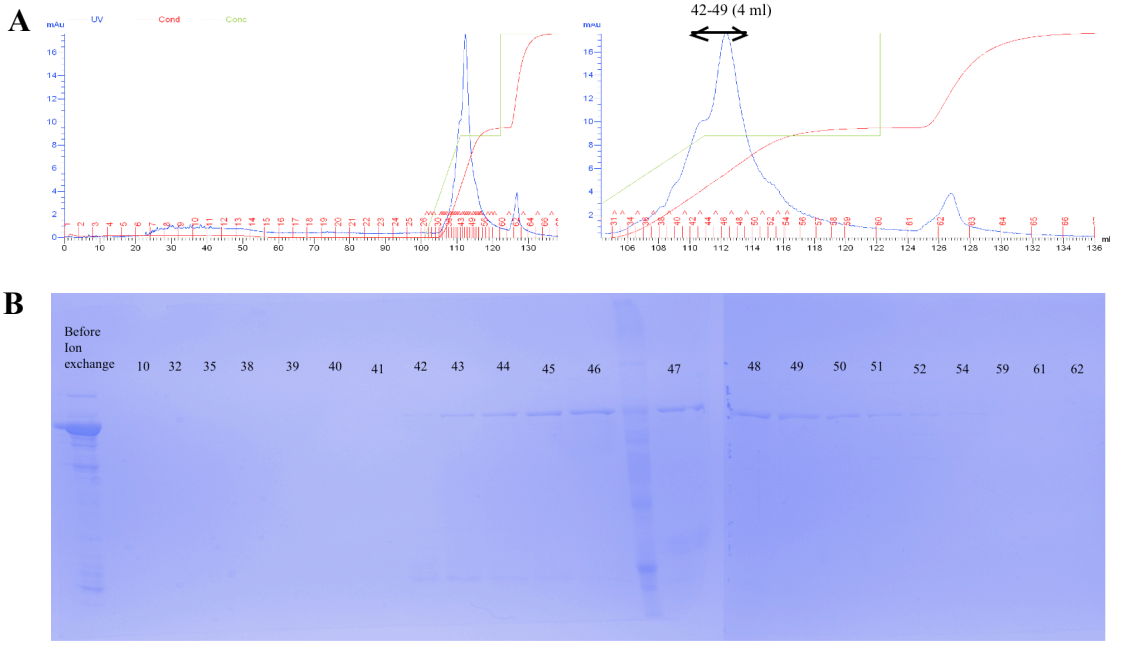

Figure 3.12. Purification of GST-CtBP2FL on Q HP column, (A) FPLC trace, (B) gel of fractions collected

After purification, fractions 42 to 49 were collected (Figure 3.12) and dialysed in 12-14 kDa MWCO dialysis tubing against 1 litre of PBS and 15% glycerol at 4 °C overnight. After dialysis, the material was collected and the protein concentration was determined using Bio-Rad. The concentration of GST-CtBP2 was 0.055 µg/µl. Gel analysis was also carried out to confirm protein concentration (0.05 µg/µl) (Figure 3.13). The protein was aliquoted into 5 µl single use aliquots, then snap frozen and stored at -80 °C.

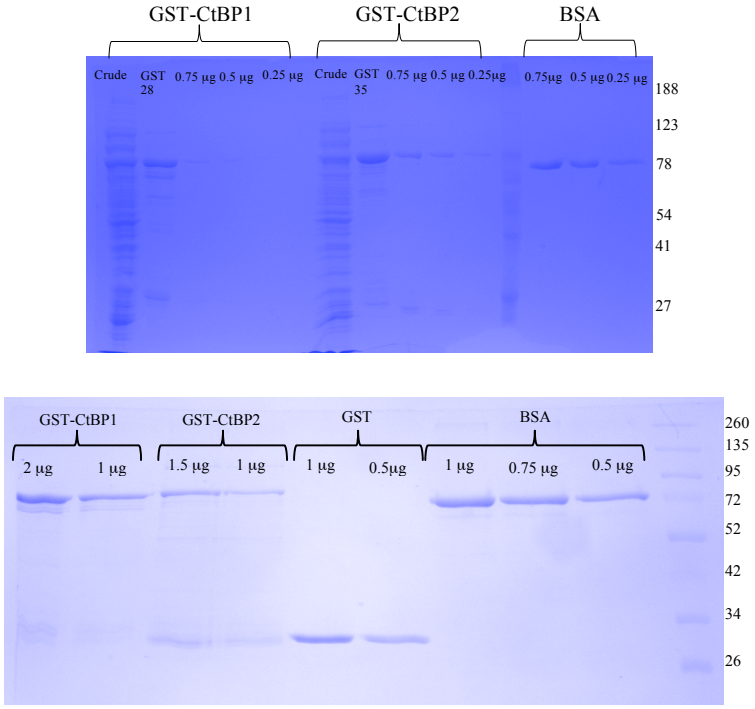

Figure 3.13. GST-CtBP vs. BSA to determine protein concentration.

3.3 Enzyme-linked immunosorbent assay (ELISA)

ELISAs were used for the quantification analysis of the effect of the cyclic peptide on the homo- and hetrodimerisation of CtBPs. The screen involves the immobilisation of either GST-CtBP1 or GST-CtBP2 (depending on the screen) onto the glutathione plates, followed by the addition of His-CtBP protein and peptide. Mouse anti His primary antibody was used to recognise the His on the second CtBP protein, followed by sheep anti-mouse HRP (horseradish peroxidase) secondary antibody illustrated in Figure 3.14. This allows recognition of the primary antibody and quantification of the protein interaction. The activity of the inhibitor can be monitored by a concentration-dependent

reduction in the horseradish peroxidase signal, because of the disruption of the complex. SuperSignal ELISA femto Maximum Sensitivity Substrate was used; this is a highly sensitive, chemiluminescent, HRP substrate for ELISA detection and quantification. The SuperSignal substrate generates detectable light within one minute of addition to trace amount of soluble HRP, saving incubation time. The SuperSignal ELISA femto Maximum Sensitivity Substrate is made up of luminol/enhancer and a stable peroxide buffer.

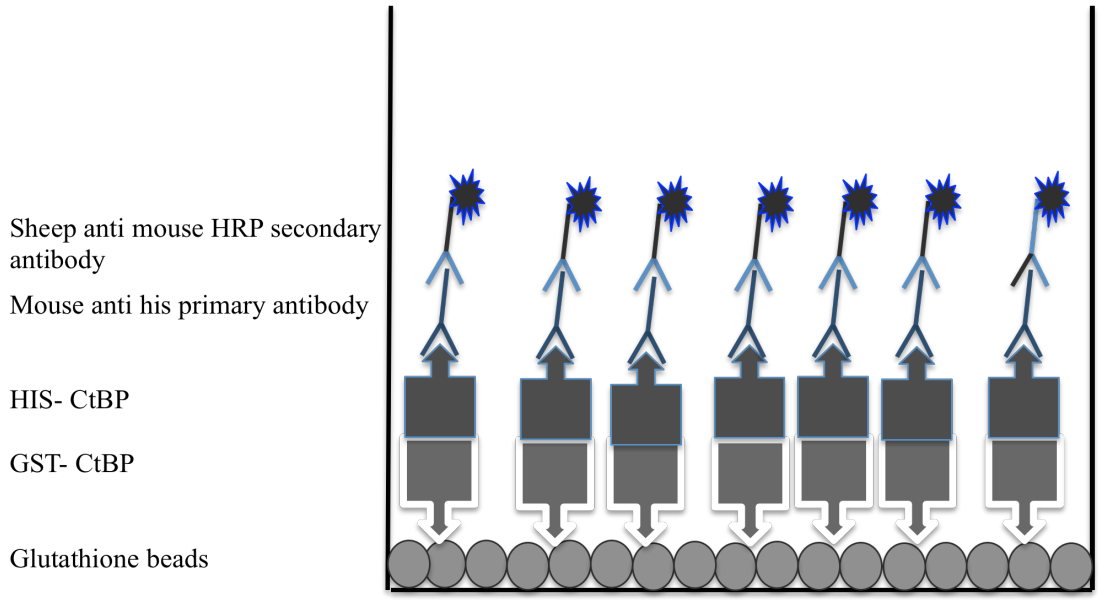

Figure 3.14. Diagram illustrating the ELISA setup.

Horseradish peroxidase (HRP) is a 40kDa protein that catalyses the oxidation of substrates by hydrogen peroxide, resulting in a coloured or fluorescent product or the release of light as a by-product. HRP functions optimally at a near to neutral pH. The high turnover rate, stability, low cost and wide availability of substrates, makes HRP enzymes the choice for most applications.

Chemiluminescence has a large linear response for detection and quantification over a wide range of protein concentrations. Chemiluminescence yields the greatest sensitivity of any available detection method. In a chemiluminescence ELISA, the substrate is the limiting reagent in the reaction; as it is exhausted, light production decreases and eventually ceases. It is important to optimise the conditions and use appropriate antibody dilutions in order to produce a stable output of light, producing consistent and

sensitive results. Luminol is one of the most widely used chemiluminescent reagents and its oxidation by peroxide results in creation of an excited state product, 3-aminophthalate. This product decays to a lower energy state by releasing photons of light (Figure 3.15).

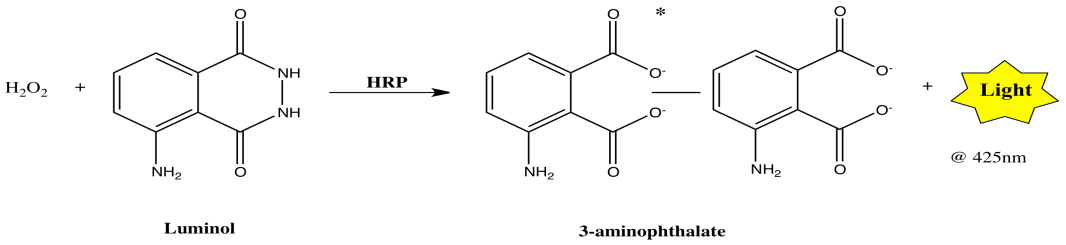

Figure 3.15. Luminol is oxidised in the presence of horseradish peroxidase and hydrogen peroxide to form an excited state (3-aminophthalate). The 3-aminophthalate emits light at 425nm as it decays to the ground state.

The blocking and washing step are important during an ELISA. The binding capacity of micro plate wells is typically higher than the amount of protein coated in each well. The remaining surface area must be blocked to prevent antibodies or other proteins from adsorbing to the plate during subsequent steps. A blocking buffer is a solution of irrelevant protein, mixture of proteins, or other compound that may be able to adsorb to all remaining binding surfaces on the plate. The ideal blocking buffer will bind to all potential sites of nonspecific interaction, eliminating background, without preventing protein binding. This will improve sensitivity of an assay by reducing background signal and improving the signal-to-noise ratio. During the development of the ELISA, BSA (Bovine serum Albumin) made up in TBS (Tris Buffered Saline) with 0.05% tween was used as a blocking buffer. Sets of control experiments were set up to determine the optimum conditions for the ELISA. Both protease free (Bovine serum Albumin protease free powder, Cat 700-101P, Gemini Bio Products) BSA and globulin free BSA (Albumin from bovine, A7638, Sigma) were tried, it was found that the protease free BSA gave a lower background signal. Wells blocked with globulin free BSA gave higher readings when wells were treated with just His-CtBP1 and His-CtBP2. (Figure 3.16). A control experiment was also run using 1% BSA and 3% BSA. The 3% BSA blocking buffer showed an improved signal-to-noise ratio.

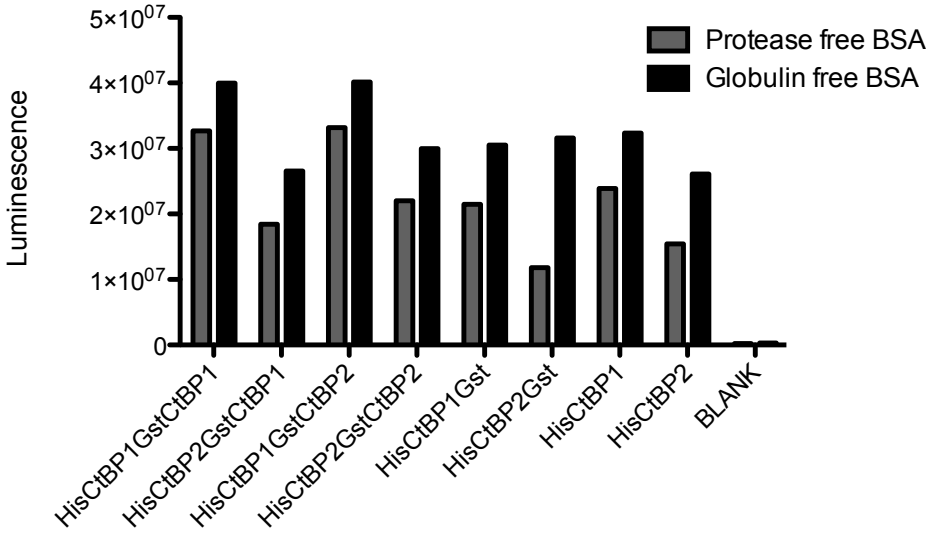

Figure 3.16. Graph showing a comparison between protease free BSA and Globulin free BSA in different ELISA conditions.

To investigate the amount of GST-CtBP1 protein required for the experiment, serial dilutions of the protein were plated. The protein was prepared in wash buffer (TBS/0.05% Tween-20). It was important to incorporate washes between each step to wash away any unbound protein or antibody. Initially two quick washes and one 5 min wash was carried out. This was increased to three 5 min washes and that showed improvements in unspecific binding. The R41 anti-GSTCtBP1[111] antibody was used to detect the protein, followed by a goat anti-rabbit HRP labelled antibody was used for quantification. As the concentration of protein increased, the signal increased and maximum signal was obtained at 100 ng. 100 ng of GST and GST-CtBP1 was used (Figure 3.17). A titration of GST-CtBP2 was then carried out using the same conditions and antibodies as for the GST-CtBP1 titration assay. 200 ng of GST and GST-CtBP2 was used.

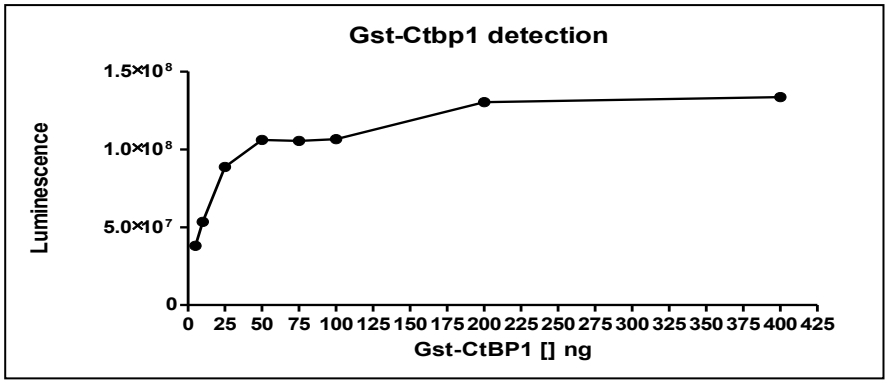

Figure 3.17. Graph showing change in luminescence reading as GST-CtBP1 concentration increases.

The His-CtBP2 protein was titrated into plates treated with GST-CtBP2 in order to investigate the amount of His-CtBP2 required for the CtBP2 homodimeric and CtBP heterodimeric assay. The plates were first treated with GST-CtBP2 and GST alone to see how much background binding was occurring (i.e. His-CtBP2 just binding to the GST protein). Plates were washed and blocked before the addition of His-CtBP2 and the protein was added with and without the addition of NADH (1 mM) (NADH should promote dimerisation of the CtBPs). A 1/2000 dilution of mouse anti-his antibody was added to detect the bound His-CtBP2 protein and a 1/2000 dilution of sheep anti mouse HRP labelled secondary antibody that was used for quantification and detection of primary antibody. After the addition of SuperSignal the absorbance was measured at 425nm on the plate reader. The optimal amount chosen was 600 ng as it gave a better signal to noise ratio and gave a greater difference between the +/- NADH (Figure 3.18). The same experiment was carried out for His-CtBP1, the optimum amount chosen was 600 ng.

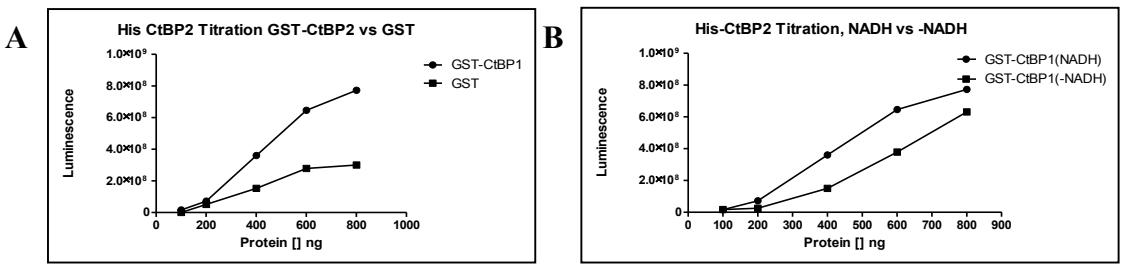

Figure 3.18. Graphs showing titration of His-CtBP2, (A) Titration into wells with GST-CtBP2 and GST, (B) Titration with and without NADH.

0.5 mM was taken as the optimal NADH value, this value was chosen based on work carried out by mirnexami *et al*.[111] It was found that when the antibody is not sufficiently diluted, the amount of enzyme present is too high and the substrate is used up quickly and a stable output of light will not be reached. A 1/2000 dilution was initially used for both antibodies, but this was not the optimum dilution and it resulted in the signal burning out and gave a 0 reading on the plate reader. It can be clearly seen from Figure 3.19 that the GST-CtBP1 has turned a darker colour then the GST alone indicating that there is more dimerised protein present.

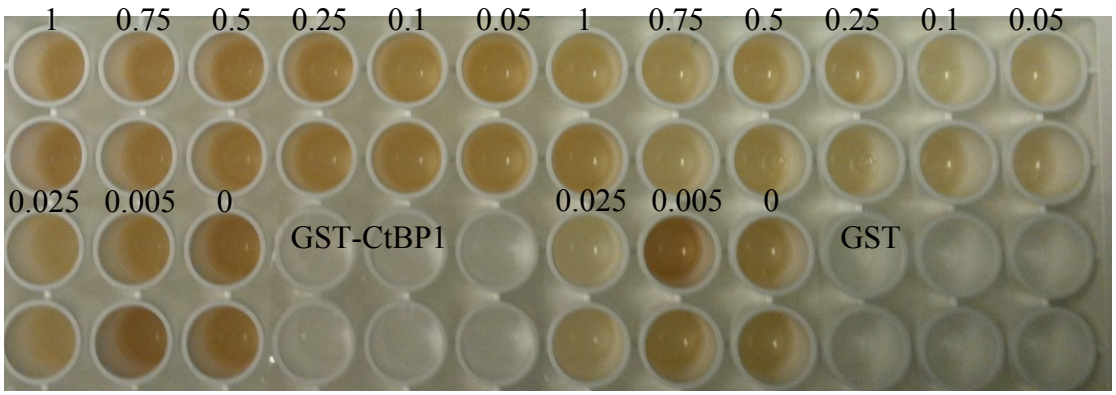

Figure 3.19. An experimental plate showing the effect of signal burn out. Left hand side shows GST-CtBP1 coated wells; right hand side shows GST coated wells.

An antibody titration was carried out in the CtBP1 homodomeric ELISA in order to discover the optimum dilution. 600 ng of His-CtBP1, 100 ng of GST-CtBP1 and 0.5 mM of NADH was used. The same assay was run substituting GST-CtBP1 with GST alone (taken as background signal). Initially two experiments were carried out: in the first experiment the primary antibody was kept at a dilution of 1/2000; in the second, the primary antibody was kept at a dilution of 1/5000. The secondary antibody was titrated at a dilution 1/1000 to 1/6000 (A and B Figure 3.20). A higher signal to noise ratio was obtained when the primary antibody was diluted 1/5000. The experiment was then repeated using higher dilutions of secondary antibody against 1/5000 and 1/10000 dilutions of primary antibody in order to further optimise the conditions (C and D Figure 3.20). The maximum signal to noise ratio was obtained when a 1/5000 dilution for the primary antibody and a 1/10000 dilution for the secondary antibody were used.

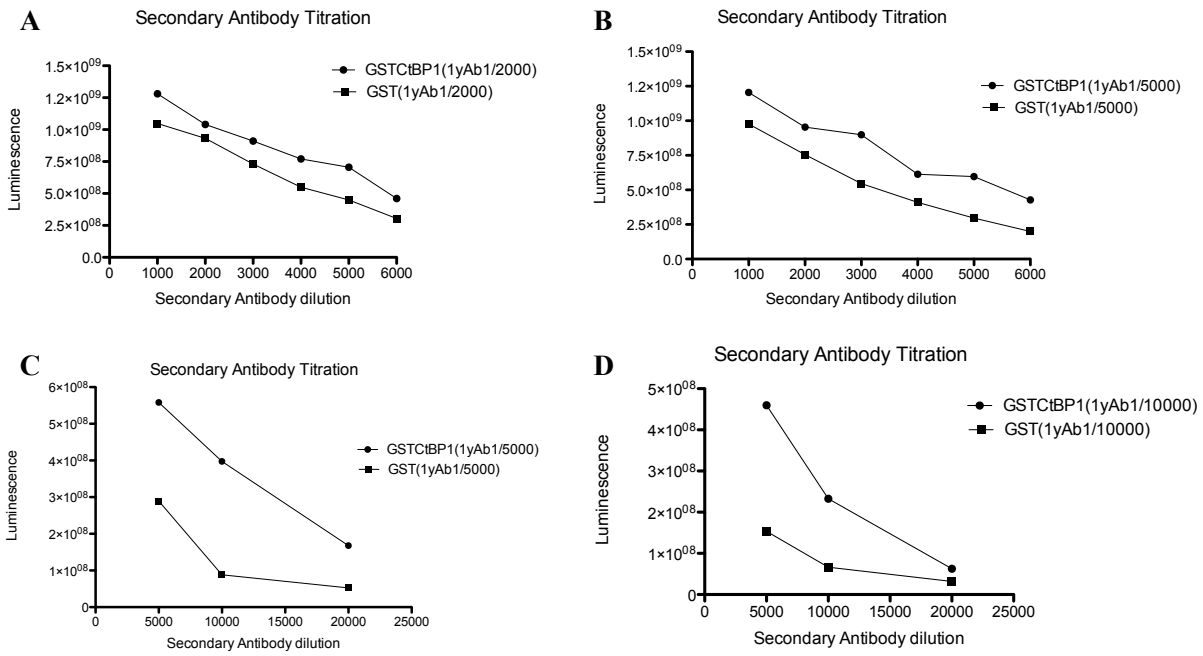

Figure 3.20. Titration of secondary antibody, (A) 1/2000 dilution of primary antibody, (B) 1/5000 dilution of primary antibody, (C) 1/5000 dilution of primary antibody, (D) 1/10000 dilution of primary antibody.

In summary the optimised conditions for the ELISA was to use 100 ng GST-CtBP1, 200 ng GST-CtBP2, 600 ng of both His-CtBP1 and His-CtBP2, 3% BSA/TBS 0.05% tween for blocking, a 1/5000 dilution for the primary antibody, a 1/10000 dilution for the secondary antibody and finally three washes at 5 min each after each step. GST was used as a control at the same concentration as the GST-CtBP protein. In initial experiments 0.5 mM NADH was mixed with the His-CtBP protein before adding it to the wells. This was then changed to first adding the His-CtBP protein and allowing it to react for 30 min then adding the 0.5 mM NADH and allowing it to react for a further 1 hr. The reason behind this was that if His-CtBP and NADH are mixed beforehand the proteins might dimerise before adding to the assay therefore preventing dimerisation of His-CtBP with GST-CtBP. The experimental procedure for the CtBP heterodimeric system and the CtBP1 and CtBP2 homodimeric system is described in sections 6.3.3.3, 6.3.3.1 and 6.3.3.2 respectively.

Once the ELISA had been optimised Peptide 6 and 61 were tested in all the assays (CtBP1 homodimeric, CtBP2 Homodimeric and CtBP heterodimeric). The peptide was

added to the His-CtBPs at different concentrations and allowed to react for 30 min at rt before the addition of NADH in binding buffer and the reaction was continued for a further 1 hr at rt. Each individual experiment was carried out in duplicate wells. All experiments with GST-CtBP were run in parallel with experiments with GST. The GST readings were subtracted from the GST-CtBP readings as background. Three repeats of each experiment were done and the results were normalised (Figure 3.21-Figure 3.28 are all normalised plots). The following steps were carried out for normalisation:

- The average of each duplicate well was taken and the GST background was subtracted for each concentration (average-background) this was done for all three repeats.
- The sum ($\sum$) of all the average-background was taken.
- The highest sum ($\sum_1$) from the three repeats was taken and divided by the sum of individual experiment ($\sum_1/\sum_2$). This was done for all three triplicates.
- This value was multiplied by the average-background value to give the normalized value at each concentration.

Normalisation was carried out due to the variation of the readings between experiments this could be because of the slight time variation between adding the SuperSignal and taking the reading on the plate reader. We hypothesise that both peptide 6 and 61 would have an inhibitory effect on the CtBP1 homodimeric assay and the CtBP heterodimeric assay but only Peptide 61 would have an effect on the CtBP2 homodimeric assay. This is because SICLOPPS screen shows that Peptide 61 prevents dimerisation of CtBP1 and CtBP2 whereas Peptide 6 only inhibited the dimerisation of CtBP1 (Figure 2.27).

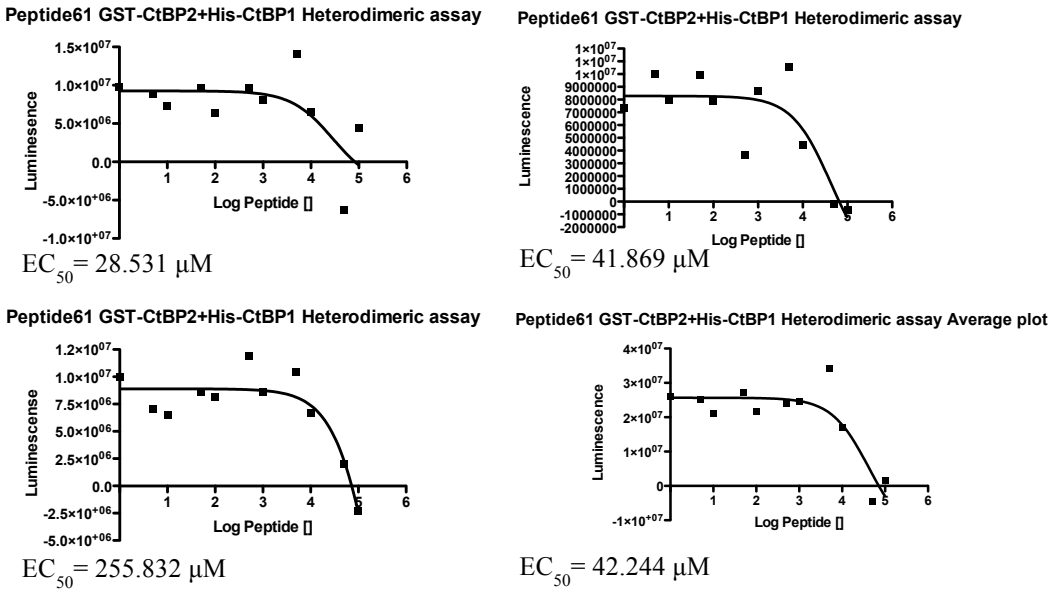

Figure 3.21. Peptide 61 titrations into CtBP heterodimeric assay (GST-CtBP2 and His-CtBP1), three repeats and average plot.

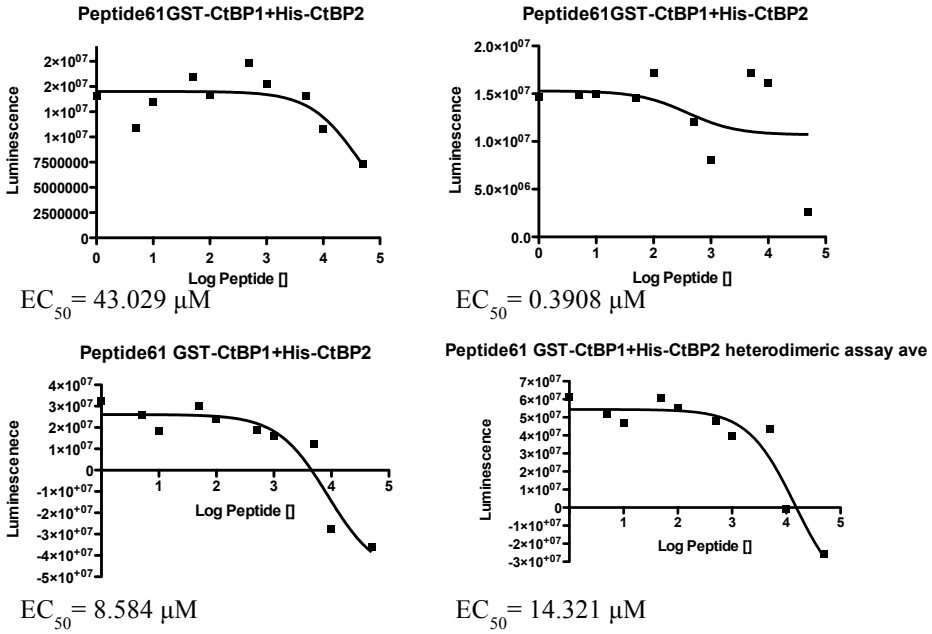

Figure 3.22. Peptide 61 titrations into the CtBP heterodimeric assay (GST-CtBP1 and His-CtBP2), three repeats and average plot.

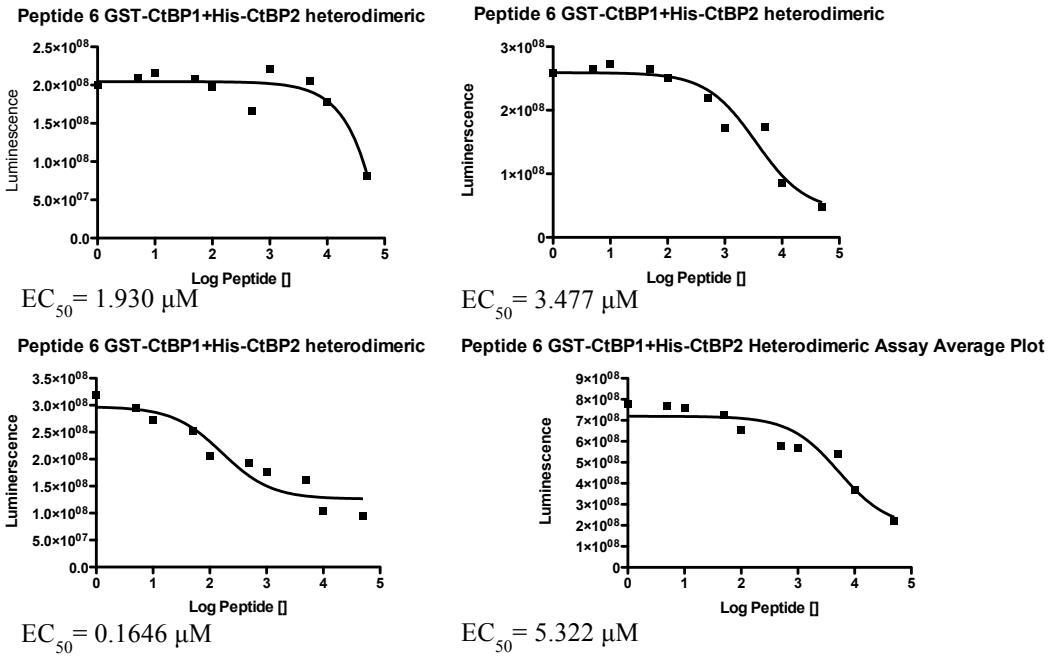

EC_{50}= 1.930 μM

EC_{50}= 3.477 μM

EC_{50}= 0.1646 μM

EC_{50}= 5.322 μM

Figure 3.23. Peptide 6 titrations into the CtBP heterodimeric assay (GST-CtBP1 and His-CtBP2), three repeats and average plot.

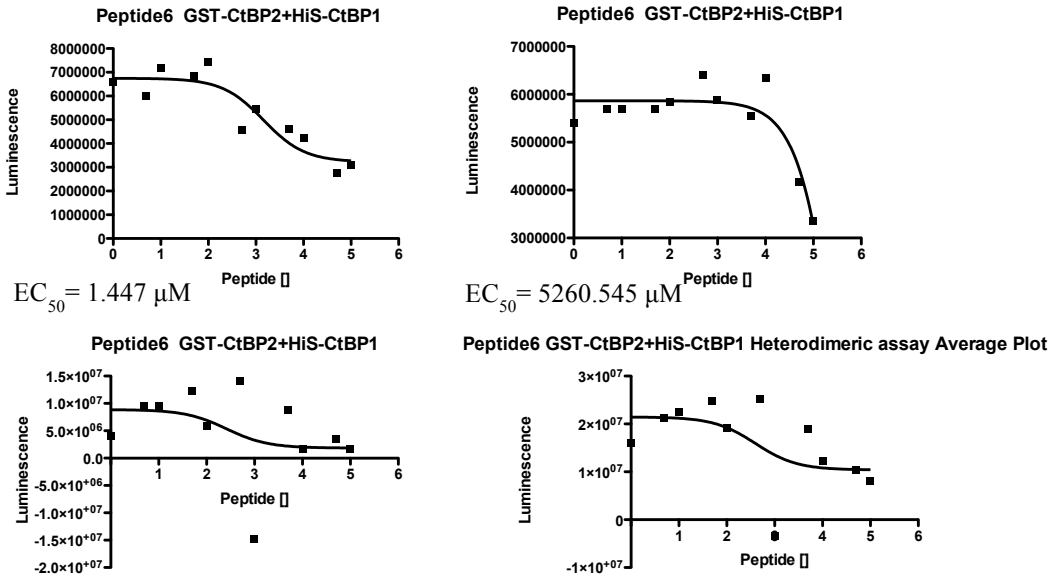

EC_{50}= 1.447 μM

EC_{50}= 5260.545 μM

EC_{50}= 0.2595 μM

EC_{50}= 0.3954 μM

Figure 3.24. Peptide 6 titrations into the CtBP heterodimeric assay (GST-CtBP2 and His-CtBP1), three repeats and average plot.

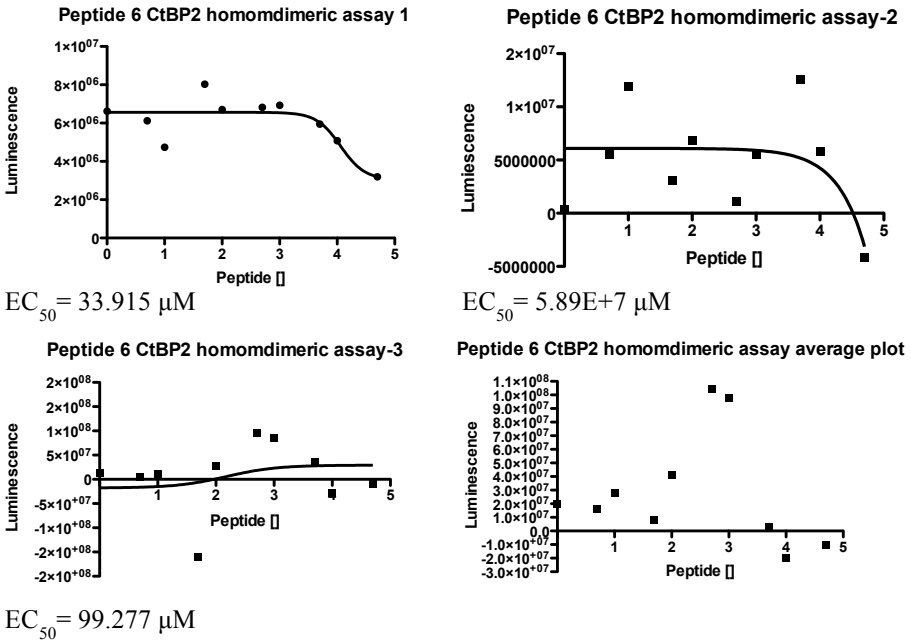

EC_{50}= 33.915 µM

EC_{50}= 5.89E+7 µM

EC_{50}= 99.277 µM

Figure 3.25. Peptide 6 titration into the CtBP2 Homodimeric assay. Three repeats and average plot.

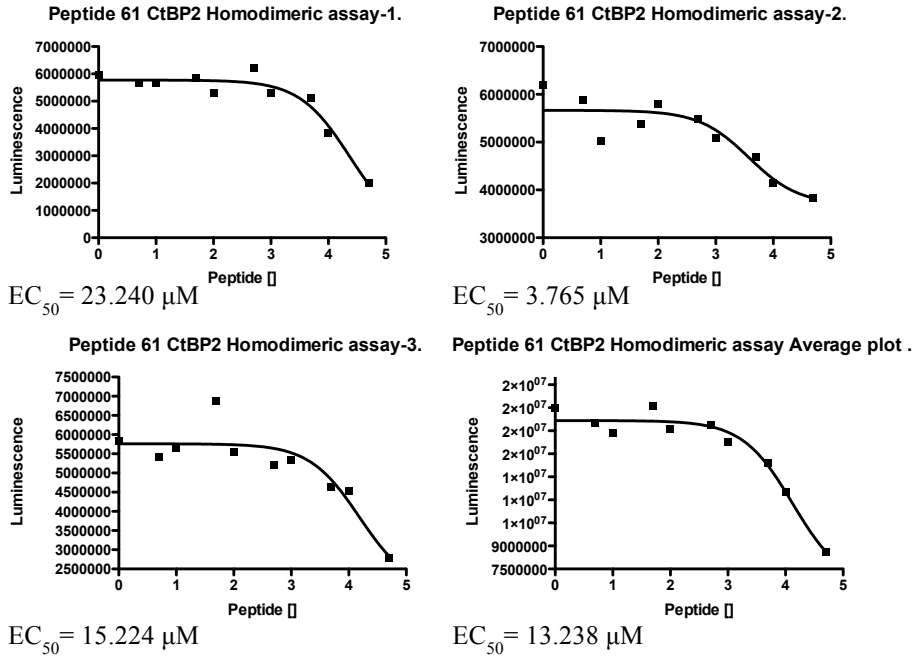

EC_{50}= 23.240 µM

EC_{50}= 3.765 µM

EC_{50}= 15.224 µM

EC_{50}= 13.238 µM

Figure 3.26. Peptide 61 titration into the CtBP2 Homodimeric assay. Three repeats and average plot.

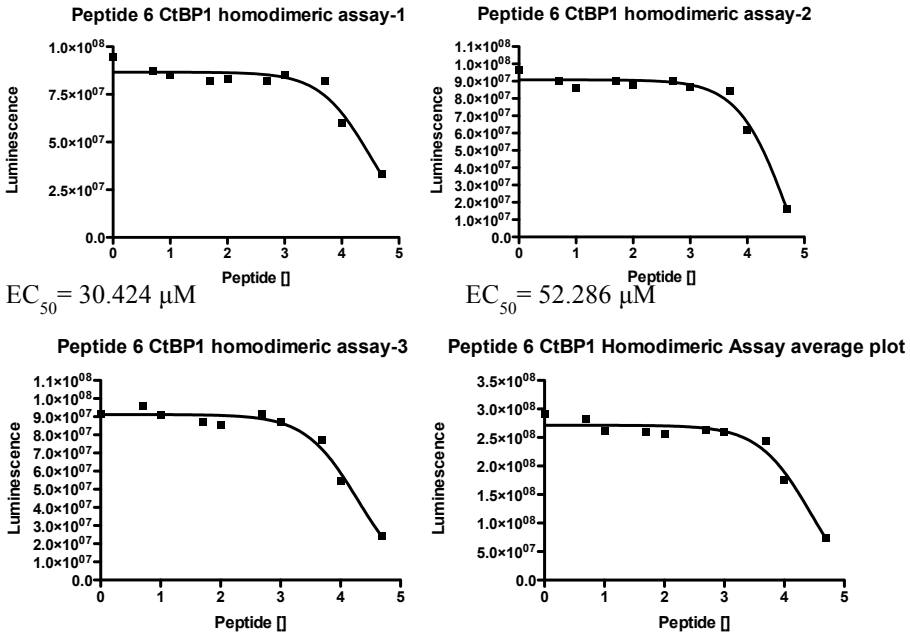

Figure 3.27. Peptide 6 titration into the CtBP1 Homodimeric assay. Three repeats and average plot.

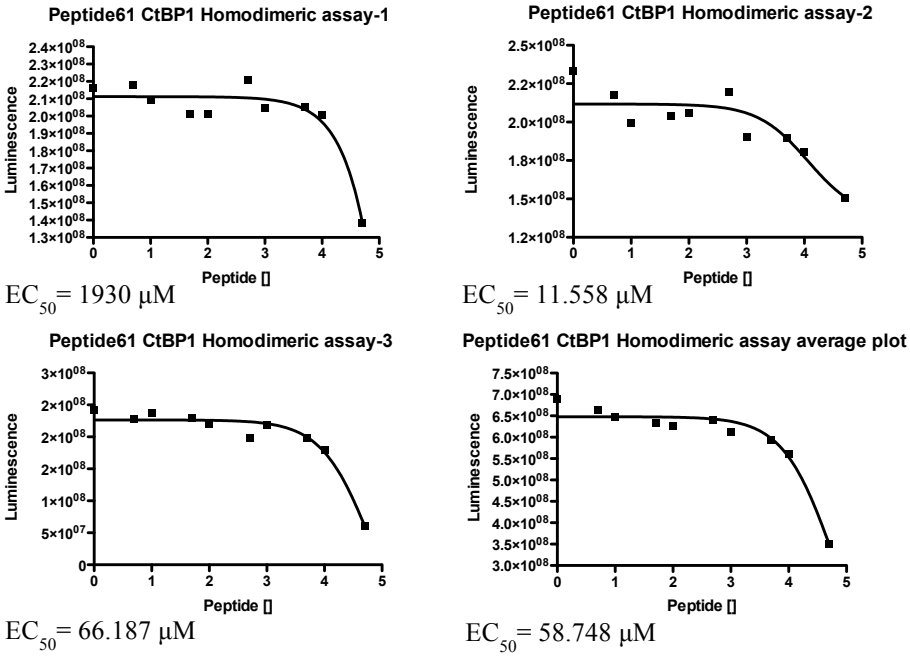

Figure 3.28. Peptide 61 titration into the CtBP1 Homodimeric assay. Three repeats and average plot.

Marked inhibition of the CtBP protein-protein interactions occurred in the presence of both peptide 6 and 61 in the μM range. Analysis of EC_{50} (half maximal effective concentration) values was carried out using the Prism software. EC_{50} refers to the concentration of a drug required to induce a response halfway between the baseline and maximum responses.

Variations in the results were observed for the two heterodimeric assays and the order in which the CtBP1 and CtBP2 protein was added appeared to have an effect. Peptide 61 gave a lower EC_{50} when CtBP1 was coated on to the plate compared to when CtBP2 was coated (14.32 μM (Figure 3.22) compared to 42.224 μM (Figure 3.21)) Peptide 6 gave a lower EC_{50} when CtBP2 was coated first, 0.395 μM (Figure 3.24) in comparison with when CtBP1 was coated, 5.3 μM (Figure 3.23). Peptide 61 also had a lower EC_{50} for the CtBP2 homodimeric assay compared to the CtBP1 homodimeric assay (13.32 μM (Figure 3.26) compared 58.75 μM (Figure 3.28)). Peptide 6 gave a lower EC_{50} for both heterodimeric assays and the CtBP1 homodimeric assay. These effects may be due to the way the peptides bind to the protein, or the protein interaction being weaker therefore requiring less peptide. Table 3.1 Shows EC50 values for both peptide 6 and 61 in the different ELISA assays. Both estimate values and prism values are given, as the prism curve fitting is not reliable.

	EC50 (μM) (Estimate)	EC50 (μM) (prism)
Pep61 CtBP2 Homo	10000	13238
Pep61 CtBP1 Homo	25000	58748
Pep6 CtBP1 Homo	9000	27743
Pep61 CtBP heter (GST-CtBP2: His-CtBP1)	1000	42.2
Pep61 CtBP Heter (GST-CtBP1: His-CtBP2	500	14.3
Pep6 CtBP heter (GST-CtBP2: His-CtBP1)	500	0.3954
Pep 6 CtBP heter (GST-CtBP1: His-CtBP2)	100	5.3

Table 3.1 Table showing EC50 results for each peptide in the different ELISA assays. Both estimate and prism values are given.

The CtBP2 homodimeric assay with peptide 6 did not work very well (Figure 3.25). The first assay worked as would be expected for peptide 6 where a signal was obtained from the dimerising proteins but there was not an effective decrease in signal as peptide was added. The subsequent two experiments did not work, as there is no signal over the background. This could be due to the proteins going off or issues with blocking therefore higher background signal was obtained.

Overall the ELISA allowed us to show CtBP dimerisation *in vitro* and the importance of NADH in improving dimerisation. Both peptide 6 and 61 have shown inhibitory effects. Further experimental work is required to determine whether the peptides work as competitive or non-competitive inhibitors. The assay can be used to test other compounds identified in the SICLOPPS screen, or any modified compounds of peptide 6 and 61 that may be made in the future to improve the inhibitor activity of the peptides. The CtBP2 homodimeric assay requires further development, as the results obtained from this assay are inconsistent. It would be of interest for future work to have crystal structures of the CtBPs with the peptide to see how the peptides binds to the protein and carry out subsequent experiments to determine binding efficiency of the peptides.

4. *In vivo* effects of CtBP Dimerisation Inhibition

Overview

Results and discussion

- Time lapse
  - Microinjection
  - TAT-Tagged time lapse
- Immunoflourescence analysis
  - Mitotic Index and Cells with Micronuclei
- MTS
- Colony forming assay
- Flow Cytometry
- P53 Activity
- Cell Migration Assay

Given the multiple roles and forms of CtBPs in cells, conventional methods (such as gene knockout or siRNA knockdown) are not ideally suited for deciphering their mechanisms as they eliminate the target protein from the whole system rather than a single function. Cyclic peptides that specifically inhibit homodimerisation of CtBP1 and those that inhibit the dimerisation of CtBP1 and CtBP2 were uncovered by SICLOPPS screening via the bacterial reverse two-hybrid system, for inhibitors of CtBP1 homodimerisation. The uncovered cyclic peptides specifically inhibit the protein-protein interaction of CtBPs without affecting their cellular levels. This phenotype can therefore be directly assigned to the protein-protein interaction of CtBP, rather than their presence or absence from the cell. The peptides were tested in a number of assays to try and further understand how CtBPs function.

4.1 Time Lapse

4.1.1 Microinjection

It has previously been shown that one of the most distinctive phenotypes caused by the combined inhibition of CtBP1 and CtBP2 protein synthesis is loss of mitotic fidelity. This effect on mitosis is an important determinant of the loss of cancer cell viability by CtBP depletion.[58] It has been shown that the maintenance of mitotic fidelity by CtBPs requires that they are active in the nucleus and that they are able to bind DNA-binding transcriptional repressors and/or chromatin modifying enzymes. It is yet unknown if it is required for CtBP to dimerise in order to maintain mitotic fidelity and therefore we have tried to address this question using cyclic peptide inhibitors of CtBP dimerisation. Peptide 6 and 61 were microinjected into synchronized MCF-7 breast cancer cells in early S phase. The fidelity of subsequent mitosis was determined by time-lapse video microscopy.

To permit the reliable analysis of the effect of peptides on the first mitosis post-microinjection, the cells were injected at a defined time after release from serum-starvation-induced G1 arrest. Optimization of conditions for cell synchronization and release was carried out by CN Birts *et al*.[86] Following subsequent re-stimulation with serum, it took approximately 30 hr for the first cells to enter mitosis.

Microinjection was carried out 20 hr after serum re-stimulation. Cells were injected in the cytoplasm with peptide. Dextran-FITC was co-injected to allow cells to be followed for a further 48 hr by fluorescent live cell imaging. Dextran-FITC was also injected on its own as a control. Mitotic events were scored as aberrant if there was a failed abscission, extended rounding during mitosis or the death of one or both daughter cells directly after mitosis. Peptide 61 was first tested at 25 μM and 50 μM; at 25 μM the peptide did not cause aberrant mitosis, but at 50 μM up to 50% of mitotic cells were aberrant (Figure 4.1). The experiment was repeated but this time injecting cells with 50 μM of peptide 6 and 61 in order to confirm previous results of peptide 61 and to test the effects of peptide 6. Figure 4.2 shows that this approach had minimal non-specific toxicity to the cells. Injection with peptide did not increase cell death or reduce the ability of cells to enter first mitosis. Compared to control-injected cells peptide 61, which inhibits the homodimeriation of both CtBP1 and CtBP2, caused a significant ($P<0.001$) increase in the percentage of mitosis that were aberrant from 1.6% to 31.3% (Figure 4.2). This suggests that a proportion of the cells undergo cell division without segregating their DNA, leading to an increase in cells with 4N DNA.

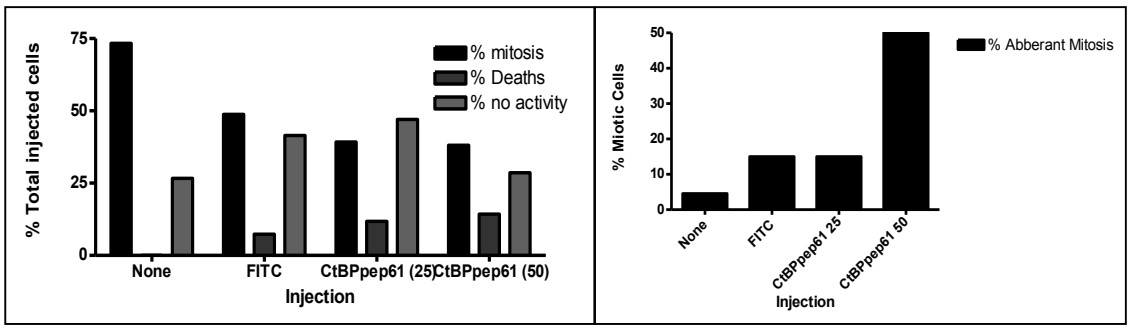

Figure 4.1. Peptide 61 (25 μM and 50 μM) treated cells were monitored by live cell imaging over a period of 48 hr post-serum re-stimulation. The percentage of cells in which the first event was either mitosis or death was recorded. The cells that underwent mitosis were subjected to further analysis, as indicated.

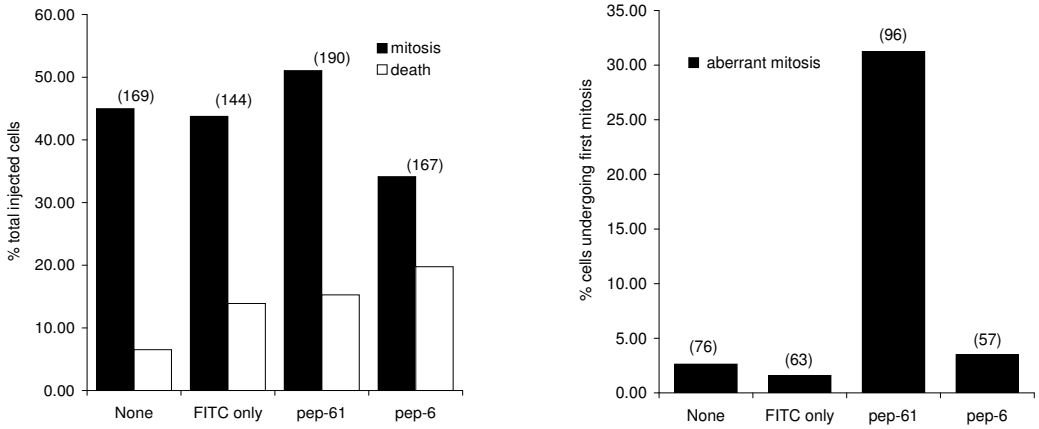

Figure 4.2. Peptide 61 and peptide 6 treated cells were monitored by live cell imaging over a period of 48 hr post-serum re-stimulation. The percentage of cells in which the first event was either mitosis or death was recorded. The cells that underwent mitosis were subjected to further analysis, as indicated.

The length of time spent by each microinjected cell in mitosis was also quantified (Figure 4.3); FITC injected cells spent an average of 1.3 hr in mitosis and peptide injected cells spent an average of 3 hr in mitosis. Bergman *et al* observed a similar observation where CtBP siRNA resulted in a striking increase in the average time spent in mitosis. The delay is a consequence of cells spending a longer period of time in prometaphase, which can indicate prolonged activation of the spindle assembly checkpoint.[58]

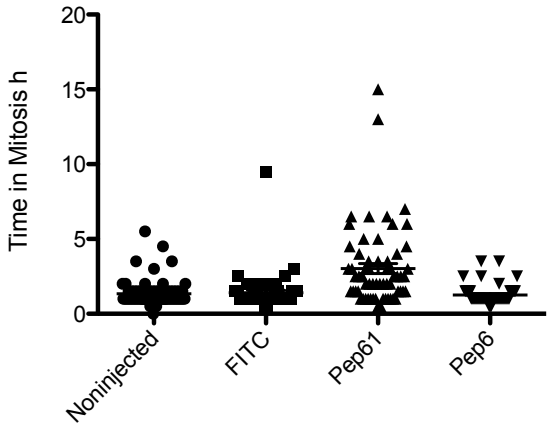

Figure 4.3. Time taken for peptide 61 and peptide 6 treated cells to complete mitosis. The bars through clusters of time points represent the mean times taken to complete mitosis.

Previous work using siRNA has shown that both CtBP1 and CtBP2 have to be blocked in order to see this effect on mitosis.[58] Peptide 6, which is specific to CtBP1, did not have any effect on the mitotic fidelity of the MCF-7 cells (Figure 4.2), suggesting that CtBP2 homodimers may be sufficient to maintain the fidelity of mitosis. Cells were transfected with CtBP2 siRNA using INTERFERin siRNA transfection reagent in order to knockout CtBP2. Following CtBP2 siRNA transfection cells were treated with peptide 6. Small interfering RNA (siRNA) are involved in RNA interference (RNAi) pathway, where they interferes with the expression of specific genes by hybridizing to its corresponding RNA sequence in target mRNA. This then activates degradation of mRNA. Once the target mRNA is degraded, the mRNA cannot be translated into protein. The siRNA pathway is illustrated (Figure 4.4).

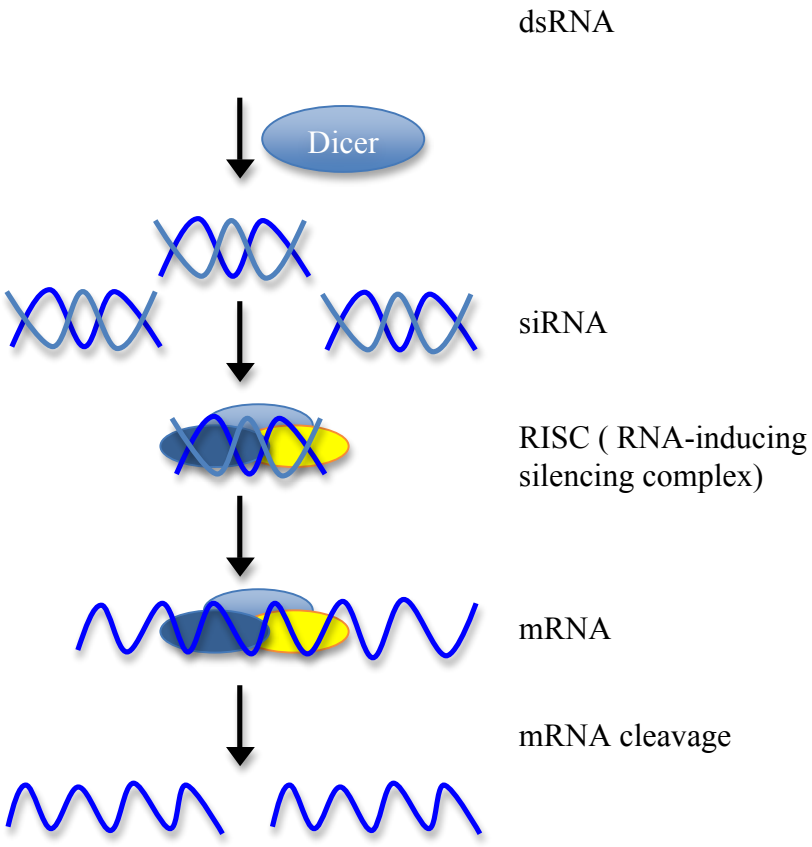

Figure 4.4. Diagram illustrating the siRNA pathway.

As can be seen in Figure 4.5 peptide 6 with CtBP2 siRNA showed a significant ($p<0.0001$) increase in the frequency of aberrant mitosis to 43.8% compared to 3.3% in the control injections. CtBP2 siRNA itself did not result in aberrant mitosis, unless combined with CtBP1 siRNA. A control experiment was carried out using a scrambled control siRNA that does not have an effect on CtBPs to confirm that the increase in aberrant mitosis was not due to the addition of siRNA. The time spent in mitosis for each microinjected cell was quantified. FITC injected cells spent an average of 1.3 hr in mitosis and peptide injected cells spent an average of 3.5 hr in mitosis (Figure 4.6).

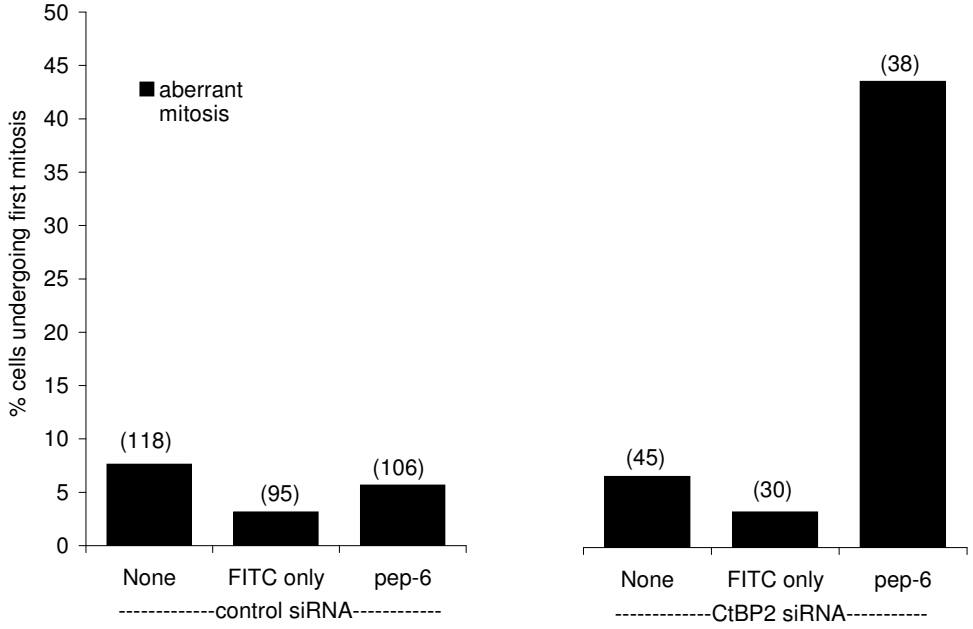

Figure 4.5. Peptide 6 with control siRNA (left hand side) and peptide 6 with CtBP2 siRNA (right hand side) treated cells were tracked by live cell imaging over a period of 48 hr post-serum re-stimulation. The cells that underwent aberrant mitosis were monitored, as indicated.

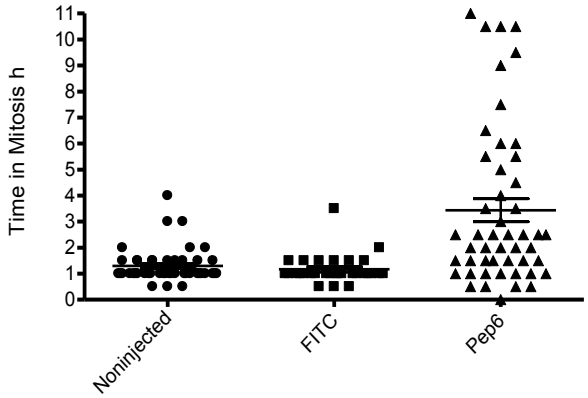

Figure 4.6. Time taken for peptide 6 and CtBP2 siRNA treated cells to complete mitosis. The bars through clusters of time points represent the mean times taken to complete mitosis.

4.1.2 Tat-tagged peptides

In order to establish whether the effects of the peptides were independent of any potential influence of their mechanism of delivery into the cell, peptide 6 and 61 were coupled to the cell penetrating HIV-Tat peptide as previously described for other SICLOPP-derived cyclic peptides.[26] MCF-7 cells were treated with peptide 61Tat-tagged at 25 μM and 50 μM similar effects were observed but to lesser extent compared to the microinjection, 31% compared to 11% and 13% (Figure 4.7). Therefore the experiment was repeated testing peptide 6, peptide 61 and Tat at 50 μM and 100 μM (Figure 4.8). Tat was used as a control on its own as Tat should not have an effect. In cells treated with 50 μM and 100 μM of peptide 61 there were 27% and 22% aberrant mitosis respectively in comparison with 4% and 5% for peptide 6 and Tat respectively.

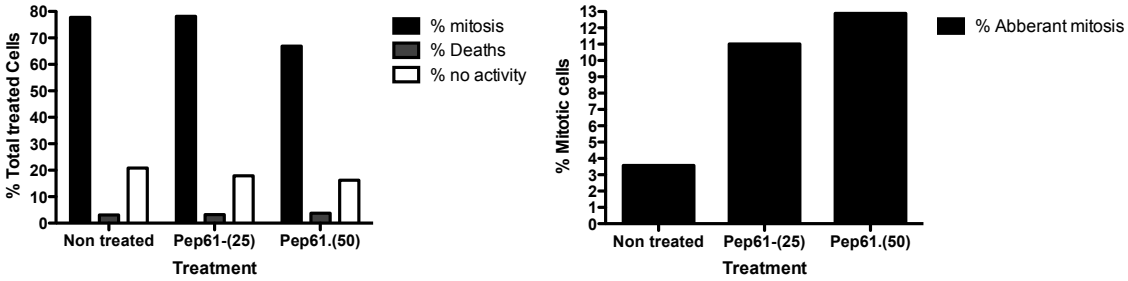

Figure 4.7. Tat-tagged peptide 61 (25 μM and 50 μM) treated cells were monitored by live cell imaging over a period of 48 hr post-serum re-stimulation. The percentage of cells in which the first event was either mitosis or death was recorded. The cells that underwent mitosis were subjected to further analysis, as indicated.

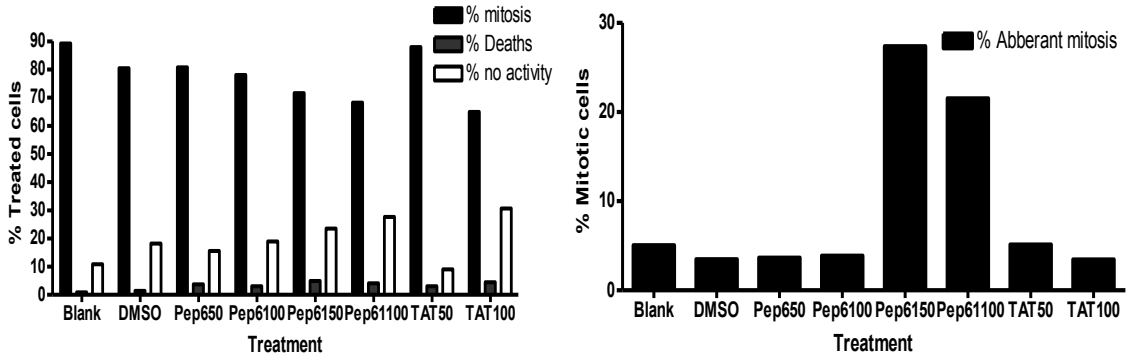

Figure 4.8. Tat-tagged peptide 61 (50 μM and 100 μM) treated MCF-7 cells were monitored by live cell imaging over a period of 48 hr post-serum re-stimulation. The percentage of cells in which the first event was either mitosis or death was recorded. The cells that underwent mitosis were subjected to further analysis, as indicated.

The time spent in mitosis for each Tat-tagged treated cell was quantified (Figure 4.9). Non-treated and Tat treated cells spent an average of 1.3 hr in mitosis and peptide 61 treated cells spent an average of 3.5 hr in mitosis.

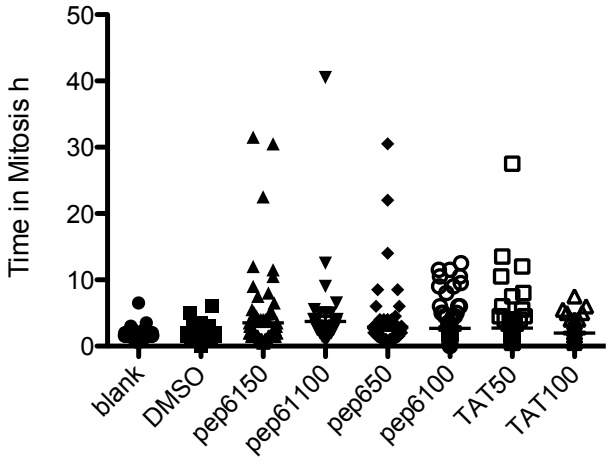

Figure 4.9. Time taken for Tat, Tat-tagged peptide 6 and peptide 61 MCF-7 treated cells to complete mitosis. The bars through clusters of time points represent the mean times taken to complete mitosis.

MDA-MB231 cells were treated with peptide 6, peptide 61 and Tat at 50μM and 100 μM. As with MCF-7 peptide 6 did not have an effect where as peptide 61 caused aberrant mitosis but the effect was not as great as with MCF-7 cells (27% compared to 12%, Figure 4.10). There was an increase in time spent in mitosis from 1.5 hr in Tat treated cell to 4 hr following peptide 61 treatment (Figure 4.11). MDA-MB 231 cells are p53 mutated cells and therefore we would have expected to see more death in peptide treated cells that have undergone chromosome segregation defects, as previously seen by siRNA treated cells.[58] MDA-MB231 cells are more mobile then MCF-7 cells, making it more difficult to analyse and follow during live cell imaging. Therefore, for further live cell imaging experiments only MCF-7 cells were used.

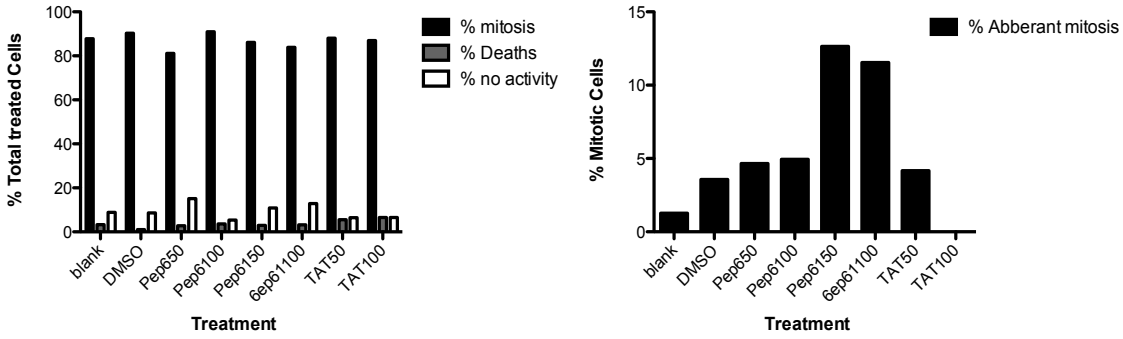

Figure 4.10. Tat, Tat-tagged peptide 61and peptide 6 (50 μM and 100 μM) and DMSO treated and non-treated MDA-MB231 cells were monitored by live cell imaging over a period of 48 hr post-serum re-stimulation. The percentage of cells in which the first event was either mitosis or death was recorded. The cells that underwent mitosis were subjected to further analysis, as indicated.

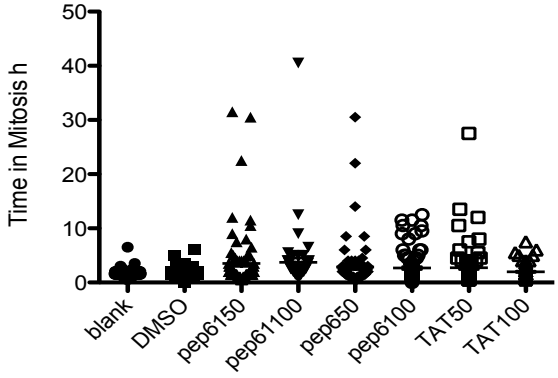

Figure 4.11. Time taken for Tat, Tat-tagged peptide 6 and peptide 61 MCF-7 treated cells to complete mitosis. The bars through clusters of time points represent the mean times taken to complete mitosis.

After live cell imaging, cells were counted in the first and last image to work out the percentage increase in cells (Figure 4.12). Treatment with peptide 61 in both MCF-7 cells and MDA-MB231 cells led to a smaller increase in cell number compared to Tat and peptide 6 treated cells. The above analysis (Figure 4.10) has shown that this decrease in cell number is not due to cell death. Therefore, the decrease in the percentage increase of cells could be due to the fact that more cells went through aberrant mitosis (one binucleate cell instead of two individual cells) and cells were spending longer in mitosis and/or undergoing cell cycle arrest after the first mitosis.

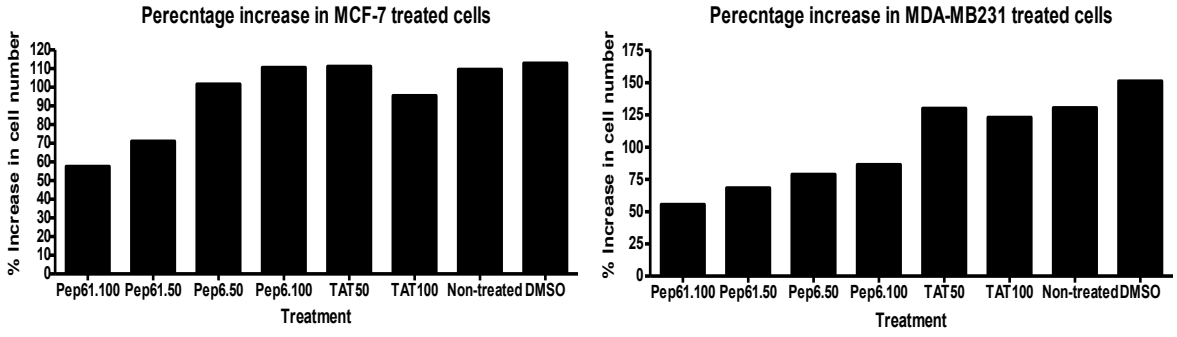

Figure 4.12. MCF-7 and MDA-MB231 treated Cells counted in the first image and last image during live cell imaging to calculate the percentage increase in cell number.

As with the microinjection experiments Tat-tagged peptide 6 did not have an effect on aberrant mitosis. Therefore, the experiment was repeated this time by treating the cell with CtBP2 siRNA prior to treatment with Tat-tagged peptide 6 (Figure 4.13). This resulted in a significant increase in aberrant mitosis ($P<0.0001$), 6% and 1% for Tat 50 μM and 100 μM to 16% and 30% for CtBP2 siRNA with peptide 6 50 μM and 100 μM, respectively. Figure 4.14 shows images captured during live cell imaging, the red circle follows an example of a cell that goes through aberrant mitosis. The cell looks as if it has split to two cells but then comes back together giving a single binucleate cell, due to failed abscission. The time spent in mitosis for each Tat-tagged treated cell was quantified. Non-treated and Tat treated cells spent an average of 1.5 hr in mitosis; cells treated with peptide 6 and CtBP2 siRNA spent an average of 3.5 hr in mitosis (Figure 4.15).

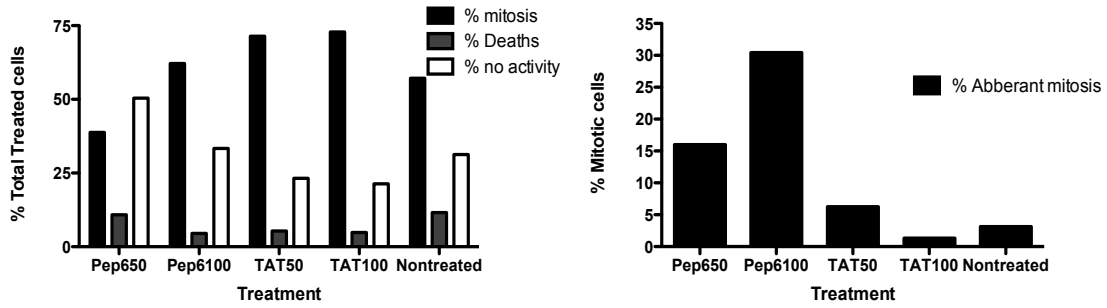

Figure 4.13. Tat, Tat-tagged peptide 6 with CtBP2 siRNA treated cells were tracked by live cell imaging over a period of 48 hr post-serum re-stimulation. The cells that underwent aberrant mitosis were monitored.

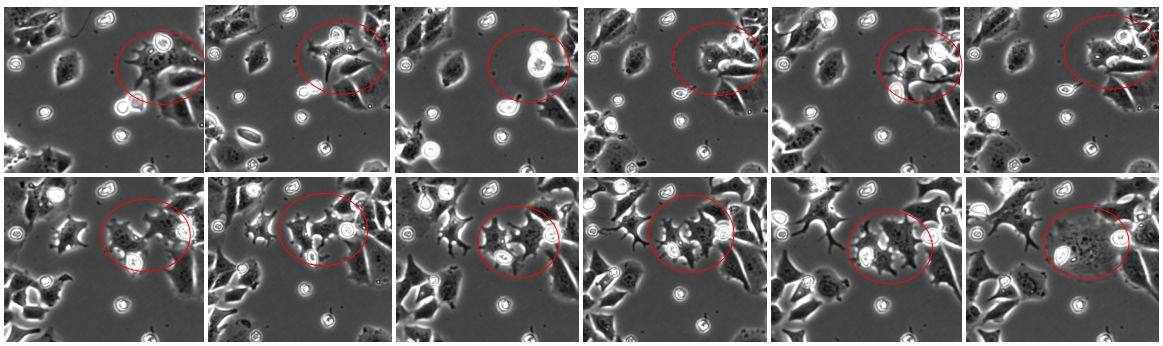

Figure 4.14. MCF-7 cells treated with CtBP2 siRNA and peptide 6 Tat-tagged induces aberrant mitosis.

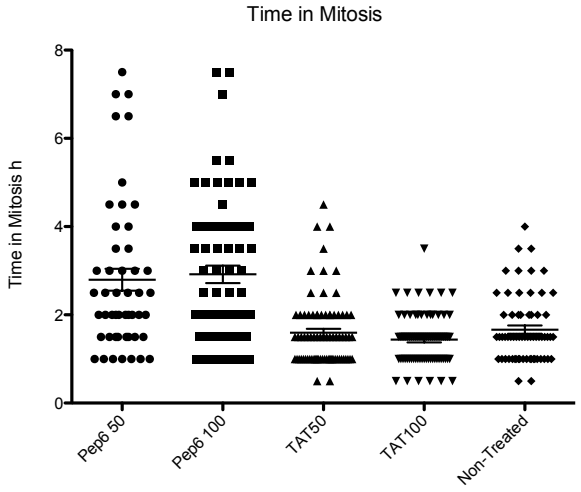

Figure 4.15. Time taken for Tat, Tat-tagged peptide 6 with CtBP2 siRNA treated cells to complete mitosis was monitored. The bars through clusters of time points represent the mean times taken to complete mitosis.

X-ray crystallography and mutational studies have determined that CtBP homo- and heterodimerisation is dependent upon critical residues in the central dehydrogenase-homology domain of the protein. Therefore, isolated dehydrogenase domain CtBPDD could be used as an alternative tool to disrupt CtBP1 and CtBP2 homo- and heter-dimerisation in cells. A double point mutant (R147A, R169L the CtBP2 dehydrogenase domain) would disrupt this CtBP-binding activity of this domain, without affecting its gross structure, and this serves as a well-defined negative control, CtBPDDM. When injected into synchronized MCF-7 cell by Dr Charles Birts, CtBPDD but not CtBP2DDM resulted in a significant ($p<0001$) increase in the proportion of mitotic events that failed to progress normally[86] (Figure 4.16). This data supports the results for the peptide treated cells that illustrate that CtBP dimerisation is important in maintaining mitotic fidelity.

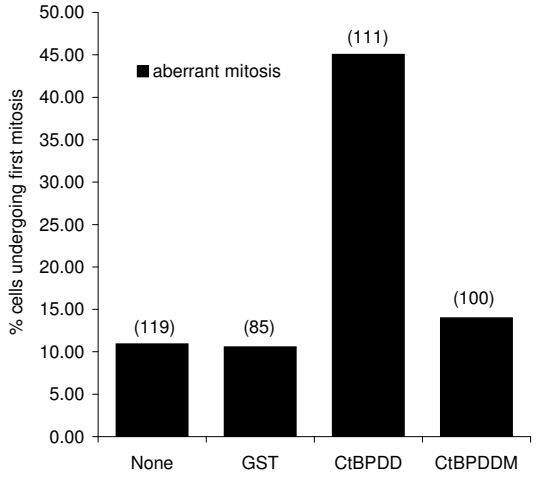

Figure 4.16. GST, CtBPDD and CtBPDDM treated cells were tracked by live cell imaging over a period of 48 hr post-serum re-stimulation. The cells that underwent aberrant mitosis were monitored, as indicated.

4.1.3 Immunofluorescence analysis

4.1.3.1 Mitotic Index and Cells with Micronuclei

Mitotic Index is defined as the ratio between the number of cells in mitosis and the total number of cells. Mitotic Index is calculated by counting the number of cells containing visible chromosomes divided by the total number of cells in the field of view. In order to analyse the phenotype of CtBP-depleted cells, detailed morphological analysis of DAPI-stained cell nuclei was carried out (Figure 4.17). DAPI is a fluorescent stain that binds strongly to A-T rich regions in DNA. Along with the mitotic index, cells with micronuclei were also counted. Micronuclei can arise from whole chromosomes, which lag at mitosis due to, for example, damaged kinetochore or faulty spindle apparatus, or from acentric chromosome fragments created by DNA breaks. There was a significant increase in the occurrence of micronuclei, from 6% of the Tat treated cells to 16.5% following peptide 61 treatment. Compared to the untreated cells peptide 61 resulted in a significant reduction in the mitotic index similar to that observed with CtBP siRNA. Peptide 6 and Tat on its own illustrated a less of an effect (Figure 4.18). This was supported with a siRNA control experiment (Figure 4.19), where cells were treated with CtBP siRNA, both CtBP1 and CtBP2 siRNA, and CtBP1 and CtBP2 siRNA

individually. Individually CtBP1 and CtBP2 had little effect, similar to that observed with peptide 6, which only block CtBP1. Cells treated with CtBP siRNA and CtBP1 and CtBP2 siRNA together showed significant increase in cells with micronuclei, similar to that observed with peptide 61, which blocks CtBP1 and CtBP2.

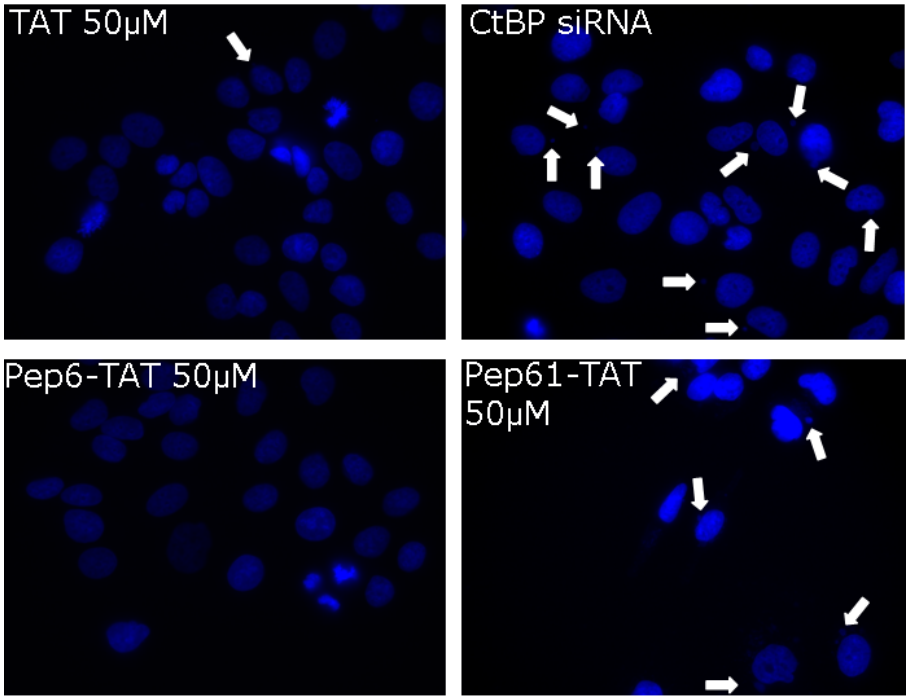

Figure 4.17. DAPI-stained MCF-7 nuclei of control treated cells and peptide 61 treated cells. Micronuclei indicated with white arrows (in collaboration with Dr Charles Birts).

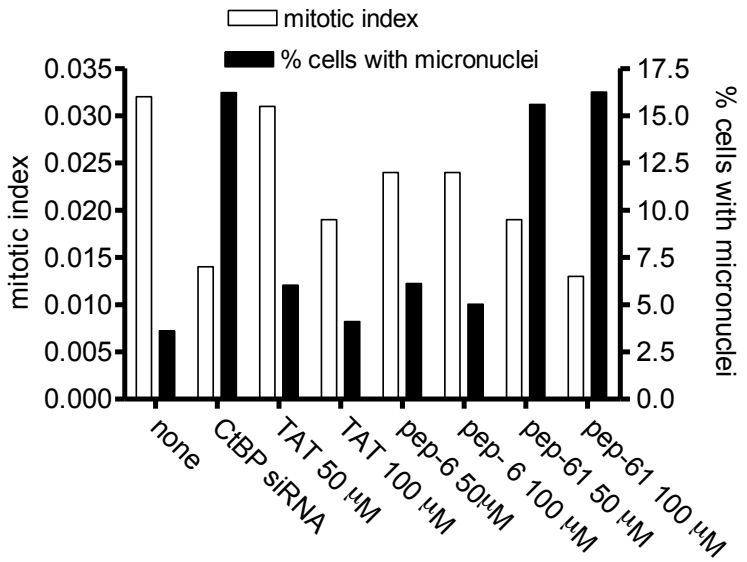

Figure 4.18. Quantification of micronuclei in MCF-7 cells 3 day post-transfection with CtBP siRNA, TAT, peptide 6 and 61 at 50 and 100 μM (Dr Charles Birts).

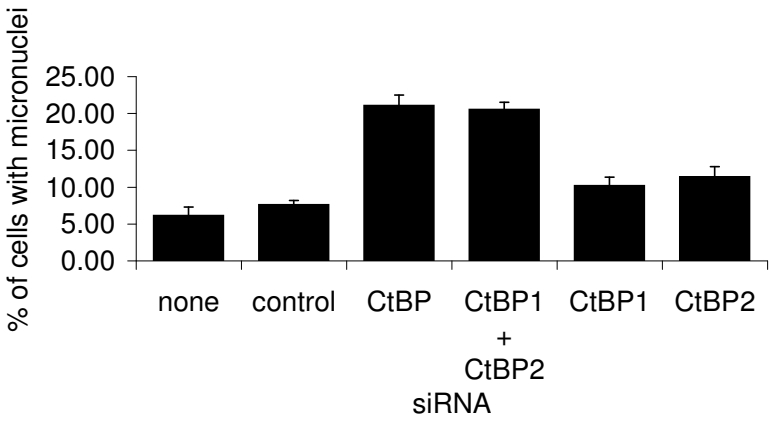

Figure 4.19. Quantification of micronuclei in MCF-7 cells 3 day post-transfection with control, CtBP, CtBP1 + CtBP2, CtBP1 and CtBP2 siRNA (Dr Charles Birts).

It has previously been shown that CtBP siRNA down regulated CtBP expression within 24 hr.[58] CtBP siRNA similarly reduced CtBP abundance. We have demonstrated that the uncovered cyclic peptides specifically inhibit the protein-protein interaction of CtBPs without affecting their cellular level (illustrated in the immunoblot Figure 4.20

carried out by Dr Charles Birts). Therefore any phenotypes observed can therefore be directly assigned to the protein-protein interaction of CtBP, rather than their presence or absence from the cell.

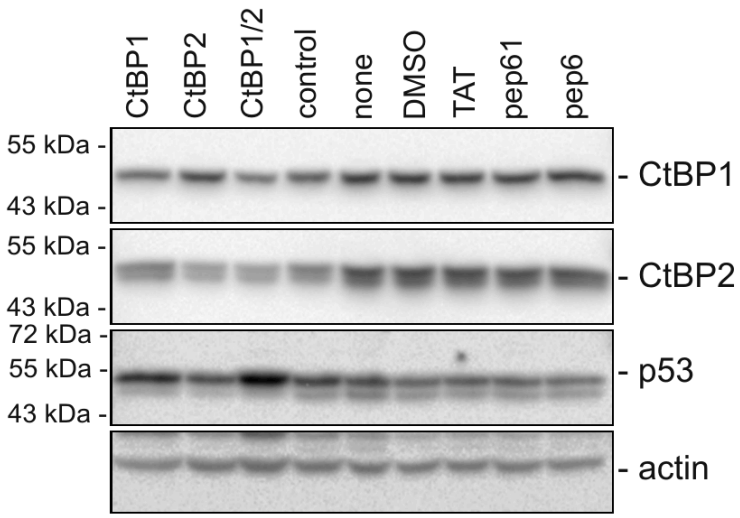

Figure 4.20. Immunoblot confirming effects of siRNAs and peptide on the abundance of their targets in MCF-7 cells. The abundance of the p53 protein was also examined.

4.1.4 MTS assays.

MTS [3-(4,5-dimethylthiazol-2-yl)-5-(3-carboxymethoxyphenyl)-2-(4-sulfophenyl)-2H-tetrazolium] is a Tetrazolium-based assay. The MTS assay was carried out to complement the experiments from cell counting in the live cell imaging. Metabolism in viable cells produces "reducing equivalents" such as NADH or NADPH. These reducing compounds pass their electrons to an intermediate electron transfer reagent that can reduce the tetrazolium product, MTS, into an aqueous, soluble formazan. The CellTiter 96$^{(R)}$ Aqueous products are MTS assays for determining the number of viable cells in culture and therefore the combined effects of inhibition of cell division and induction of cell death over the treatment period can be monitored.

Cells were initially treated with Tat-tagged peptide 6 and 61 (at a concentration of 0, 0.5, 1, 5, 10, 25, 50, 100 μM). 48hr post treatment the MTS was run (Figure 4.21). DMEM was added on its own as a background control and the peptides were run in triplicate. As the peptide concentration increases there is a decrease in signal indicating

a decrease in the presence of viable cells. In MDA-MB231 cells 50 μM of peptide 6 and 10 μM of peptide 61 were sufficient for maximum decrease in signal. In MCF-7 cells 50μM of peptide 6 and 25 μM of peptide 61 were sufficient for maximum decrease in signal. Survival was plotted as a percentage of untreated cells. In MCF-7 cells the signal decreased to 69% and 53% for peptide 6 and 61 respectively from 0-100 μM. In MDA-MB231 cells the signal decreased to 54% and 64% for peptide 6 and 61 respectively from 0-100 μM.

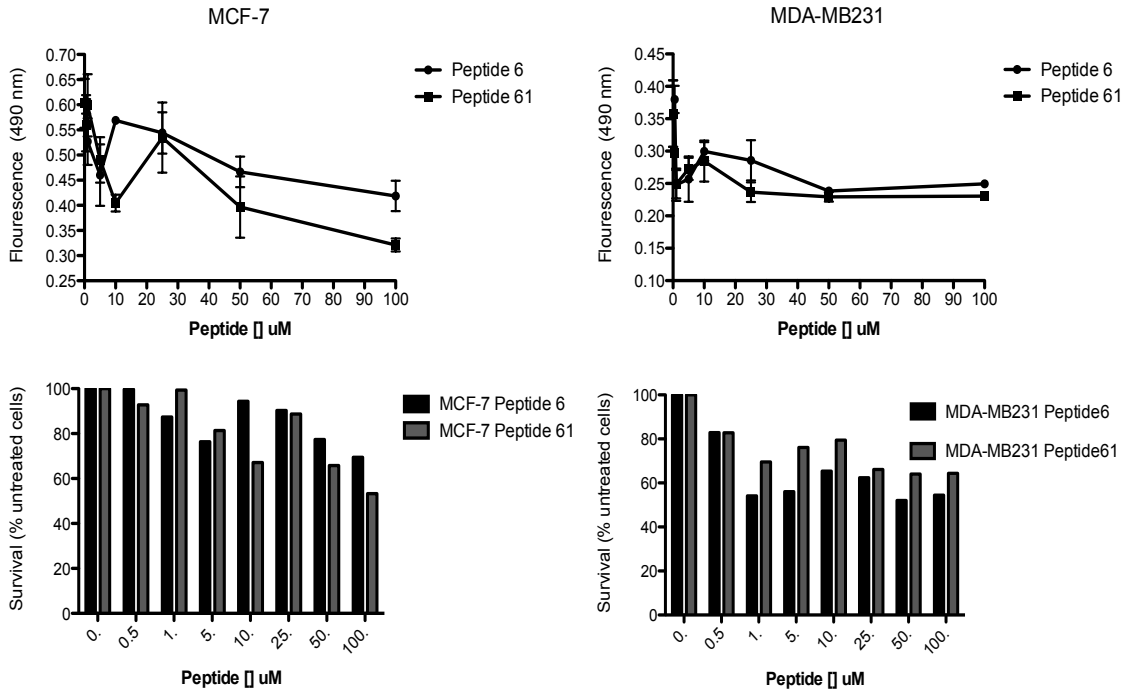

Figure 4.21. Graph showing results from the MTS assay; the graphs above show how the fluorescent signal decreases as the peptide concentration increases in MDA-MB231 and MCF-7 cells respectively; the graphs below shows the percentage of signal at each concentration compared to untreated cells.

The experiment was repeated but this time Tat was also used as a control to ensure Tat was not having an effect on the cells (Figure 4.22). MCF-7 and MDA-MB231 cells were treated with peptide 6, 61 and Tat at concentrations of 0.1, 1, 3, 10, 30 and 100 μM. In MDA-MB231 cells 10 μM of peptide 6 and 30 μM of peptide 61 were sufficient for maximum decrease in signal. In MCF-7 cells 30 μM of peptide 6 and 10 μM of peptide 61 were sufficient for maximum decrease in signal. In MCF-7 cells the signal decreased to 45%, 51%, 82% for peptide 6, 61 and Tat respectively from 0-100 μM. In

MDA-MB231 cells the signal decreased to 31%, 69% and 83% for peptide 6, 61 and Tat respectively from 0-100 μM. Tat did not lead to a significant decrease in signal compared to peptide 6 and 61.

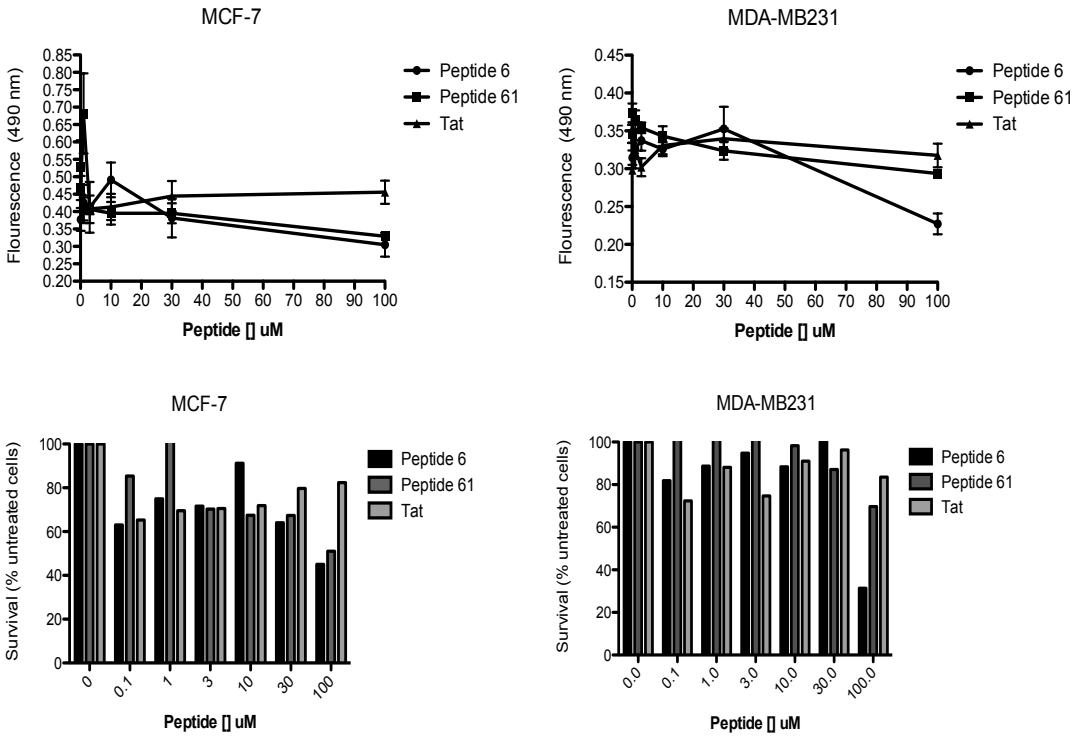

Figure 4.22. Graph showing results from the MTS assay; the graphs above show how the fluorescent signal decreases and peptide concentration increases in MDA-MB231 and MCF-7 cells respectively; the graphs below shows the percentage of signal at each concentration compared to untreated cells.

4.1.5 Colony Forming Assay

The results from the MTS assay were not conclusive, therefore colony-forming assays were carried out as this assay is a more sensitive measure of the ability of the peptides to inhibit cellular proliferative capacity than MTS. Also a more visual view of the effect of the peptides on the ability of single breast cancer cells to establish colonies can be obtained. Tat alone was used as a control. Peptide 61 resulted in a decrease in the number of colonies present in MCF-7 and MDA-MB-231 10 d post-transfection, whereas peptide 6 resulted in a decrease in colony number in MDA-MB-231 cells. This is in agreement with the live cell imaging analysis (Figure 4.13).

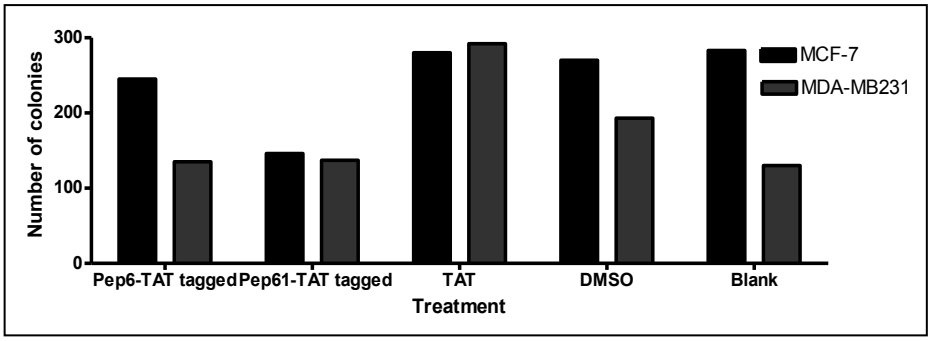

Figure 4.23. Colony-forming assay for both MCF-7 and MDA-MB231 cells 10 days post-transfection with peptide 6, peptide 61 and TAT.

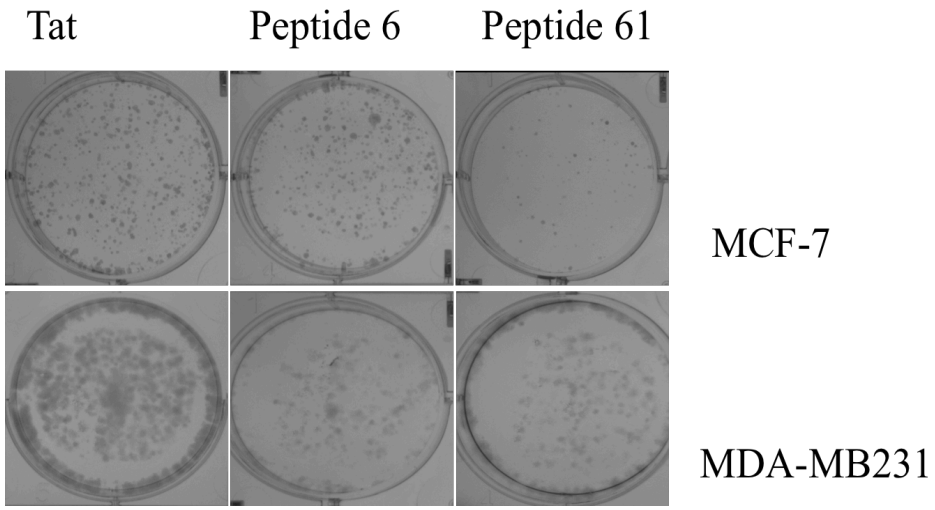

Figure 4.24. Giemsa staining of MCF-7 and MDA-MB231 cell colonies 10 days post-transfection with Tat, peptide 6 and 61.

4.1.6 Flow Cytometry

Different cells can be identified by measuring the fluorescence they emit when they pass a laser beam in a flow cytometer. In a fluorescence-activated cell sorter (FACS), which is an instrument based on flow cytometry, the cells can be identified and separated from each other. To investigate whether breast cancer cells arrest in a specific point of the cell cycle after treatment with peptides, flow cytometry analysis of DNA content was carried out. Cells from the time-lapse experiment were trypsinised and collected in centrifuge tubes and centrifuged. After subsequent washes with PBS and 70% ethanol the pellet was stored at 4 °C until propidium iodide (PI) staining was

carried out. PI intercalates into double-stranded nucleic acids. It is excluded by viable cells but can penetrate cell membranes of dying or dead cells and is used as a DNA stain for flow cytometry. The staining and flow cytometry was carried out by Dr Charles Birts. The analysis did not show a significant effect of the peptides. This may have been due the fact that there were not enough cells for analysis as the samples were small. Due to time constraints the experiment has not yet been repeated.

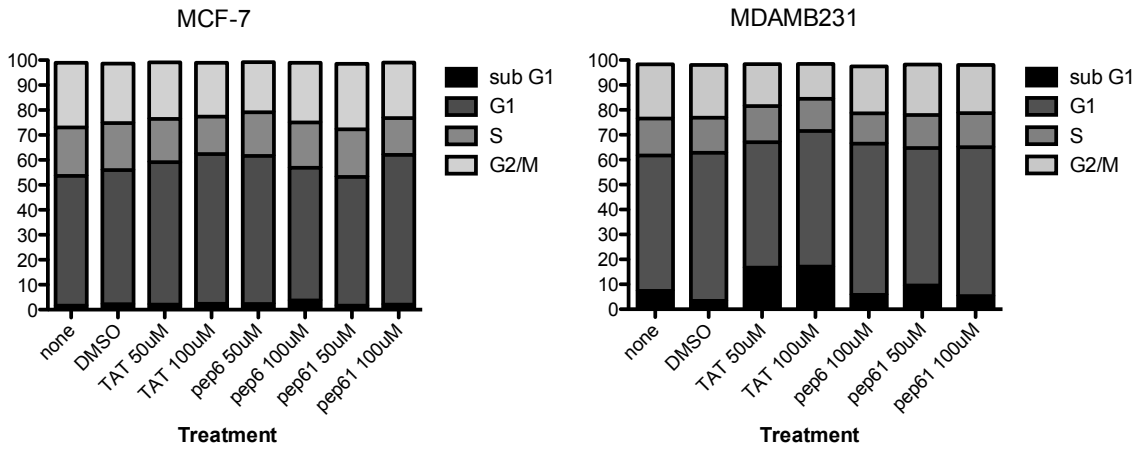

Figure 4.25. Analysis of cellular content by flow cytometry.

4.1.7 P53 activity

The tumor protein 53 (p53), is a tumor suppressor protein that in humans is encoded by the *TP53* gene.[113] p53 is crucial in multicellular organisms, where it regulates the cell cycle and thus functions as a tumor suppressor that is involved in preventing cancer. The regulation of p53 function is tightly controlled through several mechanisms including p53 transcription and translation, protein stability and post-translational modifications. P53 is mostly located in the cytoplasm. When DNA damage occurs, p53 gets imported into the nucleus via its NLS and undergoes tetramization, binds and activates DNA damage-response genes.[114]

It has previously been shown by Bergman *et al* that inhibition of CtBP expression in MCF-7 cells caused an increase in p53 protein abundance, and up regulation of its transcriptional target, $p21^{WAF1}$ (cyclin-dependent kinase inhibitor 1). The $p21^{WAF1}$ protein binds to and inhibits the activity of cyclin-CDK2 or –CDK4 complexes, and thus functions as a regulator of cell cycle progression at G_1.[58] To investigate whether the

peptides led to an increase in p53 protein abundance, MCF-7 cells were treated with peptide 6 and 61. 2 d post-transfection immunofluorescence staining was carried out. A p53 primary antibody was used followed by a Rabbit-α-mouse FITC (1:50) secondary antibody (FITC stains areas containing p53 green). Cells were counterstained with DAPI during secondary antibody incubation (stains the nucleus blue). Sufficient Blocking and washing was required to prevent unspecific binding of the antibodies. For blocking, 10% FCS in PBS was used; for washing 5 min washing with PBS was carried out; for the final wash two 5 min washes with PBS and one 5 min wash with water was carried out. Nutlin (Figure 4.26 C) was used as a positive control as it inhibits the interaction between MDM2 and p53, thus stabilizing p53.

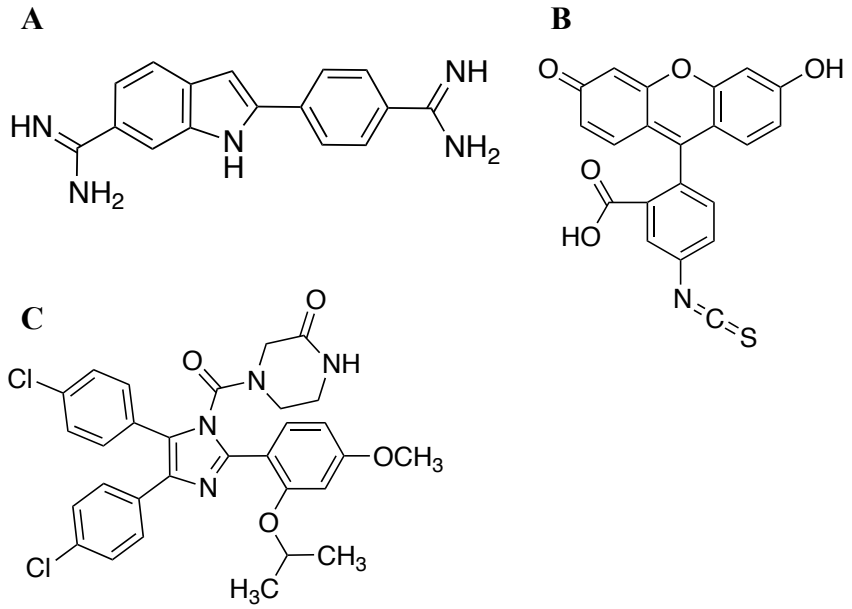

Figure 4.26. Structure of (A) DAPI, (B) FITC and (C) Nutlin.

Treatment with peptide 6 and 61 did not lead to a significant increase in p53 up regulation in comparison with nutlin (Figure 4.27). It can be seen that the majority of p53 protein is located in the cytoplasm. These results are supported by the immunoblot in Figure 4.20, which show that treatment with peptide 6 and 61 did not cause an increase in p53 abundance whereas cells treated with both CtBP1 and CtBP2 siRNA showed an increase. This may be due to the fact that CtBP siRNA leads to a reduction of cellular CtBP levels whereas the peptides break up dimerisation but do not affect cellular levels. Further investigation is required.

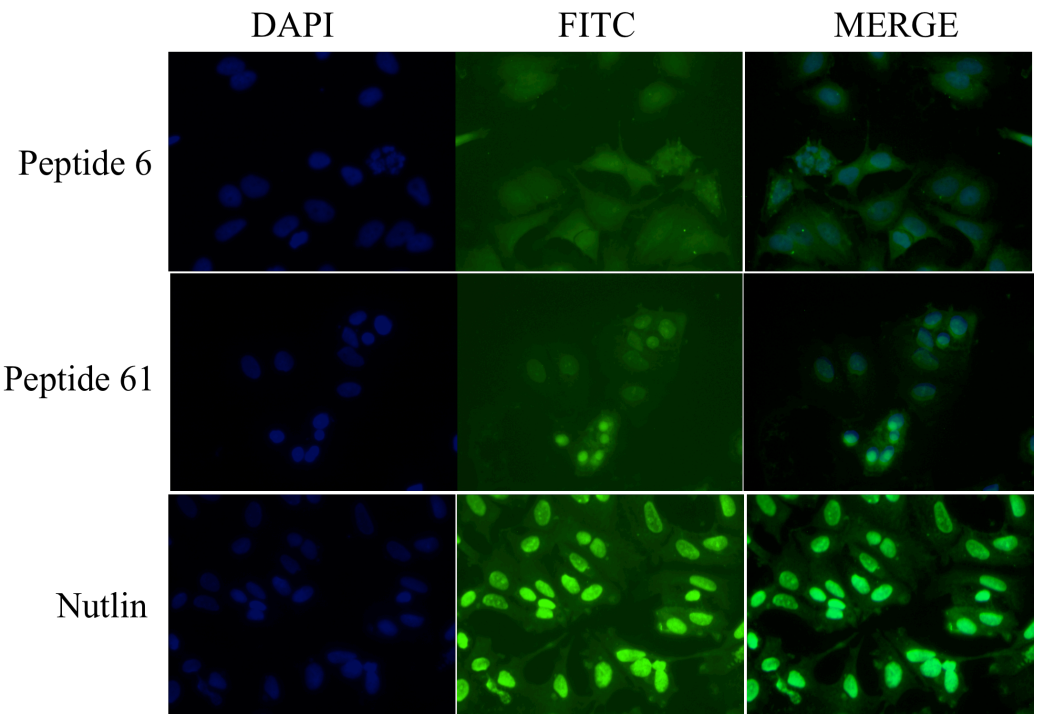

Figure 4.27. Immunofluorescence staining for p53 in MCF-7 cells treated with peptide 6, peptide 61 and nutlin.

4.1.8 Cell Migration Assay

Effect of Peptide 6 on MCF-7 single cell migration towards collagen

The study of cell invasion and migration is of great importance to enable a better understanding of underlying biological and molecular mechanisms. Cell invasion is the intrusion and destruction of adjacent tissues particularly with respect to cancer cells. Cell migration is the movement of cells from one area to another generally in response to chemical signals and is important in diverse physiological and pathological processes including embryonic development, cell differentiation, wound healing, immune response, inflammation and cancer metastasis.

Transwell migration assay used for studying the motility of different cells including metastatic cancer cells. The assay relies on a permeable layer of support, usually a microporous membrane that is tissue culture treated, which is positioned between two compartments that mimic two different microenvironments for cell growth. Cells on one side of the compartment can migrate through the micropores on the membrane in response to a chemoattractant. Migrated cells can then be quantified by methods as

simple as fix/stain and count. A typical set up for the migration assay in a single well of a 24 well plate is illustrated in Figure 4.28.

All migration assays were carried out by Marta Chrzan. Cells were incubated with peptide 6 and Tat in the presence of collagen IV for 30 min at 4 °C prior to plating in Transwells (40,000 cell/well). Cells were also treated with BSA and collagen IV only as controls. Integrin-mediated migration was induced with collagen IV (10μg/ml). BSA was used to measure non-specific migration. The migration assay illustrated that peptide6 and peptide61 lowered the number of migrated cells to almost half of that for the control Tat on its own (Figure 4.29, Figure 4.30).

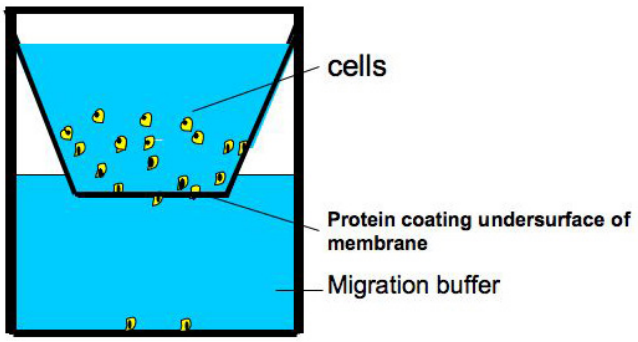

Figure 4.28. A typical set up for the migration assay in a single well of a 24 well plate.

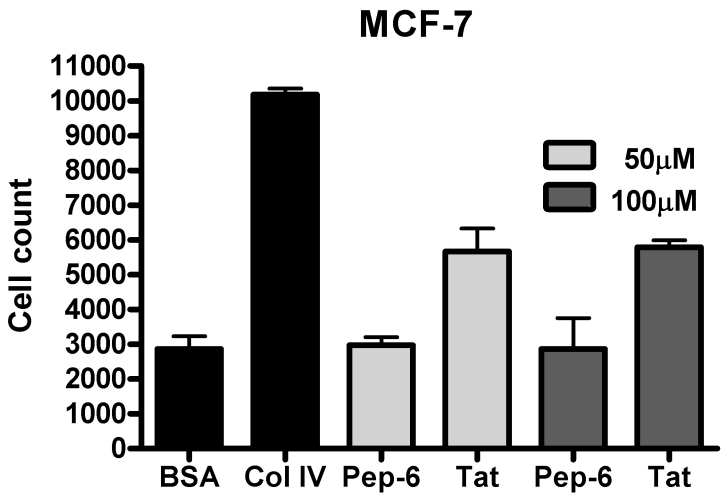

Figure 4.29. Cell migration assay results of MCF cells treated with peptide 6 and Tat.

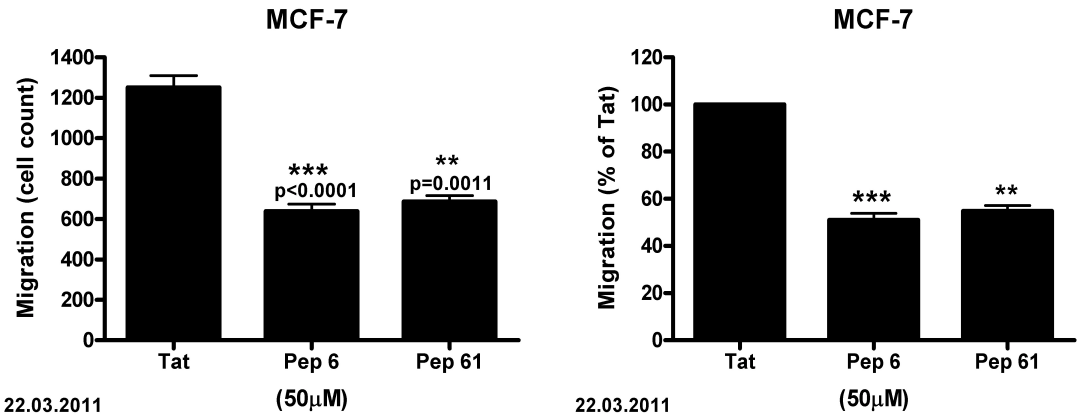

Figure 4.30. Cell migration assay results of MCF-7 cells treated with Tat, peptide 6 and 61; the left hand side illustrates cell count for cells that have migrated across the membrane; the right hand side shows migration as a percentage of Tat.

There are certain drawbacks of the transwells assay. For example, the migrated cells must be stained with chemical dyes or labelled with fluorescent molecules. In most cases the membrane is removed from the insert then counted manually using a microscope or evaluated using a spectrometer. That can be labour intensive and lead to limited throughput. Also, labelling may alter gene expression profiles and lead to intra-assay variability because of differences in labelling efficiency. Cell counting can also be inconsistent and irreproducible.

Roche xCELLigence provides kinetic information about cell migration by dynamically recording the entire cell migration and invasion process in real time without labelling cells. Information about cell growth, morphological changes and cell death can be obtained. This assay considerably improves invasion and migration assay quality. As cells migrate from the upper chamber to the lower chamber in response to chemoattractant, they contract and adhere to the electronic sensors on the underside of the membrane resulting in an increase in impedance. The impedance increase correlates to increasing number of migrated cells on the underside of the membrane, and cell-index values reflecting impedance changes are automatically and continuously recorded

by the RTCA DP instrument. Therefore cell migration activity can be monitored via cell index profile.

The xCELLigence data (Figure 4.31) confirms the finding that for peptide 6, cells initially migrate across the membrane but then the amount of migration levels off at around 2 hr. Whereas, the control Tat is constantly migrating across the membrane. Peptide 61 constantly migrating across the membrane too but at a slower rate compared to the Tat and that could account for the lower cell count. Towards the end of the assay, the levels seem to drop for all three assays this could be due the fact that the cells have been with out serum for too long and the cells are therefore are dying.

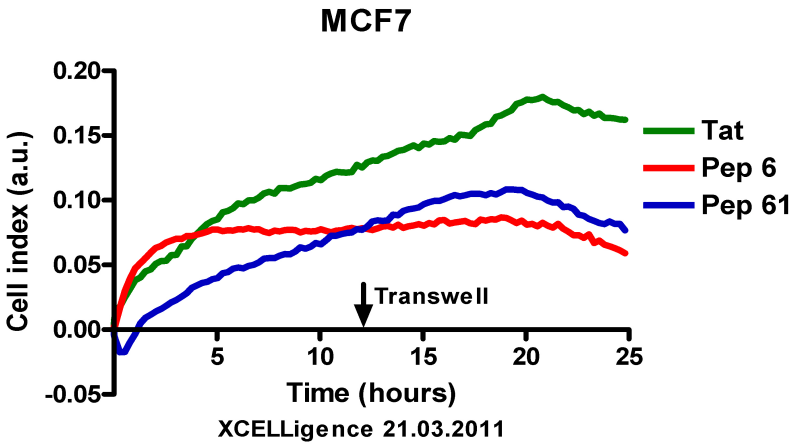

Figure 4.31. Graph illustrating the migration profile of MCF-7 cells treated with Tat, peptide 6 and 61.

The RTHS and SICLOPPS have been combined to uncover cyclic peptide inhibitors of CtBP1 and CtBP2 dimerisation (Chapter 2). This is important to study the effect of disrupting dimerisation of CtBPs in cancer cells. Peptide 6 and 61 showed similar effects to CtBP siRNA without causing a decrease in cellular levels of CtBP. In the SICLOPPS screen peptide 6 showed inhibition of CtBP1 whereas Peptide 61 showed inhibition of both CtBP1 and CtBP2. This was supported by the *in vivo* studies in this chapter. When studying the mitotic fidelity of cells peptide 61 showed an increase in aberrant mitosis and time spent in mitosis, whereas peptide 6 only showed this effect in the presence of CtBP2 siRNA. Thus confirming the importance both CtBP1 and CtBP2 dimerisation in maintaining mitotic fidelity.

5. Conclusion

There has been an increasing amount of evidence linking CtBPs to tumorigenesis and tumor progression. CtBPs are transcriptional corepressors that promote cell survival, migration and invasion.[76b, 68, 69] The ability of CtBP1 and CtBP2 to homodimerise and heterodimerise has previously been reported. The CtBP nucleotide binding domain plays an important role in dimerisation. NADH is able to bind in the nucleotide binding domain with high affinity and is important for CtBP dimerisation and CtBP regulated transcriptional co-repressor activity.[115, 42, 116] Many models have been postulated implicating the importance of CtBP dimers as bridge linking transcription factors and effectors.[69, 48]

CtBP inhibition is a therapeutic target in cancer therapy due to the potentially druggable dehydrogenase domain. Straza et al have reported a dehydrogenase 4-methylthio-2-oxobutyric acid (MTOB) CtBP inhibitor. MTOB induced p53-independent apoptosis in a variety of human cancer cells and it led to a loss of cell viability. High levels of CtBPs were detected in colon cancer. Therefore, colon cancer exhibits heightened sensitivity to anti-CtBP therapy. MTOB induced apoptosis and reduced tumor burden in human colon cancer cells.[117]

In this study RTHS and SICLOPPS have been combined to uncover cyclic peptide inhibitors of CtBP1 and CtBP2 dimerisation. It is important to study the effect of disrupting dimerisation of CtBPs in cancer cells. Peptide 6 and 61 showed similar effects to CtBP siRNA without causing a decrease in cellular levels of CtBP. In the SICLOPPS screen peptide 6 showed inhibition of CtBP1 whereas peptide 61 showed inhibition of both CtBP1 and CtBP2. When studying the mitotic fidelity of cells, peptide 61 showed an increase in aberrant mitosis and time spent in mitosis, whereas peptide 6 only showed this effect in the presence of CtBP2 siRNA. This confirms the importance of both CtBP1 and CtBP2 in maintaining mitotic fidelity.

It has previously been shown that RNAi mediated knockdown of CTBP1 and CtBP2 leads to a decrease in cell invasion and migration.[118, 119] Treatment of MCF-7 cells with peptide 6 and 61 led to a decrease in migration. That indicates the importance of CtBP dimerisation in cell migration and the ability of CtBPs to recruit DNA binding

transcription factors. To further understand the effects of peptide 6 and 61 in the recruitment of transcription factors, it would be of interest, as part of future work, to send the peptide treated cells for microarray analysis to investigate the changes in gene expression.

Our mechanism of combining the RTHS and SICLOPPS allows us to obtain small molecule tools that are useful for improving our understanding of disease mechanism and developing new therapies. Peptide 6 and 61 inhibit CtBP dimerisation and they could be candidate drugs for cancer, or they could help identify new drug targets. The peptides have shown to have an influence on MCF-7 breast cancer cells without having a toxic effect on the cells. There are issues with regard to delivery of the peptides across the cell membrane. So, a more efficient way of delivering the peptides into the cells is required other then microinjection and Tat-tagging, in order to make them more suitable as a therapeutic drugs. Cyclic peptides have a greater potential as therapeutic agents compared to the linear peptide due to increased chemical and enzymatic stability and receptor selectivity which arises from the restricted conformational flexibility.[120]

The initial step in drug research to improve a potential therapeutic drug is simplification. Not all the amino acids in the peptide are required to achieve biological effects. Therefore it is important to establish which amino acids are of importance for the peptides activity. Alanine scanning is a technique used to identify specific amino acid residues that are responsible for the protein function, stability and conformation. Alanine is used because of its small inert methyl functional group. Alanine is used to substitute each non-alanine residue one at a time. Alanine scanning of peptide 6 and 61 can be carried out to determine which residues are essential for the function of the peptides. Another method for generating compounds with drug-like permeability and oral bioavailability is N-methylation. N-methylation has shown to improve pharmacological properties such as lipophilicity, proteolytic stability, bioavailability and conformational rigidity.[120-121] These peptides can then be tested in the ELISA to see how the residue substitution and N-methylation affects the activity of the peptide. Active peptides can then be further tested in animal permeability studies.

We need to better understand how the peptides function and bind to CtBPs. Therefore, further work would involve the crystallisation of CtBPs and peptides. To date, all crystallisation that has been carried out on CtBPs has excluded the C-terminal due to the

high mobility or disorder of the C-terminal region in the full-length protein that may maintain an unstructured conformation, preventing the formation of productive crystal contacts. For the ELISA the full length CtBP was used, and therefore the CtBP-pET28 vectors can be modified to exclude the C-terminal. Compared to the ELISA more protein is required and an extra gel filtration step is also required.

Reference

1. Fry, D. C.; Vassilev, L. T., Targeting protein-protein interactions for cancer therapy. *Journal of Molecular Medicine-Jmm* **2005,** *83* (12), 955-963.

2. Eggert, U. S.; Field, C. M.; Mitchison, T. J., Small molecules in an RNAi world. *Mol Biosyst* **2006,** *2* (2), 93-6.

3. Tu, Z.; Argmann, C.; Wong, K. K.; Mitnaul, L. J.; Edwards, S.; Sach, I. C.; Zhu, J.; Schadt, E. E., Integrating siRNA and protein-protein interaction data to identify an expanded insulin signaling network. *Genome Res* **2009,** *19* (6), 1057-67.

4. Underwood, L., siRNA gene silencing for therapeutic purposes. *MMG 445 Basic Biotechnology* **2010,** *6*, 59-64.

5. Fletcher, S.; Hamilton, A. D., Targeting protein-protein interactions by rational design: mimicry of protein surfaces. *Journal of the Royal Society Interface* **2006,** *3* (7), 215-233.

6. Guney, E.; Tuncbag, N.; Keskin, O.; Gursoy, A., HotSprint: database of computational hot spots in protein interfaces. *Nucleic Acids Research* **2008,** *36*, D662-D666.

7. Chene, P., Drugs targeting protein-protein interactions. *Chemmedchem* **2006,** *1* (4), 400-411.

8. Moreira, I. S.; Fernandes, P. A.; Ramos, M. J., Hot spots-A review of the protein-protein interface determinant amino-acid residues. *Proteins-Structure Function and Bioinformatics* **2007,** *68* (4), 803-812.

9. Zhong, S. J.; Macias, A. T.; MacKerell, A. D., Computational identification of inhibitors of protein-protein interactions. *Current Topics in Medicinal Chemistry* **2007,** *7* (1), 63-82.

10. Vidal, M.; Legrain, P., Yeast forward and reverse 'n'-hybrid systems. *Nucleic Acids Research* **1999,** *27* (4), 919-929.

11. Liu, Y.; Kim, I.; Zhao, H., Protein interaction predictions from diverse sources. *Drug Discovery Today* **2008,** *13* (9-10), 409-416.

12. (a) Kuroda, K.; Kato, M.; Mima, J.; Ueda, M., Systems for the detection and analysis of protein-protein interactions. *Applied Microbiology and Biotechnology* **2006,** *71* (2), 127-136; (b) Karimova, G.; Pidoux, J.; Ullmann, A.; Ladant, D., A bacterial two-hybrid system based on a reconstituted signal transduction pathway. *Proceedings of*

the National Academy of Sciences of the United States of America **1998,** *95* (10), 5752-5756.

13. Vidal, M.; Brachmann, R. K.; Fattaey, A.; Harlow, E.; Boeke, J. D., Reverse two-hybrid and one-hybrid systems to detect dissociation of protein-protein and DNA-protein interactions. *Proceedings of the National Academy of Sciences of the United States of America* **1996,** *93* (19), 10315-20.

14. Vidal M, E. H., Prospects for drug screening using the reverse two-hybrid system. *Trends Biotechnol.* **1999,** *17* (9), 374-81.

15. Hannink*, C. A. L. a. M., The reverse two-hybrid system: a genetic scheme for selection against specific protein/protein interactions. *Nucleic Acids Research* **1996,** *24* (17), 3341-3347.

16. Joung, J. K.; Ramm, E. I.; Pabo, C. O., A bacterial two-hybrid selection system for studying protein-DNA and protein-protein interactions. *Proceedings of the National Academy of Sciences of the United States of America* **2000,** *97* (13), 7382-7387.

17. (a) Tavassoli, A.; Benkovic, S. J., Genetically selected cyclic-peptide inhibitors of AICAR transformylase homodimerization. *Angewandte Chemie-International Edition* **2005,** *44* (18), 2760-2763; (b) Horswill, A. R.; Savinov, S. N.; Benkovic, S. J., A systematic method for identifying small-molecule modulators of protein-protein interactions. *Proceedings of the National Academy of Sciences of the United States of America* **2004,** *101* (44), 15591-15596.

18. Ladant, D.; Karimova, G., Genetic systems for analyzing protein-protein interactions in bacteria. *Res Microbiol* **2000,** *151* (9), 711-20.

19. Bushman, F. D.; Ptashne, M., Activation of transcription by the bacteriophage 434 repressor. *Proc Natl Acad Sci U S A* **1986,** *83* (24), 9353-7.

20. Hollis, M.; Valenzuela, D.; Pioli, D.; Wharton, R.; Ptashne, M., A repressor heterodimer binds to a chimeric operator. *Proc Natl Acad Sci U S A* **1988,** *85* (16), 5834-8.

21. Donner, A. L.; Carlson, P. A.; Koudelka, G. B., Dimerization specificity of P22 and 434 repressors is determined by multiple polypeptide segments. *J Bacteriol* **1997,** *179* (4), 1253-61.

22. Di Lallo, G.; Castagnoli, L.; Ghelardini, P.; Paolozzi, L., A two-hybrid system based on chimeric operator recognition for studying protein homo/heterodimerization in *Escherichia coli*. *Microbiology* **2001,** *147* (Pt 6), 1651-6.

23. Horswill, A. R.; Benkovic, S. J., Cyclic peptides, a chemical genetics tool for biologists. *Cell Cycle* **2005,** *4* (4), 552-555.

24. Brilli, M.; Fani, R., Molecular evolution of hisB genes. *J. Mol. Evol.* **2004,** *58* (2), 225-237.

25. Miranda, E.; Forafonov, F.; Tavassoli, A., Deciphering interactions used by the influenza virus NS1 protein to silence the host antiviral sensor protein RIG-I using a bacterial reverse two-hybrid system. *Mol Biosyst* **2011,** *7* (4), 1042-5.

26. Tavassoli, A.; Lu, Q.; Gam, J.; Pan, H.; Benkovic, S. J.; Cohen, S. N., Inhibition of HIV budding by a genetically selected cyclic peptide targeting the Gag-TSG101 interaction. *ACS Chem Biol* **2008,** *3* (12), 757-64.

27. Sancheti, H.; Camarero, J. A., "Splicing up" drug discovery. Cell-based expression and screening of genetically-encoded libraries of backbone-cyclized polypeptides. *Adv Drug Deliv Rev* **2009,** *61* (11), 908-17.

28. Buller, F.; Mannocci, L.; Scheuermann, J.; Neri, D., Drug discovery with DNA-encoded chemical libraries. *Bioconjug Chem* **2010,** *21* (9), 1571-80.

29. Scheuermann, J.; Dumelin, C. E.; Melkko, S.; Neri, D., DNA-encoded chemical libraries. *J Biotechnol* **2006,** *126* (4), 568-81.

30. Giebel LB, C. R., Milligan DL, Young DC, Arze R, Johnson CR., Screening of cyclic peptide phage libraries identifies ligands that bind streptavidin with high affinities. *Biochem J* **1995,** *34* (47), 15430-5.

31. Tavassoli, A.; Benkovic, S. J., Split-intein mediated circular ligation used in the synthesis of cyclic peptide libraries in *E-coli*. *Nature Protocols* **2007,** *2* (5), 1126-1133.

32. Cheriyan, M.; Perler, F. B., Protein splicing: A versatile tool for drug discovery. *Adv Drug Deliv Rev* **2009,** *61* (11), 899-907.

33. Scott, C. P.; Abel-Santos, E.; Jones, A. D.; Benkovic, S. J., Structural requirements for the biosynthesis of backbone cyclic peptide libraries. *Chem Biol* **2001,** *8* (8), 801-15.

34. Scott, C. P.; Abel-Santos, E.; Wall, M.; Wahnon, D. C.; Benkovic, S. J., Production of cyclic peptides and proteins in vivo. *Proceedings of the National Academy of Sciences of the United States of America* **1999,** *96* (24), 13638-13643.

35. Deschuyteneer, G.; Garcia, S.; Michiels, B.; Baudoux, B.; Degand, H.; Morsomme, P.; Soumillion, P., Intein-mediated cyclization of randomized peptides in the periplasm of *Escherichia coli* and their extracellular secretion. *ACS Chem Biol* **2010,** *5* (7), 691-700.

36. Naumann, T. A.; Tavassoli, A.; Benkovic, S. J., Genetic selection of cyclic peptide Dam methyltransferase inhibitors. *Chembiochem* **2008,** *9* (2), 194-7.

37. Cheng, L.; Naumann, T. A.; Horswill, A. R.; Hong, S. J.; Venters, B. J.; Tomsho, J. W.; Benkovic, S. J.; Keiler, K. C., Discovery of antibacterial cyclic peptides that inhibit the ClpXP protease. *Protein Sci* **2007,** *16* (8), 1535-42.

38. Kinsella, T. M.; Ohashi, C. T.; Harder, A. G.; Yam, G. C.; Li, W.; Peelle, B.; Pali, E. S.; Bennett, M. K.; Molineaux, S. M.; Anderson, D. A.; Masuda, E. S.; Payan, D. G., Retrovirally delivered random cyclic Peptide libraries yield inhibitors of interleukin-4 signaling in human B cells. *J Biol Chem* **2002,** *277* (40), 37512-8.

39. Zhao, L. J.; Subramanian, T.; Chinnadurai, G., Inhibition of transcriptional activation and cell proliferation activities of adenovirus E1A by the unique N-terminal domain of CtBP2. *Oncogene* **2008,** *27* (39), 5214-5222.

40. Chinnadurai, G., CtBP, an unconventional transcriptional corepressor in development and oncogenesis. *Molecular Cell* **2002,** *9* (2), 213-224.

41. Nardini, M.; Svergun, D.; Konarev, P. V.; Spano, S.; Fasano, M.; Bracco, C.; Pesce, A.; Donadini, A.; Cericola, C.; Secundo, F.; Luini, A.; Corda, D.; Bolognesi, M., The C-terminal domain of the transcriptional corepressor CtBP is intrinsically unstructured. *Protein Sci* **2006,** *15* (5), 1042-50.

42. Kumar, V.; Carlson, J. E.; Ohgi, K. A.; Edwards, T. A.; Rose, D. W.; Escalante, C. R.; Rosenfeld, M. G.; Aggarwal, A. K., Transcription corepressor CtBP is an NAD(+)-regulated dehydrogenase. *Molecular Cell* **2002,** *10* (4), 857-869.

43. Ghosh, S.; George, S.; Roy, U.; Ramachandran, D.; Kolthur-Seetharam, U., NAD: A master regulator of transcription. *Biochim Biophys Acta*.

44. Nardini, M.; Valente, C.; Ricagno, S.; Luini, A.; Corda, D.; Bolognesi, M., CtBP1/BARS Gly172 -> Glu mutant structure: Impairing NAD(H)-binding and dimerization. *Biochemical and Biophysical Research Communications* **2009,** *381* (1), 70-74.

45. Kuppuswamy, M.; Vijayalingam, S.; Zhao, L. J.; Zhou, Y.; Subramanian, T.; Ryerse, J.; Chinnadurai, G., Role of the PLDLS-binding cleft region of CtBP1 in recruitment of core and auxiliary components of the corepressor complex. *Mol Cell Biol* **2008,** *28* (1), 269-81.

46. Thio, S. S.; Bonventre, J. V.; Hsu, S. I., The CtBP2 co-repressor is regulated by NADH-dependent dimerization and possesses a novel N-terminal repression domain. *Nucleic Acids Res* **2004,** *32* (5), 1836-47.

47. Quinlan, K. G.; Verger, A.; Kwok, A.; Lee, S. H.; Perdomo, J.; Nardini, M.; Bolognesi, M.; Crossley, M., Role of the C-terminal binding protein PXDLS motif binding cleft in protein interactions and transcriptional repression. *Mol Cell Biol* **2006,** *26* (21), 8202-13.

48. Chinnadurai, G., Transcriptional regulation by C-terminal binding proteins. *Int J Biochem Cell Biol* **2007,** *39* (9), 1593-607.

49. Chinnadurai, G., CtBP, an unconventional transcriptional corepressor in development and oncogenesis. *Mol Cell* **2002,** *9* (2), 213-24.

50. Kumar, R.; Wang, R. A.; Barnes, C. J., Coregulators and chromatin remodeling in transcriptional control. *Mol Carcinog* **2004,** *41* (4), 221-30.

51. Spyer, M.; Allday, M. J., The transcriptional co-repressor C-terminal binding protein (CtBP) associates with centrosomes during mitosis. *Cell Cycle* **2006,** *5* (5), 530-7.

52. Bergman, L. M.; Morris, L.; Darley, M.; Mirnezami, A. H.; Gunatilake, S. C.; Blaydes, J. P., Role of the unique N-terminal domain of CtBP2 in determining the subcellular localisation of CtBP family proteins. *BMC Cell Biol* **2006,** *7*, 35.

53. Chinnadurai, G., Transcriptional regulation by C-terminal binding proteins. *Int. J. Biochem. Cell Biol.* **2007,** *39* (9), 1593-1607.

54. Hildebrand, J. D.; Soriano, P., Overlapping and unique roles for C-terminal binding protein 1 (CtBP1) and CtBP2 during mouse development. *Mol Cell Biol* **2002,** *22* (15), 5296-307.

55. Sewalt, R. G.; Gunster, M. J.; van der Vlag, J.; Satijn, D. P.; Otte, A. P., C-Terminal binding protein is a transcriptional repressor that interacts with a specific class of vertebrate Polycomb proteins. *Mol Cell Biol* **1999,** *19* (1), 777-87.

56. Fang, M.; Li, J.; Blauwkamp, T.; Bhambhani, C.; Campbell, N.; Cadigan, K. M., C-terminal-binding protein directly activates and represses Wnt transcriptional targets in Drosophila. *EMBO J* **2006,** *25* (12), 2735-45.

57. Straza, M. W.; Paliwal, S.; Kovi, R. C.; Rajeshkumar, B.; Trenh, P.; Parker, D.; Whalen, G. F.; Lyle, S.; Schiffer, C. A.; Grossman, S. R., Therapeutic targeting of C-terminal binding protein in human cancer. *Cell Cycle* **2010,** *9* (18).

58. Bergman, L. M.; Birts, C. N.; Darley, M.; Gabrielli, B.; Blaydes, J. P., CtBPs promote cell survival through the maintenance of mitotic fidelity. *Mol Cell Biol* **2009,** *29* (16), 4539-51.

59. Zhang, Q.; Yoshimatsu, Y.; Hildebrand, J.; Frisch, S. M.; Goodman, R. H., Homeodomain interacting protein kinase 2 promotes apoptosis by downregulating the transcriptional corepressor CtBP. *Cell* **2003,** *115* (2), 177-186.

60. Kim, J. H.; Youn, H. D., C-terminal binding protein maintains mitochondrial activities. *Cell Death Differ* **2009,** *16* (4), 584-92.

61. Boyd, J. M.; Subramanian, T.; Schaeper, U.; Laregina, M.; Bayley, S.; Chinnadurai, G., A Region in the C-Terminus of Adenovirus-2/5 E1a Protein Is Required for Association with a Cellular Phosphoprotein and Important for the Negative Modulation of T24-Ras Mediated Transformation, Tumorigenesis and Metastasis. *Embo Journal* **1993,** *12* (2), 469-478.

62. Frisch, S. M., E1A as a tumor suppressor gene: commentary re S. Madhusudan et al. A multicenter Phase I gene therapy clinical trial involving intraperitoneal administration of E1A-lipid complex in patients with recurrent epithelial ovarian cancer overexpressing HER-2/neu oncogene. *Clin Cancer Res* **2004,** *10* (9), 2905-7.

63. Di, L. J.; Fernandez, A. G.; De Siervi, A.; Longo, D. L.; Gardner, K., Transcriptional regulation of BRCA1 expression by a metabolic switch. *Nat Struct Mol Biol* **2010,** *17* (12), 1406-13.

64. Deng, Y.; Liu, J.; Han, G.; Lu, S. L.; Wang, S. Y.; Malkoski, S.; Tan, A. C.; Deng, C.; Wang, X. J.; Zhang, Q., Redox-dependent Brca1 transcriptional regulation by an NADH-sensor CtBP1. *Oncogene* **2010,** *29* (50), 6603-8.

65. Grooteclaes, M.; Deveraux, Q.; Hildebrand, J.; Zhang, Q. H.; Goodman, R. H.; Frisch, S. M., C-terminal-binding protein corepresses epithelial and proapoptotic gene expression programs. *Proceedings of the National Academy of Sciences of the United States of America* **2003,** *100* (8), 4568-4573.

66. Sanchez-Tillo, E.; Lazaro, A.; Torrent, R.; Cuatrecasas, M.; Vaquero, E. C.; Castells, A.; Engel, P.; Postigo, A., ZEB1 represses E-cadherin and induces an EMT by recruiting the SWI/SNF chromatin-remodeling protein BRG1. *Oncogene* **2010,** *29* (24), 3490-500.

67. Hanahan, D.; Weinberg, R. A., The hallmarks of cancer. *Cell* **2000,** *100* (1), 57-70.

68. Zhang, Q. H.; Wang, S. Y.; Nottke, A. C.; Rocheleau, J. V.; Piston, D. W.; Goodman, R. H., Redox sensor CtBP mediates hypoxia-induced tumor cell migration. *Proceedings of the National Academy of Sciences of the United States of America* **2006,** *103* (24), 9029-9033.

69. Chinnadurai, G., The transcriptional corepressor CtBP: a foe of multiple tumor suppressors. *Cancer Res* **2009,** *69* (3), 731-4.

70. Wang, J.; Lee, S.; Teh, C. E.; Bunting, K.; Ma, L.; Shannon, M. F., The transcription repressor, ZEB1, cooperates with CtBP2 and HDAC1 to suppress IL-2 gene activation in T cells. *Int Immunol* **2009,** *21* (3), 227-35.

71. Papadopoulou, V.; Postigo, A.; Sanchez-Tillo, E.; Porter, A. C.; Wagner, S. D., ZEB1 and CtBP form a repressive complex at a distal promoter element of the BCL6 locus. *Biochem J* **2010,** *427* (3), 541-50.

72. Pena, C.; Garcia, J. M.; Garcia, V.; Silva, J.; Dominguez, G.; Rodriguez, R.; Maximiano, C.; Garcia de Herreros, A.; Munoz, A.; Bonilla, F., The expression levels of the transcriptional regulators p300 and CtBP modulate the correlations between SNAIL, ZEB1, E-cadherin and vitamin D receptor in human colon carcinomas. *Int J Cancer* **2006,** *119* (9), 2098-104.

73. Grooteclaes, M. L.; Frisch, S. M., Evidence for a function of CtBP in epithelial gene regulation and anoikis. *Oncogene* **2000,** *19* (33), 3823-8.

74. Wang, S. Y.; Iordanov, M.; Zhang, Q., c-Jun NH2-terminal kinase promotes apoptosis by down-regulating the transcriptional co-repressor CtBP. *J Biol Chem* **2006,** *281* (46), 34810-5.

75. Birts, C. N.; Harding, R.; Soosaipillai, G. B.; Halder, T.; Azim-Araghi, A.; Darley, M.; Cutress, R. I.; Bateman, A. C.; Blaydes, J. P., Expression of ctBP family protein isoforms in breast cancer and their role in chemoresistance. *Biol Cell* **2010**.

76. (a) Paliwal, S.; Pande, S.; Kovi, R. C.; Sharpless, N. E.; Bardeesy, N.; Grossman, S. R., Targeting of C-terminal binding protein (CtBP) by ARF results in p53-independent apoptosis. *Mol Cell Biol* **2006,** *26* (6), 2360-72; (b) Paliwal, S.; Kovi, R. C.; Nath, B.; Chen, Y. W.; Lewis, B. C.; Grossman, S. R., The alternative reading frame tumor suppressor antagonizes hypoxia-induced cancer cell migration via interaction with the COOH-terminal binding protein corepressor. *Cancer Res* **2007,** *67* (19), 9322-9.

77. Kovi, R. C.; Paliwal, S.; Pande, S.; Grossman, S. R., An ARF/CtBP2 complex regulates BH3-only gene expression and p53-independent apoptosis. *Cell Death Differ* **2010,** *17* (3), 513-21.

78. Bergman, L. M.; Morris, L.; Darley, M.; Mirnezami, A. H.; Gunatilake, S. C.; Blaydes, J. P., Role of the unique N-terminal domain of CtBP2 in determining the subcellular localisation of CtBP family proteins. *BMC Cell Biol.* **2006,** *7*, 10.

79. Aoki, K.; Taketo, M. M., Adenomatous polyposis coli (APC): a multi-functional tumor suppressor gene. *J Cell Sci* **2007,** *120* (Pt 19), 3327-35.

80. Johnstone, R. W.; Ruefli, A. A.; Lowe, S. W., Apoptosis: a link between cancer genetics and chemotherapy. *Cell* **2002,** *108* (2), 153-64.

81. Colanzi A, H. C. C., Persico A, Cericola C, Turacchio G, Bonazzi M, Luini A, Corda D., The Golgi mitotic checkpoint is controlled by BARS-dependent fission of the Golgi ribbon into separate stacks in G2. *EMBO J.* **2007,** *26* (10), 2465-76.

82. Colanzi, A.; Corda, D., Mitosis controls the Golgi and the Golgi controls mitosis. *Curr Opin Cell Biol* **2007,** *19* (4), 386-93.

83. Yang, J. S.; Lee, S. Y.; Spano, S.; Gad, H.; Zhang, L. L.; Nie, Z. Z.; Bonazzi, M.; Corda, D.; Luini, A.; Hsu, V. W., A role for BARS at the fission step of COPI vesicle formation from Golgi membrane. *Embo Journal* **2005,** *24* (23), 4133-4143.

84. Bergman, L. M.; Blaydes, J. P., C-terminal binding proteins: Emerging roles in cell survival and tumorigenesis. *Apoptosis* **2006,** *11* (6), 879-888.

85. Bergman, L. M.; Birts, C. N.; Darley, M.; Gabrielli, B.; Blaydes, J. P., CtBPs Promote Cell Survival through the Maintenance of Mitotic Fidelity. *Molecular and Cellular Biology* **2009,** *29* (16), 4539-4551.

86. Birts, C. N.; Bergman, L. M.; Blaydes, J. P., CtBPs promote mitotic fidelity through their activities in the cell nucleus. *Oncogene* **2011,** *30* (11), 1272-80.

87. Shin, H. J.; Baek, K. H.; Jeon, A. H.; Kim, S. J.; Jang, K. L.; Sung, Y. C.; Kim, C. M.; Lee, C. W., Inhibition of histone deacetylase activity increases chromosomal instability by the aberrant regulation of mitotic checkpoint activation. *Oncogene* **2003,** *22* (25), 3853-8.

88. Cimini, D.; Mattiuzzo, M.; Torosantucci, L.; Degrassi, F., Histone hyperacetylation in mitosis prevents sister chromatid separation and produces chromosome segregation defects. *Mol Biol Cell* **2003,** *14* (9), 3821-33.

89. Stevens, F. E.; Beamish, H.; Warrener, R.; Gabrielli, B., Histone deacetylase inhibitors induce mitotic slippage. *Oncogene* **2008,** *27* (10), 1345-54.

90. Warrener, R.; Beamish, H.; Burgess, A.; Waterhouse, N. J.; Giles, N.; Fairlie, D.; Gabrielli, B., Tumor cell-selective cytotoxicity by targeting cell cycle checkpoints. *FASEB J* **2003,** *17* (11), 1550-2.

91. Dieck, S. T.; Brandstatter, J. H., Ribbon synapses of the retina. *Cell and Tissue Research* **2006,** *326* (2), 339-346.

92. Wan, L.; Almers, W.; Chen, W., Two ribeye genes in teleosts: the role of Ribeye in ribbon formation and bipolar cell development. *J Neurosci* **2005,** *25* (4), 941-9.
93. Schmitz, F.; Konigstorfer, A.; Sudhof, T. C., RIBEYE, a component of synaptic ribbons: a protein's journey through evolution provides insight into synaptic ribbon function. *Neuron* **2000,** *28* (3), 857-72.
94. tom Dieck S, A. W., Kessels MM, Qualmann B, Regus H, Brauner D, Fejtová A, Bracko O, Gundelfinger ED, Brandstätter JH., Molecular dissection of the photoreceptor ribbon synapse: physical interaction of Bassoon and RIBEYE is essential for the assembly of the ribbon complex. *j Cell Biol* **2005,** *168* (5), 825-36.
95. Kim, G. T.; Shoda, K.; Tsuge, T.; Cho, K. H.; Uchimiya, H.; Yokoyama, R.; Nishitani, K.; Tsukaya, H., The ANGUSTIFOLIA gene of Arabidopsis, a plant CtBP gene, regulates leaf-cell expansion, the arrangement of cortical microtubules in leaf cells and expression of a gene involved in cell-wall formation. *EMBO J* **2002,** *21* (6), 1267-79.
96. Zhang YW, A. D., Conserved catalytic and C-terminal regulatory domains of the C-terminal binding protein corepressor fine-tune the transcriptional response in development. *Mol Cell Biol.* **2011,** *31*
(2), 375-84.
97. Van Hateren, N.; Shenton, T.; Borycki, A. G., Expression of avian C-terminal binding proteins (Ctbp1 and Ctbp2) during embryonic development. *Dev Dyn* **2006,** *235* (2), 490-5.
98. Nibu, Y.; Zhang, H.; Levine, M., Interaction of short-range repressors with Drosophila CtBP in the embryo. *Science* **1998,** *280* (5360), 101-4.
99. (a) Van Hateren N, S. T., Borycki AG Expression of avian C-terminal binding proteins (Ctbp1 and Ctbp2) during embryonic development. **2006,** *235* (2), 490-495; (b) Chinnadurai, G., CtBP family proteins: more than transcriptional corepressors. *Bioessays* **2003,** *25* (1), 9-12.
100. Zhang, O. H.; Yoshimatsu, Y.; Hildebrand, J.; Frisch, S. M.; Goodman, R. H., Homeodomain interacting protein kinase 2 promotes apoptosis by downregulating the transcriptional corepressor CtBP. *Cell* **2003,** *115* (2), 177-186.
101. Tarleton, H. P.; Lemischka, I. R., Delayed differentiation in embryonic stem cells and mesodermal progenitors in the absence of CtBP2. *Mech Dev* **2010,** *127* (1-2), 107-19.

102. Stern MD, A. H., Cho KH, Kim GT, Horiguchi G, Roccaro GA, Guevara E, Sun HH, Negeri D, Tsukaya H, Nibu Structurally related Arabidopsis ANGUSTIFOLIA is functionally distinct from the transcriptional corepressor CtBP. *Dev Genes Evol.* **2007,** *217* (11-12), 759-69.

103. Folkers U, K. V., Schöbinger U, Falk S, Krishnakumar S, Pollock MA, Oppenheimer DG, Day I, Reddy AS, Jürgens G, Hülskamp M., The cell morphogenesis gene ANGUSTIFOLIA encodes a CtBP/BARS-like protein and is involved in the control of the microtubule cytoskeleton. *EMBO J* **2002 Mar 15;,** *21* (16), 1280-8.

104. Haldimann, A.; Wanner, B. L., Conditional-replication, integration, excision, and retrieval plasmid-host systems for gene structure-function studies of bacteria. *Journal of Bacteriology* **2001,** *183* (21), 6384-6393.

105. Lu Zhou, K. Z., and Barry L. Wanner, *Chromosomal Expression of Foreign and Native Genes From Regulatable Promoter in Escherichia coli*. 2004; Vol. 267.

106. Tavassoli, A.; Benkovic, S. J., Split-intein mediated circular ligation used in the synthesis of cyclic peptide libraries in E. coli. *Nat Protoc* **2007,** *2* (5), 1126-33.

107. Sawant, R.; Torchilin, V., Intracellular transduction using cell-penetrating peptides. *Mol Biosyst* **2010,** *6* (4), 628-40.

108. Brooks, H.; Lebleu, B.; Vives, E., Tat peptide-mediated cellular delivery: back to basics. *Adv Drug Deliv Rev* **2005,** *57* (4), 559-77.

109. Sieber, P., An improved method for anchoring of 9-fluorenylmthoxycarbonyl-amino acids to II-alkoxybenzyl alcohol resins. *Tetrahedron Letters* **1987,** *28* (49), 6147-6150.

110. Balasubramanian, P.; Zhao, L. J.; Chinnadurai, G., Nicotinamide adenine dinucleotide stimulates oligomerization, interaction with adenovirus E1A and an intrinsic dehydrogenase activity of CtBP. *FEBS Lett* **2003,** *537* (1-3), 157-60.

111. Mirnezami, A. H. F.; Campbell, S. J.; Primrose, J. N.; Johnson, P. W. M.; Blaydes, J. P., Hdm2 recruits the hypoxia sensitive transcriptional co-repressor CtBP2 to negatively regulate p53-dependant transcription. *Clinical Science (London)* **2003,** *104* (Supplement 49), 29P.

112. Berg JM, T. J., Stryer L., The Purification of Proteins Is an Essential First Step in Understanding Their Function. In *Biochemistry. 5th edition.*, W. H. Freeman and Company.: New York, 2002.

113. McBride OW, M. D., Givol D., The gene for human p53 cellular tumor antigen is located on chromosome 17 short arm (17p13). *Proc Natl Acad Sci U S A* **1986,** *83* (1), 130-4.

114. O'Brate, A.; Giannakakou, P., The importance of p53 location: nuclear or cytoplasmic zip code? *Drug Resist Updat* **2003,** *6* (6), 313-22.

115. Thio, S. S. C.; Bonventre, J. V.; Hsu, S. I. H., The CtBP2 co-repressor is regulated by NADH-dependent dimerization and possesses a novel N-terminal repression domain. *Nucleic Acids Research* **2004,** *32* (5), 1836-1847.

116. Zhang, Q.; Piston, D. W.; Goodman, R. H., Regulation of corepressor function by nuclear NADH. *Science* **2002,** *295* (5561), 1895-7.

117. Straza, M. W.; Paliwal, S.; Kovi, R. C.; Rajeshkumar, B.; Trenh, P.; Parker, D.; Whalen, G. F.; Lyle, S.; Schiffer, C. A.; Grossman, S. R., Therapeutic targeting of C-terminal binding protein in human cancer. *Cell Cycle 9* (18), 3740-3750.

118. Chen, Y. D.; Zheng, S.; Yu, J. K.; Hu, X., Artificial neural networks analysis of surface-enhanced laser desorption/ionization mass spectra of serum protein pattern distinguishes colorectal cancer from healthy population. *Clin Cancer Res* **2004,** *10* (24), 8380-5.

119. Zhang, Q.; Wang, S. Y.; Nottke, A. C.; Rocheleau, J. V.; Piston, D. W.; Goodman, R. H., Redox sensor CtBP mediates hypoxia-induced tumor cell migration. *Proc Natl Acad Sci U S A* **2006,** *103* (24), 9029-33.

120. Ovadia, O.; Greenberg, S.; Chatterjee, J.; Laufer, B.; Opperer, F.; Kessler, H.; Gilon, C.; Hoffman, A., The effect of multiple N-methylation on intestinal permeability of cyclic hexapeptides. *Mol Pharm* **2011,** *8* (2), 479-87.

121. Chatterjee, J.; Gilon, C.; Hoffman, A.; Kessler, H., N-methylation of peptides: a new perspective in medicinal chemistry. *Acc Chem Res* **2008,** *41* (10), 1331-42.

6 Experimental

Polymerase chain reaction (PCR) was carried out using Eppendorf mastercycler personal and BioRad MyCycler Thermal cycler. DNA purification was carried out using QIAquick PCR Purification Kit (QIAGEN, Germany) and Promega Wizard plus Mini Prep DNA Purification System (Promega UK Ltd, UK). DNA concentration was measured using Nano Drop ND-1000 spectrophotometer (NanoDrop Technologies, USA). Agarose gels were run using Bio Rad Power Pack basic and imaged on BioRad Universal Hood II imager using QuantityOne software by BioRad (Bio-Rad Laboratories Ltd, UK) imaging system. Transformation by electroporation was carried out on the Bio Rad pulse controller and gene pulsar. Optical density of cell cultures was measured using the Thermo Electron Corporation BioMate 3. PDraw was used to choose restriction enzymes, work out annealing temperature, and design primers. Sequencing was carried out by MWG (Germany). Molecular biology reagents were purchased from New England Biolabs or Promega.

Bacterial strains SNS126, SNS118 and DH5α and plasmids pTHCP14, pTHCP16, pAH68 and pAH69 were provided by Professor Benkovic at Pennsylvania State University (USA). Bacterial strains GM2929 and BL21 were provided by Dr Roach from The University of Southampton (UK). The plasmid strains containing the cDNA of CtBP1 and CtBP2 were provided by Dr Jeremy Blaydes from the Faculty of Medicine University of Southampton. The pET28 vector was provided by Patric Duriez from the Faculty of Medicine University of Southampton.

6.1 Screening and selection of peptide

6.1.1 Reagents

All solutions were sterilised by either autoclaving for 20 min at 115 °C on liquid media cycle or filtration through a 0.22 μm filter (Millipore, U.S.A) as required.

6.1.1.1 Tris-acetate-EDTA (TAE) Buffer 50x

Tris Base	242 g, 2 M
Glacial acetic acid	57.1 mL, 1 M
EDTA pH 8	100 mL, 0.5 M
Water	Adjust to 1 L

Adjust to pH 8.0 using dilute NaOH.

1x solution is made by adding 20 mL (50x) to 1 L of sterilised deionised water

6.1.1.2 Phosphate Buffered Saline (PBS)

Sodium Chloride	125 mM
Sodium Phoshate	16 mM
Sodium Hydrogen Phosphate	10 mM

pH 7.3

6.1.1.3 2X O-Nitrophenyl-Beta-D-Galactopyranoside (ONPG) assay Buffer.

	Final Concentration
$Na_2HPO_412H_2O$	120 mM
$NaH_2PO_42H_2O$	80 mM
$MgCl_26H_2O$	2 mM
2-mercaptoethanol	100 mM
ONPG (sigma)	1.33 mg/mL

6.1.1.4 Z buffer

	Quantity	Final concentrations
Sodium phosphate monobasic	0.851 g	60 mM
Sodium phosphate dibasic	0.522 g	40 mM
Potassium Chloride	74 mg	10 mM
Magnesium Sulphate	0.245 g	10 mM
B-mercaptoethanol	280 µL	40 mM
Sterile distilled water	Make up 100 mL	

Table 6.1. Composition of Z buffer.

6.1.1.5 Luria-bertani (LB) broth

LB-Broth powder (Fisher Scientific, UK) 6.25 g/250 mL

6.1.1.6 LB agar plates

LB-Agar powder (Fisher Scientific, UK) 10 g/250 mL

LB agar powder (10 g) (Fisher Scientific) was dissolved in water (250 mL) and autoclaved for 20 min at 115 °C on the liquid media cycle. The media was allowed to solidify. When required the media was microwaved until liquid, then allowed to cool to around 50 ºC. Once cooled the required antibiotics were added. The media was then mixed gently to prevent bubbles from forming and then poured into sterile petri dishes. Plates were left to solidify, and then stored in the fridge. When required, the plates were dried in the incubator for 30 min at 37 °C. Antibiotic concentrations used for plasmids were as follows: Ampicillin (100 µg/mL), Chloramphenicol (25 µg/mL), Kanamycin (50 µg/mL) and Spectinomycin (50 µg/mL). For resistance coming from the chromosome the quantity of antibiotics used was halved.

6.1.1.7 Minimal media plates

Agar powder (3.75 g) (Fisher Scientific) was dissolved in Water (200 mL) and autoclaved for 20 min at 115 °C on the liquid media cycle. Minimal media (50 mL) (6.1.1.8) was added. The bottle of agar was stored in the oven at 60 °C to stop it from solidifying. 10 different plates were prepared; mixtures for each plate were prepared in

falcon tubes. 1 and 2 were control plates: 1 containing Kan (0 μg/mL), 3AT (0 mM) and IPTG (0 μL), the other containing Kan (0 μg/mL), 3AT (0 mM) and IPTG (200 μL), Tubes 3 to 10 all contained 3AT (250 μL, 5 μM), and Kan (125 μL, 50 μg/mL) and the levels of IPTG added to each was varied (0-100 μM). Glycerol (50%, 10mL), $MgSO_4$ (250 μL) and Spectinomycin (625 μL) was added to the agar and mixed. The agar mixture (25 mL) was then added to individual falcon tube and poured into the plates. The plates were allowed to dry in the incubator for 2 hr at 37 °C before use. Cells were drop spotted onto the plates with a 10-fold dilution.

6.1.1.8 Composition of minimal media

$(NH_4)_2SO_4$	5 g
KH_2PO_4	22.5 g
K_2HPO_4	52.5 g
Sodium citrate.H_2O	2.5 g
Sterile distilled water	1 L

6.1.1.9 SOC medium

LB Growth media	50 mL
$MgCl_2$	1 M, 500 mL
$MgSO_4$	2M, 500 mL

6.1.2 DNA manipulation

PCR were carried out using Eppendorf master cycle gradient. DNA purification was carried out using Qiagen QIAquick columns and QIAprep spin column. DNA concentration was measured using the Nano Drop ND-1000 V312 spectrophotometer. Agarose gels were run using the Bio Rad Power Pack 3000 and imaged with gene genius bio imaging system. Transformation by electroporation was carried out on the Bio Rad pulse controller and gene pulser. Optical density of cell cultures was measured using the Thermo Electron Corporation BioMate 3. PDraw was used to choose restriction enzymes, work out annealing temperature, and design primers.

6.1.2.1 Bacterial Cultures

The required sample was scraped using a pipette tip from the frozen stock in the -80 °C freezer, or from the LB agar plate and mixed in LB media (10 mL). The culture was then grown in the incubator o/n at 37 °C with shaking unless otherwise stated.

6.1.2.2 Polymerase chain reaction (PCR)

PCR reactions were carried out using deep vent polymerase (New England Biolabs) and Gotaq (Promega).

	Volume (µL)	Stock concentration	Total quantity
GoTaq Buffer	10	5 x	1 x
dNTPs	5	2 mM	10 nmol
Forward Primer	1	10 µM	0.01 nmol
Reverse Primer	1	10 µM	0.01 nmol
Template	1	50-150 ng/ µL	50-150 ng
GoTaq polymerase	0.25	5 u/ µL	1.25 U
Sterile distilled water	31.75		
Total	50		

Table 6.2. Composition of GoTaq (Promega) reaction mixture.

	Volume (µL)	Stock concentration	Total quantity
Thermopol Buffer	5	10 x	1 x
dNTPs	5	2 mM	10 nmol
Forward Primer	1	10 µM	0.01 nmol
Reverse Primer	1	10 µM	0.01 nmol
Template	1	50-150 ng/ µL	50-150 ng
Deepvent polymerase	1	2 u/ µL	2 U
Sterile distilled water	36		
Total	50		

Table 6.3. Composition of deep vent (New England Biolab) reaction mixture.

Typical reaction cycle

Initial denaturation	94 °C for 2 min	
Denaturation	94 °C for 30 sec	35 cycles
Annealing	45 °C-65 °C for 30 sec	
Extension	72 °C for 1 min	
Final Extension	72 °C for 2 min	

Annealing temperature is dependent on primer sequence. Extension time is dependent on the length of the gene.

Following amplification, the product was confirmed by restriction endonuclease digestion and agarose gel electrophoresis. The amplified product was then purified using QIAGEN QIAquick purification system. All primers (Table 6.4) were synthesised by Eurofins MWG Operon.

Primer	Sequence (5'-3')
CtBP1F	GTTGTT GTCGAC ATGGGCAGCTCGCAC
CtBP1R	GTTGTT TCGCGA CTA GTCAACAACACTATT
CtBP2F	GTTGTT CTCGAG ATGGCC CTTGTG GATA
CtBP2R	GTTGTT TCGCGA CTATTG CTCGTT GGGGT
NADHF	CTCATTGGCTTTGCGCGCACGGGGCAG
NADHR	CTGCCCCGTGCGCGCAAAGCCAATGAG
CtBP2dimF(SalI)	GTTGTTGTCGACATGAGTACAGGCTGCTGTACAG
CtBP2dimR(SacI)	GTTGTTGAGCTCCTATGGCTGGCAACTAGAAGGCAC
CtBP1dimF(SmaI)	GTTGTTCCCGGGATGGTTGACATTGATTATTGAC
CtBP1dimR(KpnI)	GTTGTTGGTACCCTAAAGTGCGAGCTGCCCATGAATTC
CtBP1FNdeI	GGG AAT TCC ATA TGA TGG GCA GCT CGC ACT TGC TC
Ctbp1XhoI	GTT GTT CTC GAG CTA CAA CTG GTC ACT GGC GTG GTC
CtBP2F(NdeI)	GGG AAT TCC ATA TGA TGG CCC TTG TGG ATA AGC A
CtBP2R(XhoI)	GTT GTT CTC GAG CTA TTG CTC GTT GGG GTG CTC TCG
P1	GGAATCAATGCCTGAGTG
P2	ACTTAACGGCTGACATGG
P3	ACGAGTATCGAGATGGCA
P4	GGCATCAACAGCACATTC
C+5	GGAATTCGCC AATGGGGCGA TCGCCCACAA TTGCNNSNNS NNSNNSNNST GCTTAAGTTT TGGC
CBD F	GTTGTTAAGCTTTCATTCAAGCTGCCACAAGG
Zipper F	GGAATTCGCCAATGGGGCGATCGCC
SGW+6	GGAATTCGCCAATGGGGCGATCGCCCACAATAGCGGCTGGN NSNNSNNSNNSNNSNNSTGCTTAAGTTTTGGC
SGW+5	GGAATTCGCCAATGGGGCGATCGCCCACAATAGCGGCTGGN NSNNSNNSNNSNNSTGCTTAAGTTTTGGC
SGW+4	GGAATTCGCCAATGGGGCGATCGCCCACAATAGCGGCTGGN NSNNSNNSNNSTGCTTAAGTTTTGGC

Table 6.4. Primer sequences.

6.1.2.3 DNA Purification:

The DNA sample was mixed with PBI (5 xs the concentration of DNA) in an eppendorf. The mixture was then added to QIAGEN QIAquick spin column and

centrifuged in the microcentrifuge for 1 min at 1300 rpm. The flow through was discarded and the column was reinserted into the collection tube. PE (750 µl) was added to the column and centrifuged for 1 min. Again the flow through was discarded and the column was centrifuged for a further min. The collection tube was then discarded. The column was inserted into an eppendorf and eluted with autoclaved water (50 µl). Purified DNA was then stored at -20 ºC.

6.1.2.4 Promega plasmid Prep:

O/n culture of required cells was set up (6.1.2.1). Cells were centrifuged for 10 min at 4 ºC and 13000 rpm. The flow through was discarded. The cells were thoroughly re-suspended with cell re-suspension solution (250 µl) and added to an eppendrof. Cell lysis solution (250 µl) was added to the tube and inverted 4 times to mix and incubated at rt for 2 min. An alkaline protease solution (10 µl) was then added and inverted 4 times to mix and incubated at rt for 5 min. Neutralisation solution (350 µl) was added and inverted 4 times to mix. The mixture was then centrifuged for 10 min at 13000 rpm. The pellet was discarded and the solution was added to a QIAGEN QIAquick Spin columns. The mixture was then centrifuged for 1 min at 13000 rpm and the flow through was discarded. Wash solution (750 µl) was added and centrifuged for a further min, and the flow through discarded. Wash solution (250 µl) was added and centrifuged for 1 min; the flow through was discarded and centrifuged for a further 2 min. The spin column was transferred to an eppendorf and eluted with water (50 µl). The column was discarded and the DNA was stored at -20 ºC.

6.1.2.5 Digestion:

A variety of restriction enzymes (from Promega and New England Bio-labs) were employed. Digestions were set up in PCR tubes, the total volume made up to 50 µl. Single digestion or double digestion (cleaving DNA substrate with 2 restriction enzymes simultaneously) were set up, depending on the compatibility of the two enzymes.

	Volume (µL)	Stock concentration	Total quantity
Plasmid	44	50-300 ng/ µL	2.2-13 ng
Buffer	5	10 x	1 x
Restriction enzyme	1	10 U/ µL	10 U
Total	50		

Table 6.5. Restriction Enzyme digestion mixture.

	Volume (µL)	Stock concentration	Total quantity
Plasmid	39	50-300 ng/ µL	2.2-13 ng
Buffer	5	10 x	1 x
BSA	5	1 mg/mL	
Restriction enzyme	1	10 U/ µL	10 U
Total	50		

Table 6.6. Digestion requiring Bovine Serum albumin (BSA).

6.1.2.6 Ligation:

Ligation of the plasmid backbone and gene insert was set up in PCR tube according to Table 6.7, using DNA quantities calculated following Promega protocol as below. The mixture was vortexed before adding the ligase and gently pipetted after. The reaction was carried out for 4 hr at rt or for 16 hr at 4 ºC. The ligase enzyme was killed before transforming into chemically or electrocompetent cells by heating at 70 ºC for 10 min then cooling to 4 ºC

$$\frac{\text{Ng of vector x Kb size insert}}{\text{Kb size insert}} = \text{ng of insert}$$

	Volume (μL)	Stock concentration	Total quantity
Buffer	1	10 x	1x
Linear plasmid	4-7.5	5-50 ng/ μL	35-200 ng
Insert	0.5-4	5-50 ng/ μL	2.5-100 ng
T4 Ligase	1	3 U μL	3 U
Total	10		

Table 6.7. Composition of ligation mixture.

6.1.2.7 Agarose Gel Electrophoresis

Agarose gel electrophoresis was employed to size fractionate DNA for analysis or eluting from the gel. 1% agarose gel was prepared by dissolving agarose powder (2 g) in 1x TAE buffer (200 mL) by heating in the microwave. Ethidium Bromide was included in the gel matrix at 0.05 μg/mL to enable fluorescent visualisation of DNA fragments under ultraviolet light (UV). Agarose gels were submerged in TAE buffer in a horizontal electrophoresis apparatus. Samples (5 μL analysis and 50 μL gel purification) were mixed with loading dye (1 μL per 5 μL sample) and loaded into the sample wells. A DNA ladder was used to determine the size of the DNA fragment. Electrophoresis was conducted at 90 mA for 30 min at rt. After electrophoresis, gels were placed on a UV light box for visualisation of the DNA separation pattern.

6.1.2.8 Gel purification:

The MinElute Gel Extraction kit was used for purification. Digested plasmid (50 μl) was mixed with the loading dye (10 μl), and then loaded onto the gel. The gel was then ran and imaged (UV light kept on for minimum amount of time to avoid DNA damage). The gene band of interest was cut from the agarose gel with a clean sharp scalpel. The gel slice was weighed in an eppendorf tube. Three volumes of buffer QC to 1 volume of gel (eg. 300 μl of buffer QC to each 100 mg of gel, maximum amount of gel per spin is 400 mg) were added to the tube. The gel was melted at 65 ºC (~15 min); the tube was vortexed every 2-3 min to help the gel dissolve. Isopropanol (1 gel volume) was added

and inverted several times to mix. The mix was then purified by adding PE (750 µl) and centrifuging for 1 min at 13000 rpm and eluted with distilled water.

6.1.2.9 Preparation of chemically competent cells for transformation:

E.coli strains were grown o/n at 37 ºC in LB (10 mL) without antibiotics. The culture (50 µl) was then transferred to fresh LB Media (50 mL), with no antibiotics. The cultures were incubated at 37 ºC until the OD_{600} had reached 0.4-0.6. The culture was then centrifuged (10 min, 4 ºC, 13000 rpm). The supernatants decanted off and the cells were re-suspended in ice cold TBF I Buffer (10 mL) (Table 6.8) then centrifuged (10 min, 4 ºC, 13000 rpm). The supernatant was discarded and the cells were re-suspended in ice-cold TBF II buffer (1 mL) (Table 6.9). Cells (100 µl) were aliquoted into PCR tubes (this was done on dry ice). The PCR tubes were put into a falcon tube and stored in the -80 ºC freezer until they were required.

	Quantity	Final Concentration
Potassium acetate	0.588 g	30 mM
Rubidium Chloride	2.42 g	100 mM
Calcium Chloride	0.294 g	10 mM
Manganese chloride	2 g	50 mM
Glycerol	30 mL	15% v/v
Sterile deionised water	Adjust to 200 mL	

Adjust to pH 5.8 with 1% acetic acid.

Table 6.8. Composition of TBFI buffer.

	Quantity	Final Concentration
MOPS	0.21 g	10 mM
Rubidium Chloride	0.121 g	10 mM
Calcium Chloride	1.10 g	75 mM
Glycerol	15 mL	15% v/v
Sterile deionised water	Adjust to 100 mL	

Adjust to pH 6.5 with dilute NaOH

Table 6.9. Composition of TBFII buffer.

6.1.2.10 Preparation of electrocompetent cells

Cells were cultured o/n in LB media (5 mL) without antibiotic. 5mL of the culture was then transferred to fresh LB media (500 mL), with no antibiotic, until the OD_{600} had reached 0.4-0.6. The culture was centrifuged (3100 rpm, 15 min, 4 °C). Supernatant decanted off and cells were washed by re-suspension in 500 mL of ice-cold glycerol solution (10% w/v) followed by centrifugation (3100 rpm, 10 min, 4 °C). Washes were repeated a further two times with 250 mL, then 20 mL. The cells were then re-suspended in 1 mL of glycerol solution (10% w/v) and aliquoted into 100 µL portions and immediately frozen using dry ice and stored at -80 °C until needed.

6.1.2.11 Transformation:

1. Using chemically competent cells

100 µL of competent cells were thawed on ice. 5 µL of Plasmid DNA was added and the mixture incubated on ice for 30 min. The samples were then heat shocked at 42 ºC for 45 sec and transferred to ice to cool for 1-2 min. 895 µL SOC media was added to a tube and the cells were then added. The solution was then shaken at 37 ºC for 1 hr. 100 µL of recovery solution was transferred onto 90 mm LB agar plates supplemented with the appropriate selection antibiotic. Plates were then incubated at 37 ºC o/n. Colonies of transformed bacteria were selected on the following day.

2. Using electro-competent cells

The aliquot of electro competent cells (kept in -80 ºC freezer) were allowed to thraw on ice for 10 min. 5 µL of plasmid was added to the cells and the plasmid mixture was then transferred to the electroporative cuvette and an electric charge was passed through the sample and immediately after SOC medium (895 µL) was added. The mixture was then transferred to a culture tube and shaken at 37 ºC for one hr. 100 µL of recovery solution was transferred onto 90 mm LB agar plates supplemented with the appropriate selection antibiotic. Plates were then incubated at 37 ºC o/n. Colonies of transformed bacteria were selected the following day.

6.1.2.12 Colony PCR:

Batches of PCR mix were prepared containing the required template and primers. 10 µL of PCR mix was added to colony PCR tube. Individual colonies were picked with pipette tip and swirled into PCR mix. The PCR reaction was run and the gel was run to check whether the colonies contained the correct insert.

	Volume (µL)	Stock concentration	Total quantity
GoTaq green Buffer	20	5 x	1 x
dNTPs	1	2 mM	10 nmol
Forward Primer	2	10 µM	0.01 nmol
Reverse Primer	2	10 µM	0.01 nmol
GoTaq polymerase	0.5	5 u/ µL	2 U
Sterile distilled water	65.5		
Total	100		

Table 6.10. Composition of colony PCR.

6.1.3 Construction of RTHS

6.1.3.1 Construction of CtBP1 RTHS CtBP1-16

The pTHCP16 plasmid was transformed into GM2929.

The cDNA of Ctbp1 (1320 bp) was amplified by PCR by using Deep Vent (New England Biolabs) with Forward primer: CtBP1F 5'-GTTGTTGTCGACATGGGCAGCTCGCAC-3' and reverse primer: CtBP1 R 5'-GTTGTTTCGCGACTAGTCAACAACACTATT-3' with annealing temperature of 54 ºC and extension time of 1.35 min. The PCR product and isolated GM2929 pTHCP16 plasmid were digested with *SalI* using buffer 1 and BSA followed by *NruI* using buffer 3. The digested plasmid and insert were ligated o/n at 4 ºC and then transformed into chemically competent DH5α cells and grown o/n on LB Agar plates containing ampicillin (100 µg/mL). Positive colonies were identified by colony PCR and the plasmid was isolated.

6.1.3.2 Construction of pAH68-CtBP1/pTHCP16

The CtBP1-pTCHP16 plasmid was digested with *HpaI* using buffer 4 followed by *NruI* using buffer 3. The construct was isolated and purified by gel purification from the agarose gel using QIAGEN purification kit. The pAH68 plasmid was digested with SmaI using buffer 4 at 25 ºC. The vector was then treated with Shrimp alkaline phosphotase (Promega) for 1 hr at 37 ºC; the enzyme was then heat inactivated by incubating at 65 ºC for 30 min. The isolated RTHS construct and linearised pAH68 were ligated o/n at 4 ºC. The ligase enzyme was heat inactivated before transformation by heating at 70 ºC for 10 min. The ligated mixture was then transformed into chemically competent DH5α pir cells and plated onto agar plate containing ampicillin (100 µg/mL) and incubated o/n at 37 ºC. Colony PCR was carried out to identify positive colonies.

6.1.3.3 Construction of CtBP1/SNS118

The pAH68-CtBP1-pTHCP16 plasmid (5 µL) was added to the SNS118 + pAH69 cells (100 µL) and the plasmid mixture was then transferred to the electroporative cuvette and an electric charge was passed through the sample and immediately after SOC medium (895 µL) was added. The mixture was then transferred to a culture tube and shaken at 30 ºC for 1 hr. The temperature of the incubator was increased to 42 ºC. While the shaker was increasing in temperature the recovery solution was shaken in the water bath at 42 ºC for a few min. The total incubation time at 42 ºC was 30 min. The

recovery solution (5 µL, made up to 100 µL with distilled water) was then plated onto agar plates containing ampicillin and spectinomycin, and then incubated at 37 ºC o/n. Colony PCR using predesigned primers P1, P2, P3 and P4 (Table 6.4) was carried out to see whether the incorporation was successful.

6.1.3.4 Construction of CtBP2 RTHS CtBP2-16

The cDNA of Ctbp2 was amplified by PCR by using Deep Vent (New England Biolabs) with Forward primer: CtBP2 F 5'- GTTGTTCTCGAGATGGCCCTTGTGGATA-3' and reverse primer: CtBP2 R 5'-GTTGTTTCGCGACTATTGCTCGTTGGGGT-3' with annealing temperature of 55 ºC and extension time of 1.35 min. The PCR product and isolated GM2929 pTHCP16 plasmid were digested with *XhoI* using buffer 2 and BSA followed by *NruI* using buffer 3. The digested plasmid and insert were ligated o/n at 4 ºC and then transformed into chemically competent DH5α cells and grown o/n on LB Agar plates containing ampicillin (100 µg/mL). Positive colonies were identified by colony PCR and the plasmid was isolated.

6.1.3.5 Construction of pAH68-CtBP2/pTHCP16

The CtBP2/pTHCP16 plasmid was digested with *HpaI* using buffer 4 followed by *NruI* using buffer 3. The construct was isolated and purified by gel purification on agarose gel using QIAGEN purification kit. The pAH68 plasmid was digested with *SmaI* using buffer 4 at 25 ºC. The vector was then treated with Shrimp alkaline phosphotase (Promega) for 1 hr at 37 ºC; the enzyme was then heat inactivated by incubating at 65 ºC for 30 min. The isolated RTHS construct and linearised pAH68 were ligated o/n at 4 ºC. The ligase enzyme was heat inactivated by heating at 70 ºC for 10 min. The ligated mixture was then transformed into chemically competent DH5α pir cells and plated onto agar plate containing ampicillin (100 µg/mL) and incubated o/n at 37 ºC. Colony PCR was carried out to identify positive colonies.

6.1.3.6 Construction of CtBP2/SNS118

The same procedure as 6.1.3.3 was followed.

6.1.3.7 Mutation of NADH domain of CTBP2

6.1.3.7.1 Mega primer method

Firstly two sets of PCR were run; one using the CtBP2 forward primer: CtBP2 F 5'-GTTGTT CTCGAG ATGGCC CTTGTG GATA-3' and the reverse mutation primer NADHF 5'-CTGCCCCGTGCGCGCAAAGCCAATGAG-3', with an annealing temperature of 55 ºC and an extension time of 45 sec. The second PCR was run using the CtBP2 reverse primer: CtBP2 R 5'-GTTGTT TCGCGA CTATTG CTCGTT GGGGT-3' and the forward mutation primer NADHF 5'-CTCATTGGCTTTGCGCGCACGGGGCAG-3', with an annealing temperature of 56 ºC and an extension time of 50 sec. The PCR products were then combined and a PCR was run using the CtBP2 forward and reverse primer. The PCR was then cloned into the pTCHP16 plasmid following the same procedure as 6.1.3.4. The construct was then cloned onto the chromosome of SNS118 following the procedures in 6.1.3.5 and 6.1.3.6.

6.1.3.8 Construction of CtBP1dim-CtBP2dim/pTHCP14

CtBP2dim 82-330 truncation was amplified by PCR using Deep Vent (New England Biolabs) with the forward primer: CtBP2dimF(SalI) 5'-GTTGTTGTCGACATGAGTACAGGCTGCTGTACAG-3' and the reverse primer: CtBP2dimR (SacI) 5'-GTTGTTGAGCTCCTATGGCTGGCAACTAGAAGGCAC-3' with an annealing temperature of 56°C and extension time of 50 sec. The PCR product and isolated plasmid was digested using *SalI*-HF and *SacI*-HF (buffer 4 and BSA). The digested vector and insert were ligated o/n at 4°C then transformed into chemically competent DH5α and grown o/n on agar plate containing ampicillin (100 μg/mL). Positive colonies were identified by colony PCR and the CtBP2dim/pTHCP14 was plasmid isolated.

CtBP1dim 76-324 truncation was then amplified by PCR using Deep Vent (New England Biolabs) with forward primer: CtBP1dimF (SmaI) 5'-

GTTGTTCCCGGGATGGTTGACATTGATTATTGAC-3' and reverse primer: CtBP1dimR (KpnI) 5'-GTTGTTGGTACCCTAAAGTGCGAGCTGCCCATGAATTC-3' with an annealing temperature of 54°C and extension time 50 sec. The PCR product and isolated CtBP2dim/pTHCP14 plasmid was digested using *SmaI* (buffer 4 and BSA at 25 °C) followed by *KpnI* (buffer 1 and BSA). The digested vector and insert were ligated o/n at 4°C then transformed into chemically competent DH5α and grown o/n on agar plate containing ampicillin (100 µg/mL). Positive colonies were identified by colony PCR and the CtBP1dim-CtBP2dim/pTHCP14 plasmid was isolated.

6.1.3.9 ONPG (Ortho-Nitrophenyl-β-galactosidase) Assays:

The CtBP-pTHCP16 was transformed into SNS118 cells. Positive colonies were grown in o/n cultures containing 10 mL LB, 50 µl amp and 25 µl spec. The o/n culture was sub cultured into 8 tubes, by adding 5 mL LB and 50 µl of o/n culture to each, (each tube was numbered to avoid mix up). The cultures were then incubated at 37 ºC for a further 2 hrs in the shaker. The OD_{600} was measured (should be around 0.5-0.7). IPTG (100 mmol) was then added to each tube: in 1 50 µL; in 2 25 µL; in 3 12.5 µL; in 4 50 µL; in 5 25µL; in 6 12.5 µL; in 7 5µL and no IPTG was added in to the 8^{th} tube.

The cultures were then incubated for a further 1hr at 37 ºC. The OD_{600} was measured for all the samples. Sample assays were then run (4 samples at a time). Into an eppindorf 0.15 mL of culture, 0.55 mL of Z-buffer was added. A control was also set up containing 0.15 mL of water and 0.2 mL of Z-buffer. 1 drop of $CHCl_3$ and 1 drop 1% SDS was added. The mixture was then vortexed for 10 sec. The sample was incubated at 37 ºC for 1 min, then 0.2 mL ONPG was added and the sample was incubated at 37 ºC. The timer was started at time of incubation. When the colour change was observed (from clear to yellow) the reaction was stopped by the addition of 0.5 mL of Na_2CO_3. The timer was stopped; the incubation time of each sample was noted. The sample was then centrifuged for 1 min; the OD_{400} was measured for each sample. The results were then plotted using excel.

6.1.4 Constructing SICLOPPS library

6.1.4.1 C+5

The C-terminal intein from pARCBD was amplified using GoTaq (promega), using C+5 forward primers- 5'-GGAATTCGCC AATGGGGCGA TCGCCCACAA TTGCNNSNNS NNSNNSNNST GCTTAAGTTT TGGC-3' with the CBD reverse primer- 5'-GTTGTTAAGCTTTCATTCAAGCTGCCACAAGG-3' with annealing temperature of 55 ºC and extension time of 1 min 15 sec. The PCR product was purified with the QIAGEN kit and then used as the template for subsequent PCR reaction using the ZIPPER forward primer- 5'-GGAATTCGCCAATGGGGCGATCGCC-3' and the same CBD reverse primer as above with an annealing temperature of 55 ºC and extension time of 1 min 15 sec. The PCR product and isolated blank pARCBD plasmid were digested using *BglI* (buffer 3) followed by *HindIII* (buffer 2). Digested vector was treated with shrimp alkaline phosphatase at 37 ºC for 1 hr, the enzyme was then inactivated by incubating at 65 ºC for 30 min. Digested vector and insert were ligated o/n at 4 ºC then dialyzed for 2hr. Ligation (3 µL) product was transformed into electrocompetent NEB10β and grown o/n on agar plates containing chloramphenical (50 µg/mL). Dilutions of the recovery solution were plated to work out the library size (10^3, 10^5, 10^7), and the remaining recovery solution was grown in 20 mL LB and Chloramphenicol. The library plasmid was then purified.

6.1.4.2 SWG+6

The same protocol as for the C+5 library was followed but the C+5 forward primer was replaced with the SWG+6 forward primer- 5'GGAATTCGCCAATGGGGCGATCGCCCACAATAGCGGCTGGNNSNNSNNSNNSNNSNNSTGCTTAAGTTTTGGC-3'.

6.1.4.3 SWG+5

The same protocol as for the C+5 library was followed but the C+5 forward primer was replaced with the SWG+5 forward primer- 5'GGAATTCGCCAATGGGGCGATCGCCCACAATAGCGGCTGGNNSNNSNNSNNSNNSTGCTTAAGTTTTGGC-3'.

6.1.4.4 SGW+4

The same protocol as for the C+5 library was followed but the C+5 forward primer was replaced with the SWG+4 forward primer-
5'GGAATTCGCCAATGGGGCGATCGCCCACAATAGCGGCTGGNNSNNSNNSNNSTGCTTAAGTTTTGGC-3'.

6.1.4.5 Genetic selection

SICLOPPS libraries were transformed into CtBP1-68-8.1 in SNS118 cells. The recovery was centrifuged (10 min); the cells were then re-suspended in a mixture of minimal media A, 50% glycerol and water. Dilutions were then plated onto minimal media supplemented with L- (+)-arabinose, 3-AT (625 µl, 2.5 mM), kanamycin (625 µl, 25 mM) and IPTG (500 µl). Plates were then incubated in the incubator for 3 to 4 days at 37 ºC. Surviving colonies were restreaked onto rich media containing spectinomycin and chloramphenicol. Surviving colonies from these plates were then drop spotted onto the same minimal media plates with and without arabinose. Plasmids from those strains whose growth depended on the presence of arabinose were isolated and retransformed into the original selection strain. Transformants were drop spotted onto minimal media plates with and without arabinose to check activity. The most active plasmids were then transformed into other selection strains (ATIC and P6-UEV).

6.1.5 Construction of Expression Vectors

6.1.5.1 Construction of CtBP1-pET28

The full length Ctbp1 coding sequence (1320 bp) was amplified by PCR by using Deep Vent (New England Biolabs) with forward primer: CtBP1FNdeI 5'-GGGAATTCCATATGATGGGCAGCTCGCACTTGCTC -3' and reverse primer: CtBP1XhoI 5'- GTTGTTCTCGAGCTACAACTGGTCACTGGCGTGGTC -3' with an annealing temperature of 57 ºC and extension time of 1.35 min. The PCR product and isolated pET28 vector was digested with *XhoI* and *NdeI* using buffer 4 and BSA. The

reaction mixture was incubated at 65 ºC for 20 min to inactivate the enzyme. The digested plasmid and insert were ligated o/n at 4 ºC then transformed into chemically competent Bl21 cells and grown o/n on LB Agar plates containing kanamycin (100 µg/mL). Positive colonies were identified by colony PCR and positive plasmids were isolated.

6.1.5.2 Construction of CtBP2-pET28

The full length Ctbp2 coding sequence was amplified by PCR by using Deep Vent (New England Biolabs) with forward primer: CtBP2F (NdeI) 5'-GGGAATTCCATATGATGGCCCTTGTGGATAAGCA-3' and reverse primer: CtBP2R (XhoI) 5'-GTTGTTCTCGAGCTATTGCTCGTTGGGGTGCTCTCG-3' with annealing temperature of 56 ºC and extension time of 1.35 min. The PCR product and isolated pET28 vector was digested with *XhoI* and *NdeI* using buffer 4 and BSA. The reaction mixture was incubated at 65 ºC for 20 min to inactivate the enzyme. The digested plasmid and insert were ligated o/n at 4 ºC then transformed into chemically competent Bl21 cells and grown o/n on LB Agar plates containing kanamycin (100 µg/mL). Positive colonies were identified by colony PCR and positive plasmids were isolated.

6.1.6 Peptide synthesis

Peptides were synthesised by "solid phase" chemical synthesis, starting with the carboxyl-terminal amino acid attached to the solid phase, and adding one amino acid at a time to the amino terminal end to build the peptide.

6.1.6.1 Loading Wang Resin.

The Wang resin (500 mg, 0.55 mmol, 1eq) and Fmoc protected amino acid (2eq) were dissolved in DMF (3 mL) and gently stirred at rt for 15 min. Pyridine (1.47 µL, 1.82 mmol, 3.3 eq) and 2, 6-dichlorobenzoyl chloride (158 µL, 1.1 mmol, 2 eq) were added to the reaction mixture and stirred at rt for 15 hr. The reaction was filtered and washed with DMF (3x 15 mL), DCM (3 x 15 mL) and diethyl ether (3x 15 mL). The reaction was dried under vacuo.

6.1.6.2 Measuring Loading

Loaded resin (6.1 mg) was dissolved in 20% piperidine/DMF (10mL) and left for 15 min. The mixture was diluted with 20% piperidine/DMF giving a final volume of 50 mL. The absorbance at 302 nm was measured and the loading was calculated using the following equation,

Loading = ((A x V)/(ε x w)) x 1000

A = Absorbance at 302 nm

V = Volume

W = Mass of resin

ε = Molar extinction co-efficient of adduct at 302 = 7800 m^{-1}.

6.1.6.3 Capping

Benzoyl Chloride (150 μL), pyridine (150 μL) and DCM (4 mL) was added to the loaded resin and reacted in the bubbler at rt for 2 hr.

6.1.6.4 Coupling

The Fmoc protected amino acid (3eq) was dissolved in DCM/DMF (4:1, 1.5 mL). PyBop (3eq, 0.702 mmol, 365 mg) was added followed by DIPEA. The mixture was added to the resin and agitated (2 hrs) and then washed with DMF (3x 15 mL), DCM (3 x 15 mL) and diethyl ether (3x 15 mL). Addition of protected amino acid was verified via quantitative Ninhydrin test (straw yellow colour).

6.1.6.5 Deprotection

20% piperidine/DMF (10 mL) was added to the Fmoc protected peptidyl resin in the reaction vessel. The suspended resin was then agitated for 30 min then washed with DMF (3x 15 mL), DCM (3x 15 mL) and diethyl ether (3x 15 mL). Removal of the Fmoc group was confirmed by quantitative Ninhydrin test (purple colour).

6.1.6.6 Ninhydrin Test.

Solution A: 0.5 g ninhydrin in 10 mL EtOH

Solution B: 0.4 mL of 0.001 M KCN aq in 20 mL pyridine.

A small amount of resin was added to a reaction vial. Solution A (100 μL) and solution B (25 μL) was added to the vessel, the mixture was heated to 150 °C until a colour change was observerd.

6.1.6.7 Cleavage from resin

On completion the resin was placed in a flask and a mixture of 94.0% TFA: 2.5% water: 2.5% EDT: 1%TIS (10-25 mL/g resin) was added. EDT was only added in the presence of Cys and Met (all equipment in contact with EDT was soaked in bleach due to strong odour). The reaction was stirred for 3 h at rt. The resin was removed via filtration and washed with TFA. The filtrates were combined and concentrated in vacuo and re-dissolved in the minimum amount of TFA. The mixture was ether precipitated via the addition of cold ether (8-10 fold volume), the reaction was carried out in a falcon tube. The solution underwent centrifugation and the residual solution was decanted off leaving the peptide pellet.

6.1.6.8 Addition of the Aldrithiol group

The peptide was dissolved in DMF. Aldrithiol (10 equivalents) was added to the solution and the reaction and stirred o/n (reaction went a lime green colour). The mixture was concentrated in vacuo and ether precipitated twice to remove excess aldrithiol.

6.1.6.9 Cyclisation reaction

Linear peptide (1eq) was reacted with EDC (3eq) and HOBt (6eq) DMF. The reaction mixture was stirred for 24 h. The reaction mixture was concentrated in vacuo and ether precipitated.

6.1.6.10 Reduction of disulfide bonds with 1,3-propanedithiol

The peptide was dissolved in degassed MeOH (1-3 mg/mL). 1,3-propanedithiol (5-fold excess relative to thiol) was added and the reaction was stirred under nitrogen for 6 hrs. The mixture was concentrated in vacuo and ether precipitated. The peptide was then purified via HPLC.

6.1.6.11 Reduction of disulphide bond with TCEP

The cyclic peptide (1eq) was dissolved in DMF (10 mL) and a solution of TCEP (1eq) in water (0.5 mL) was added. The mixture was stirred for 1 hr under Ar. The reaction was monitored by HPLC and controlled by MS. The solvent was removed and the products were precipitated with cold ether.

6.1.6.12 Tat-Tagging

The peptide from crude extract 6.1.6.11 was then coupled with Tat (2eq). The Tat-tagged product was purified via HPLC (RP-HPLC separation using Atlantis® T3 Prep OBD™ column, 19 mm x100 mm, 5 µm C_{18}, 17 mL/min). Crude peptide mixtures were subjected to reverse-phase chromatography, on a Waters HPLC system by using water/acetonitrile gradient with 0.1% trifluoroacetic acid. A typical program was 95:5 (water:acetonitrile) for 1 min and then the flow was then changed to 50:50 over 10 min and held for 15 minutes before reducing the flow was reduced to 95:5 for 5 min.

6.1.6.13 Synthesis of Tat

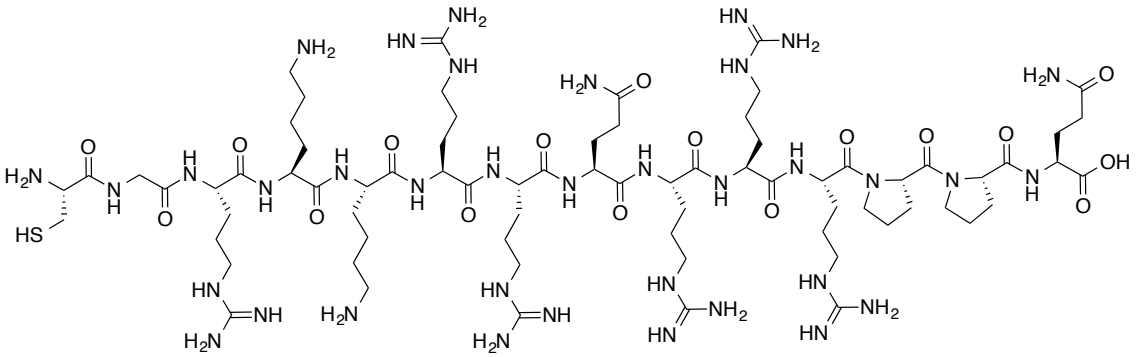

The reagents in Table 6.11 were used to synthesise the linear peptide. The coupling (6.1.6.4) and deprotection (6.1.6.5) steps were followed as mentioned above.

Reagent	Equivalents	Concentration	Mass (mg)
Fmoc-Gln(Trt)-O-wang resin	1	0.47	700
Fmoc-Pro-OH	3	1.32	663.96
Fmoc-Pro-OH	3	1.32	663.96
Fmoc-Arg(Pmc)-OH (x2)	3	0.99	654
Fmoc-Arg(Pmc)-OH (x2)	3	0.99	654
Fmoc-Arg(Pmc)-OH (x2)	3	0.99	654
Fmoc-Gly(Trt)-OH	3	0.99	603.9
Fmoc-Arg(Pmc)-OH (x2)	3	0.99	654
Fmoc-Arg(Pmc)-OH (x2)	3	0.99	654
Fmoc-Lys(Boc)	3	0.99	463.9
Fmoc-Lys(Boc)	3	0.99	463.9
Fmoc-Arg(Pmc)-OH (x2)	3	0.99	654
Fmoc-Gly-OH	3	0.99	290
Fmoc-Cys(Trt)-OH	3	0.99	579
PyBop	3	0.99	514.8
DIPEA	6	1.98	345 μl

Table 6.11. Reagents for the synthesis of Tat.

Note: Arginine requires double coupling. Proline gives a slight red colour in the Kaiser test.

On completion the Tat/resin (1.867 g) was placed in flask and a mixture of 94.0% TFA (43.9 μL): 2.5% water (1.2 μL): 2.5% TIS (1.2 μL): 1% EDT (0.467 μL) was added. The reaction was stirred for 3 hr at rt. The resin was removed via filtration and washed with TFA. The filtrates were combined and concentrated in vacuo and re-dissolved in minimum amount of TFA and ether precipitated via the addition of an 8-10 fold volume of cold ether (carried out in falcon tube). The solution underwent centrifugation and residual solution was decanted off leaving the peptide pellet.

Tat peptide (1eq, 0.62 mmol, 1.125 g) was dissolved in DMF (100 mL). Aldrithiol (10 eq, 6.2mmol, 1.366 μg) was added to the reaction and stirred o/n (reaction went a lime green colour). The mixture was concentrated in vacuo and ether precipitated twice

to remove excess aldrithiol. The product was then purified via 95:5 (water:acetonitrile) for 1 min and then the flow was then changed to 50:50 over 10 min and held for 15 minutes before reducing the flow was reduced to 95:5 for 5 min, (retention time 11 min). The mass was confirmed via high mass electron ionisation (HM ESI+) mass spectrometry:$(M+H)^+$ 1822.2, $(M+2H)^+$ 911.4, $(M+3H)^+$ 607.9, $(M+4H)^+$ 456.

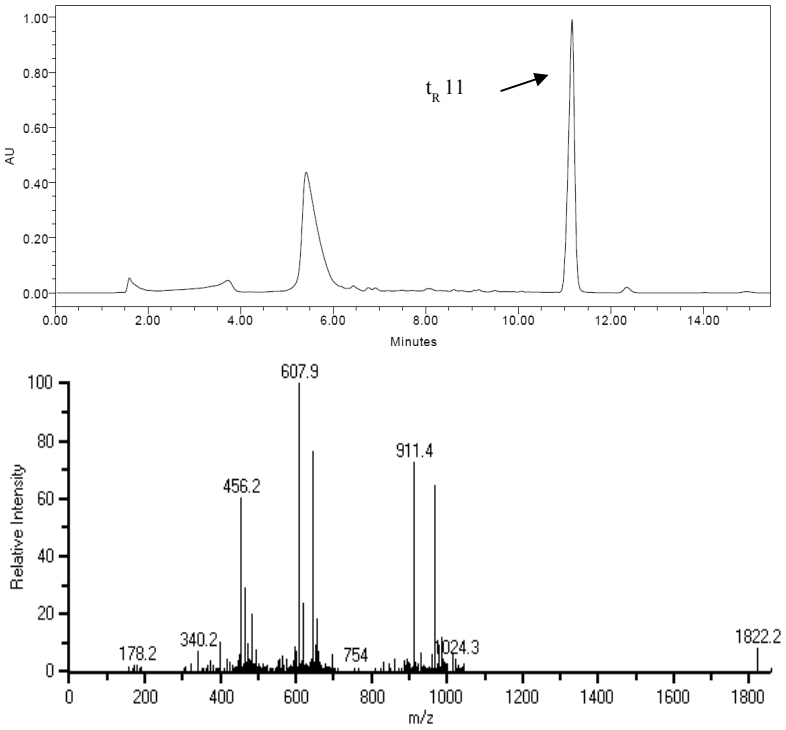

Figure 6.1. HPLC trace and mass spec trace of Tat peptide.

6.1.6.14 Peptide 61

6.1.6.14.1 Synthesis of GWTVVRMYS (Peptide 61)

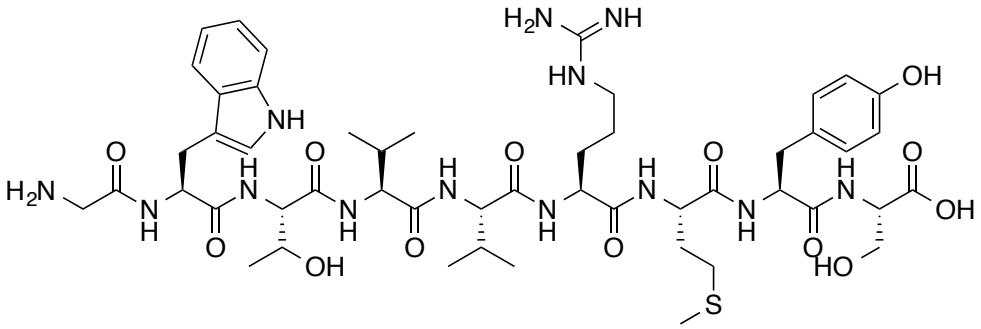

The Wang resin (500 mg, 0.55 mmol, 1eq) and Fmoc-Ser(tBu)-OH (421.74 mg, 1.1 mmol, 2eq) were dissolved in DMF (3 mL) and gently stirred at rt for 15 min. Pyridine (1.47 μL, 1.82 mmol, 3.3 eq) and Benzoyl Chloride (158 μL, 1.1 mmol, 2 eq) was added to the reaction mixture and stirred at rt for 15 hr. The reaction was filtered and washed with DMF (3x 15 mL), DCM (3 x 15 mL) and diethyl ether (3x 15 mL). The reaction was dried under vacuo. Loading was 0.94 mmol g^{-1}. The amino acid was capped by adding Benzoyl Chloride (150 μL), pyridine (150 μL) and DCM (4 mL) to the loaded resin and reacting in the bubbler for 2 hr at rt.

The reagents in Table 6.12 were used to synthesise the linear peptide, the coupling (6.1.6.4), deprotection (6.1.6.5) steps were followed as mentioned above.

Reagent	Equivalents	Concentration	Mass (g)
Fmoc-Ser(tBu)-O-Wang resin	1	0.166	0.24
Fmoc-Tyr(tBu)-OH	3	0.498	246.8
Fmoc-Met-OH	3	0.498	185
Fmoc-Arg(Pmc)-OH	3	0.498	329.2
Fmoc-Val-OH	3	0.498	169.3
Fmoc-Val-OH	3	0.498	169.3
Fmoc-Thr(tBu)-OH	3	0.498	198
Fmoc-Trp(Boc)-OH	3	0.498	262
Fmoc-Gly-OH	3	0.498	146
PyBop	3	0.498	259
DIPEA	6	1	96 μL

Table 6.12. Reagents for the synthesis of linear peptide 61 (GWTVVRMYS).

On completion, peptide 61/resin (600 mg) was placed in a flask and a mixture of 94.0% TFA (7.18 mL): 2.5% water (0.29 μL): 2.5% EDT (0.29 μL): 1% TIS (0.6 μL) was added. The reaction was stirred for 3 h at rt. The resin was removed via filtration and washed with TFA. The filtrates were combined and concentrated in vacuo and re-dissolved in minimum amount of TFA and ether precipitated via the addition of an 8-10 fold volume of cold ether (carried out in falcon tube). The solution underwent centrifugation and residual solution was decanted off leaving the peptide pellet. The crude product was purified via HPLC 95:5 (water:acetonitrile) for 1 min and then the flow was then changed to 40:60 over 10 min and held for 15 minutes before reducing the flow was reduced to 95:5 for 5 min, (retention time 8.6 min). The presence of the product was confirmed via HM ESI+ mass spectrometry: $(M+H)^+$1099.1.

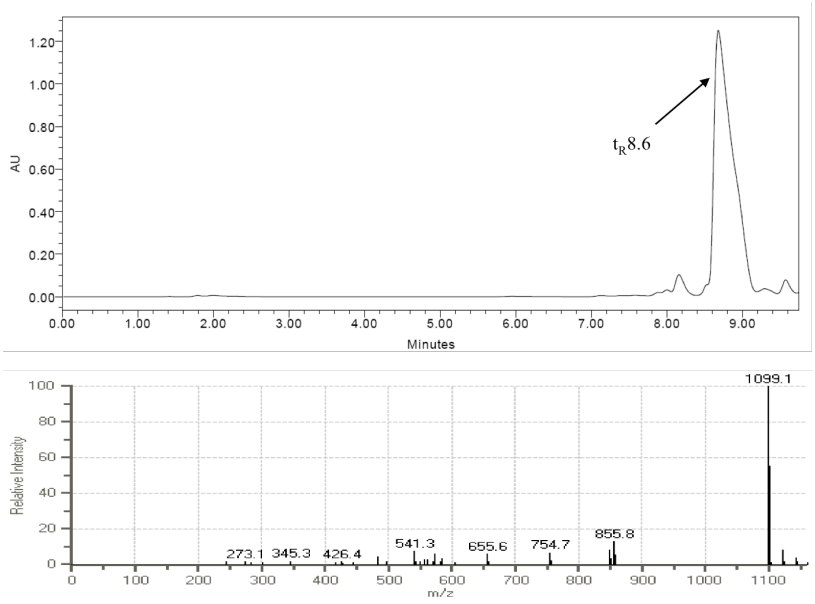

Figure 6.2. HPLC trace and mass spec trace of linear peptide 61.

6.1.6.14.2 Cyclisation of GWTVVRMYS

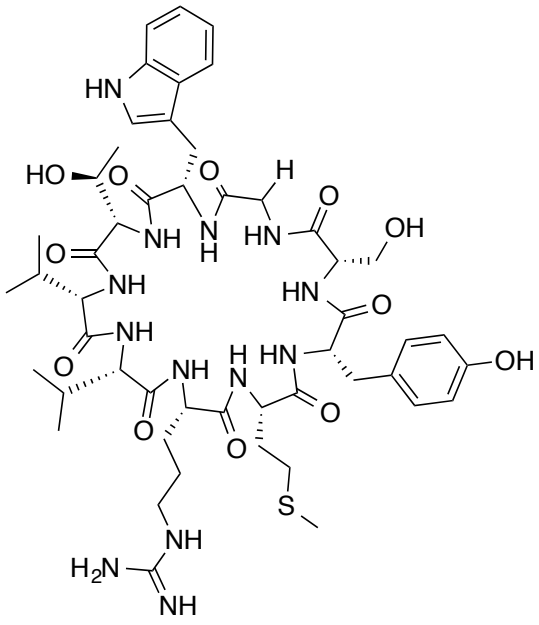

Linear peptide (1eq, 0.128 mmol 0.141g) was reacted with EDC (3eq, 0.39 mmol, 76 mg) and HOBt (6eq, 0.768 mmol, 103 mg) DMF (150 mL). The reaction mixture was stirred for 24 h. The reaction mixture was concentrated in vacuo and ether precipitated. The crude product was purified via HPLC 95:5 (water:acetonitrile) for 1 min and then the flow was then changed to 50:50 over 10 min and held for 15 minutes before reducing the flow was reduced to 95:5 for 5 min, (retention time 9.19 min). The

presence of the product was confirmed using HM ESI+ mass spectrometry:$(M+H)^+$ 1081. The purified product (36.7 mg) was freeze dried and stored at -80 °C

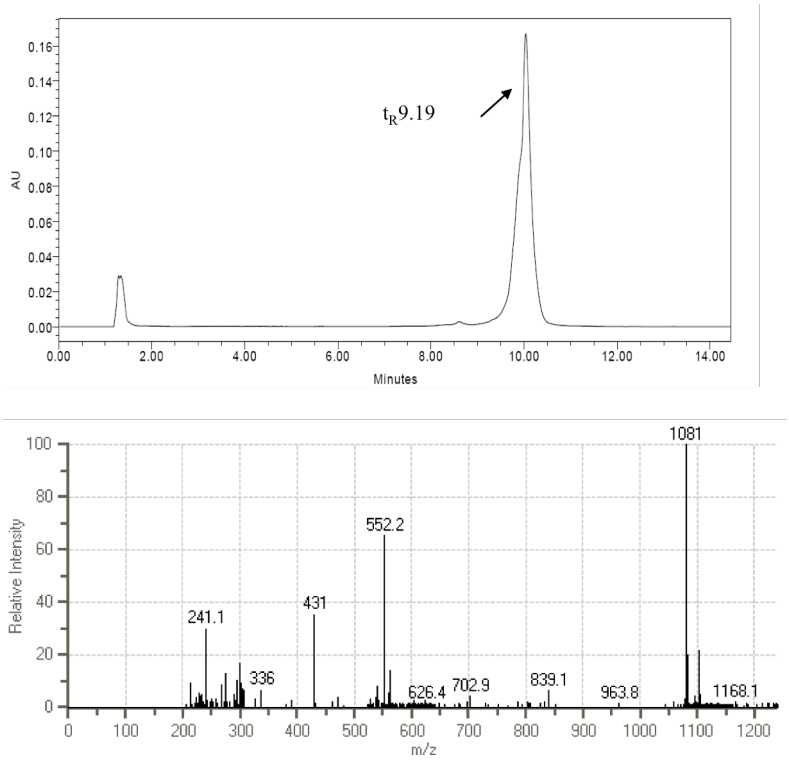

Figure 6.3. HPLC trace and mass spec trace of cyclic peptide 61.

6.1.6.15 Peptide 61 Tat-Tagged

6.1.6.15.1 Synthesis of CGWTVVRMY

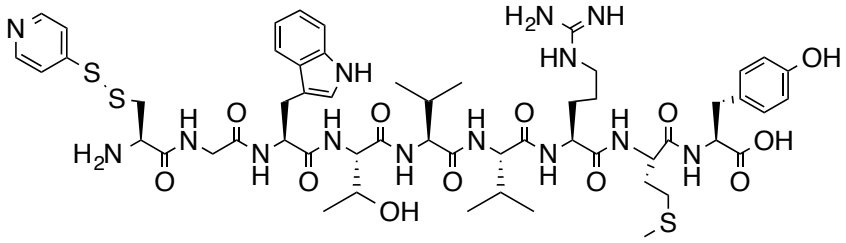

The Wang resin (1200 mg, 1.32 mmol, 1eq) and Fmoc-Tyr(tBu)-OH (1308 mg, 2.64 mmol, 2eq) were dissolved in DMF (12 mL) and gently stirred at rt for 15 min. Pyridine (352 µL, 4.36 mmol, 3.3 eq) and Benzoyl Chloride (306 µL, 2.64 mmol, 2 eq) was added to the reaction mixture and stirred at rt for 15 hr. The reaction was filtered and washed with DMF (3x 15 mL), DCM (3 x 15 mL) and diethyl ether (3x 15 mL). The reaction was dried under vacuo. Loading was 0.56 mmol g^{-1}. Benzoyl Chloride

(150 µL), pyridine (150 µL) and DCM (4 mL) was added to the loaded resin and reacted in the bubbler at rt for 2 hr to cap the amino acid.

The reagents in Table 6.13 were used to synthesise the linear peptide, the coupling (6.1.6.4), deprotection (6.1.6.5) steps were followed as mentioned above.

Reagent	Equivalents	Concentration	Mass (g)
Fmoc-Gly-O-Wang resin	1	0.79	1
Fmoc-Cys(Trt)-OH	3	2.37	1.386
Fmoc-Tyr(tBu)-OH	3	2.37	1.117
Fmoc-Met-OH	3	2.37	0.880
Fmoc-Arg(Pmc)-OH	3	2.37	1.567
Fmoc-Val-OH	3	2.37	0.791
Fmoc-Val-OH	3	2.37	0.791
Fmoc-Thr(tBu)-OH	3	2.37	0.941
Fmoc-Trp(Boc)-OH	3	2.37	1.248
PyBop	3	2.37	1.232
DIPEA	6	4.74	825 µL

Table 6.13. Reagents for the synthesis of linear peptide 61cys (CGWTVVRMY).

On completion, peptide 61Cys/resin (2.5718 g) was placed in a flask and a mixture of 94.0% TFA (60 mL): 2.5% water (1.6 µL): 2.5% EDT (1.6 µL): 1% TIS (0.6 µL) was added. The reaction was stirred for 3 h at rt. The resin was removed via filtration and washed with TFA. The filtrates were combined and concentrated in vacuo and re-dissolved in minimum amount of TFA and ether precipitated via the addition of an 8-10 fold volume of cold ether (carried out in falcon tube). The solution underwent centrifugation and residual solution was decanted off leaving the peptide pellet.

Peptide 61Cys (1eq, 0.9 mmol, 1.114 g) was dissolved in DMF. Aldrithiol (10 eq, 9 mmol, 1.98 g) was added to the reaction and stirred o/n (reaction went a lime green colour). The mixture was concentrated in vacuo and ether precipitated twice to remove excess aldrithiol. The crude product was purified via HPLC 95:5 (water:acetonitrile) for 1 min and then the flow was then changed to 60:40 over 10 min and held for 15 minutes before reducing the flow was reduced to 95:5 for 5 min, (retention time 7.76 min). The

presence of the product was confirmed via HM ESI+ mass spectrometry: $(M+H)^+$ 1224.1. The peptide was dried o/n in the desiccator.

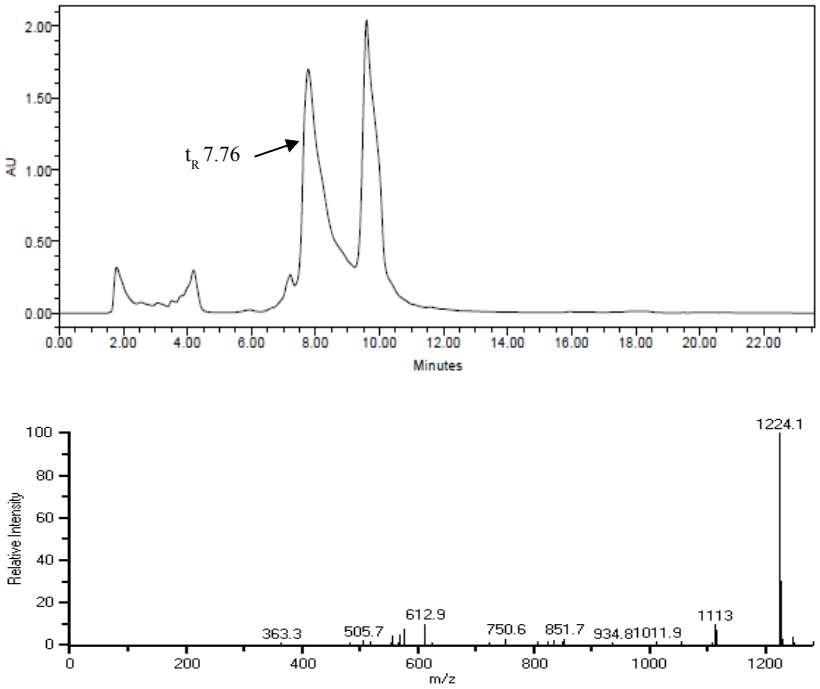

Figure 6.4. HPLC trace and mass spec trace of linear peptide 61cys.

6.1.6.15.2 Synthesis of Cyclic CGWTVVRMY

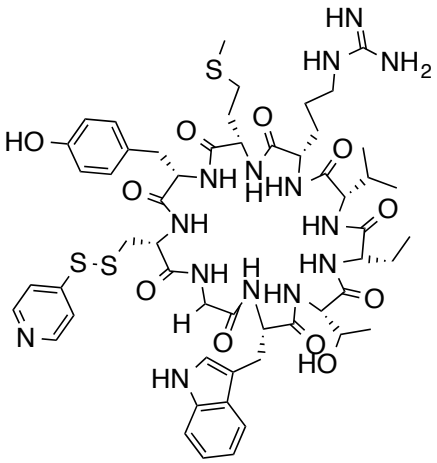

Linear peptide (1eq, 0.173 mmol 0.212g) was reacted with EDC (3eq, 0.52 mmol, 63 mg) and HOBt (6eq, 1.56 mmol, 210 mg) DMF (200 mL). The reaction mixture was stirred for 24 h. The reaction mixture was concentrated in vacuo and ether precipitated. The crude product was purified via HPLC 95:5 (water:acetonitrile) for 1 min and then the flow was then changed to 60:40 over 10 min and held for 15 minutes before

reducing the flow was reduced to 95:5 for 5 min, (retention time 7.9 min). The presence of the product was confirmed via HM ESI+ mass spectrometry: $(M+H)^+$ 1206, $(M+2H)^+$ 603.9.

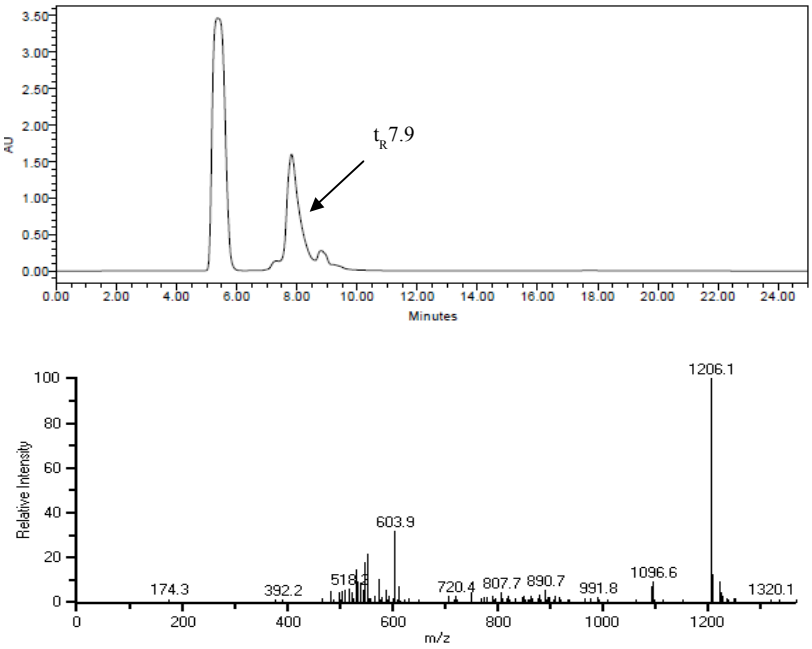

Figure 6.5. HPLC trace and mass spec trace of cyclic peptide 61cys.

6.1.6.15.3 Tat-tagging of cyclic- CGWTVVRMY

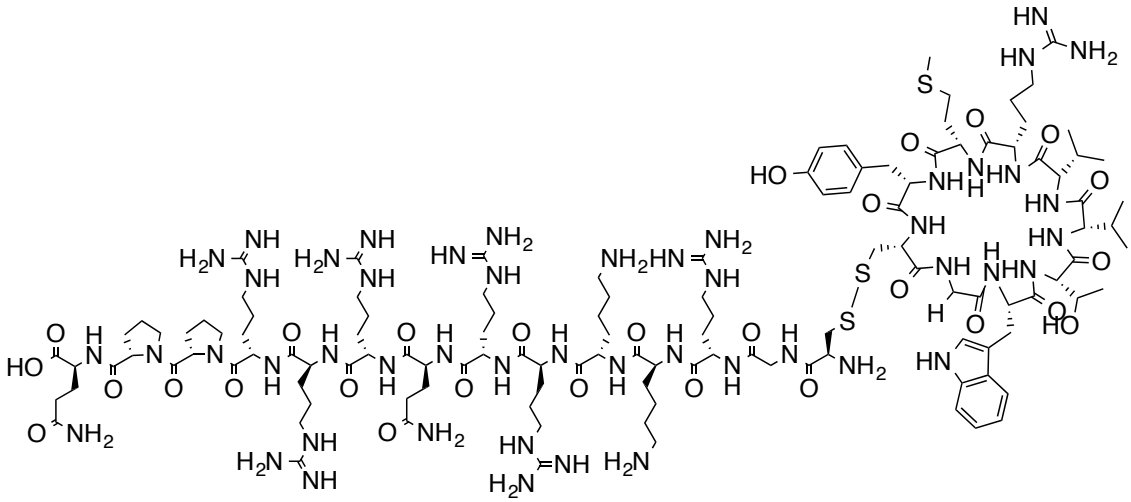

Tcep (1eq, 0.075 mmol, 21.5 mg), DMF (9 mL) and H_2O (0.05mL) were added to the cyclic peptide 61cys (1eq, 0.075 mmol 91 mg) and the mixture was stirred for 1 hr. The peptide was added to Tat-S-S-Py (2eq, 114.8 mg) and DMF (2 mL) and reacted for 3 hr. The crude product was purified via HPLC 95:5 (water:acetonitrile) for 1 min and then

the flow was then changed to 50:50 over 10 min and held for 15 minutes before reducing the flow was reduced to 95:5 for 5 min, (retention time 9.4 min). The presence of the product was confirmed via HM ESI+ mass spectrometry: $(M+2H)^+$ 1459, $(M+3H)^+$ 973.5, $(M+4H)^+$ 730.3, $(M+5H)^+$ 584

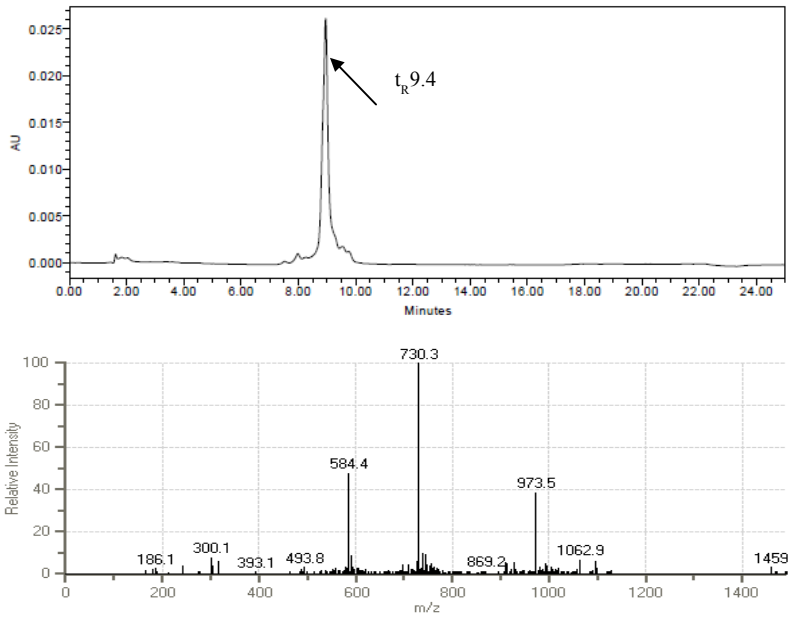

Figure 6.6. HPLC trace and mass spec trace of Tat-Tagged peptide 61cys.

6.1.6.16 Peptide 6

6.1.6.16.1 Synthesis of GWNTVRSS (Peptide 6)

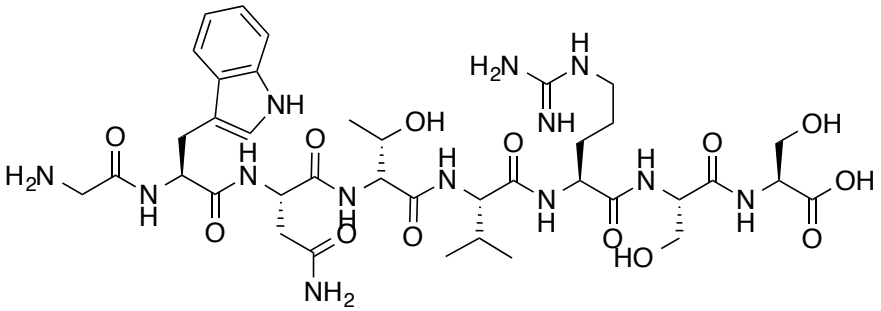

The Wang resin (500 mg, 0.55 mmol, 1eq) and Fmoc-Ser(tBu)-OH (421.74 mg, 1.1 mmol, 2eq) were dissolved in DMF (3 mL) and gently stirred at rt for 15 min. Pyridine (1.47 µL, 1.82 mmol, 3.3 eq) and Benzoyl Chloride (158 µL, 1.1 mmol, 2 eq) was added to the reaction mixture and stirred at rt for 15 hr. The reaction was filtered

and washed with DMF (3x 15 mL), DCM (3 x 15 mL) and diethyl ether (3x 15 mL). The reaction was dried under vacuo. Loading was 0.94 mmol g^{-1}. The amino acid was capped by adding Benzoyl Chloride (150 µL), pyridine (150 µL) and DCM (4 mL) to the loaded resin and reacting in the bubbler at rt for 2 hr.

The reagents in Table 6.14 were used to synthesise the linear peptide, and the coupling (6.1.6.4) and deprotection (6.1.6.5) steps were followed as mentioned above.

Reagent	Equivalents	Concentration	Mass (g)
Fmoc-Ser(tBu)-O-Wang resin	1	0.69	1
Fmoc-Ser(tBu)-OH	3	2.07	0.794
Fmoc-Arg(Pmc)-OH	3	2.07	1.368
Fmoc-Val-OH	3	2.07	0.703
Fmoc-Thr(tBu)-OH	3	2.07	0.823
Fmoc-Asn(Trt)-OH	3	2.07	0.821
Fmoc-Trp(Boc)-OH	3	2.07	1.09
Fmoc-Gly-OH	3	2.07	0.607
PyBop	3	2.07	1.076
DIPEA	6	6.21	1081 µL

Table 6.14. Reagents for the synthesis of linear peptide 6 (GWNTVRSS).

On completion, peptide 6/resin (1.449 g) was placed in a flask and a mixture of 95% TFA (34.4 mL): 2.5% water (0.9 µL): 2.5% TIS (0.9 µL) was added. The reaction was stirred for 3 h at rt. The resin was removed via filtration and washed with TFA. The filtrates were combined and concentrated in vacuo and re-dissolved in minimum amount of TFA and ether precipitated via the addition of an 8-10 fold volume of cold ether (carried out in falcon tube). The solution underwent centrifugation and residual solution was decanted off leaving the peptide pellet. The crude product was purified via HPLC 95:5 (water:acetonitrile) for 1 min and then the flow was then changed to 60:40 over 10 min and held for 15 minutes before reducing the flow was reduced to 95:5 for 5 min, (retention time 6.1 min). The presence of the product was confirmed via HM ESI+ mass spectrometry: $(M+H)^+$ 906.9, $(M+2H)^+$ 454.1

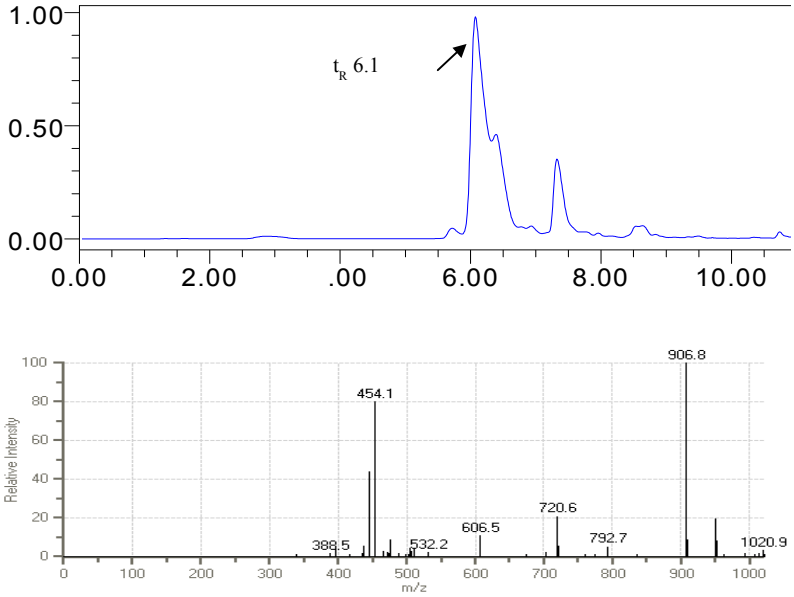

Figure 6.7. HPLC trace and mass spec trace of linear peptide 6.

6.1.6.16.2 Synthesis of Cyclic- GWNTVRSS

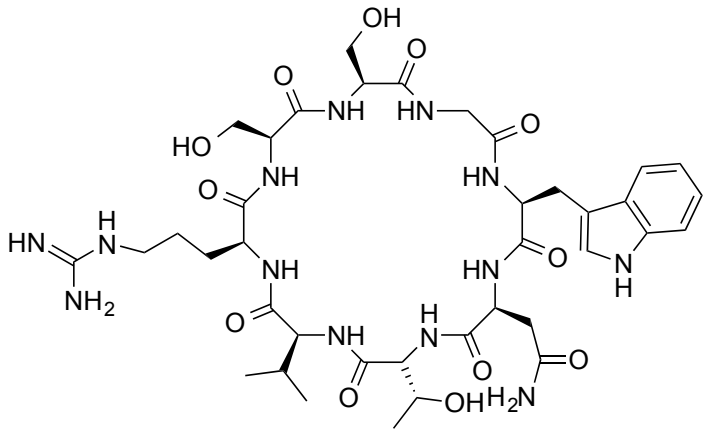

Linear peptide (1eq, 0.132 mmol 0.120 g) was reacted with EDC (3eq, 0.79 mmol, 75 mg) and HOBt (6eq, 0.79 mmol, 107.4 mg) and DMF (150 mL). The reaction mixture was stirred for 24 h. The reaction mixture was concentrated in vacuo and ether precipitated. The crude product was purified via HPLC 95:5 (water:acetonitrile) for 1 min and then the flow was then changed to 50:50 over 10 min and held for 15 minutes before reducing the flow was reduced to 95:5 for 5 min, (retention time 7.9 min). The

presence of the product was confirmed via HM ESI+ mass spectrometry $(M+H)^+$888.8. The cyclic peptide 6 (79 mg) was freeze dried and stored in the -80 °C freezer.

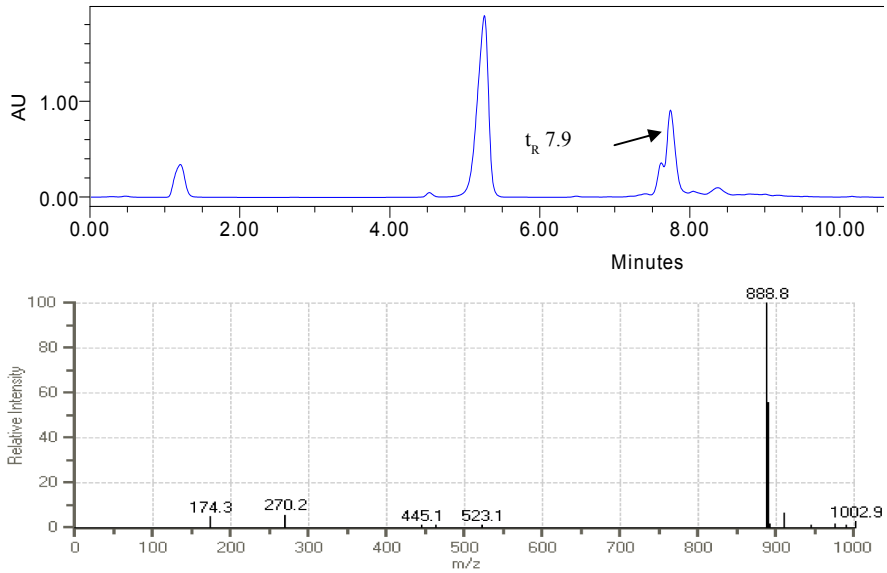

Figure 6.8. HPLC trace and mass spec trace of cyclic peptide 6.

6.1.6.17 Peptide 6 Tat-Tagged

6.1.6.17.1 Synthesis of GWNTVRCS

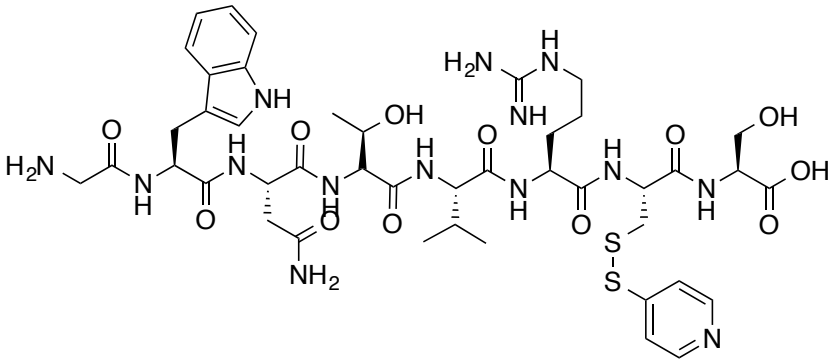

The linear peptide was synthesised on the peptide synthesiser. The reagents in Table 6.15 were loaded onto the machine. Amino acids were dissolved in DMF before loading, and the Fmoc-Ser(tBu)-O-Wang resin (loading of 0.69 mmol g^{-1}) was added directly to the reaction vessel. The reaction was run on a 0.25 mM scale. Coupling of Fmoc-Arg(Pmc)-OH was carried out twice. Each coupling step was followed by a

deprotection step as normal; however the final amino acid was left protected and was deprotected manually before cleavage from the resin.

Reagent	Mass (g)	Reagent volume (mL)
Fmoc-Ser(tBu)-O-Wang resin	0.362	-
Fmoc-Cys(Trt)-OH	0.59	5
Fmoc-Arg(Pmc)-OH	1.43	11
Fmoc-Val-OH	0.41	6
Fmoc-Thr(tBu)-OH	0.48	6
Fmoc-Asn(Trt)-OH	0.72	6
Fmoc-Trp(Boc)-OH	0.63	6
Fmoc-Gly-OH	0.30	5
PyBop	4.68	18
DIPEA/NMP	-	3.1/5.9
DMF	-	1012

Table 6.15. Reagents for the synthesis of linear peptide 6cys (CGWNTVRS).

The resin was cleaved by adding 94% TFA (36 mL), 2.5% H_2O (0.96 µL), 2.5% EDT (0.96 µL) and 1% TIS (0.4 µL) was added to the peptide (1.93 g). The reaction was stirred for 3 h at rt. The resin was removed via filtration and washed with TFA. The filtrates were combined and concentrated in vacuo and re-dissolved in a minimum amount of TFA and ether precipitated via the addition of an 8-10 fold volume of cold ether (carried out in falcon tube). The solution underwent centrifugation and the residual solution was decanted off leaving the peptide pellet.

Peptide 6 Cys (1eq, 0.83 mmol, 1 g) was dissolved in DMF. Aldrithiol (10 eq, 8.3 mmol, 1.829 g) was added to the reaction and stirred o/n (reaction went a lime green colour). The mixture was concentrated in vacuo and ether precipitated twice to remove excess aldrithiol. The crude product was purified via HPLC 95:5 (water:acetonitrile) for 1 min and then the flow was then changed to 60:40 over 10 min and held for 15 minutes before reducing the flow was reduced to 95:5 for 5 min, (retention time 6.9 min). The presence of the product was confirmed via HM ESI+ mass spectrometry $(M+H)^+$ 1031.9, $(M+2H)^+$ 516.7. The peptide was dried o/n in the desiccator.

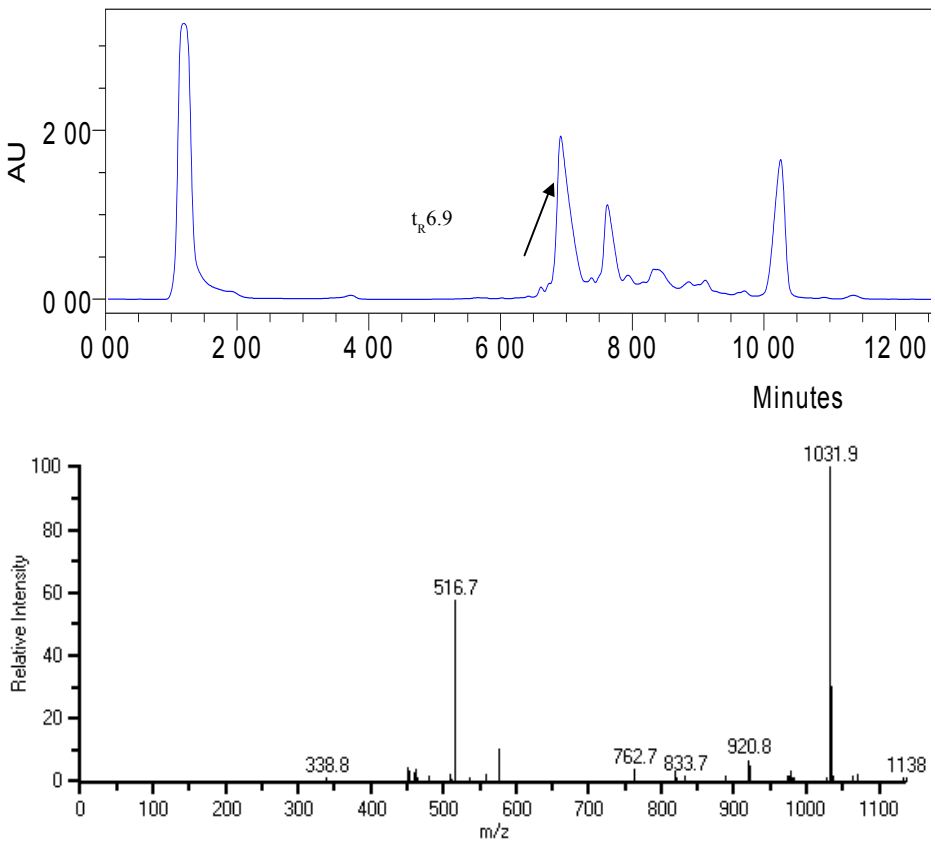

Figure 6.9. HPLC trace and mass spec trace of linear peptide 6cys.

6.1.6.17.2 Synthesis of Cyclic-CGWNTVRS

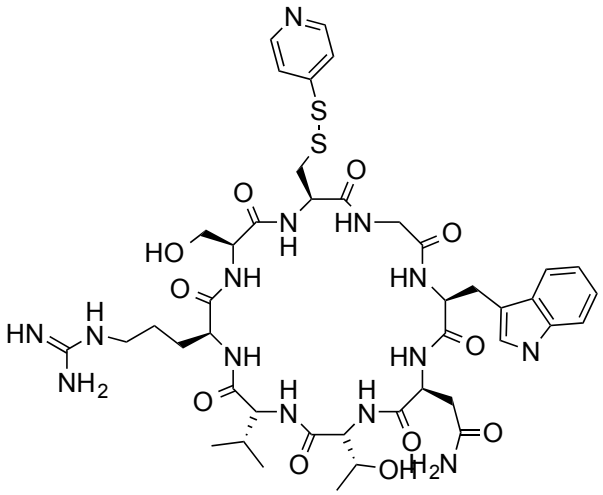

Linear peptide (1eq, 0.193 mmol 0.200 g) was reacted with EDC (3eq, 0.579 mmol, 114.2 mg) and HOBt (6eq, 1.737 mmol, 234.7 mg) and DMF (200 mL). The reaction mixture was stirred for 24 h. The reaction mixture was concentrated in vacuo and ether precipitated. The crude product was purified via HPLC 95:5 (water:acetonitrile) for 1 min and then the flow was then changed to 50:50 over 10 min and held for 15 minutes before reducing the flow was reduced to 95:5 for 5 min, (retention time 7.7 min). The presence of the product was confirmed via HM ESI+ mass spectrometry: $(M+H)^+$ 1013.9, $(M+2H)^+$ 507.7.

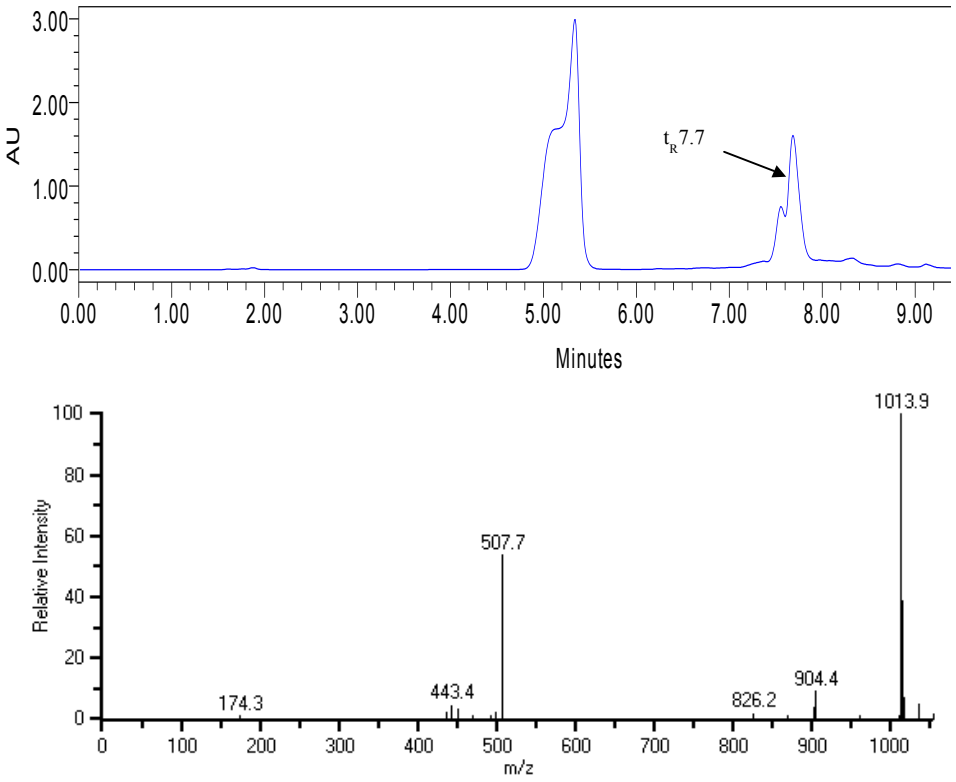

Figure 6.10. HPLC trace and mass spec trace of cyclic peptide 6cys.

6.1.6.17.3 Tat-tagging of cyclic-CGWNTVRS

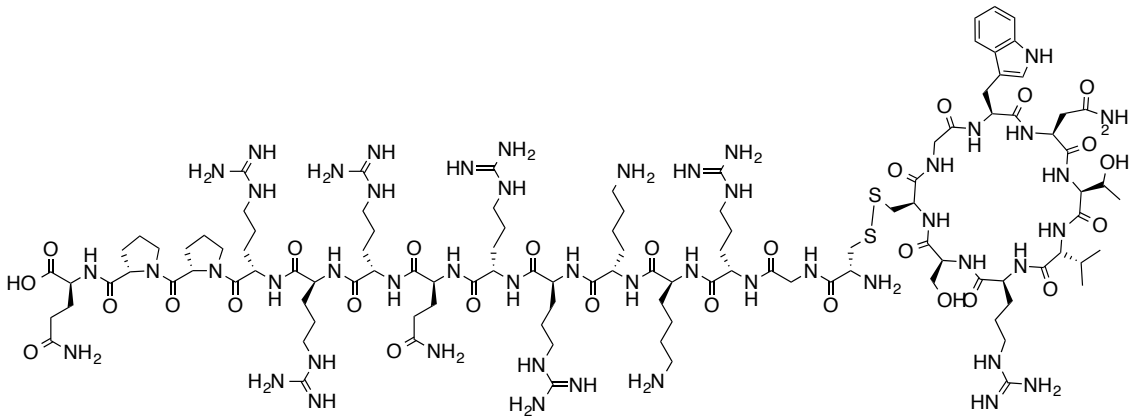

Tcep (1eq, 0.02 mmol, 5.7 mg), DMF (2 mL) and H_2O (0.05mL) was added to cyclic peptide 6cys (1eq, 0.02 mmol 20 mg) and the mixture was stirred for 1 hr. The peptide was added to Tat-S-S-Py (2eq, 0.04 mmol, 77.3 mg) and DMF (2 mL) and the mixture was stirred for 3 hr. The crude product was purified via HPLC 95:5 (water:acetonitrile) for 1 min and then the flow was then changed to 60:40 over 10 min and held for 15 minutes before reducing the flow was reduced to 95:5 for 5 min, (retention time 7.1).

The presence of the product was confirmed via HM ESI+ mass spectrometry: $(M+2H)^+$ 1362.9, $(M+3H)^+$ 909.3, $(M+4H)^+$ 682.6, $(M+5H)^+$ 545.9.

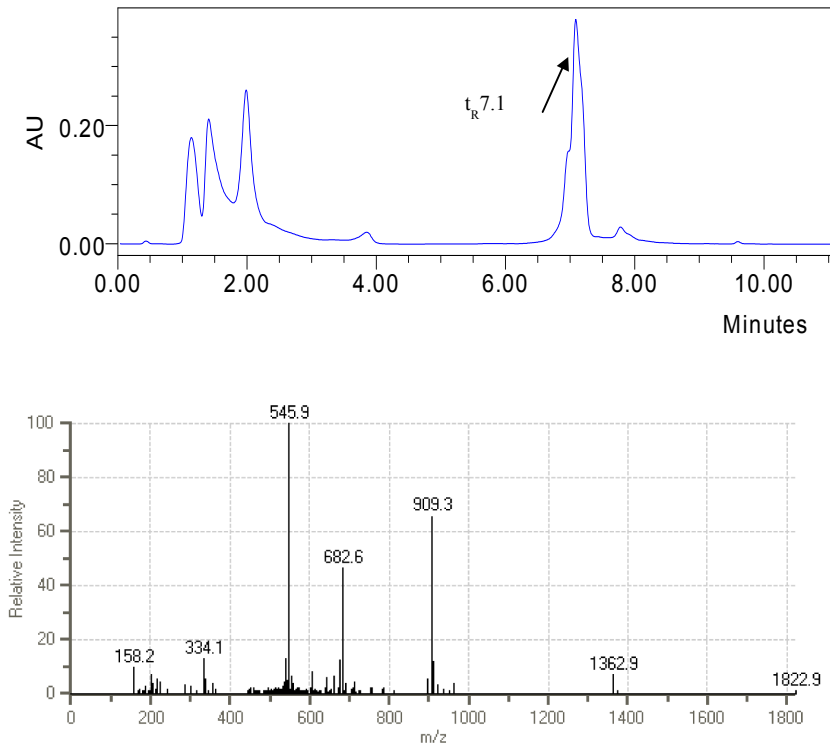

Figure 6.11. HPLC trace and mass spec trace of Tat-tagged peptide 6cys.

6.1.6.18 Peptide 33

6.1.6.18.1 Synthesis of CNRYYF (Peptide 33)

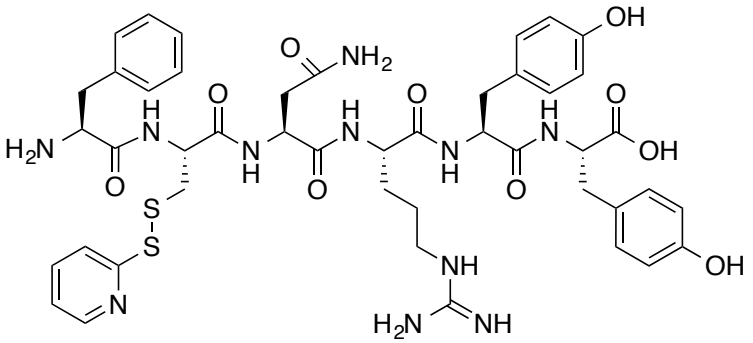

The reagents in Table 6.16 were used to synthesise the linear peptide and the coupling (6.1.6.4) and deprotection (6.1.6.5) steps were followed as mentioned above.

Reagent	Equivalents	Concentration	Mass (g)
Fmoc-Tyr(tBu)-O-Wang resin	1	0.56	1
Fmoc-Arg(Pmc)-OH (x2)	3	2.1	1.338
Fmoc-Asn(Trt)-OH	3	1.68	0.831
Fmoc-Cys(Trt)-OH	3	1.68	1228.5
Fmoc-Phe(tBu)-OH	3	1.68	0.813
Fmoc-Try(tBu)-OH	3	1.68	1.041
PyBop	3	1.68	1.092
DIPEA	6	3.36	403 µL

Table 6.16. Reagents for synthesis of linear peptide 33 (CNRYYF).

On completion, peptide 33/resin (1.929 g) was placed in a flask and a mixture of 95.0% TFA (45.82 mL): 2.5% water (1.21 µL): 2.5% TIS (1.21 µL) was added. The reaction was stirred for 3 h at rt. The resin was removed via filtration and washed with TFA. The filtrates were combined and concentrated in vacuo and re-dissolved in a minimum amount of TFA and ether precipitated via the addition of an 8-10 fold volume of cold ether (carried out in falcon tube). The solution underwent centrifugation and the residual solution was decanted off leaving the peptide pellet.

Peptide 33 (1eq, 0.639 mmol, 0.622 mg) was dissolved in DMF. Aldrithiol (10 eq, 6.39mmol, 1.4 g) was added to the reaction and stirred o/n (reaction went a lime green colour). The mixture was concentrated in vacuo and ether precipitated twice to remove excess aldrithiol. The crude product was purified via HPLC 95:5 (water:acetonitrile) for 1 min and then the flow was then changed to 50:50 over 10 min and held for 15 minutes before reducing the flow was reduced to 95:5 for 5 min, (retention time 7.7 min). The presence of the product was confirmed via HM ESI+ mass spectrometry:$(M+H)^+$ 974.6. The peptide was dried o/n in the desiccators.

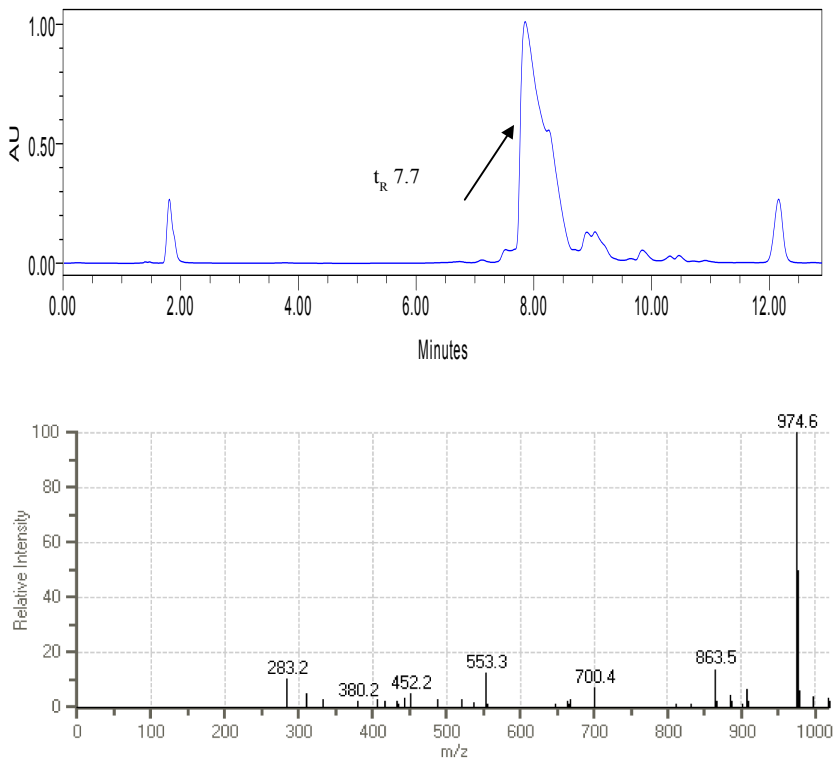

Figure 6.12. HPLC trace and mass spec trace of linear peptide 33.

6.1.6.18.2 Synthesis of Cyclic-CNRYYF

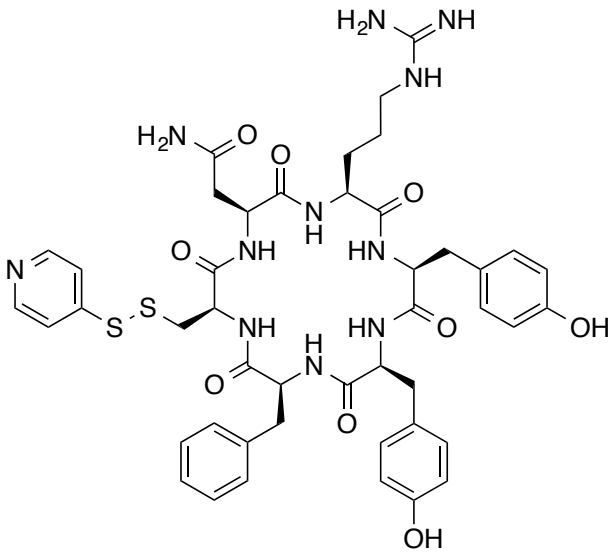

Linear peptide (1eq, 0.23 mmol 0.244g) was reacted with EDC (3eq, 0.69 mmol, 136.4 mg) and HOBt (6eq, 2.07 mmol, 279.7 mg) DMF (250 mL). The reaction mixture

was stirred for 24 h. The reaction mixture was concentrated in vacuo and ether precipitated. The crude product was purified via HPLC 95:5 (water:acetonitrile) for 1 min and then the flow was then changed to 50:50 over 10 min and held for 15 minutes before reducing the flow was reduced to 95:5 for 5 min, (retention time 10.4 min). The presence of the product was confirmed via HM ESI+ mass spectrometry: $(M+H)^+$ 953.7.

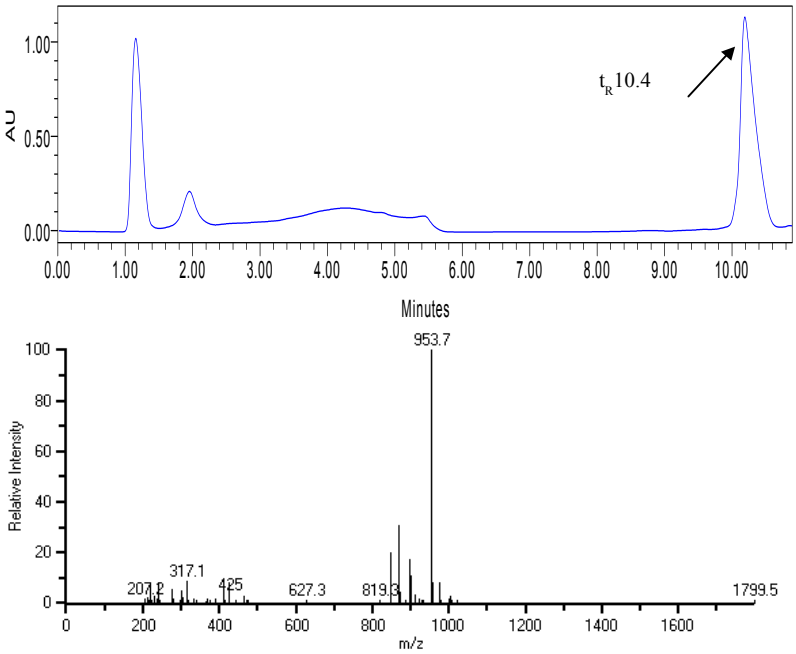

Figure 6.13. HPLC trace and mass spec trace of cyclic peptide 33 (protected).

6.1.6.19 Peptide 32

6.1.6.19.1 Synthesis of CRYFNV (Peptide 32)

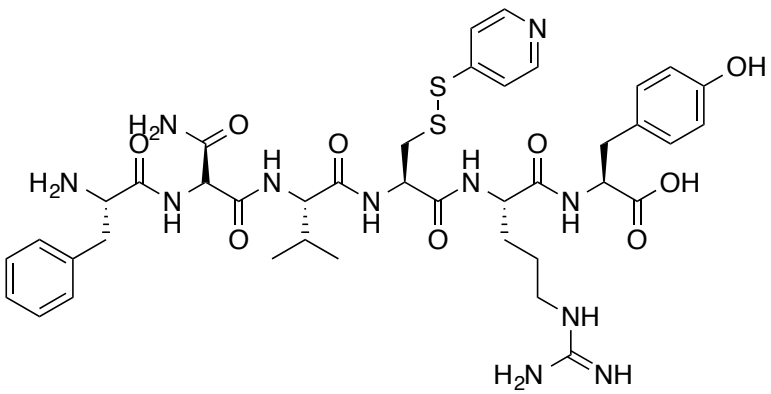

The reagents in Table 6.17 were used to synthesise the linear peptide and the coupling (6.1.6.4) and deprotection (6.1.6.5) steps were followed as mentioned above.

Reagent	Equivalents	Concentration	Mass (g)
Fmoc-Tyr(tBu)-O-Wang resin	1	0.358	0.639
Fmoc-Arg(Pmc)-OH (x2)	3	1.07	0.710
Fmoc-Cys(Trt)-OH	3	1.07	0.543
Fmoc-Val-OH	3	1.07	0.365
Fmoc-Asn(Trt)-OH	3	1.07	0.460
Fmoc-Phe(tBu)-OH	3	1.07	0.416
PyBop	3	1.07	0.558
DIPEA	6	2.15	374 µL

Table 6.17. Reagents for synthesis of linear peptide 32 (CRYFNV).

On completion, peptide 32/resin (0.895 g) was placed in a flask and a mixture of 94.0% TFA (21 mL): 2.5% water (0.6 µL): 2.5% TIS (0.6 µL): 1% EDT (0.222 µL) was added. The reaction was stirred for 3 h at rt. The resin was removed via filtration and washed with TFA. The filtrates were combined and concentrated in vacuo and re-dissolved in the minimum amount of TFA and ether precipitated via the addition of an 8-10 fold volume of cold ether (carried out in falcon tube). The solution underwent centrifugation and the residual solution was decanted off leaving the peptide pellet.

Peptide 32 (1eq, 0.34 mmol, 271 mg) was dissolved in DMF (250 mL). Aldrithiol (10eq, 3.4 mmol, 749 mg) was added to the reaction and stirred o/n (reaction was a lime green colour). The mixture was concentrated in vacuo and ether precipitated twice to remove excess aldrithiol. The crude product was purified via HPLC 95:5 (water:acetonitrile) for 1 min and then the flow was then changed to 50:50 over 10 min and held for 15 minutes before reducing the flow was reduced to 95:5 for 5 min, (retention time 10.4 min). The presence of the product was confirmed via HM ESI+ mass spectrometry:$(M+^{15}N)^+$ 910.7. The peptide was dried o/n in the desiccator.

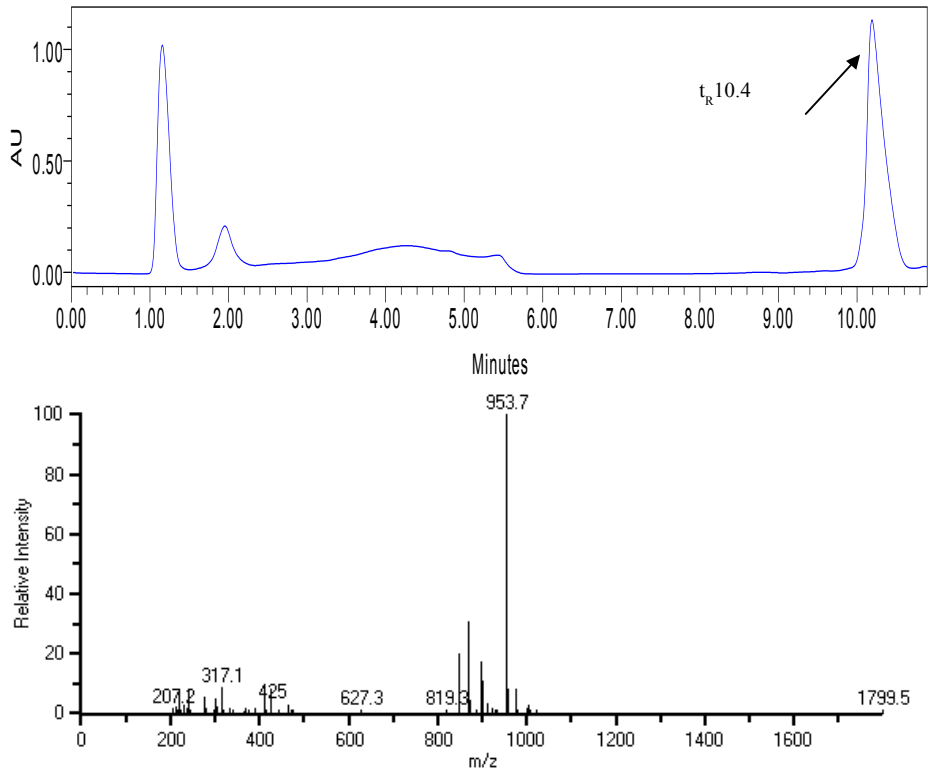

Figure 6.14. HPLC trace and mass spec trace of linear peptide 32.

6.1.6.19.2 Synthesis of Cyclic-CRYFNV (cysteine protected)

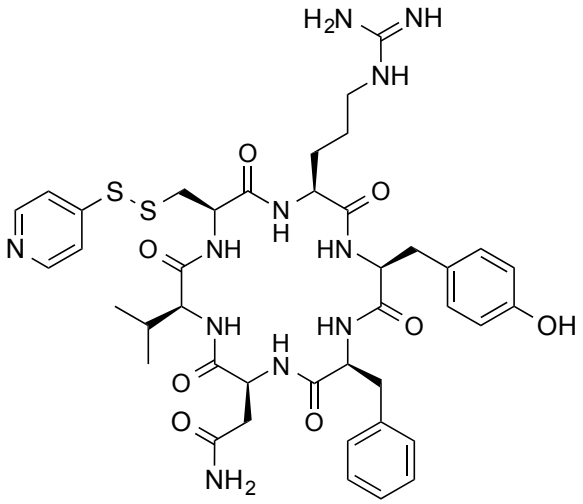

Linear peptide (1eq, 0.1 mmol 91 mg) was reacted with EDC (3eq, 0.3 mmol, 59.31 mg) and HOBt (6eq, 0.6 mmol, 81.1 mg) in DMF. The reaction mixture was stirred for 24 h. The reaction mixture was concentrated in vacuo and ether precipitated.

The crude product was purified via HPLC 95:5 (water:acetonitrile) for 1 min and then the flow was then changed to 50:50 over 10 min and held for 15 minutes before reducing the flow was reduced to 95:5 for 5 min, (retention time 10 min). The presence of the product was confirmed via HM ESI+ mass spectrometry: $(M+H)^+$ 892.

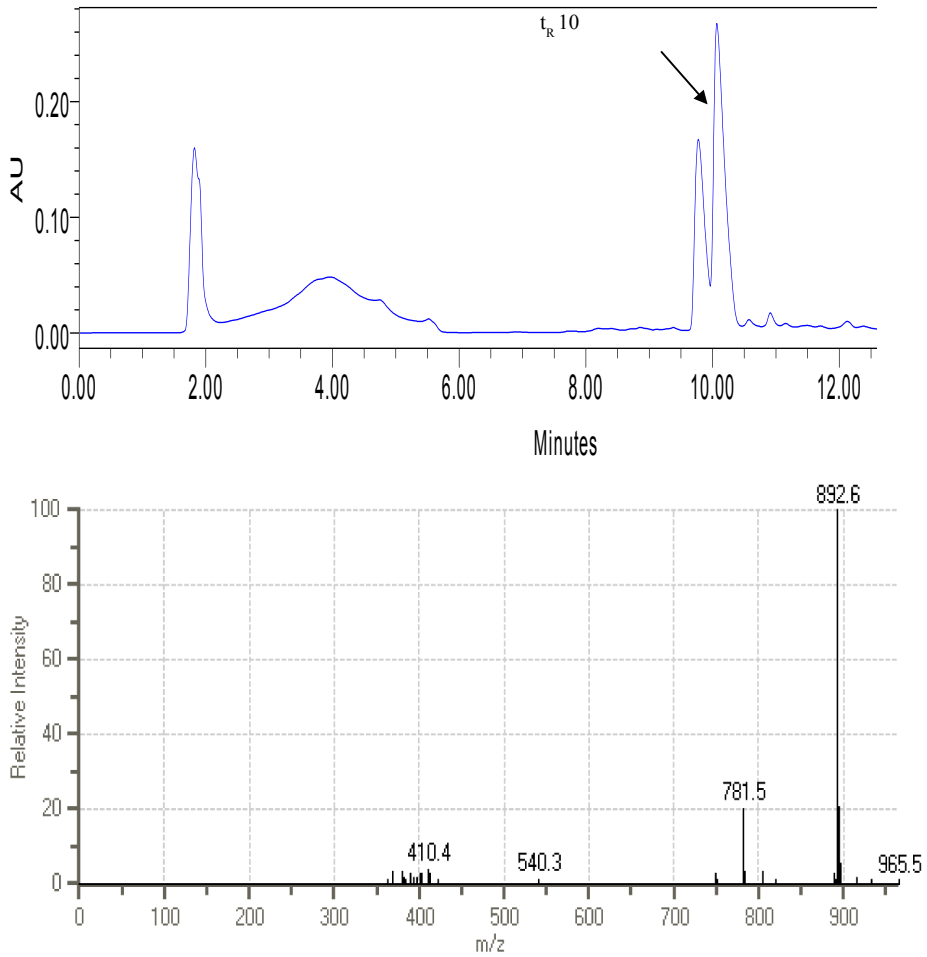

Figure 6.15. HPLC trace and mass spec trace of cyclic peptide 32 (cysteine protected).

6.1.6.19.3 Cyclic-CRYFNV (Removal of Aldrithiol group)

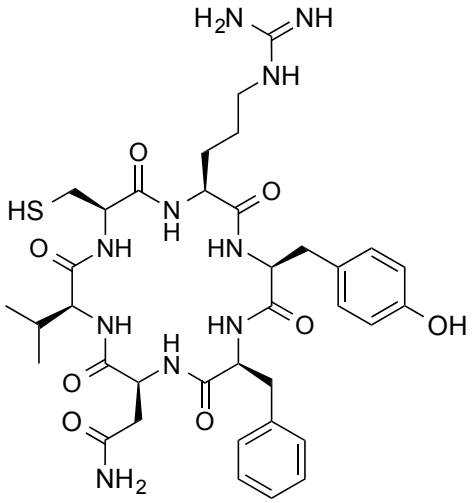

The peptide (1eq, 2.5 mmol, 22 mg) was dissolved in degassed MeOH (44 mL) and propandithiol (4eq, 18.75 mmol, 2.2 μL) was added. The reaction was stirred for 6 hr. The crude product was purified via HPLC 95:5 (water:acetonitrile) for 1 min and then the flow was then changed to 50:50 over 10 min and held for 15 minutes before reducing the flow was reduced to 95:5 for 5 min, (retention time 12.2 min). The presence of the product was confirmed via HM ESI+ mass spectrometry: $(M+H)^+$ 783. The purified product was freeze dried and stored in the -80 °C freezer.

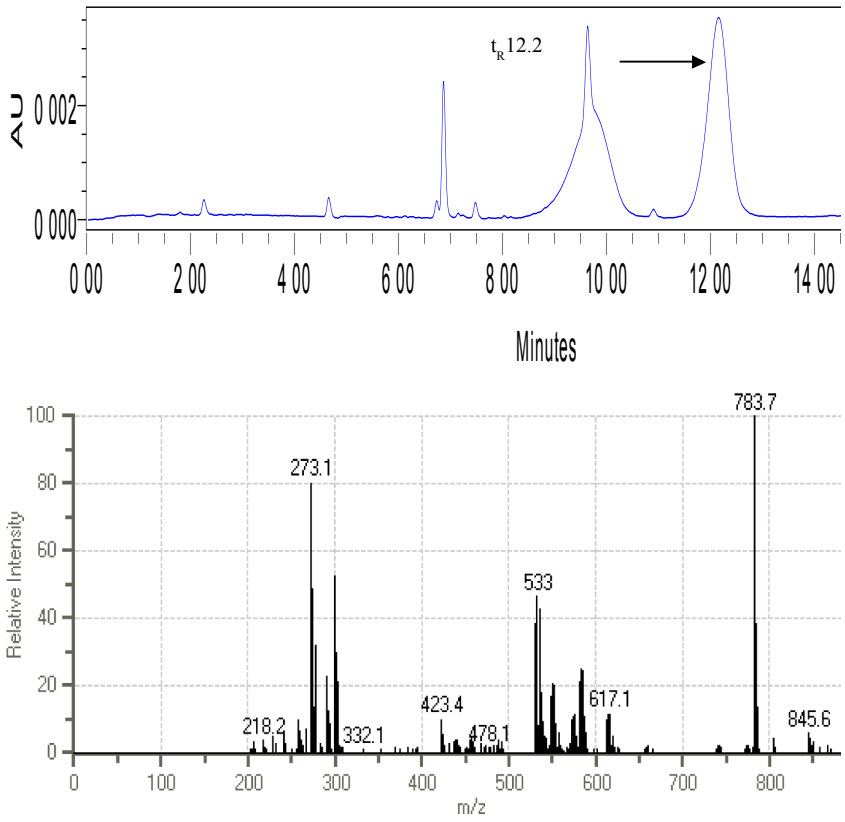

Figure 6.16. HPLC trace and mass spec trace of cyclic peptide 32.

6.2 In vivo effects of CtBP Dimerisation Inhibition

6.2.1 Mammalian Cell Reagents

Thermo scientific Griener, U.K supplied all tissue culture plastic ware.

Invitrogen Life technologies, UK:

Hank's Balanced Salt Solution (HBSS)

- (1X) liquid without Calcium and Magnesium

Dulbecco's modified Eagle's medium (DMEM)

Trypsin-EDTA

Peninillin/Streptomycin/L-Glutamine 100X concentration

Penicillin G 10 mg/mL

Streptomycin	10 mg/mL
L-Glutamine	29.2 mg/mL

Promega, U.K

CellTiter 96® AQ_{ueous} One Solution Cell Proliferation assay 20 µl/well

PAA Laboratories, Austria

Foetal Calf Serum (FCS)

6.2.2 Mammalian cell culture techniques

6.2.2.1 Cell line, culture conditions and cell passage

Cell lines MCF-7 and MDA-MB231 were cultured at 37 °C in a humidified atmosphere containing 10% CO_2 (HERA Vell, Heraeus), with DMEM supplemented with 10% (v/v) FCS and 1% (v/v) penicillin/streptomycin/glutamine. All media were pre-warmed to 37 °C before use, and the culture media was renewed every 48-72 hr.

Cell passaging was performed by removing the culture medium and washing the cells with HPSS solution. Following this cells were treated with trypsin (typically 1 mL for a 75 cm^2 flask) and incubated at 37 °C for 5 min or until all cells had detached. Fresh growth medium was then added and cells plated at the required density.

6.2.2.2 Cryopreservation and thawing of cells

Monolayers were disassociated by trypsinisation as described (6.2.2.1) and cells re-suspended in complete growth media. Cells were collected by Centrifugation at 1399 rpm (Sorvall legend ™ RT, Rotor 6445) for 3 min. Cells were re-suspended in 2 mL of freezing media (50% (v/v) DMEM, 40% (v/v) FCS and 10% (v/v) Dimethyl Sulfoxide (DMSO) and transferred to cryovials (greiner, U.K), Cryovials were placed in an insulated Styrofoam box (Nalgen U.K) which was sealed and stored at -80 °C. 24 hrs later the vials were transferred to liquid nitrogen for long term storage.

Cells were thawed by removing the cryovial from the liquid nitrogen and allowing rapid thawing at 37 °C. Once thawed the cells were added carefully to 10 mL or pre- warmed

growth media. Cells were collected by centrifugation at 3000 rpm (Sorvall legend ^{TM} RT, Rotor 6445) for 3 min and re-suspended in the desired volume of complete media prior to culture and stored in the incubator.

6.2.3 Transfection

Transfection was carried out using INTERFERin^{TM} siRNA transfection reagent from Source Bioscience Lifescience. Cells were plated 24 hrs prior to transfection, typically in 60 mm dishes. 3.75 µL, 25 nM CtBP2 siRNA was added to an eppendorf containing 400 µL of optimum and vortexed. 15 µL of Interferin was added and vortexed for a further 10 sec and left to stand for 10 min before adding to the media. Cells were then returned to the incubator for 4 hr. At the end of the incubation time the media was replaced with fresh media.

6.2.4 Time-Lapse Experiments

6.2.4.1 Peptide Microinjection Time-lapse Experiment

6.2.4.1.1 Preparation of MCF-7 Cells for Microinjection with Peptide 6 and Peptide 61

The media (trypsin and DMEM) was pre-warmed in a 37 ºC water bath. The fumehood and gloves were sprayed with ethanol to ensure sterility. The media was removed from the T flask containing the cells using the aspirator and pipette. 10 mL of HPPS media was added to the flask. The media was then removed. 1 mL of Trypsin was added to the flask (ensuring that the surface was covered), and the flask was left in the incubator for ~5 min. The flask was checked under the microscope to see whether the cells had lifted. DMEM was added to the flask and transferred into a falcon tube (to prevent cells from adhering to the plate again). The cells were counted using a hemocytometer (require 10^5 cells). The required amount was replated into the flask. 200 µL of cells was added to the centre of the 60mm dish (where the marking for microinjection was) and incubated for 30 min at 37 ºC. 3mL DMEM was added to the plate and incubate at 37 ºC for 24 h. The media was removed and washed with DMEM no adds media a couple of times. 3 mL of

DMEM no adds media was added to the plate and incubated at 37 ºC for 40 h. The media was removed and replaced with DMEM and incubated at 37 ºC for 30 h.

6.2.4.1.1 Preparation of CtBP2 siRNA treated MCF-7 Cells for Microinjection with Peptide 6

200 µL of cells was added to the centre of the 60mm dish (where the marking for microinjection was) and incubated for 30 min at 37 ºC. 3mL DMEM was added to the plate and incubated at 37 ºC for 24 h. The media was removed and washed with DMEM no adds media a couple of times. 3 mL of DMEM no adds media was added to the plate and incubated at 37 ºC for 40 h. Transfection with CtBP2 siRNA was carried out as described in 6.2.3. Instead of replacing the media after 4 hr, media was replaced with DMEM media after 8hr. The cells were microinjected 24 hr later.

6.2.4.1.2 Microinjection

Cells were plated in 60 mm dishes prior to microinjection. Media was replaced with Leibovitz's L-15 medium containing serum to control pH during microinjection, which was performed with an eppendorf microinjection system (Femtojet and InjectMan N12), mounted on an Axiovert 35M microscope with heated stage. The peptide was injected into the Cytoplasm; Dextran-FITC was co-injected to allow cells to be followed (4 µL was loaded into the injection needle. The Pressure varied with the sample. Injection time was set to 1/2 sec.

6.2.4.2 Running Time-lapse Microscopy

Fluorescence time-lapse microscopy of MCF-7 cells was performed using an Olympus IX81 microscope with CO_2- and temperature-controlled environmental chamber controlled by SIS Cell P software, for a period of 48 hr. Image J software was used for analysis.

IX81 Multiple fluorescence (mFIP) set up was as follows:

- Switch on the microscope, stage controller, mercury bulb and computer etc
- Create a folder in the data folder on the hard drive (to hold images of run).

- Start Cell^P log into the microscope (password ‘a’) and bring up the microscope and camera control windows.
- Bring up the Define Fluorescence Acquisition window – acquire > Multiple fluorescence > define Fluorescence acquisition (should have phase and FITC) > Select phase method, click preview focus the image and the exposure time, then set focus level by clicking focus stop the preview by clicking on the snap shot > Select the FITC, click start preview, focus image and adjust exposure time, then click read and stop the preview > Save the method.
- Define ISP – acquire > define ISP > flow tab, cycle setup number of frames and cycle repeat times > under acquire mode select mFIP method from above > under save image select folder created earlier > settings tab provide a path name > macro tab tick sequence apply preprocessing and click define and type IXC::ixSetShutterOpen(TRUE,FALSE); > Add sequence find image and then read image do this for all images then save and run.

6.2.4.3 Tat-Tagged time-lapse experiment

6.2.4.3.1 Testing Tat-Tagged Peptide 6, 61 and Tat

Cells (40,000) were dosed and plated into 24 well plates. Peptides 6, 61 and Tat were tested at a concentration of 50 μM and 100 μM. Once the cells had adhered to the plate, the plate was loaded onto the time-lapse microscope using phase imaging.

6.2.4.3.2 Testing Tat-Tagged Peptide 6 with CtBP2 siRNA

MCF-7 and MDA-MB231 cells were treated with CtBP2 siRNA following the transfection protocol above (6.2.3). CtBP2 siRNA treated cells were then dosed and plated into 24 well plates. Peptide 6 and Tat were treated at a concentration of 50 μM and 100 μM. Once the cells had adhered to the plate, the plate was loaded onto the time-lapse microscope using phase imaging.

6.2.5 Immunoflourescence analysis

Cells were grown on coverslips in 24 well plates; the media was removed and washed with PBS. The cells were fixed with 4% paraformaldehyde in PBS for 10 min. Wells were washed with PBS, 1 mM Glycine and 0.2% Triton X-100/PBS (2 mL) was added and incubated for 15 min at rt, The wells were washed with PBS and then blocked for 30 min in 10% FCS/PBS. The p53 primary antibody (1:100) in 0.6% BSA/PBS (100 μL) was added and incubated for 1 hr. The wells were then washed with PBS for 5 min. The Rabbit-α-mouse FITC secondary antibody (1:50) in 0.6% BSA (100 μL) and DAPI (1:1000) was added and incubated in a humidified box for 90 min. Coverslips were mounted onto slides with fluorescent mounting medium (DakoCytomation). All cells were visualized using a Zeiss Axiovert 200 fluorescence microscope with a 40 xs or 100 xs objective. Images were collected using an Orca-ER digital camera (Hamamatsu) and processed using Openlab 3.5.1 Software (Improvision). Identical exposure times were applied for different images within the same experiment.

6.2.6 3-(4,5-dimethylthiazol-2-yl)-5-(3-carboxymethoxyphenyl)-2-(4-sulfophenol)-2H-tetrazolium (MTS) assay

For cell MTS assays, the cells were plated at 4000 cells per a well in 96 well plates. Cells were left to adhere for 24 hr at 37 ºC in a humidified atmosphere containing 10% CO_2 (HERA Vell, Heareus). Media was replaced with 100 μL medium containing serial dilution of the peptides. The final concentration of solvent DMSO, was 1/200 in all wells. All conditions were assayed in triplicate. After 48 h the media was removed and replaced with fresh medium before performing an MTS-based assay (CellTitre Aqueous One Cell Proliferation assay, Promega). 10 μL of CellTitre Aqueous one solution reagent was added to each well, the plate was incubated at 37 °C in a humidified 5% CO_2 atmosphere for 3 hrs to allow the colorimetric reaction to occur. The reduction of MTS inner salt to the coloured water soluble product formazan was measured at 490 nm using a plate reader (Thermo Fischer scientific Varioskan Flash).

6.2.7 Colony forming assay

2500 cells were dosed and plated into 96 well plates with 50 mM of peptide. Cells were detached with trypsin 2 days post-transfection in 96-well plates and 10% of the volume

of harvested cells was replated into 6-well plates. The cells were grown for a further 10 days with a change of growth medium every 3 to 4 days. Colonies were fixed with MeOH and stained with Giemsa (Sigma) and counted manually.

6.2.8 MeOH fixing and Giemsa staining of cells

Media was removed from the plates and washed with PBS (1 mL). MeOH (1 mL) was added and left for 5 min, rinsed then left to air dry. Giemsa stain (1:20 dilution) was added and left for 60 min. Plates were washed with water for 4 min and then with PBS and left to air-dry.

6.2.9 Preparation of cell pellets and fixation from adherent mammalian cells for DNA content of cells by propidium iodide (PI) staining flow cytometry.

Plates were removed from the incubator. The media was removed and added to the microcentrifuge tube. Wells were washed with PBS and added to centrifuge tubes. Trypsin was added to the plates to detach the cells. Wells were washed with the media in the microcentrifuge tubes. Everything was collected in the microcentrifuge tubes and centrifuged for 5 min at 1000g (3000 rpm). The supernatant was removed and the cell pellet was re-suspended in PBS (1 mL). The microcentrifuge tubes were centrifuged for 5 min at 1000g (3000 rpm), the supernatant was removed and the cells were re-suspended in 70% Ethanol/water and stored at 4 °C.

Staining and flow cytometry was carried out by Dr Charles Birts. The ethanol suspended cells were centrifuged at 1000g (no breaking) and the supernatant was removed. PBS (1 mL) was added to the samples and mixed by pipetting up and down. The samples were left for 1 min and re-centrifuged. The supernatant was removed and the pellet was re-suspended in 0.5-1 mL PI staining solution. The sample was incubated at 37 °C for 15 min the at rt for 30 min. Flow cytometry was carried out according to the instructions in the operating manual.

6.3 In vitro Analysis of Peptides Developing ELISA

6.3.1 Protein Purification Reagents

Protease inhibitor cocktail tablets (Roche)

Sample Buffer (for SDS-PAGE)

	Final Concentration
Tri-Hydrochloric Acid pH6.8	50 mM
Sodium Dodecyl Sulphate	12% (w/v)
Bromophenol Blue	0.1% (w/v)

Supplemented with 10% Dithiothreitol (DTT) added fresh

6.3.1.1 10X concentration Protein Running Buffer

Tris Base	30 g
Glycine	144 g
Sodium Dodecyl Sulphate	10 g
H_2O	to 1 L

6.3.1.2 10X Tris-Glycine (TG)

Tris Base	29 g
Glycine	145 g
H20	to 1 L

6.3.1.3 Transfer Buffer

10X TG	100 mL
H_2O	700 mL
Methanol	200 mL

6.3.1.4 Coomassie Blue

Glacial Acetic acid	10% (v/v)
Ethanol	10% (v/v)
Distilled water	45% (v/v)
Coomassie Blue Powder	0.05% (w/v)

6.3.1.5 10 mL Lysis Buffer

(10 mL of lysis buffer per g pellet)

Composition of lysis buffer

	Amount	Stock	Final concentration
TrisHCl pH 8	200 µL	1 M	20 mM
NaCl	625 µL	4 M	250 mM
Triton X	100 µL	20%	0.2%
Lysozyme	2 µL	1000 x	
DNASI	50 µL	2 mg/mL	125 µg/mL
MgCl	100 µL	1 M	10 mM0.

Table 6.18. Composition of lysis buffer

6.3.1.6 Binding Buffer (500 mL)

	Amount	Stock	Final concentration
TrisHCl (Fisher) pH 7.4	10 mL	1 M	20 mM
NaCl (Fisher)	43.75 mL	4 M	350 mM

Table 6.19. Composition of Binding buffer.

6.3.1.7 Elution Buffer (100 mL)

Imidazole (1.7 g, 250 mM) was mixed with the binding buffer (100 mL). The pH was adjusted to 7.4.

6.3.2 Protein Quantification

6.3.2.1 Recombinant protein production and purification

E. Coli BL21 and RIPL competent cells were used for production of recombinant GST fusion protein and His fusion protein as they give high-level expression and are protease-deficient strain.

6.3.2.2 Protein Purification

6.3.2.2.1 Cell culture and Lysis

Cell cultures and induction was kindly set up by Dr Patrick Duriez. Competent cells transformed with the appropriate vector were cultured o/n at 37 °C with shaking in 5-10 mL of LB media supplement with antibiotics. The culture was then subcultured o/n in LB medium (50 mL). Another subculture (500 mL) was set up and once the OD reached 0.6 induction was carried. IPTG (0.2 mM) was added and the culture was incubated for a further 2 hr at 25 °C. The culture was centrifuged at 4000 rpm at 4 °C for 25 min and the supernatant was discarded. The pellet was subsequently re-suspended in 50 mL of ice-cold PBS and split into two 50 mL tubes. The samples were centrifuged at 4000 rpm at 4 °C for 10 min the supernatant was discarded and the pellet was stored at –20 °C until required.

The pellet was thawed and lysed with lysis buffer (10 mL/mg) (kept on ice). Sample was left on ice for 10 min, then freezed/thawed using dry ice. Sonication was applied (4x 20 min pulses at 6.5) and the tubes were kept on ice. The lysed cells were centrifuged at 15000 rpm at 4 °C for 20 min and the sample were collected before and after centrifugation. The pellet (insoluble protein) was discarded and the supernatant (soluble protein) was kept for further purification.

6.3.2.2.2 Purification on FPLC Column

Once cells were lysed, the supernatant was filtered and loaded onto the column (GSTrap column (GE Healthcare) for GST-CtBP protein and HisTrap column (GE Healthcare)

for His-CtBP protein). The column was then washed with binding buffer. Sodium pyruvate (50 mL, 0.25 mM) was made up in binding buffer. 15 ml was applied to fill line A and the column, and the FPLC was paused for 20 min. The rest of the sodium pyruvate/binding buffer was then washed through over 10 min (30 min of total contact with sodium pyruvate). Binding buffer was then applied. Wash buffer was then applied in line B in a stepwise manner: first 4% (20 mM imidazole) then 8% (40 mM imidazole) then a10 ml gradient from 16% to 100% (20-250 mM imidazole) was applied to elute the purified protein. Fractions were collected throughout the run and then run on the SDS-PAGE gel in order to identify fractions containing the protein.

6.3.2.2.3 Purification on Beads (Ni-NTA Superflow, Qiagen))

1.5 mL of 75% beads was washed with 15 mL of PBS (to prepare 2 mL of 50% beads). 1 mL of 50% beads was added to 50 mL of supernatant. The beads were incubated o/n at 4 °C under rotation. After o/n capture the beads were centrifuged at 1300 rpm, and the supernatant was retained and loaded on the gel (unbound). The beads were washed with 50 mL binding buffer twice (saving both washes). The beads were then incubated with 0.25 mM sodium pyruvate in binding buffer for 30 min at 4 °C under rotation (wash 3). The beads were incubated with binding buffer and 20 mM imidazole for 20 min at 4 °C under rotation (wash 4).

The beads were then transferred onto a column and mounted onto the FPLC. Wash buffer was then applied in a stepwise manner: 16% (40 mM imidazole), 20% (50 mM imidazole) and 24% (60 mM imidazole). Finally, a 18 mL gradient from 24% to 100% (60-250 mM) was applied. Fractions were collected throughout the run and then run on the SDS-PAGE gel in order to identify fractions containing the protein. The retained washes collected from the beads were also run on the SDS-PAGE gel to confirm that the protein was not lost in the washes.

6.3.2.3 Sodium Dodecyl Sulphate – Polyacrylamide Gel Electrophoresis (SDS-PAGE)

SDS-PAGE was used to analyse protein samples from cell extracts and protein purification samples. Proteins were separated by SDS-PAGE prior to further analysis

using 12% gradient Tris-HCL SDS-polyacrylamide gels. Samples were heated to 95 °C for 5 min prior to loading. 20 μg of protein was loaded onto the gel in 1 x protein running buffer (6.3.1.1) and broad range protein marker (New England Biolabs, U.K) was used as a molecular weight markers. Electrophoresis was conducted at 200 V for 1 hr or until the dye front reached the bottom of the gel in mini-protean III cells (Bio-Rad, U.K)

Resolving gel (12%)

40% Acrylamide-Bis (29:1)	3.0 mL
Water	5.4 mL
1.5 M Tris pH 8.8	2.5 mL
20% SDS	50 μL
10% Ammonium Persulphate	100 μL
TEMED	5 μL

6.3.2.4 Coomassie Blue Stain

Coomassie Blue Staining was used to quantify protein levels on 12% gradient Tris-HCL SDS-polyacrylamide gels. Coomassie blue binds non-specifically to all proteins with approximately 1:1 stoichiometry. After completion of SDS-PAGE, the gel was removed from the mini-protean III cells (Bio-Rad, U.K.). The gel was incubated with shaking in Coomassie blue for 1 hr at room temperature. The gel was then washed with boiling water to distain for 20 min at room temperature. The process was repeated 2 times to remove excess stain. The gel was placed on Whatmann paper 3 mm and wrapped in cellophane prior to drying under vacuum at 80 °C for 1 hr.

6.3.2.5 Protein quantification

Bio-Rad's protein assay reagent, which provides a simple calorimetric assay for measuring total protein concentration in a sample, was used (Bio-Rad, UK). Protein was added into the wells of a 96 well plate at different concentrations. 50 μL of neat Bio-rad

reagent was added. The plate was then assayed on the plate reader to measure the absorbance at 595 nm. Protein concentration could then be calculated using a standard curve of known Bovine Serum Albumin concentration against absorbance.

6.3.3 ELISA

Binding Buffer - TBS pH 7.4 (500 mL)

	Molecular weight	Mass	Final concentration
TrisHCl	157.6	3.94	50 mM
NaCl	58.44	4.38	150 mM

Table 6.20. Composition of Binding buffer

Wash buffer – TBS + 0.05% tween-20-20 pH7.4 (200 mL)

100 µL of tween-20 was added to 200 mL of binding buffer.

6.3.3.1 CtBP1 Homodimeric assay

The glutathione coated 96 well plate (15240 thermo Scientific) was rinsed three times with wash buffer (200 µL). Purified GST-CtBP1 protein was prepared in wash buffer (100 ng, 100 µL) and was applied to duplicate wells. GST in wash buffer (100 ng, 100 µL) was applied to separate duplicate wells to measure background. The plate was covered and incubated at room temperature for 1 hr. The wells were washed three times with wash buffer (200 µL) for 5 min. The wells were blocked using 3% BSA (Bovine serum Albumin protease free powder, Cat 700-101P, Gemini Bio Products) in TBS (200 µL). Dilutions of the peptide (0, 1, 5, 10, 50, 100, 500, 1000, 5000, 10000 and 50000 nM) was mixed with purified His-CtBP1 protein (600 ng, 100 µL) and added to the wells for 30 min. NADH (Sigma-Aldrich, CAS Number: 104809-32-7) (0.5 mM) was added to the wells giving a final volume of 150 µL per well. The plate was incubated at room temperature for 1 hr. Wells were washed three times with wash buffer (200 µL) for 5 min. A 1/5000 dilution of mouse anti-His antibody was prepared

in 3% BSA-TBS/0.05% tween-20 and 100 µL was added to each well. The plate was covered and incubated at room temperature for 90 min. Plates were washed three times with wash buffer (200 µL) for 5 min. A 1/10000 dilution of sheep anti mouse HRP labelled secondary antibody was prepared in 3% BSA-TBS/0.05% tween-20 and 100 µL was applied to each well. The plate was covered and incubated at room temperature for 1 hr. Wells were washed three times with wash buffer (200 µL) for 5 min. Super signal (100 µL) (thermo Scientific) was applied to each well. The Luminescence measured was on the plate reader (Thermo Fischer scientific Varioskan Flash).

6.3.3.2 CtBP2 Homodimeric assay

The glutathione coated 96 well plate (15240 thermo Scientific) was rinsed three times with wash buffer (200 µL). Purified GST-CtBP2 protein was prepared in wash buffer (200 ng, 100 µL) and was applied to duplicate wells. GST in wash buffer (200 ng, 100 µL) was applied to separate duplicate wells to measure the background. The plate was covered and incubated at room temperature for 1 hr. The wells were washed three times with wash buffer (200 µL) for 5 min. The wells were blocked using 3% BSA (Bovine serum Albumin protease free powder, Cat 700-101P, Gemini Bio Products) TBS/0.05% tween-20 (200µL). Dilutions of the peptide (0, 1, 5, 10, 50, 100, 500, 1000, 5000, 10000 and 50000 nM) was mixed with purified His-CtBP2 protein (600 ng, 100 µL) and added to the wells for 30 min. NADH (0.5 mM) was added to the wells giving a final volume of 150 µL per well. The plate was incubated at room temperature for 1 hr. The wells were washed three times with wash buffer (200 µL) for 5 min. A 1/5000 dilution of mouse anti-His antibody was prepared in 3% BSA-TBS/0.05% tween-20 and 100 µL was added to each well. The plate was covered and incubated at room temperature for 90 min. The wells were washed three times with wash buffer (200 µL) for 5 min. A 1/10000 dilution of sheep anti mouse HRP labelled secondary antibody was prepared in 3% BSA-TBS/0.05% tween-20 and 100 µL was applied to each well. The plate was covered and incubated at room temperature for 1h. Wells were washed three times with wash buffer (200 µL) for 5 min. Super signal (100 µL) (thermo Scientific) was applied to each well. The Luminescence was measured on the plate reader (Thermo Fischer scientific Varioskan Flash).

6.3.3.3 CtBP Heterodimeric assay

The glutathione coated 96 well plate (15240 thermo Scientific) was rinsed three times with wash buffer (200 µL). Purified GST-CtBP2 protein was prepared in wash buffer (200 ng, 100 µL) and was applied to duplicate wells. GST in wash buffer (200 ng, 100 µL) was applied to separate duplicate wells to measure the background. The plate was covered and incubated at room temperature for 1 hr. Plates were washed three times with wash buffer (200 µL) for 5 min. The wells were blocked using 3% BSA (Bovine serum Albumin protease free powder, Cat 700-101P, Gemini Bio Products) in TBS (200 µL). Dilutions of the peptide (0, 1, 5, 10, 50, 100, 500, 1000, 5000, 10000 and 50000 nM) was mixed with purified His-CtBP1 protein (600ng, 100 µL) and added to the wells for 30 min. NADH (0.5 mM) was added to the wells giving a final volume of 150 µL per well. The plate was incubated at room temperature for 1 hr. The wells were washed three times with wash buffer (200 µL) for 5 min. A 1/5000 dilution of mouse anti-His antibody was prepared in 3% BSA-TBS/0.05% tween-20 and 100 µL was added to each well. The plate was covered and incubated at room temperature for 90 min. The wells were washed three times with wash buffer (200 µL) for 5 min. A 1/10000 dilution of sheep anti mouse HRP labelled secondary antibody was prepared in 3% BSA-TBS/0.05% tween-20 and 100 µL was applied to each well. The plate was covered and incubated at room temperature for 1 hr. Wells were washed three times with wash buffer (200 µL) for 5 min. Super signal (100 µL) (thermo Scientific) was applied to each well. The Luminescence was measured on the plate reader (Thermo Fischer scientific Varioskan Flash).